

PLASTIC RESPONSE OF SHIP STRUCTURE  
SUBJECT OF ICE LOADING

JACOB ABRAHAM







**PLASTIC RESPONSE OF SHIP STRUCTURE  
SUBJECT TO ICE LOADING**

by

© JACOB ABRAHAM, B.Tech.

A thesis submitted to the School of Graduate Studies  
in partial fulfillment of the requirements for the degree of  
Master of Engineering

Faculty of Engineering and Applied Science  
Memorial University of Newfoundland

September 2008

St. John's

Newfoundland

Canada

## TABLE OF CONTENTS

Abstract	
Acknowledgements	
List of figures	
List of tables	
Nomenclature	
<b>1 INTRODUCTION.....</b>	<b>1</b>
1.1 THE ARCTIC – THE NEW FRONTIER .....	1
1.2 BACKGROUND OF RESEARCH .....	2
1.3 POST YIELD BEHAVIOR OF A FRAME .....	3
1.3.1 <i>Material model</i> .....	3
1.3.2 <i>Yield, plastic hinge and collapse</i> .....	4
1.4 ICE-STRUCTURE INTERACTION .....	5
1.4.1 <i>Pressure-area relationship</i> .....	6
1.4.2 <i>Ice loading considered in present study</i> .....	7
1.5 CURRENT ICE CLASS VESSEL DESIGN PRACTICE.....	9
1.5.1 <i>Ice classes</i> .....	9
1.5.2 <i>Hull areas</i> .....	9
1.5.3 <i>Design ice load</i> .....	9
1.5.4 <i>Shell plating and framing requirements</i> .....	10
1.5.5 <i>Structural stability of framing</i> .....	10
1.5.6 <i>Corrosion/abrasion allowance</i> .....	10
1.5.7 <i>Material requirement</i> .....	10
1.6 LITERATURE REVIEW .....	11
1.6.1 <i>Experimental studies</i> .....	12
1.6.2 <i>Analytical and numerical studies</i> .....	13
1.6.3 <i>Analytical studies related to ice loading</i> .....	15
1.6.4 <i>Stiffened panel - collapse modes</i> .....	16
1.7 SCOPE OF RESEARCH .....	19
1.7.1 <i>Validation of large grillage experiment</i> .....	20
1.7.2 <i>Load sharing in a grillage</i> .....	20
1.7.3 <i>Parametric study of capacity</i> .....	20
1.7.4 <i>Stability of flat bar stiffener</i> .....	21
<b>2 FEM VALIDATION OF LARGE GRILLAGE EXPERIMENT .....</b>	<b>23</b>
2.1 INTRODUCTION .....	23
2.2 LARGE GRILLAGE EXPERIMENT .....	25
2.2.1 <i>Large grillage geometry</i> .....	26
2.2.2 <i>Loading scheme</i> .....	26
2.2.3 <i>Boundary conditions</i> .....	26

2.2.4	<i>Results of experiment</i> .....	27
2.3	ANSYS NON-LINEAR ANALYSIS .....	30
2.3.1	<i>Types of nonlinearities</i> .....	32
2.3.2	<i>Solution options</i> .....	33
2.3.3	<i>Solution convergence</i> .....	34
2.4	FINITE ELEMENT ANALYSIS OF LARGE GRILLAGE .....	36
2.4.1	<i>Structural modeling</i> .....	36
2.4.2	<i>Finite elements</i> .....	36
2.4.3	<i>Material model</i> .....	38
2.4.4	<i>Boundary conditions</i> .....	38
2.4.5	<i>Loading</i> .....	39
2.4.6	<i>Solution</i> .....	41
2.5	RESULTS OF FE ANALYSIS USING SHELL ELEMENT .....	42
2.5.1	<i>Comparison of capacity</i> .....	42
2.5.2	<i>Comparison of deformed shape</i> .....	43
2.5.3	<i>Modeling of weld</i> .....	43
2.6	RESULTS OF FE ANALYSIS USING SOLID ELEMENT .....	47
2.6.1	<i>Comparison of capacity</i> .....	47
2.6.2	<i>Comparison of deformed shape</i> .....	48
2.7	COMPARISON OF SHELL AND SOLID ELEMENT .....	49
2.7.1	<i>Capacity comparison</i> .....	49
2.7.2	<i>Deformed shape comparison</i> .....	51
2.8	CONCLUSIONS .....	52
<b>3</b>	<b>LOAD SHARING IN A GRILLAGE</b> .....	<b>54</b>
3.1	INTRODUCTION .....	54
3.2	ICE LOAD .....	55
3.3	SINGLE FRAME ANALYSIS .....	56
3.3.1	<i>Structural model</i> .....	56
3.3.2	<i>Finite element model</i> .....	56
3.3.3	<i>Material model</i> .....	56
3.3.4	<i>Loading</i> .....	56
3.3.5	<i>Boundary conditions</i> .....	57
3.3.6	<i>Solution process</i> .....	58
3.4	SMALL GRILLAGE ANALYSIS .....	58
3.4.1	<i>Structural model</i> .....	58
3.4.2	<i>Finite element</i> .....	58
3.4.3	<i>Loading</i> .....	58
3.4.4	<i>Boundary conditions</i> .....	59
3.4.5	<i>Solution process</i> .....	60
3.5	LARGE GRILLAGE ANALYSIS .....	60
3.5.1	<i>Structural model</i> .....	60
3.5.2	<i>Finite elements</i> .....	61
3.5.3	<i>Loading</i> .....	61

3.5.4	<i>Boundary conditions</i> .....	62
3.5.5	<i>Solution</i> .....	62
3.6	CAPACITY OF A FRAME.....	63
3.6.1	<i>Twice elastic slope method</i> .....	63
3.6.2	<i>Tangent intersection method</i> .....	64
3.6.3	<i>0.1% residual strain method</i> .....	64
3.7	T STIFFENER ANALYSIS .....	66
3.7.1	<i>Frame T1</i> .....	67
3.7.2	<i>Frame T2</i> .....	69
3.7.3	<i>Frame T3</i> .....	71
3.7.4	<i>Frame T4</i> .....	73
3.7.5	<i>Frame T5</i> .....	75
3.7.6	<i>Discussion of T stiffener results</i> .....	77
3.8	FLAT BAR STIFFENER ANALYSIS .....	79
3.8.1	<i>Frame FB1</i> .....	80
3.8.2	<i>Frame FB2</i> .....	82
3.8.3	<i>Frame FB3</i> .....	84
3.8.4	<i>Frame FB4</i> .....	86
3.8.5	<i>Discussion of flat bar stiffener results</i> .....	87
3.9	CONCLUSIONS .....	89
<b>4</b>	<b>PARAMETRIC STUDY OF CAPACITY</b> .....	<b>91</b>
4.1	INTRODUCTION .....	91
4.2	FACTORS CONSIDERED FOR THE STUDY .....	94
4.3	DESIGN SPACE.....	95
4.4	DESIGN OF EXPERIMENTS .....	96
4.5	FINITE ELEMENT ANALYSIS .....	99
4.5.1	<i>Finite element</i> .....	99
4.5.2	<i>Loading</i> .....	99
4.5.3	<i>Boundary conditions</i> .....	99
4.5.4	<i>Nonlinear analysis</i> .....	101
4.5.5	<i>Result of finite element analysis</i> .....	102
4.5.6	<i>Modified tangent intersection method</i> .....	102
4.6	ANALYSIS MATRIX .....	104
4.7	CAPACITY PREDICTION MODEL .....	108
4.8	VALIDATION OF CAPACITY PREDICTION MODEL .....	110
4.9	MAJOR FACTORS AFFECTING CAPACITY .....	114
4.9.1	<i>Capacity vs. web height</i> .....	114
4.9.2	<i>Capacity vs. web height / web thickness</i> .....	115
4.9.3	<i>Capacity vs. shell thickness</i> .....	116
4.9.4	<i>Capacity vs. yield strength</i> .....	117
4.9.5	<i>Interaction of web height and web height / thickness</i> .....	118
4.9.6	<i>Interaction of web height and plate thickness</i> .....	119
4.9.7	<i>Interaction of web height and yield strength</i> .....	120

4.9.8	<i>Interaction of web height / thickness and yield strength</i> .....	121
4.9.9	<i>Interaction of plate thickness and yield strength</i> .....	122
4.10	CONCLUSIONS.....	123
<b>5</b>	<b>STABILITY OF FLAT BAR STIFFENER</b> .....	<b>125</b>
5.1	INTRODUCTION .....	125
5.2	FACTORS CONSIDERED FOR THE STUDY .....	130
5.3	DESIGN SPACE.....	131
5.4	DESIGN OF EXPERIMENT .....	132
5.5	FINITE ELEMENT ANALYSIS .....	133
5.5.1	<i>Finite element</i> .....	133
5.5.2	<i>Loading</i> .....	133
5.5.3	<i>Boundary conditions</i> .....	134
5.5.4	<i>Nonlinear analysis</i> .....	136
5.6	DEFINING STABILITY .....	137
5.7	ANALYSIS MATRIX .....	139
5.8	RESULTS OF STABILITY STUDY .....	141
5.8.1	<i>Major factors affecting web height</i> .....	141
5.8.2	<i>Web height prediction</i> .....	141
5.8.3	<i>Major factors affecting web height / web thickness ratio</i> .....	143
5.8.4	<i>Web height / thickness ratio prediction</i> .....	144
5.9	VALIDATION OF PREDICTION MODELS .....	146
5.10	CONCLUSIONS .....	150
<b>6</b>	<b>CONCLUSIONS AND RECOMMENDATIONS</b> .....	<b>154</b>
6.1	CONCLUSIONS.....	154
6.1.1	<i>FE validation study</i> .....	154
6.1.2	<i>Load sharing in a grillage</i> .....	154
6.1.3	<i>Parametric study of capacity</i> .....	155
6.1.4	<i>Stability of flat bar stiffener</i> .....	156
6.2	RECOMMENDATIONS .....	157
<b>7</b>	<b>REFERENCES</b> .....	<b>158</b>
	<b>APPENDICES</b> .....	<b>164</b>
	<b>Appendix A: Load sharing in a grillage</b> .....	<b>165</b>
	Appendix A1: Ice load estimation	
	<b>Appendix B: Parametric study of capacity</b> .....	<b>169</b>
	Appendix B1: DOE run results	

Appendix B2: Validation run results

**Appendix C: Stability of flat bar stiffener.....183**

Appendix C1: DOE run results

Appendix C2: Validation run results

## ABSTRACT

Stiffened plates are the basic structural building blocks of ships and many onshore and offshore structures. The present research explores the plastic response of a stiffened plate subjected to lateral ice loads. The Finite Element Method (FEM) is extensively used to study the plastic behavior of stiffened plates. In order to gain confidence in using FEM, a validation study of a full scale experiment is initially presented. Following the examination of experimental and numerical results for a loaded grillage, the report examines three separate but related questions concerning the design of ice capable stiffened panels.

Ship structure design normally considers single frames. This is justified because under uniform loading, all frames behave similarly - so it is reasonable to consider frames singly. In case of ice loading which is non symmetric, the symmetric boundary condition does not accurately represent the true structural behavior. The difference in load carrying capacity between frames in isolation and frames as part of a grillage, subjected to an unsymmetrical loading is studied.

The capacity of a stiffened plate depends on many factors – geometric properties, material properties, loading type etc. The current IACS Polar Rules for Ships contain plastic limit state models of frame capacity. These limit states are analytically derived using relatively simple energy methods and validated by finite element analyses. The contributions from large deformations and membrane stresses are ignored and hence these analytical solutions may not accurately estimate capacity of all frames. The reliable methods to estimate capacity are either to conduct a full scale experiment or a nonlinear finite element analysis. These methods are either very expensive or too complex. There is a need for a simple regression equation which can predict capacity taking into account all the non-linear behavior of the structure. There are ten factors which influence load carrying capacity of a frame. The study of ten factors at two levels (at high and low levels of each factor) requires 1024 ( $2^{10}$ ) ANSYS analyses. A significant reduction in the number of analyses is achieved by using “design of experiments” (DOE) method. A new

regression equation for estimating load carrying capacity of the frame is proposed and validated using independent FE analyses.

The total load carrying capacity of a stiffened plate is contributed by both shell plate and stiffener. In most situations, stiffened panels will be sensitive to buckling under axial loads. In the case of ice reinforcement, the loads are primarily normal to the shell, with minimal axial loads. The concern for frame buckling remains, although the issue is less well understood. Some stiffeners, especially those with slender webs, show a tendency to fail by local web buckling, tripping and shear buckling, causing a sudden loss of capacity and resulting in collapse of the structure. The IACS Polar Shipping Rules (URI2) contains a requirement aimed at the prevention of web buckling by specifying a maximum web height / web thickness ( $h_w/t_w$ ). While URI2 employs plastic limit states, the stability ratio is based on prevention of elastic buckling. In some cases these stability requirements have a significant impact on the design. The current rule limiting values of  $h_w/t_w$  are very conservative and do not adequately reflect the conditions that lead to instability. The FEM coupled with the DOE method is used in the study. Six factors which influence stability of a flat bar stiffener are identified. The study of six factors even at two levels (at high and low levels of each factor) requires 64 ( $2^6$ ) possible combinations of factors to be considered. A significant reduction in the number of cases is achieved by employing DOE method. The main factors affecting the plastic stability of a frame are quite different from the usual elastic buckling parameters. A new relationship is proposed for calculating the limiting web height and web slenderness.

## ACKNOWLEDGEMENTS

The research could not have been successfully completed without the encouragement and guidance of many others.

I am extremely pleased to acknowledge my deepest gratitude to my graduate program and research supervisor, Dr. Claude Daley. The guidance, encouragement and financial support provided throughout the program were invaluable.

The assistance provided by Mr. Matt Curtis of the Structures Laboratory during the Large Grillage Experiment and the guidance provided by Dr. Leonard Lye in using DOE methods is gratefully acknowledged.

The two years I spent in MUN was made enjoyable by the company of many friends I had – of which some require special mention – Suresh, Bruce, Anup and Manoj.

My wife Megi used to be a source of constant support and encouragement for timely completion of the graduate program. For all that she has done, I dedicate this report to her.

## LIST OF FIGURES

Figure 1.3.1: Stress-strain curve of structural steel.....	3
Figure 1.3.2: Load-deflection behavior of a typical frame .....	4
Figure 1.4.1: Ice structure interaction (Daley et al., 1998).....	5
Figure 1.4.2: Frame, actual ice loading and simplified ice loading .....	8
Figure 1.6.1: Roof type mechanism (Daley at al., 2001).....	16
Figure 1.6.2: Double diamond type mechanism (Hong & Amdahl, 2007).....	16
Figure 1.6.3: Failure mode I-1 (Paik & Thayamballi, 2003).....	17
Figure 1.6.4: Failure mode I-2 (Paik & Thayamballi, 2003).....	17
Figure 1.6.5: Failure mode II (Paik & Thayamballi, 2003).....	17
Figure 1.6.6: Failure mode III (Paik & Thayamballi, 2003).....	17
Figure 1.6.7: Failure mode IV (Paik & Thayamballi, 2003) .....	18
Figure 1.6.8: Failure mode V (Paik & Thayamballi, 2003).....	18
Figure 2.1.1: Single frame .....	23
Figure 2.1.2: Small grillage .....	23
Figure 2.1.3: Large grillage .....	24
Figure 2.2.1: General arrangement of large grillage.....	25
Figure 2.2.2: Large grillage on test bed (Daley & Hermanski, 2005) .....	27
Figure 2.2.3: Un-deformed and deformed stiffener during full scale experiment .....	28
Figure 2.2.4: Load vs. Deflection of full scale experiment .....	29
Figure 2.3.1: Flowchart of ANSYS non-linear analysis .....	31
Figure 2.4.1: Shell 181 geometry.....	37
Figure 2.4.2: Solid 92 geometry .....	37
Figure 2.4.3: Non-linear material model.....	38
Figure 2.4.4: Boundary conditions of large grillage.....	38
Figure 2.4.5: Plan (bottom view) and elevation of frame and indenters.....	39
Figure 2.4.6: Load steps of large grillage experiment .....	40
Figure 2.5.1: Comparison of capacity – experimental vs. shell elements.....	42

Figure 2.5.2: Comparison of deformed shape - experimental vs. shell elements .....	43
Figure 2.5.3: Modeling of weld using thin plate.....	44
Figure 2.5.4: Comparison of capacity - experimental vs. shell with and w/o weld.....	45
Figure 2.5.5: Comparison of deformed shape - experimental vs. shell with and without weld (weld modeled using plate elements).....	45
Figure 2.5.6: Modeling of weld using rigid elements .....	46
Figure 2.5.7: Comparison of deformed shape - experimental vs. shell with and without weld (weld modeled using rigid elements) .....	46
Figure 2.6.1: Comparison of capacity – experimental vs. solid elements .....	47
Figure 2.6.2: Comparison of deformed shape– experimental vs. solid elements .....	48
Figure 2.7.1: Comparison of capacity using shell and solid elements (yield stress = 315 MPa and post yield modulus = 1000 MPa).....	49
Figure 2.7.2: Comparison of capacity using shell and solid elements (yield stress = 315 MPa and post yield modulus = 2000 MPa).....	50
Figure 2.7.3: Comparison of deformed shape using shell and solid elements.....	51
Figure 3.2.1: Frame, actual ice loading and simplified ice loading .....	55
Figure 3.3.1: Loading considered for single frame analysis .....	56
Figure 3.3.2: Symmetric boundary condition at transverse edges .....	57
Figure 3.3.3: Fixed boundary condition at longitudinal ends .....	57
Figure 3.4.1: Loading considered for small grillage analysis .....	59
Figure 3.4.2: Boundary conditions considered for small grillage analysis.....	60
Figure 3.5.1: Loading considered for large grillage analysis.....	61
Figure 3.5.2: Boundary conditions considered for large grillage analysis .....	62
Figure 3.6.1: Definition of capacity using Twice Elastic Slope Method.....	63
Figure 3.6.2: Definition of capacity using Tangent Intersection Method.....	64
Figure 3.6.3: Definition of capacity using 0.1% Residual Strain Method.....	65
Figure 3.7.1: Results of ANSYS analysis – Frame T1 .....	68
Figure 3.7.2: Capacity - Frame T1.....	68
Figure 3.7.3: Results of ANSYS analysis – Frame T2 .....	70

Figure 3.7.4: Capacity - Frame T2.....	70
Figure 3.7.5: Results of ANSYS analysis – Frame T3 .....	72
Figure 3.7.6: Capacity - Frame T3.....	72
Figure 3.7.7: Results of ANSYS analysis – Frame T4 .....	74
Figure 3.7.8: Capacity - Frame T4.....	74
Figure 3.7.9: Results of ANSYS analysis – Frame T5 .....	76
Figure 3.7.10: Capacity - Frame T5.....	76
Figure 3.8.1: Results of ANSYS analysis – Frame FB1 .....	81
Figure 3.8.2: Results of ANSYS analysis – Frame FB2.....	83
Figure 3.8.3: Results of ANSYS analysis – Frame FB3.....	85
Figure 3.8.4: Results of ANSYS analysis – Frame FB4.....	87
Figure 4.1.1: Load-deflection behavior of a typical frame .....	92
Figure 4.5.1: Loading considered for capacity study.....	100
Figure 4.5.2: Symmetric boundary condition at transverse edges .....	100
Figure 4.5.3: Fixed boundary condition at longitudinal ends .....	101
Figure 4.5.4: Definition of capacity using Modified Tangent Intersection Method.....	103
Figure 4.7.1: Predicted vs. Actual capacity .....	109
Figure 4.8.1: Predicted vs. Actual capacity .....	113
Figure 4.9.1: Capacity vs. web height.....	114
Figure 4.9.2: Capacity vs. web height / web thickness.....	115
Figure 4.9.3: Capacity vs. shell thickness.....	116
Figure 4.9.4: Capacity vs. yield strength .....	117
Figure 4.9.5: Interaction of web height and web height / thickness .....	118
Figure 4.9.6: Interaction of web height and plate thickness .....	119
Figure 4.9.7: Interaction of web height and yield strength.....	120
Figure 4.9.8: Interaction of web height / thickness and yield strength.....	121
Figure 4.9.9: Interaction of plate thickness and yield strength.....	122
Figure 5.1.1: Local web buckling .....	125
Figure 5.1.2: Lateral torsional buckling or tripping.....	126

Figure 5.1.3:: Two frames with different web heights.....	126
Figure 5.1.4: 300 mm web height frame (capacity vs. $h_w/t_w$ ratio).....	127
Figure 5.1.5: 600 mm web height frame (capacity vs. $h_w/t_w$ ratio).....	128
Figure 5.5.1: Loading considered for stability study .....	134
Figure 5.5.2: Symmetric boundary condition at transverse edges .....	135
Figure 5.5.3: Fixed boundary condition at longitudinal ends .....	135
Figure 5.6.1: Definition of stability .....	137
Figure 5.8.1: Half normal plot of web height study.....	141
Figure 5.8.2: Predicted vs. Actual web heights .....	142
Figure 5.8.3: Allowable web height vs. plate thickness and web thickness .....	143
Figure 5.8.4: Half normal plot of $h_w/t_w$ study .....	144
Figure 5.8.5: $h_w/t_w$ ratio vs. plate thickness .....	145
Figure 5.8.6: $h_w/t_w$ ratio vs. web thickness .....	145
Figure 5.9.1: Web height – actual vs. predicted values .....	148
Figure 5.9.2: $h_w/t_w$ ratio – actual vs. predicted values .....	149
Figure 5.10.1: Three frames with different web heights.....	150
Figure 5.10.2: Capacity vs. Web Height (Yield strength = 250 MPa).....	151
Figure 5.10.3: Capacity vs. Web Height (Yield strength = 375 MPa).....	152
Figure 5.10.4: Capacity vs. Web Height (Yield strength = 500 MPa).....	152
Figure 5.10.5: Large localized strains.....	153

#### LIST OF TABLES

Table 3.7.1: T stiffener parameters .....	66
Table 3.7.2: T1 stiffener parameters .....	67
Table 3.7.3: T2 stiffener parameters .....	69
Table 3.7.4: T3 stiffener parameters .....	71
Table 3.7.5: T4 stiffener parameters .....	73
Table 3.7.6: T5 stiffener parameters .....	75
Table 3.7.7: Summary of T stiffener results .....	77

Table 3.8.1: Flat bar stiffener parameters .....	79
Table 3.8.2: FB1 stiffener parameters.....	80
Table 3.8.3: FB2 stiffener parameters.....	82
Table 3.8.4: FB3 stiffener parameters.....	84
Table 3.8.5: FB4 stiffener parameters.....	86
Table 3.8.6: Summary of flat bar stiffener results .....	88
Table 4.3.1: Parameter ranges for capacity study .....	95
Table 4.6.1: Analysis matrix for capacity study .....	104
Table 4.8.1: Validation runs of capacity.....	110
Table 5.1.1: $h_w/t_w$ limits .....	129
Table 5.3.1: Design space for stability study .....	131
Table 5.6.1: Stability vs. web height.....	138
Table 5.7.1: Analysis matrix for stability study.....	139
Table 5.9.1: Validation runs of stability .....	146

## NOMENCALTURE

ABS	American Bureau of Shipping
ALPS/HULL	Progressive collapse analysis software for ships hull
ALPS/ULSAP	Ultimate limit state assessment software for stiffened panels
CSR	Common structural rules
DNV	Det Norske Veritas
DOE	Design of Experiments
FEA	Finite Element Analysis
IACS	International Association of Classification Societies
NLFEA	Non-linear Finite Element Analysis
PULS	DNV buckling code for stiffened panels
UR	Unified Requirement
$A_w$	Area of the web
$b$	height of the ice load patch
$E$	Young's modulus
$h_w$	web height
$h_w/t_w$	web height / web thickness ratio
$k_w$	area ratio
$L$	length of frame
$P_{3h}$	pressure causing collapse for case of 2 fixed supports
$Rot_x$	rotation about x-axis
$S$	frame spacing
$t_w$	web thickness
$U_x$	displacement along x-axis
$Z_p$	plastic section modulus
$Z_{pns}$	a non-dimensional modulus
$\epsilon$	strain
$\sigma$	stress
$\sigma_y$	yield stress

## **1 INTRODUCTION**

### **1.1 The Arctic – the new frontier**

Interest in the Arctic is rapidly increasing again, driven primarily by interest in oil and other resources and by the possibility of new shipping routes.

The recent high growth rate of certain large emerging economies has increased the demand for energy. This demand is putting pressure on current oil production regions. There is a need to find new energy sources and/or extend the existing capabilities to extract oil from new and often harsher environments. Recent estimates claim that the total petroleum reserves beneath the Arctic might be in the order of 400 billion barrels. Full scale oil production from the Arctic could help to meet the growing world demand for energy.

Much of the Arctic seas are normally covered by ice year round and are not suitable for shipping except during summer months when the sea ice partially retreats. Studies now show that the Arctic may become suitable for shipping all year by 2050. The new shipping routes – the Northern Sea Route and the Northwest Passage - would greatly reduce existing travel times, saving thousands of nautical miles in travel and billions of dollars in operating expenses. The Northern Sea Route would reduce the distance between Europe and Japan from 11,000 nautical miles (via Suez Canal) to 6,500 nautical miles. Similarly, the Northwest Passage would reduce distance between Europe and West coast of USA by 2,000 nautical miles, compared to the current route via Panama Canal.

While the Arctic may become less harsh in the years to come, there is immediate interest in the Arctic now. In order to take advantage of the opportunities that the Arctic offers, new ships are required which can safely operate in an ice covered Arctic. This requires advancing our understanding about ice loads and structural responses to ice loads, which will lead to more efficient structures to meet the design challenges of Arctic. The present research explores a few subsets of structural response to ice load – plastic capacity, stiffener stability and load sharing in a grillage.

## **1.2 Background of research**

Stiffened plates are the basic structural building blocks of many onshore and offshore structures, where high strength to weight ratio is a major criteria dictating design. Ships hull structure consists of plate stiffened in both directions. The behavior of stiffened plate in the elastic region is well understood. In the recent years there has been a renewed interest in estimating plastic response of ship structures.

Ship design rules are changing from traditional working stress approach to new rules which allow plastic limit states, particularly in the case of ice class vessels. The rationale behind this move is the recognition that structure tends to have a large reserve capacity after it yields and before it finally collapses. The use of some portion of the reserve capacity for resisting loads will result in lighter structures which are easier to fabricate.

There has been some significant research going on in Memorial University of Newfoundland for the past few years about the plastic response of ships frames. Full scale experiments, analytical solutions and extensive finite element studies have been carried out as part of this research. The funding of the project was provided by Government Agencies and Classification Societies. The present study is a part of the currently ongoing research about plastic response of ships frame.

### 1.3 Post yield behavior of a frame

#### 1.3.1 Material model

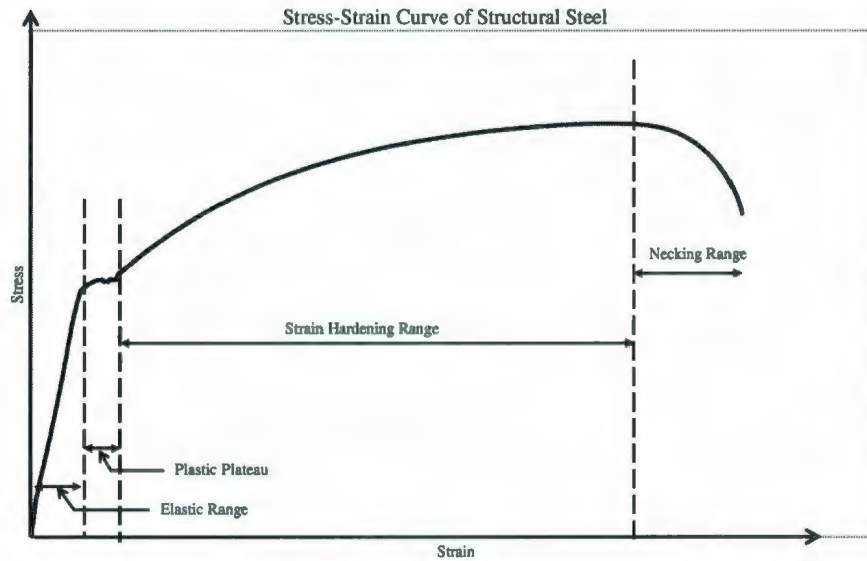


Figure 1.3.1: Stress-strain curve of structural steel

Figure 1.3.1 presents the stress-strain curve of structural steel. The stress-strain relation is linear in the elastic range. After yielding, the material 'hardens', which means that stress needed to induce plastic flow increases. The tangential stiffness (slope of stress-strain curve) in the plastic region is smaller than that in the elastic region; hence in terms of stiffness the material is 'softer'.

The stress-strain relation is non-linear in the plastic region, but can be approximated as linear in the practical ranges of structural deformation. Thus the total stress-strain is normally approximated as a bilinear curve with linear hardening. Estimated post yield modulus ranges from 0 to 2000 MPa. A factor of zero for the post yield modulus corresponds to perfectly plastic behavior.

### 1.3.2 Yield, plastic hinge and collapse

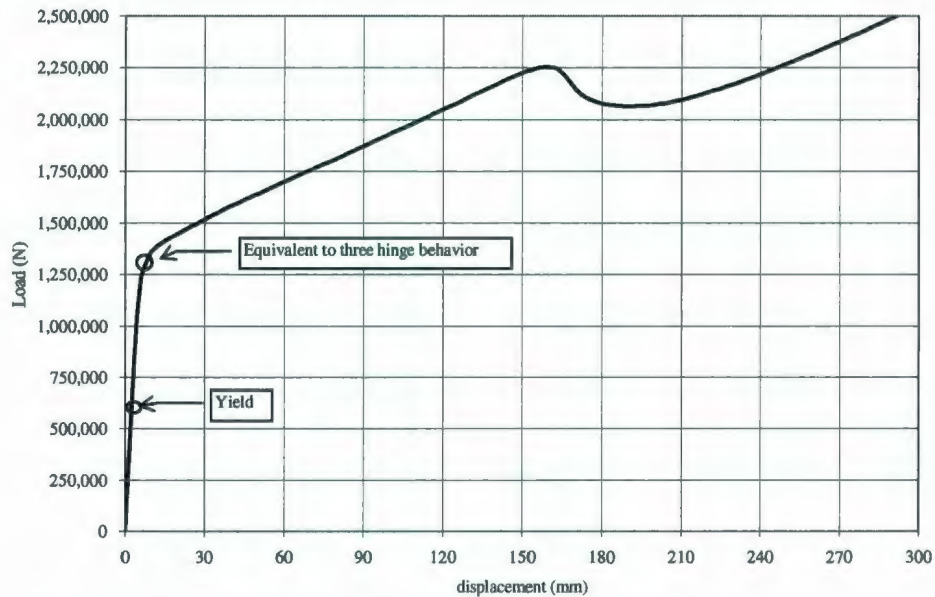


Figure 1.3.2: Load-deflection behavior of a typical frame

Figure 1.3.2 presents the response of a typical frame subjected to a concentrated patch load which is an approximation to ice loading. The initial response of the frame is linear even after the material yields. The yielding is initiated at the most highly stressed region. An increase in loading will result in growth of yielded region. When the complete cross section yields, it will result in the formation of an internal hinge at that location. If the applied load is further increased, more locations start to yield and more hinges are formed. One of the basic collapse mechanisms in the case of a fixed beam is the three-hinge formation.

Beyond the three-hinge formation, the beam can take more loads due to the additional support from membrane action (geometry change) and strain hardening. Even though the structure is deforming, the additional support of membrane and strain hardening enables the structure to bear increasing loads.

#### 1.4 Ice-structure interaction

In an ice-structure interaction event, ice gets squeezed between the structure and the remainder of the larger ice mass, as shown in Figure 1.4.1. The compressive forces cause the ice to fail near the structure, creating fractures and spalls (cracks propagating to free surface) in the ice which reduces the contact area.

The total interaction zone is characterized by three distinct regions of pressure – a critical zone, region of background pressure and areas of recently spalled ice. Critical zones are localized regions of ice where intense pressures occur over a short period of time. These areas of high pressure are continuously changing due to flaking (local cracking) of ice. Comminution (crushed ice entrapped between ice and structure) exerts background pressure which surrounds areas of high pressure. The extruded rubble exerts back pressure on the ice inhibiting crack formation inside ice.

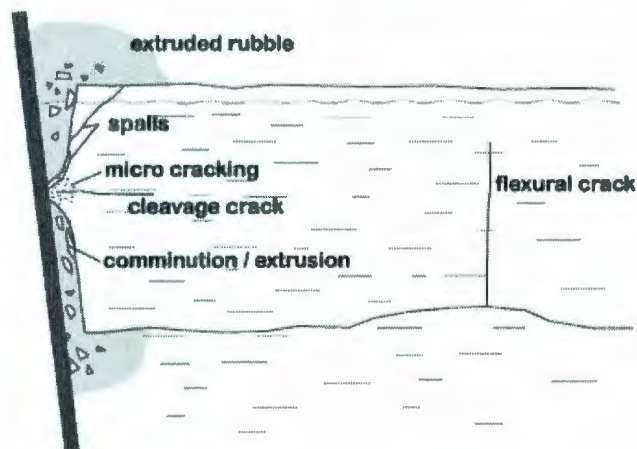


Figure 1.4.1: Ice structure interaction (Daley et al., 1998)

One of the earliest ice force models was suggested by Kurdymov and Khesin (1976). They proposed a “uniform” thickness of pulverized ice which got extruded as the collision progressed. The pressure measurements of later ship ice collision didn’t support the uniform thickness of crushed ice and uniform pressure generation. More complex ice models were proposed as time progressed.

Local pressure distribution during an ice structure interaction was studied in many ship ramming trials. Pressure sensors were fitted to the ships structure and hull responses were recorded during the trials. The major ship ramming trials were Louis S. St. Laurent (Frederking, 2000) and Canmar Kigoriak (Dome Petroleum, 1982). These tests indicated localized pressure variations within the whole area of contact. The Baltic Sea ice breaking trials onboard IB Sampo (Riska et al., 1990) and Helsinki University laboratory tests (Daley, 1991) showed line like areas of very high pressure surrounded by relatively low pressure. The local pressure was as high as 70 MPa in some cases.

#### 1.4.1 Pressure-area relationship

From the previous discussion it is clear that ice pressure is not uniform within the area of contact. The localized pressure tends to be much higher than the average pressure. Hence two pressure values are required to design a structure – one for local structural design and another for global design. This requires two distinct ways of describing the pressure of an ice collision with the area of contact – process and spatial pressure-area relationship (Daley, 2004).

##### 1.4.1.1 Process pressure-area

The process pressure-area relation describes how the average pressure relates to the total contact area. The pressure can either increase or decrease as the interaction proceeds.

The process pressure area is used to calculate the total collision force, which is used to design foundation or mooring cables.

##### 1.4.1.2 Spatial pressure-area

The spatial pressure-area describes the distribution of local pressure within the total area of contact at an instant in time. The highest pressure occurs on a small area at the peak location. The average pressure within larger areas will necessarily be smaller than the peak pressure. Hence the pressure and area are inversely related in spatial pressure area relation.

Typically, such a relation will take the following form (Daley, 2004):

$$P = C / A^e$$

where

C = average pressure (typically between 0.5 MPa to 5 MPa)

e is typically in the range of 0.25 to 0.7

The spatial pressure relation is used to determine design loads on local structure, such as plating and framing.

Both process and spatial pressure explains the same ice structure interaction in two view points and are related to each other.

#### 1.4.2 Ice loading considered in present study

The present research deals with the local design of stiffened plate; hence spatial pressure area relationship is used.

The ice load during a collision is approximated as patch load with a center peak and low pressures in near by region (Daley & Kendrick, 2008). The length of the center peak is approximated as one frame spacing. Figure 1.4.2 presents the simplified ice loading considered for the study.

Chapter 3 deals with capacity comparison in the case of large grillage, small grillage and single frame. The large grillage and small grillage pressure distribution is based on the ice load model proposed by Daley and Kendrick (2008). In the case of single frames, only the center peak load is considered. The surrounding low pressure region has been ignored for simplicity.

Single frames are studied in Chapter 4 (load carrying capacity) and Chapter 5 (stability). Only the center peak load has been considered and the surrounding low pressure region has been ignored for simplicity. The center peak load has been applied either as pressure acting on a small area (in Chapter 4) or as a prescribed displacement of nodes in a small area (in Chapter 5).

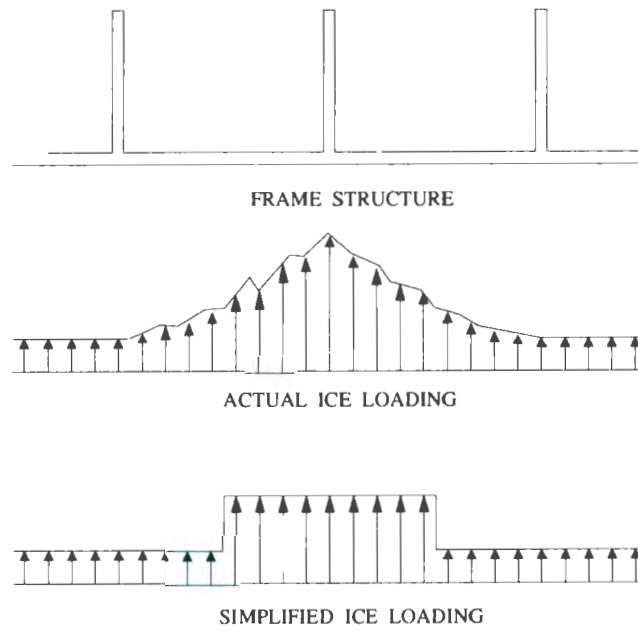


Figure 1.4.2: Frame, actual ice loading and simplified ice loading

## **1.5 Current ice class vessel design practice**

Previously ice class vessels were designed, fabricated and operated based on the rules set by individual classification societies. There are many classification societies around the world. A complex mix of ice class rules existed prior to 1992. Ice loads and limit states were defined differently by various classification societies; making comparison between ice classes difficult. It often created operational difficulties for a vessel registered in one classification society to operate in the territorial waters of another country. Beginning in 1992, International Association of Classification Societies (IACS) developed a solution to unify the various conflicting rules and regulations of various ice class vessels. IACS developed a Unified Requirement (UR) called URI in ice class vessels.

The structural requirements of an IACS class vessel are described in UR I2. Structure requirements includes that of shell plating, framing, web frames, load carrying stringers, stiffened plates, stem and stern frames, hull appendages etc.

### **1.5.1 Ice classes**

The IACS ice classes range from PC1 to PC7 - depending on the operational period and ice condition to be encountered. PC1 represents vessels that are intended to operate year round in polar waters. PC7 represents vessels intended to operate during summer/autumn in thin first year ice. Intermediate classes represent in between ice conditions.

### **1.5.2 Hull areas**

The hull of a polar class ship is divided into areas reflecting the magnitude of the loads that are expected to act upon them. There are four regions in the longitudinal direction - bow, bow intermediate (BI), mid-body (M) and stern (S). The bow intermediate, mid-body and stern regions are further divided in the vertical direction as bottom, lower and ice belt regions.

### **1.5.3 Design ice load**

Polar class ships experience a wide variety of ship-ice interactions during its operational life, but the glancing impact on the bow is considered as the design basis for calculating scantling requirements.

The design ice load is characterized by an average pressure ( $P_{avg}$ ) acting over a rectangular region of height (b) and width (w). The design ice load is defined differently for bow and non bow region.

#### 1.5.4 Shell plating and framing requirements

For designing the local structure, the average pressure is increased by the Peak Pressure Factor; to take into account the higher local pressures acting within smaller areas.

The shell plate thickness is calculated using a plastic hinge capacity.

For frames, two load scenarios are considered – a load applied at mid span and a load applied near one end of the frame. The frames are sized based on combined shear area and plastic section modulus requirements.

#### 1.5.5 Structural stability of framing

In order to prevent local web buckling, UR I2 included a maximum allowable web height to thickness ( $h_w/t_w$ ) ratios. These ratios depend on the material yield and the type of stiffener. In situations where the maximum  $h_w/t_w$  ratio is not practically attainable, stiffening of the web is required.

#### 1.5.6 Corrosion/abrasion allowance

The minimum thickness estimated by the above requirements is to be augmented by a corrosion and abrasion allowance. The allowance depends on hull area, polar class and presence/absence of effective corrosion/abrasion protection.

#### 1.5.7 Material requirement

The requirements of UR I2 are based on the assumption that brittle fracture of structural members will not occur. Minimum grades of steel to be used for various structural members are specified to avoid chances of brittle failure. The steel grade selection depends on factors like polar class, material class, thickness of the structural member etc.

## **1.6 Literature review**

A ship is designed to withstand normal operating loads without structural failure. The load acting on a ship is not always a certain quantity and sometimes exceeds the design limits due to accidental and extreme operational scenario. A ship operating in ice covered sea will have a high probability of encountering loads which exceed the design limits.

A limit state is defined as a condition in which the structure fails and becomes inadequate to perform its intended function (Paik & Thayamballi, 2003). From a structural viewpoint, there are four types of limit states - Serviceability Limit State (SLS), Ultimate Limit State (ULS), Fatigue Limit State (FLS) and Accidental Limit State (ALS).

Serviceability limits are those which cause minor inconveniences, but do not affect the ultimate functioning of the structure, for example, minor denting on the side shell of an ice breaker. Ultimate limit states are those which result in complete failure of the structure. The plastic collapse of a grillage is an example of ultimate limit state.

As the applied load is increased, structural members of the hull which are subjected to compression will buckle and that subjected to tension will yield. Beyond the onset of member buckling and yielding, the hull can withstand further loading, but the structural effectiveness of the failed members will decrease. The stresses will then be redistributed to the adjacent intact members until they also start to buckle and yield. The failure will grow progressively until an ultimate limit state is reached. The ultimate strength of the hull is an important parameter that defines the available safety factor against accidental and extreme loading.

The current rules of Classification Societies estimate ultimate capacity by using first yield and buckling with a simple correction for plasticity. These expressions are highly simplified and often give wrong estimate about the actual capacity.

The study of the ultimate strength of ships hull has been tackled by various researchers using three main approaches. The approaches can be broadly classified as:

- experimental study
- analytical study

- numerical study

Some researchers have even coupled two of the above approaches together - combining experimental with numerical or theoretical with numerical. In the coupled approach solutions were derived using one method and the second method was used to validate the proposed solutions. For example, the design equations were derived analytically and then validated using FEA (numerical study).

#### 1.6.1 Experimental studies

The most accurate method to estimate the ultimate strength of a frame is by conducting full scale experiments. The prohibitive cost of doing experiments has resulted in very few full scale tests of ships structure.

The major experimental studies on the ultimate strength of ships hull using large scale model were the following:

- Full scale test of welded steel panels subjected to axial compression and lateral pressure was conducted by Smith (1975).
- Full scale testing of the shell structure of an ice strengthened ship was carried out by Varsta et al. (1978). The test specimen had an overall dimension of 4.4m x 1.2m.
- The ultimate strength test on a 1/3 scaled model of frigate ship under sagging condition was carried out by Dow (1991). The test jig had an overall dimension of 18m x 4.0m.
- Plastic instability of ship frame was studied by Bond et al. (1995). The test panel measured 5.0 m x 2.6 m, representing mid-body hull structure along the ice-belt region of a Canadian Arctic Class 3 vessel.
- Full-scale model testing of a portion of the Juniper Class ice-belt structure was carried out by John et al. (2002) to determine failure loads. Loads were applied over a localized area to simulate the impact during level icebreaking in 24 inch thick ice. The test panel had a dimension of 5.0m x 2.6m.

- A series of full scale tests of an ice strengthened vessel subjected to ice loading was carried out by Daley et al. (2007). Eight tests were conducted as single frames fixed on both ends. A small patch load was applied at the center or near the ends. The experiments then proceeded to test two small grillages and then to two large grillages. The large grillage had a dimension of 6.8m length x 2.46m breadth.

The objective of these experimental studies was to provide data for the verification of analytical and numerical assessment tools.

#### 1.6.2 Analytical and numerical studies

The ultimate strength of ship structure was first evaluated by Caldwell (1965) using Rigid Plastic Mechanism Analysis. The effect of buckling was accounted by reducing the yield strength of the buckled region.

Smith (1977) extended the method of Caldwell and proposed a method for the collapse analysis of box girder subject to longitudinal bending. The method considered progressive stiffness loss due to both bucking and yielding.

Yao and Nikolov (1991) developed analytical solution for the progressive collapse of hull girder subjected to longitudinal bending using the computer code 'HULLST'. The stress-strain relationship was derived using elastic large deflection and rigid perfectly plastic analysis. The intersection of elastic and plastic region was taken as the ultimate compressive strength. For the rigid plastic deflection, two collapse mechanism modes were considered.

Paik and Pedersen (1996) extended the method of Yao and Nikolov by assuming three plastic collapse modes. The method was validated using non-linear FEA.

Cui and Mansour (1999) extended the method proposed by Paik and Pedersen to investigate the effect of parameters like welding distortions (amplitude and shape) and residual stresses on the ultimate compressive strength of grillage. The strength reductions due to these parameters were captured using empirical relations. The study showed that the geometric imperfections had a significant effect on the ultimate strength.

Mahendran (1997) proposed two collapse mechanisms for plate subjected to compression; roof type and flip-disc mechanisms. It was shown that a large slenderness ratio plate collapses by flip-disc mode whereas a thick plate collapses by roof mechanism.

Stiffener tripping (lateral torsional bucking) is also considered as an ultimate limit case as the frame collapses soon after stiffener tripping. Hughes and Ma (1996) proposed energy method for analyzing the tripping of flanged stiffeners subjected to axial force, end moment, lateral pressure and a combination of these loads. Rigid web and flexible web cases were studied. The verification of the method was done using FEA.

Paik et al. (1999) studied the ultimate strength of a stiffened panel subject to uni-axial compression. The plate-stiffener combination model was used to represent the stiffened panel. Three collapse modes were considered – (a) plate induced failure, (b) stiffener induced failure without rotation of stiffener and (c) lateral torsional bucking (tripping). Perry–Robertson formulation was used to calculate the collapse strength for plate induced failure and stiffener induced failure (without rotation of the stiffener). Johnson–Ostenfeld formulation was used to calculate the tripping strength. The effective width of plating between stiffeners was analytically formulated as a function of applied compressive loads and initial imperfections. The influences of stiffener web initial imperfections and rotational restraints (plate–web and web–flange intersection), on the local buckling strength were also taken into consideration. The solution developed was compared to experimental and finite element results.

Paik et al. (2001) developed design equations for the ultimate strength of plate subjected to four basic types of loading. The basic load cases considered were longitudinal compression / tension, transverse compression / tension, edge shear and lateral pressure loads. The collapse of a long and/or wide plate depends on the type of loading. Three sets of collapse loads (corresponding to longitudinal compression/tension, transverse compression/tension and edge shear) were formulated. The effect of lateral pressure was considered as secondary. The ultimate strength interaction equation of a plate subjected to combined loading was also developed. The design equations were validated using non-

linear FEA results.

An analytical method for calculating the ultimate strength of bottom plating of ship structure subject to transverse trust and lateral pressure was proposed by Fujikubo et al. (2005a). The method included the effect of plate continuity on the ultimate strength of plate. The two effects of plate continuity are: (a) increase of elastic buckling strength and (b) change of collapse mode from simply supported to clamped. The method was further extended by Fujikoba et al. (2005b) to include the effect of interaction between plate and stiffener. The overall collapse of stiffener under lateral pressure was also included as an additional failure mode. Design equations for the estimation of the ultimate strength of a continuous stiffened panel were developed, based on the results of elasto-plastic large deformation finite element analyses.

Suneel et al. (2006) developed an analytical method to calculate collapse load of stiffened plates with cut-outs subjected to axial compression. The change in strength due to cut-outs and reinforcements were studied using FEA. The FEA method was first validated using laboratory test results.

The accuracy of existing methods (like ANSYS NLFEA, PULS, ALPS/ULSAP, ALPS/HULL, and IACS CSR) used for the estimation of ultimate strength of marine structures were studied and compared by Paik et al. The following marine structures were studied:

- un-stiffened plates subject to combined biaxial compression and lateral pressure loads (Paik et al., 2008a)
- stiffened plates subject to combined biaxial compression and lateral pressure loads (Paik et al., 2008b)
- hull girders subject to bending moments (Paik et al., 2008c)

### 1.6.3 Analytical studies related to ice loading

The ship under normal operating condition is acted upon by uniform lateral load in the form of hydrostatic or dynamic pressure. Patch loading dominates the design in the case

of ice loading, which only acts over a limited length of the structure.

The plastic limit state of shell plating subjected to patch loading has recently caught the attention of many researchers due to its application to ultimate strength of ice class ships.

Daley et al. (2001) proposed roof type collapse mechanism (Figure 1.6.1) and using the work-energy principles derived analytical solutions for the collapse pressure of a beam fixed at two ends. The solutions are currently adopted by IACS for the estimation of plastic frame capacity for the design of ice class vessels. The analytical solutions were validated using extensive FEA.

Nyseth and Holtmark (2006) proposed an alternative of roof type collapse mechanism using three parallel hinge lines and presented analytical method to calculate the capacity of a plate.

Hong and Amdahl (2007) extended the roof type collapse mechanism (Figure 1.6.2) and proposed a double diamond type collapse mechanism. The collapse pressure for a plate was developed and validated using non-linear FEA. Some of the simplifications introduced in the IACS formulations were eliminated and the effect of membrane stresses was included in the method.

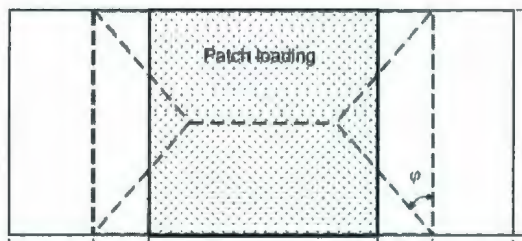


Figure 1.6.1: Roof type mechanism (Daley et al., 2001)

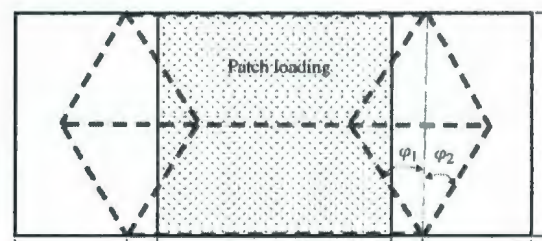


Figure 1.6.2: Double diamond type mechanism (Hong & Amdahl, 2007)

#### 1.6.4 Stiffened panel - collapse modes

The stiffened panel under predominantly compressive load shows a variety of failure modes until ultimate strength is reached (Paik & Thayamballi, 2003). The collapse modes can be categorized into six different types:

- **Mode I-1:** overall collapse of a uni-axially stiffened panel under uni-axial compression (Figure 1.6.3)
- **Mode I-2:** overall collapse of a cross-stiffened panel under uni-axial compression (Figure 1.6.4)
- **Mode II:** biaxial compressive collapse under biaxial compression (Figure 1.6.5)
- **Mode III:** beam-column type collapse under uni-axial compression (Figure 1.6.6)
- **Mode IV:** collapse by local buckling of stiffener web under uni-axial compression (Figure 1.6.7)
- **Mode V:** collapse by tripping of stiffener under uni-axial compression (Figure 1.6.8)

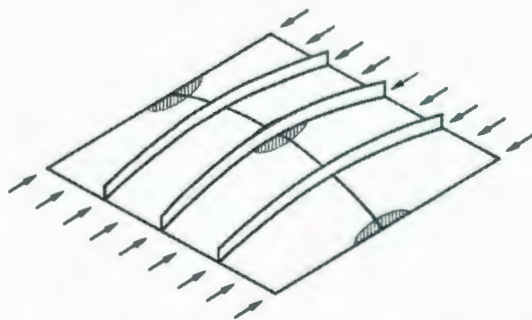


Figure 1.6.3: Failure mode I-1 (Paik & Thayamballi, 2003)

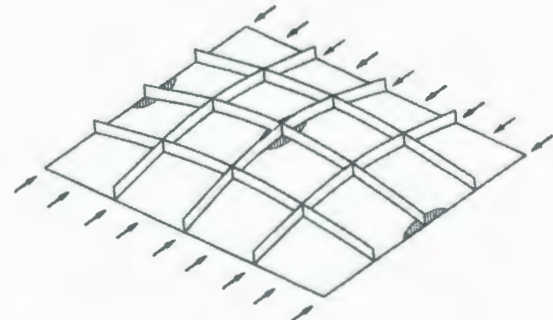


Figure 1.6.4: Failure mode I-2 (Paik & Thayamballi, 2003)

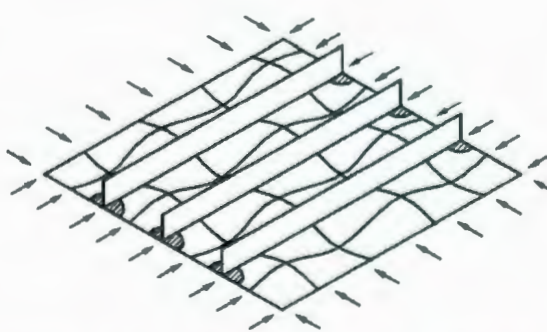


Figure 1.6.5: Failure mode II (Paik & Thayamballi, 2003)

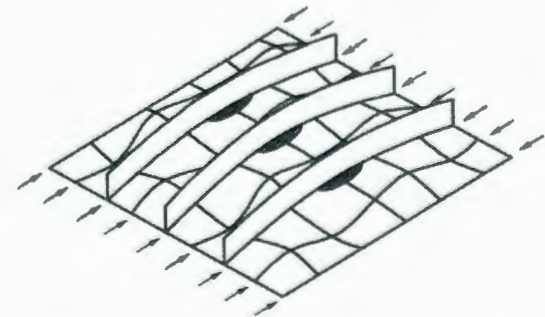


Figure 1.6.6: Failure mode III (Paik & Thayamballi, 2003)

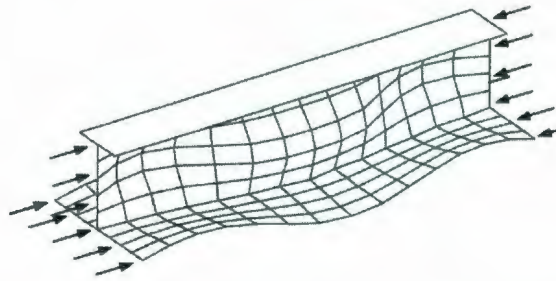


Figure 1.6.7: Failure mode IV (Paik & Thayamballi, 2003)

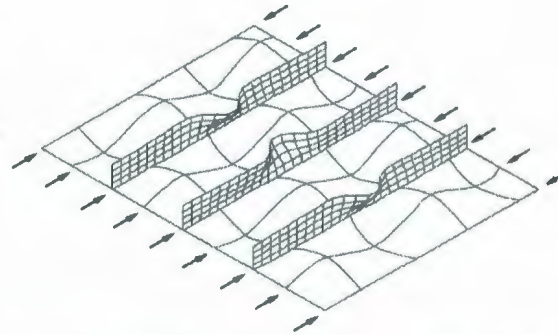


Figure 1.6.8: Failure mode V (Paik & Thayamballi, 2003)

Mode I failure occurs when the stiffeners are relatively weak. Mode I-1 is initiated by the beam-column type failure and Mode I-2 by orthotropic plate failure.

In Mode II, panel collapses due to yielding along the plate-stiffener intersection with no stiffener failure. This collapse mode typically occurs for panel subjected to predominantly biaxial compressive load and/or when the plating is stocky.

In Mode III, panel collapses due to yielding of the plate-stiffener combination at mid-span. Intermediate stiffeners (neither weak nor very strong) are susceptible to this failure mode.

Modes IV and V are stiffener induced failures due to high web slenderness and/or when the stiffener flange is inadequate to remain straight.

## **1.7 Scope of research**

The main objective of this research is to advance understanding of plastic behavior of stiffened plate subjected to ice loading. Plastic behavior is studied in terms of capacity of frame, flat bar stiffener stability and load sharing within a grillage.

The structural response beyond the elastic range is quite different for various stiffener forms and often extension of conventional wisdom results in wrong conclusions. One simple example is the T stiffener, which is the best choice in elastic design due to its high section modulus to weight ratio; whereas the plastic response can be inferior due to its tendency to fail by web local buckling resulting in sudden drop in capacity.

There are no analytical solutions currently available which represent the complete plastic response of a stiffened plate considering all possible failure modes. The plastic formulations that do exist make specific assumptions as to the type of plastic mechanisms. The choices available to study plastic response are either to do a full scale physical test or a non-linear finite element analysis.

Full scale testing is undoubtedly the best method, but the high cost of fabricating test specimen, complexities involved in accurately measuring the responses and the time required to conduct each experiment limits the number of experiments that can be practically conducted.

Finite element analysis is a fast and economic alternative compared to full scale test, but estimating non-linear response using FEA is still in its developing stages. The results from a FEA can only be used after proper validation. Hence the best option to study the non-linear response is to do a full scale experiment and validate the FE analysis results in terms of the element type, loading and solution strategy. The validated FE model can then be used to further explore the design space, within certain boundaries. By conducting more full scale experiments and validating them, the whole design space can be covered.

### 1.7.1 Validation of large grillage experiment

The first section of this report presents the finite element validation of a full scale test conducted in laboratory. The validation is done to assess the suitability of using finite element method in estimating plastic response of stiffened plate.

The results of the analysis in terms of capacity and deformation were compared using various types of finite elements – shell and solid elements. The validation also studied the effect of element size, load steps, iterative solution scheme etc. in achieving solution convergence.

The lessons learned from the validation study are used as the basis of other finite element studies carried out as part of this research.

### 1.7.2 Load sharing in a grillage

Ship structure has been traditionally designed as single frames. The main reason for considering the structure as single frames is the simplicity it offers for hand calculations.

The introduction of computers into structural design and advancements in finite element method has made it possible the analysis of complex structures like that of a ship.

The symmetric boundary condition takes care of the support provided by the adjacent structure when the loading is symmetric. In case of ice loading, which is non-symmetric, the symmetric boundary condition may not accurately represent the true structural behavior. The study explores the difference in load carrying capacity when the single frame is in isolation and when it is a part of a grillage, subjected to an unsymmetrical loading.

The study also examines the difference in behavior for various stiffener forms like flat bar and T stiffener.

### 1.7.3 Parametric study of capacity

The capacity of a stiffened plate depends on many factors – geometric, material, loading type etc. The current design rules have limited range of application and in some cases underestimate capacity.

The total number of factors affecting capacity of a frame is identified as ten - eight geometric factors and two material properties. To study these ten factors even at two levels (at high and low values of each factor) will require 1,024 ( $2^{10}$ ) FE analyses. Considering an average solution time of five hours per analysis, the total time and effort required to carry out such an exercise will become enormous thereby making it practically impossible.

Design of Experiments (DOE) offers an efficient method by which multi-factored systems can be studied using lesser number of experiments. DOE is used to systematically combine the ten factors and the effect of all factors and their interactions are found by only 77 FEA runs. The results from these FEA runs are used as input to DOE to find a regression equation for predicting capacity.

The outcome of the study is a regression equation for estimating capacity which depends on main factors and their interactions. The regression equation can be used for estimation of capacity. Validation of the regression equation has also been carried out.

#### 1.7.4 Stability of flat bar stiffener

Current design rules limit the maximum allowable web height to thickness ( $h_w/t_w$ ) ratio of various stiffener forms to avoid local buckling failure. The  $h_w/t_w$  ratios are very conservative in the case of a flat bar stiffener. The conservative estimation of  $h_w/t_w$  limits the use of flat bar stiffeners and requires the use of other stiffeners forms like L or T instead; which will increase welding and hence increase the fabrication time and cost.

The main factor hindering the wider use of flat bar is the  $h_w/t_w$  limit; hence a study was carried out to check the possibility of increasing the rule limits.

The total number of factors which influence stability of a flat bar stiffener is identified as six - four geometric factors and two material properties. The study of these six factors at two levels (at high and low values of each factor) will result in 64 ( $2^6$ ) possible combinations. Each combination requires an average of five trials to find the maximum allowable web height, making a total of 320 FEA analyses. Considering an average

solution time of ten hour per analysis, the total time and effort required to carry out such an exercise would become enormous thereby making it practically impossible.

Combining DOE and FEM, new regression equations for estimating web height and web height to thickness ratio are formulated. Validation of the regression models is also done.

## 2 FEM VALIDATION OF LARGE GRILLAGE EXPERIMENT

### 2.1 Introduction

The large grillage experiment was carried out as part of the ongoing “comprehensive study of the ultimate strength of ships frames” project, funded by Transport Canada, US Coast Guard and the US-Canada Ship Structures Committee. The intent of the experimental program was to study plastic behavior of ship frames and validate limit state equations developed for the new IACS Unified Requirements for Polar Ship Construction.

The experimental project started with the full scale testing of a series of single frames with various stiffener forms. The next stage of the project was testing of small grillage and finally the large grillage.

Ships structure consists of plate stiffened in orthogonal directions by stiffeners, also known as a grillage structure. The stiffened plate structure can be classified as Single Frame (Figure 2.1.1), Small Grillage (Figure 2.1.2) and Large Grillage (Figure 2.1.3) based on the structure considered as representative model for the whole grillage structure.



Figure 2.1.1: Single frame

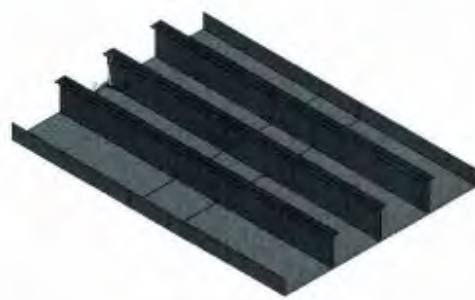


Figure 2.1.2: Small grillage

A single frame considers a stiffener with the attached shell plating as a representative model of the entire grillage structure. The web and flange of a stiffener is free to move both vertically and horizontally whereas the shell plate is restricted to move sideways due to the presence of adjacent structure. The symmetric boundary condition simulates the

support condition provided by adjacent side structure. The single frame idealizes the structure considered in design rules.

The small grillage consists of structure between two transverse stringers. The inclusion of adjacent side structures simulates the actual side boundary conditions for the middle stiffener. The two longitudinal ends are fixed to represent the boundary condition provided by heavy transverse frames in a ship structure.

A large grillage can be considered as structure within three frame spans in the longitudinal direction. At each span, a heavy transverse frame is provided which gives the necessary support at that location. The transverse frames ends and the two longitudinal ends of the large grillage are fixed. Since the points of fixities are far away from the point of application of load, these boundary conditions have no significant effect on response of the center frame. Thus in the large grillage both side and longitudinal boundary conditions of the center frame are considered to be an accurate representation of a real ships structure.



Figure 2.1.3: Large grillage

## 2.2 Large grillage experiment

Figure 2.2.1 presents the general arrangement of the large grillage used for the laboratory test.

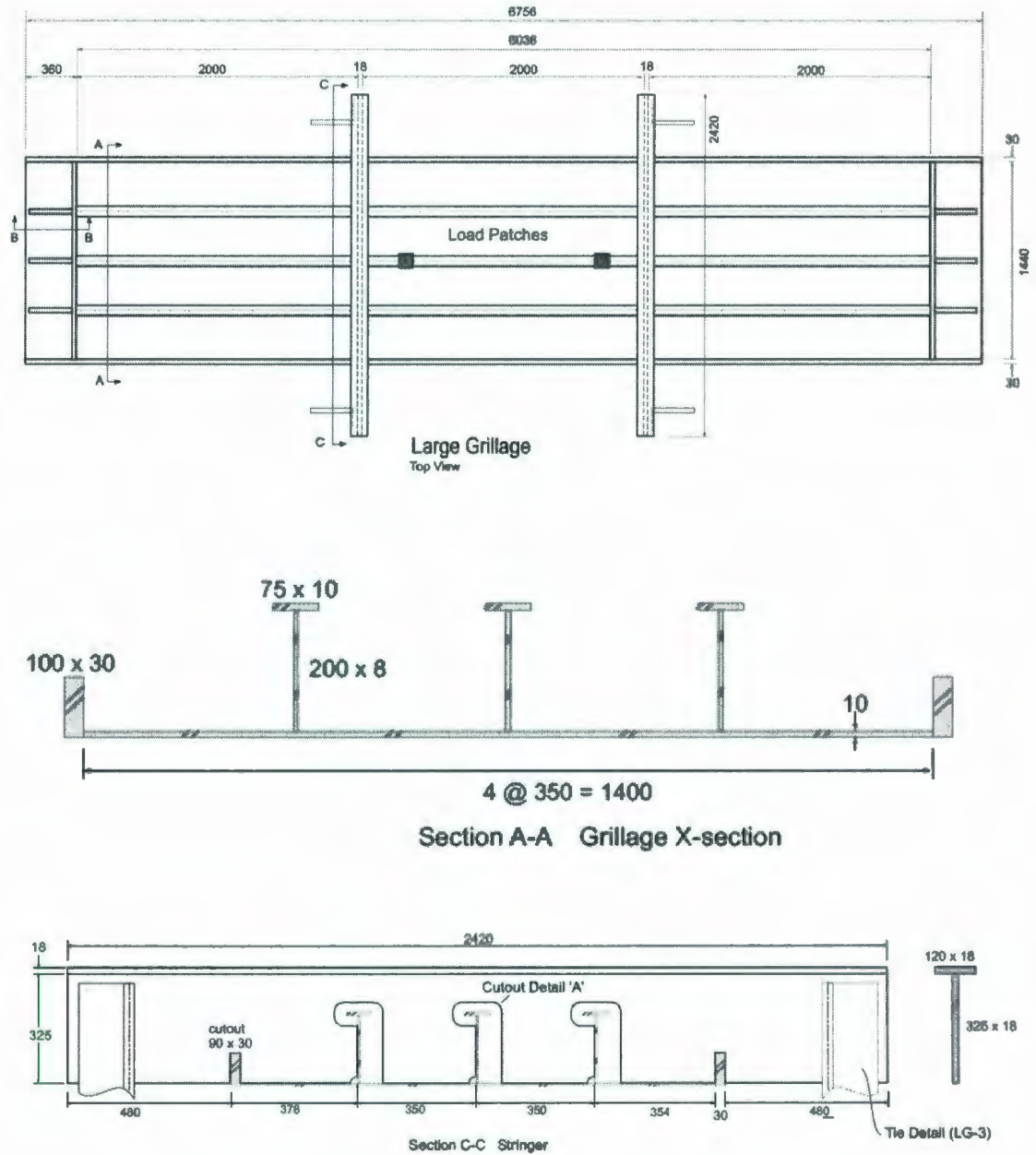


Figure 2.2.1: General arrangement of large grillage

### 2.2.1 Large grillage geometry

The large grillage structure consisted of shell plate stiffened by T stiffeners longitudinally and stringers running in the transverse direction. Thicker longitudinal stiffeners were provided on the two edges to simulate the support provided by nearby structure which are not included. The stringers consisted of T stiffeners which were heavier and deeper than the longitudinal stiffeners. The structure represents a full scale physical model of the side or bottom of a longitudinally framed ice class vessel.

### 2.2.2 Loading scheme

The grillage was loaded with a concentrated force at a small area to simulate ice load acting on the ship hull. The loading was applied at two locations within the middle bay in succession. The first load was applied 450 mm away from one of the stringers. The loading was withdrawn and the structure was allowed to relax. The second load was applied at 450 mm away from the other stringer.

A hydraulic cylinder was used to apply the required load. A thick rectangular steel block (130mm\*130mm) was placed between the cylinder head and frame, so that force is only applied on a very small area representing the peak pressure during an ice interaction.

The load was applied in steps and the measurements were recorded at each load step. The frame was loaded well into the plastic region until failure of plate or stiffener occurred.

The load was initially applied at load controlled steps. The material softens after it yields and hence it was expected to deform more as compared to the region before yielding for a given increment in load. Hence at the region near yielding, the load application was changed from load controlled to fixed increments in displacement.

### 2.2.3 Boundary conditions

The large grillage was bolted to the test bed in such a way that all displacements and rotations at the support locations are arrested. The boundary conditions are presented in Figure 2.2.2.



Figure 2.2.2: Large grillage on test bed (Daley & Hermanski, 2005)

#### 2.2.4 Results of experiment

The major responses recorded during experiment were the structural deformations and magnitude of applied load.

The deformations were measured using a Microscribe™ which had an accuracy of 0.2mm. The co-ordinates of pre defined points along the web and shell plate were recorded in each load step. The change in coordinate of each point gives the deformation of the structure. The processing of Microscribe data was done using Rhino™.

The overall force displacement behavior of the structure was obtained by combining the force and displacement data.

#### 2.2.4.1 Deformed shape

During the experiment, the web formed an arch resulting in local buckling. The un-deformed shape and deformed shape of the stiffener at the maximum load is given in Figure 2.2.3.

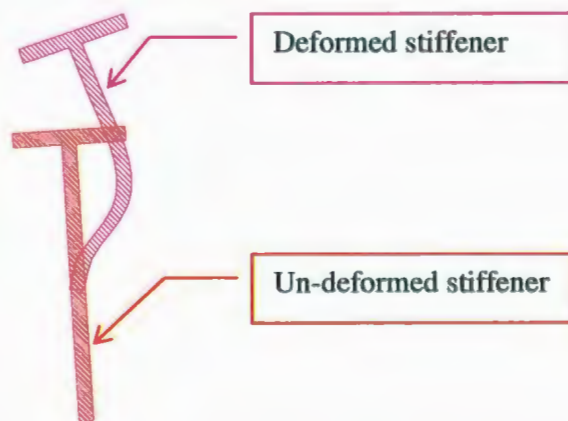


Figure 2.2.3: Un-deformed and deformed stiffener during full scale experiment

#### 2.2.4.2 Load vs. displacement

The load-displacement result of the large grillage experiment is presented in Figure 2.2.4. The displacement is measured at the centre of the hydraulic ram.

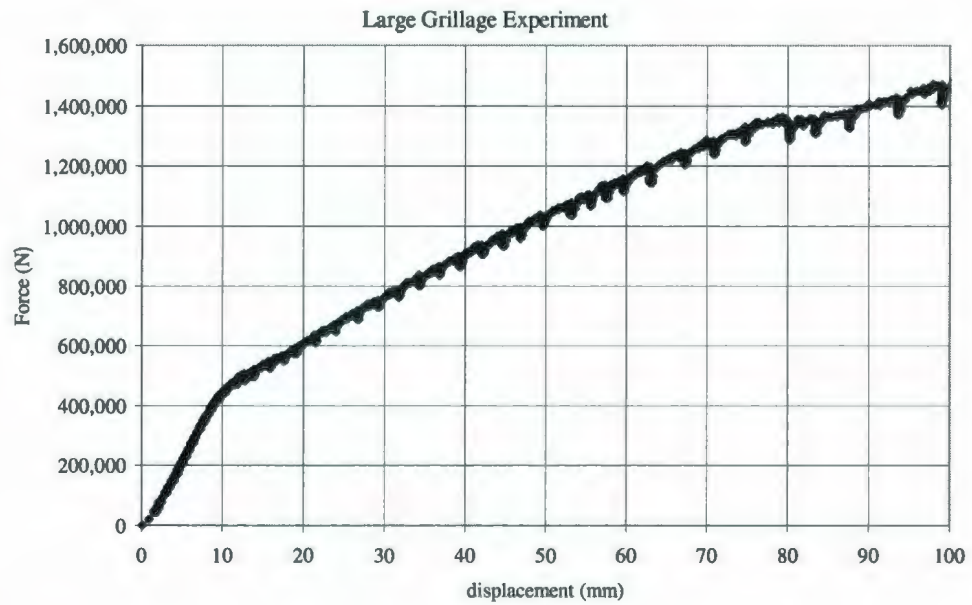


Figure 2.2.4: Load vs. Deflection of full scale experiment

### **2.3 ANSYS non-linear analysis**

ANSYS is one of the leading finite element programs used by industry and research organizations. ANSYS is capable of solving a wide range of engineering problems including structural, CFD, thermal, acoustic, electromagnetic as well as coupled physical problems like fluid-structural interaction, thermal stress analysis etc.

The ANSYS suite of finite element programs includes pre-processor for modeling complex shapes, solvers and post processors for viewing results. For complicated three dimensional solid structures, ANSYS offers an option to import geometry from other CAD software like Pro/E, such that nodes and elements can be directly generated within the imported geometric boundaries. ANSYS also supports modeling using GUI as well as using an input data file. The modeling using input data file utilizes ANSYS Parametric Design Language (APDL) commands.

APDL allows building of a finite element model using commands instead of GUI functions. Geometry, material property, boundary conditions, loading, solution options etc. are specified as parameters. APDL is suitable in situations where a series of finite element runs are required by changing parameters (for example; to study the effect of material yield, when geometry remains the same). A re-run of a FE model can be easily carried out by just changing the required parameter (rather than complete remodeling from scratch) and rerunning the modified input data file. APDL also includes standard programming functions (like macros, do loops, algebraic operations, get functions) to create a complete programming environment within ANSYS.

The basic steps involved in a non-linear finite element analysis using ANSYS are presented in Figure 2.3.1.

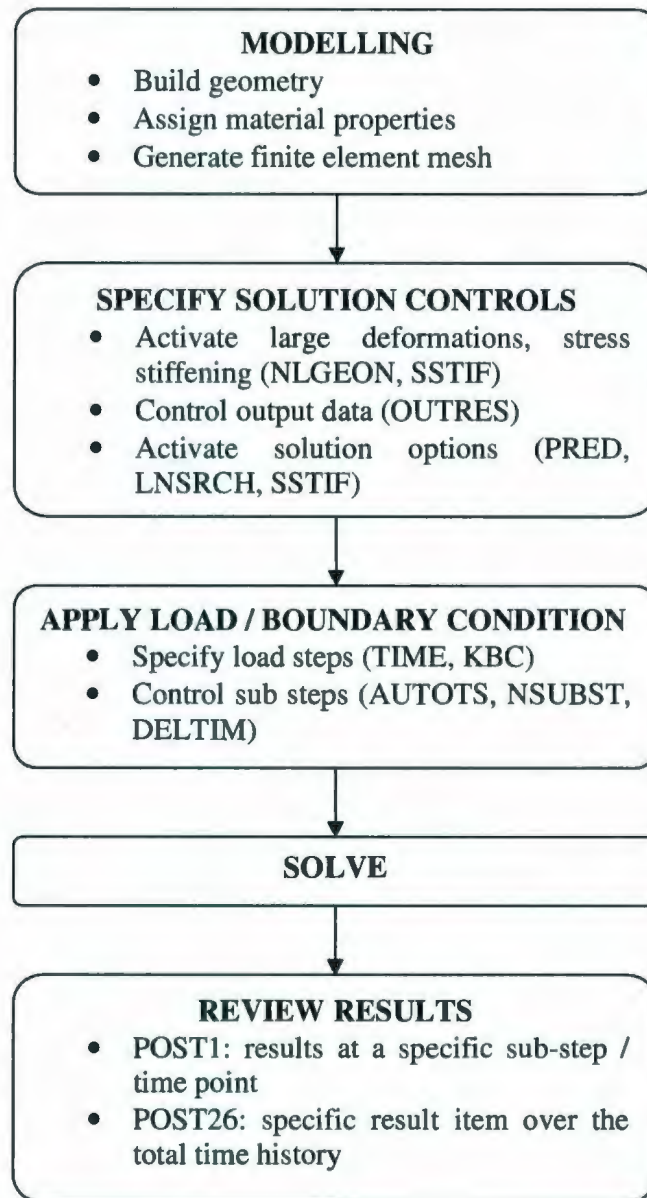


Figure 2.3.1: Flowchart of ANSYS non-linear analysis

### 2.3.1 Types of nonlinearities

There are different kinds of structural nonlinearities which are supported by ANSYS – geometric, material and boundary condition. All these nonlinearities types were present in the large grillage FE analysis.

#### 2.3.1.1 Geometric nonlinearity

For a linear analysis, the stiffness matrix is assumed to be a constant. When the structure undergoes large deformations, the stiffness matrix changes with deformation and needs to be recalculated in each load step. The governing equations are nonlinear with respect to displacement and an iterative scheme is used for solution. The most common method adopted for the iterative solution is Newton-Raphson method.

Another type of geometric non-linearity supported by ANSYS is the stress stiffening. Stress stiffening occurs in thin and highly stressed structures (like cable and membrane); whereby the out of plane stiffness is significantly affected by the state of in plane stress.

#### 2.3.1.2 Material nonlinearity

The stress-strain relationship of steel has four distinct stages:

- Linear stress strain relation up to the yield stress
- Material instability / bifurcation
- Transition to localized deformation
- Accumulation of damage resulting in fracture.

The stress-strain curve has an initial slope equivalent to the Young's Modulus (E) of the material, beyond which the material behaves non-linearly. Even though the plastic region is non-linear, it is approximated as linear with a slope equivalent to Post Yield Modulus.

#### 2.3.1.3 Boundary condition nonlinearity

In the boundary condition nonlinearity, the boundary condition is not fixed and changes during the analysis. The most common example is the contact problem, wherein there are two separate objects at the start of analysis and contact happen when the two objects

come close together. Depending on the relative stiffness of the two materials, one or both of the objects get deformed.

In the preset validation study, the response of the frame after the second indentation is compared. At the start of the analysis, there are three separate structures – frame and two indenters. The frame is loaded by the first indenter and then withdrawn. The frame is allowed to redistribute the residual stresses. The damaged frame is loaded by the second indenter at a different location. This requires the use of contact elements in the analysis.

ANSYS supports different classes of contact namely rigid-to-flexible and flexible-to-flexible. Within these classes, there are different types of contact models possible: node-to-node, node-to-surface, surface-to-surface and line-to-line.

Contact between two surfaces requires definition of a ‘contact pair’ – ‘target surface’ and ‘contact surface’. For a rigid-to-flexible contact, the target surface is the rigid surface and the contact surface is the deformable surface.

### 2.3.2 Solution options

The various iterative solution schemes available in ANSYS are:

- Newton-Raphson (default)
- Newton-Raphson with adaptive descent
- Arc-length method: this method is specifically useful in situations where there is large deformation at same load (eg: buckling)

Newton-Raphson method starts with an initial guess about the unknown displacement. The stiffness of the structure is computed based on its initial condition. Displacement is calculated for the applied loading and estimated stiffness. Based on the estimated displacement internal element forces (Newton-Raphson forces) are calculated and compared to the applied load. The difference between the applied load and internal element load is called the residual force. Convergence is achieved if the residual forces are within permitted values. If the residual forces are large, ANSYS uses the current

displacement to calculate new stiffness in the deformed position, and repeats the above procedure until the residuals are within permitted values (or convergence is achieved).

ANSYS offers features which enhances the convergence of a solution. Some of the features available in ANSYS are:

- Line search
- Automatic load stepping
- Bisection

### 2.3.3 Solution convergence

Non-linear analysis usually encounters convergence problems. The finite element modeling of the structure incorporates following techniques to achieve easier convergence:

The model is refined at the probable regions of large deformations like the vicinity of the load application. This has been achieved in two ways depending upon the type of element used –

- by defining separate areas
- by refining the mesh within certain boundaries

The shell element model was generated using areas. Separate areas are defined for regions requiring refinement. Larger element sizes are used to mesh regions of small deformations and smaller element sizes are used to mesh regions of large deformations. The method results in a very clean mesh and optimizes the number of nodes and elements. The main disadvantage of this method is the large number of key points, lines and areas required to create separate areas which can become cumbersome.

The solid element model was generated by extruding a section along an axis. Large elements were used to mesh the whole structure. The finite element model was then refined within the required boundaries.

The total load was applied in steps and solution for each load step was found successively. The load stepping forces the program to find solutions at intermediate load stages thereby avoiding large increments of load steps between solutions, which might result in convergence issues. Within each load step, a large number of sub-steps were used, so that the load was increased gradually.

The default iterative scheme of Newton-Raphson was used for solving simultaneous non-linear equations. Other iterative schemes were only tried once Newton-Raphson failed to converge. Solution enhancement features like line search, bisection and automatic load stepping were used as permitted by the selected iterative scheme.

## **2.4 Finite element analysis of large grillage**

### **2.4.1 Structural modeling**

There are two different methods for generating finite element model using ANSYS - bottom up and top down.

In bottom up method, the lowest order entities are first created, which are then combined to form higher order entities. For example, for modeling a solid cube structure, first key points are defined at the vertices. These key points are joined to create lines defining the edges. Lines are joined to form an area which represents each face. A volume is defined by combining all the faces.

In top-down solid modeling, geometric 'primitive' which describe the model (like line, area, volume etc) is first defined. Definition of a higher order primitive automatically generates the lower order primitives associated with it. ANSYS library contains both two dimensional (e.g., rectangle, circle, polygon) and three dimensional (e.g., block, cylinder, prism, sphere, cone, torus) primitives. Complex shaped are formed by Boolean operation (adding, subtracting etc) of one primitive on another.

Once the geometry is defined, controls are specified about the size and desired shape of elements to be generated. ANSYS automatically generates elements and nodes based on the controls within the specified geometry.

### **2.4.2 Finite elements**

ANSYS offers a wide variety of elements appropriate for non-linear structural analysis. The main two classes of structural elements suitable to model three dimensional structures are the shell and solid elements. Both shell and solid elements support plasticity and hence separate analyses were carried out and the results were compared with the experimental results.

#### **2.4.2.1 Shell 181 element**

The Shell 181 finite element (Figure 2.4.1) was chosen due to its suitability to model thin to moderately thick shell structures. The 4-node element has six degrees of freedom at

each node - translations in the x, y and z directions, and rotations about the x, y and z-axes.

SHELL 181 is well suited for linear, large rotation, and/or large strain nonlinear applications. Change in shell thickness is accounted for in nonlinear analyses. In the element domain, both full and reduced integration schemes are supported.

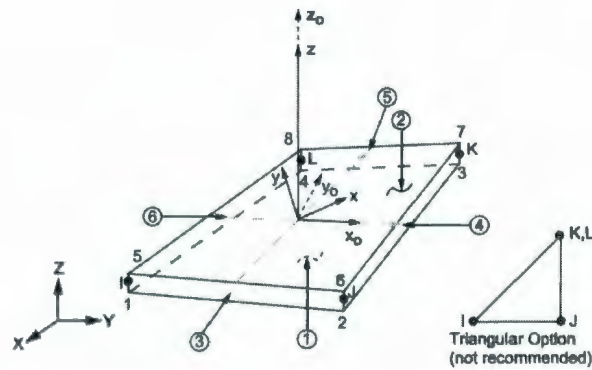


Figure 2.4.1: Shell 181 geometry

#### 2.4.2.2 Solid 92 element

The solid 92 (Figure 2.4.2) is a 10-node element having three degrees of freedom per node - translations in the nodal x, y and z directions. Solid 92 element is capable of analyzing plasticity, creep, stress stiffening, large deflection, and large strain.

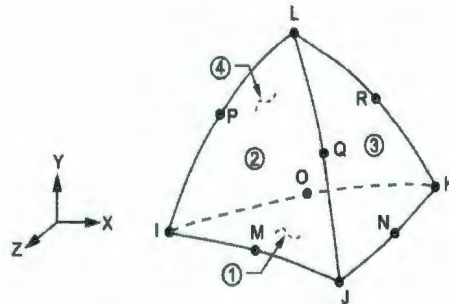


Figure 2.4.2: Solid 92 geometry

### 2.4.3 Material model

The material is considered as non-linear (Figure 2.4.3) for the analysis. The non-linear material property is idealized as bilinear with an initial slope of Young's Modulus until yield stress and with a slope of Post Yield Modulus afterwards.

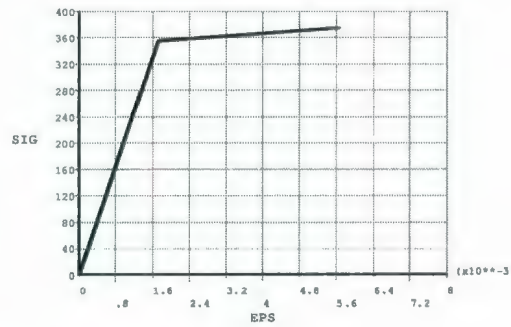


Figure 2.4.3: Non-linear material model

### 2.4.4 Boundary conditions

The large grillage was bolted to the test bed in such a way that all displacements and rotations at the support locations were arrested. This was implemented in the finite element model by specifying degree of freedom constraints for the nodes at the support locations. Boundary conditions considered for the analysis is presented in Figure 2.4.4.

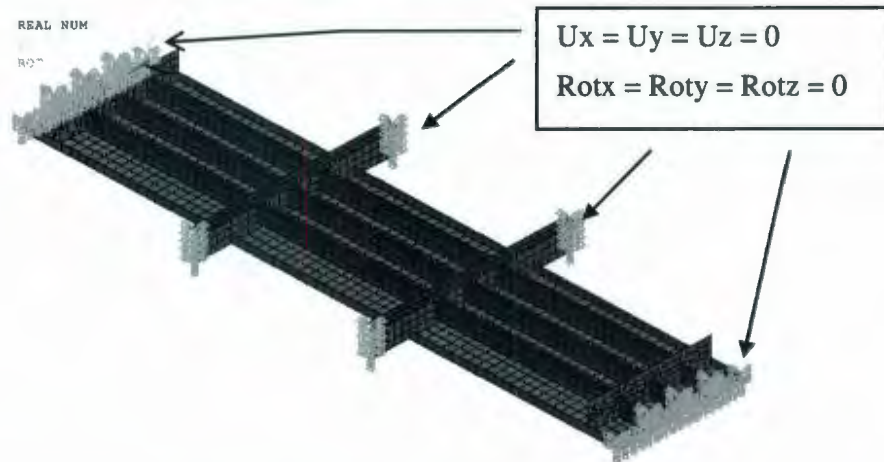


Figure 2.4.4: Boundary conditions of large grillage

### 2.4.5 Loading

A rigid indenter is used to deform the frame which simulates the loading from an ice collision. Both the rigid indenter and the flexible frame are modeled - the indenter being located at a short distance away from the frame. At the start of the analysis, the gap between indenter and frame is closed. The indenter is given a prescribed displacement equivalent to the hydraulic cylinder displacement during laboratory test. The progressive displacement of the indenter deforms the frame.

The locations of indenters relative to the large grillage are presented in Figure 2.4.5. The various steps involved in loading large grillage are presented in Figure 2.4.6.

The indenter is assumed to be rigid and the frame as flexible deformable body. Contact elements are used to model rigid-flexible contact. TARGE170 element is used to model target body (i.e., indenter) and CONTA174 element is used to model deformable body (i.e., grillage).

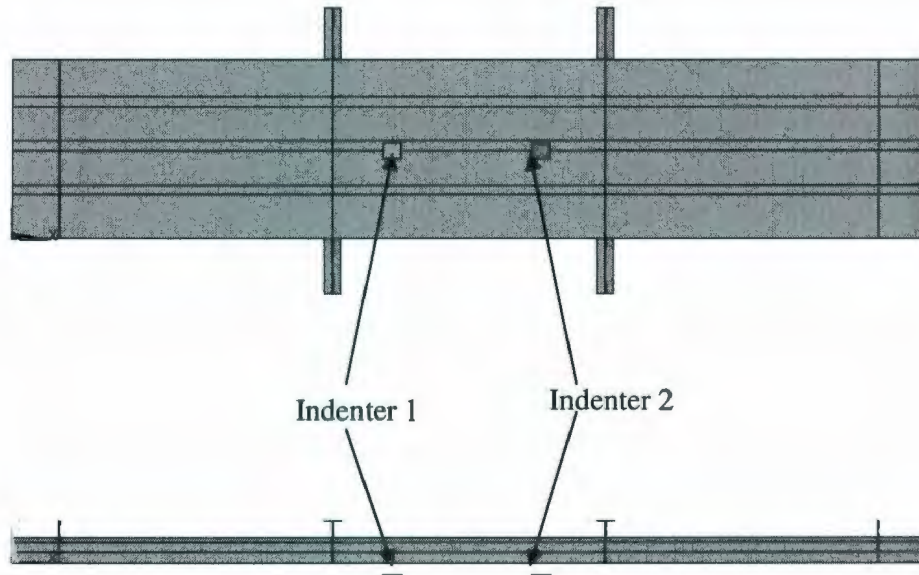
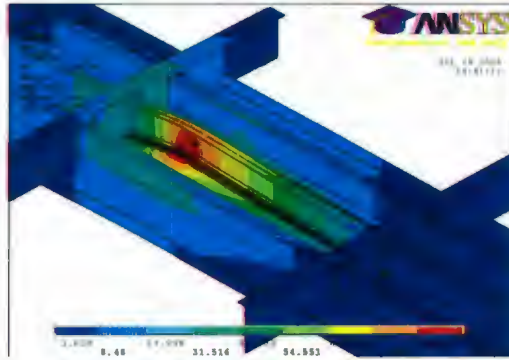
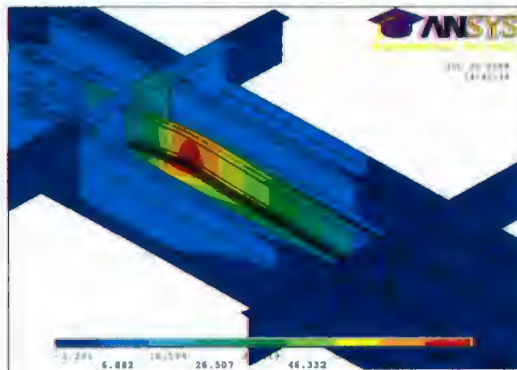


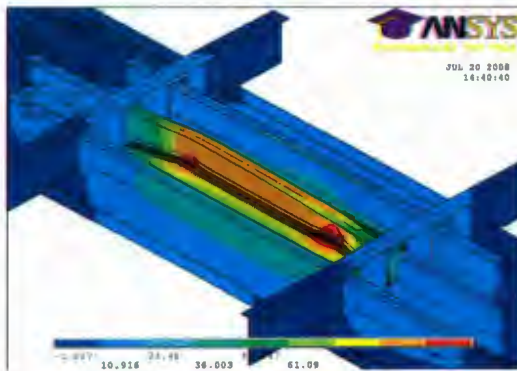
Figure 2.4.5: Plan (bottom view) and elevation of frame and indenters



Step 1: Grillage loaded by the first indenter



Step 2: First indenter withdrawn and the structure is allowed to redistribute residual stresses



Step 3: Grillage loaded by the second indenter

Figure 2.4.6: Load steps of large grillage experiment

#### 2.4.6 Solution

Both large deformations and stress stiffening were employed in the solution phase.

The reaction at the support nodes were summed up for each load sub-step, which is equal to the applied force at each sub-step.

## 2.5 Results of FE analysis using shell element

### 2.5.1 Comparison of capacity

Figure 2.5.1 presents the comparison of capacity between experimental results and ANSYS analysis using shell elements.

In the absence of mill certificate of the frame material, the analysis was carried out for a range of material property values – yield stress and post yield modulus. The closest match between the laboratory test and FEA was obtained for yield stress of 315 MPa and Post yield modulus of 1000 MPa.

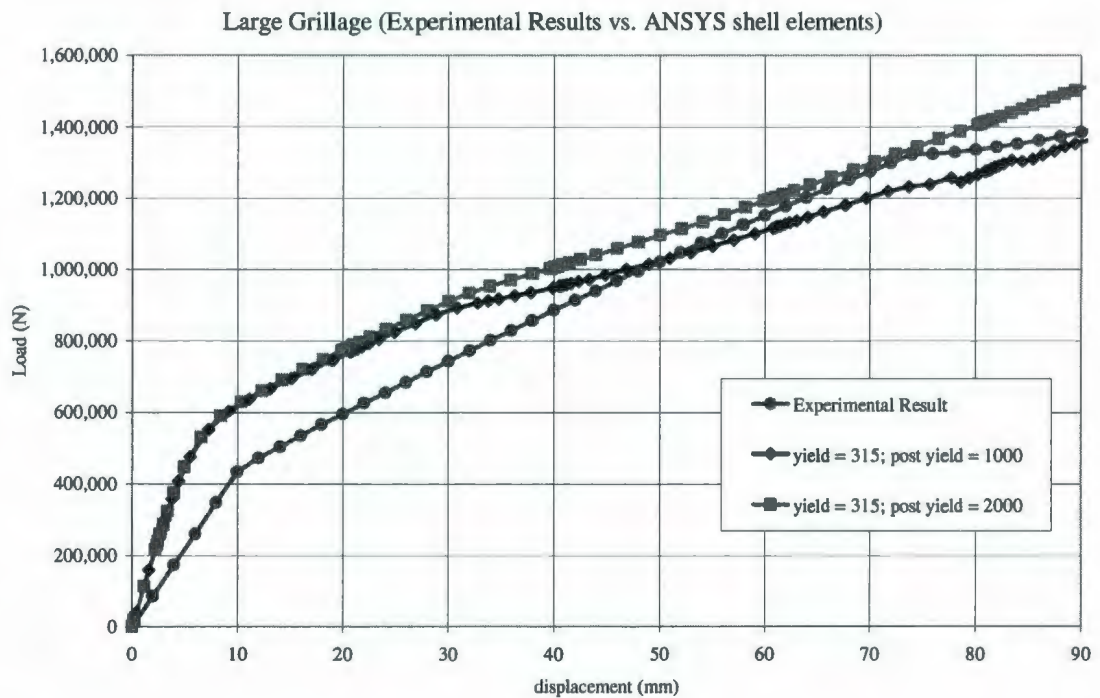


Figure 2.5.1: Comparison of capacity – experimental vs. shell elements

The load required to produce a displacement of 90mm (the maximum displacement in laboratory test) is marginally less for the 1000 MPa case, compared to 8% higher for the 2000 MPa case.

### 2.5.2 Comparison of deformed shape

Figure 2.5.2 presents the comparison of deformed shape between experimental results and ANSYS analysis using shell elements. The results of analysis using shell elements have shown that the deformations are not in good agreement with experimental results.

The shell elements tend to deform excessively, particularly at the intersection between web and shell plate. The high deformation might be due to non-inclusion of weld between web and shell which results in rotational stiffness at the joint lesser than actual values.

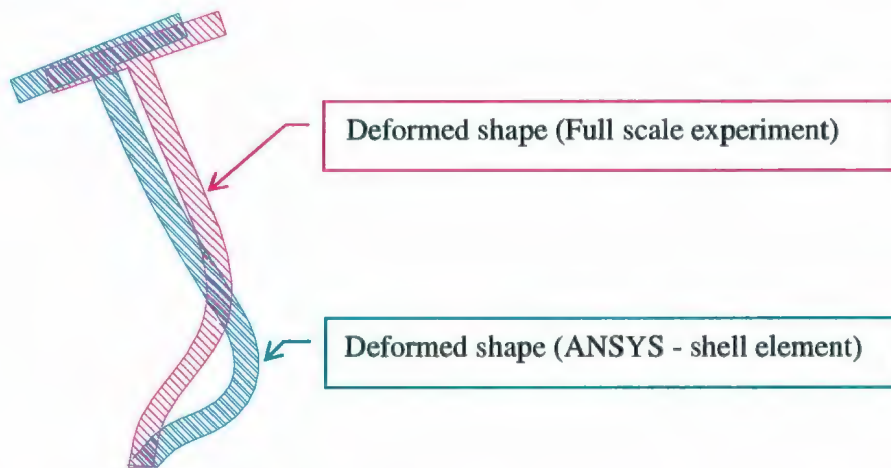


Figure 2.5.2: Comparison of deformed shape - experimental vs. shell elements

### 2.5.3 Modeling of weld

The analysis using shell elements was studied further to confirm whether the excessive deformation was due to absence of weld between web and shell plate.

The fillet welds at both sides of the web makes the web locally thicker than the web alone and hence provide additional rotational stiffness. In the finite element model the web at the intersection with the shell plate is weak due to absence of weld and hence can rotate excessively. It was anticipated that modeling of weld will provide the required rotational

stiffness to the joint connecting web and shell plate and will restrain the web from excessive deformation.

The weld was modeled using the following options:

- A thin plate (4mm) is used to connect web and shell.
- Rigid elements connecting web and shell
- Defining the intersection region (of web and shell) as rigid

#### 2.5.3.1 Thin plate modeled as weld

Modeling of the weld was accomplished by using a thin plate to connect the web and the shell plate, as shown in Figure 2.5.3.

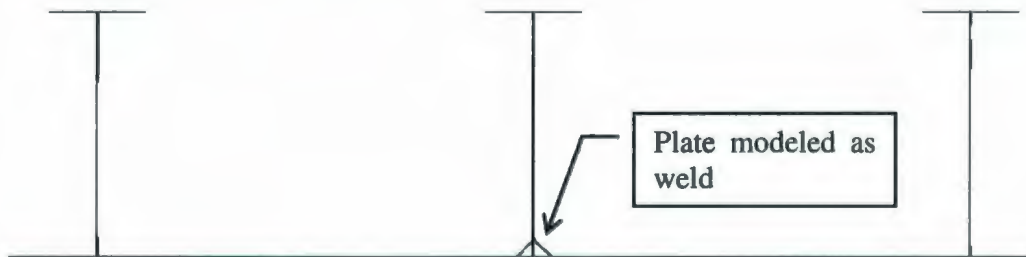


Figure 2.5.3: Modeling of weld using thin plate

Figure 2.5.4 presents the comparison of capacity between experimental results and ANSYS analysis using shell elements - with and without modeling weld. The results of analysis have shown that the load carrying capacity of the frame has marginally increased (around 7%) by including the weld.

Figure 2.5.5 presents the comparison of deformed shape between experimental results and ANSYS analysis using shell elements - with and without modeling weld. The results of the analysis have shown that excessive deformation in the case of shell element is prevented by modeling the weld.

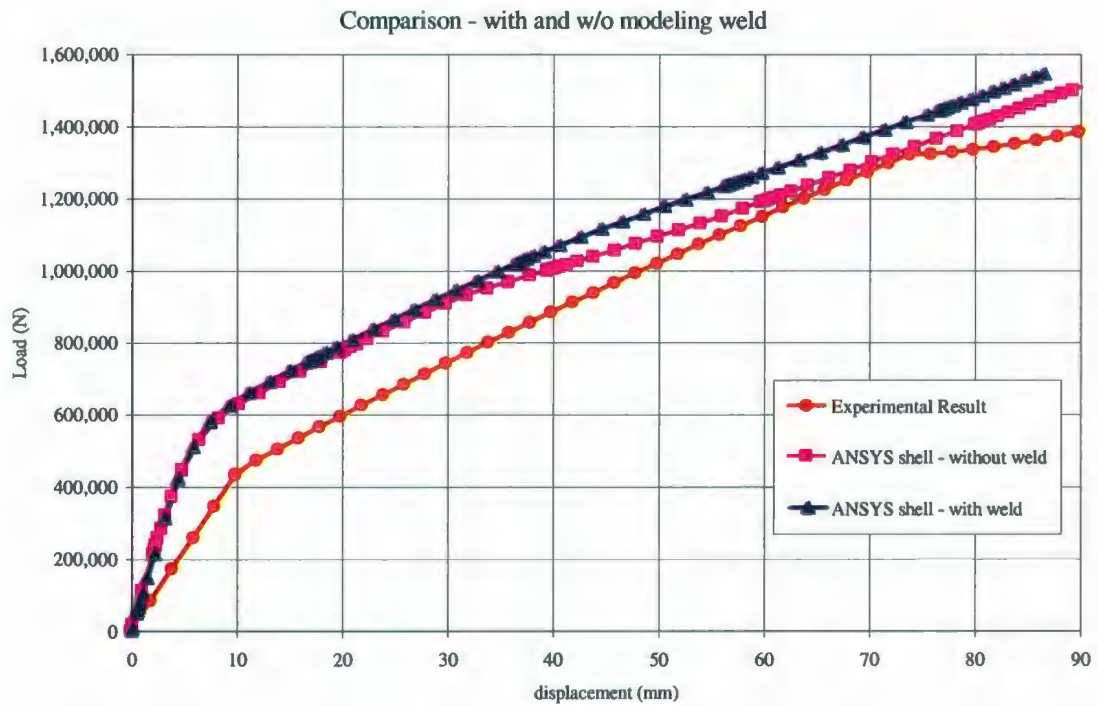


Figure 2.5.4: Comparison of capacity - experimental vs. shell with and w/o weld

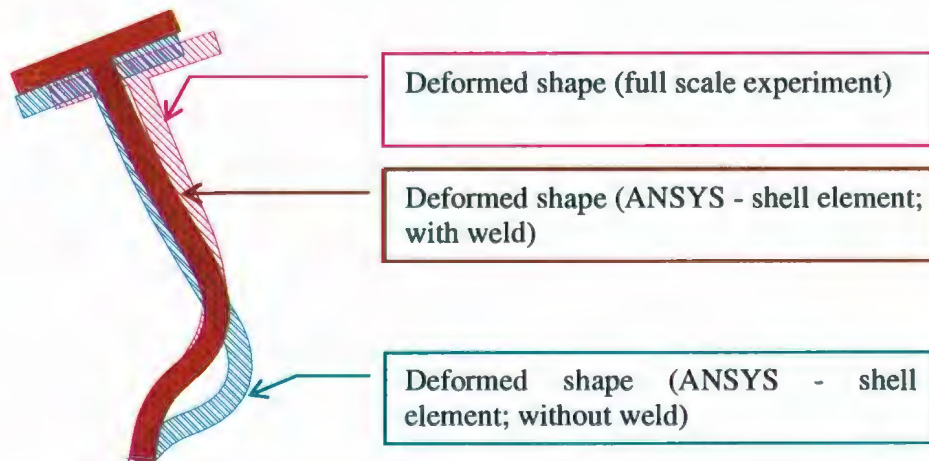


Figure 2.5.5: Comparison of deformed shape - experimental vs. shell with and without weld (weld modeled using plate elements)

### 2.5.3.2 Rigid elements connecting web and shell

Modeling of the weld was accomplished by using rigid elements to connect the web and the shell plate, as shown in Figure 2.5.6.

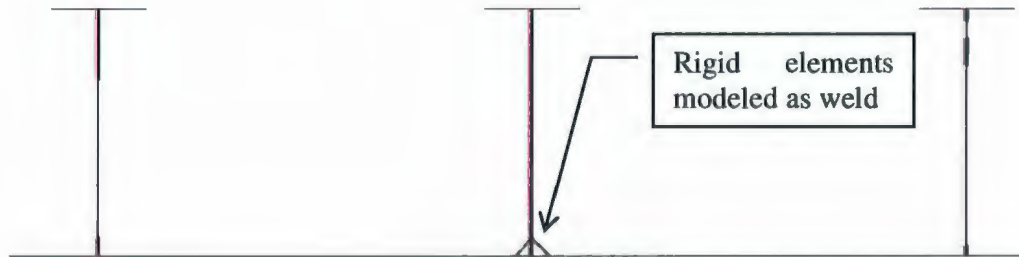


Figure 2.5.6: Modeling of weld using rigid elements

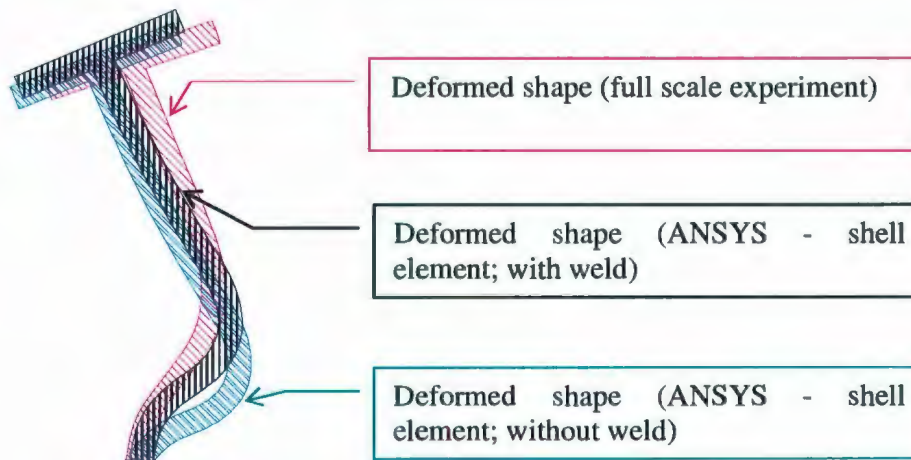


Figure 2.5.7: Comparison of deformed shape - experimental vs. shell with and without weld (weld modeled using rigid elements)

The results of the analysis have shown that excessive deformation in the case of shell element is prevented by modeling the weld, as shown in Figure 2.5.7.

## 2.6 Results of FE analysis using solid element

### 2.6.1 Comparison of capacity

Figure 2.6.1 presents the comparison of capacity between experimental results and ANSYS analysis using solid elements.

In the absence of mill certificate of the frame material, the analysis is carried out for a range of material property values – yield stress and post yield modulus. The closest match between the laboratory test and FEA is obtained for yield stress of 315 MPa and Post yield modulus of 1000 MPa.

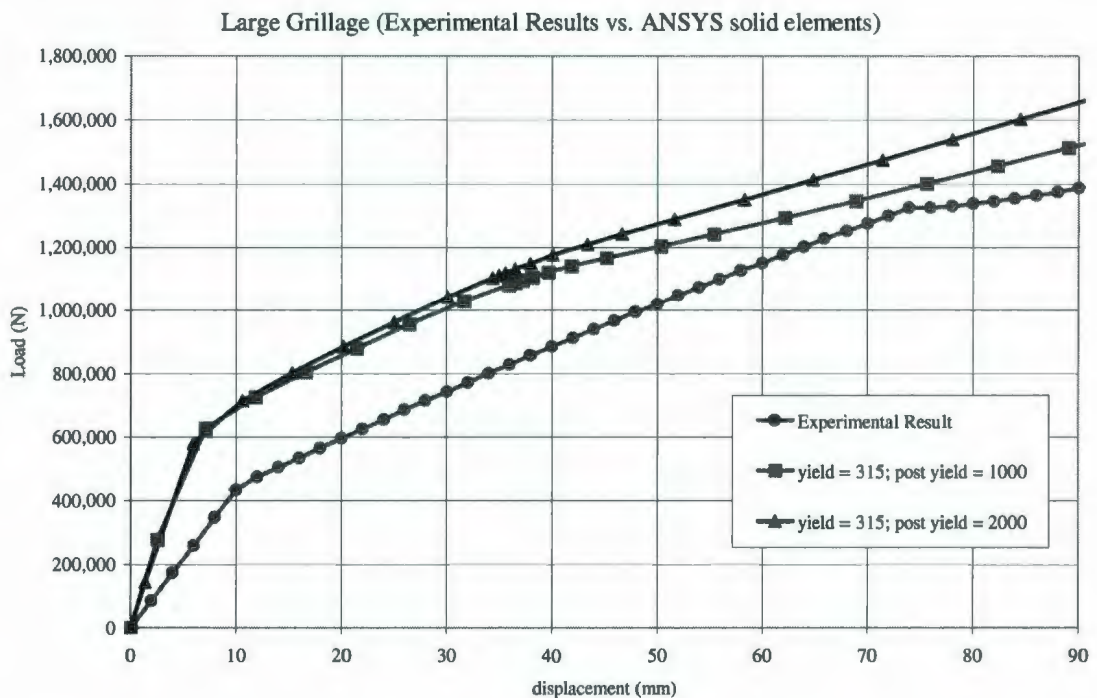


Figure 2.6.1: Comparison of capacity – experimental vs. solid elements

The load required to produce a displacement of 90mm (the maximum displacement in laboratory test) is 9% higher for the 1000 MPa case, compared to 20% higher for the 2000 MPa case.

### 2.6.2 Comparison of deformed shape

Figure 2.6.2 presents the comparison of deformed shape between experimental results and ANSYS analysis using solid elements.

The results of finite element analysis using solid element has shown similar deformation pattern as in the experimental result.

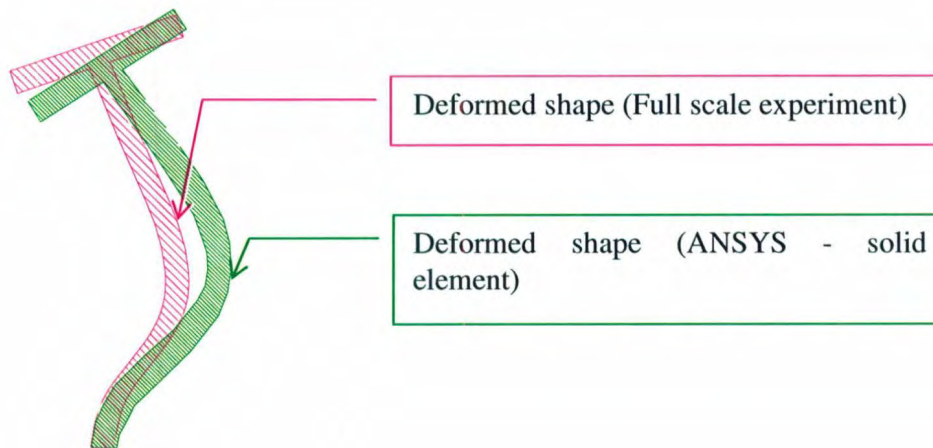


Figure 2.6.2: Comparison of deformed shape– experimental vs. solid elements

## 2.7 Comparison of shell and solid element

### 2.7.1 Capacity comparison

Figure 2.7.1 and 2.7.2 presents the comparison of the finite element analysis using shell and solid elements for a given set of material properties.

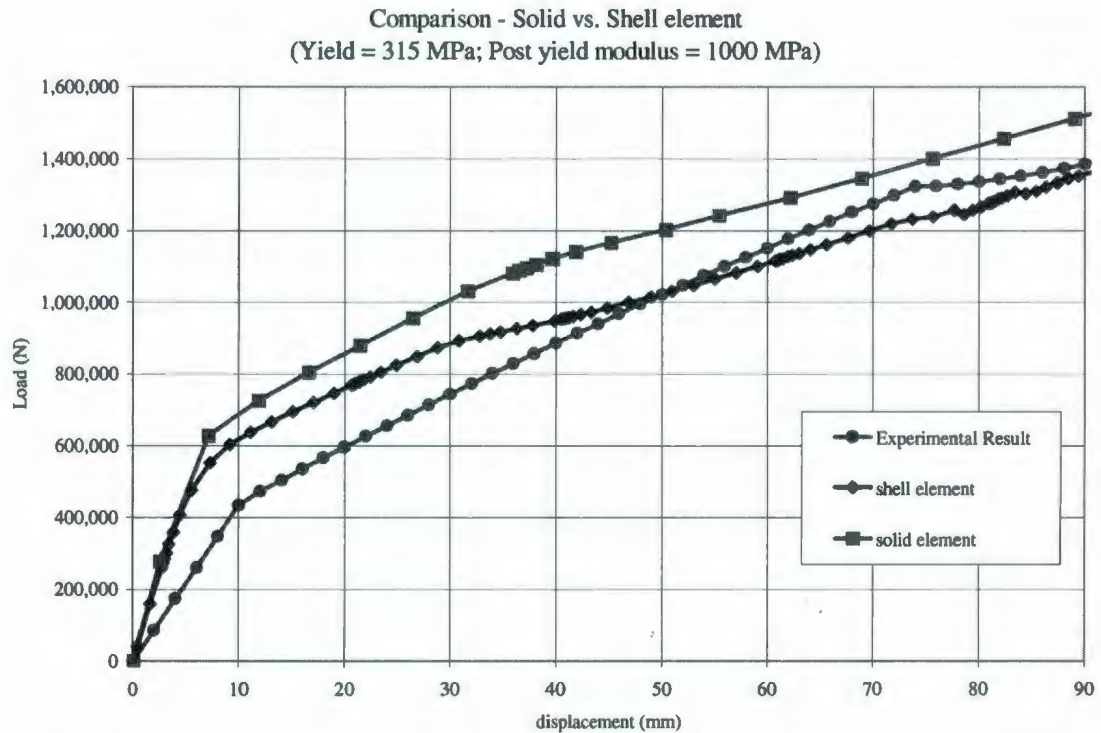


Figure 2.7.1: Comparison of capacity using shell and solid elements (yield stress = 315 MPa and post yield modulus = 1000 MPa)

The load required to produce a displacement of 90mm (the maximum displacement in laboratory test) is 11.7% higher for the solid element compared to shell element, for the 315 yield stress and 1000 MPa post yield modulus case (Figure 2.7.1).

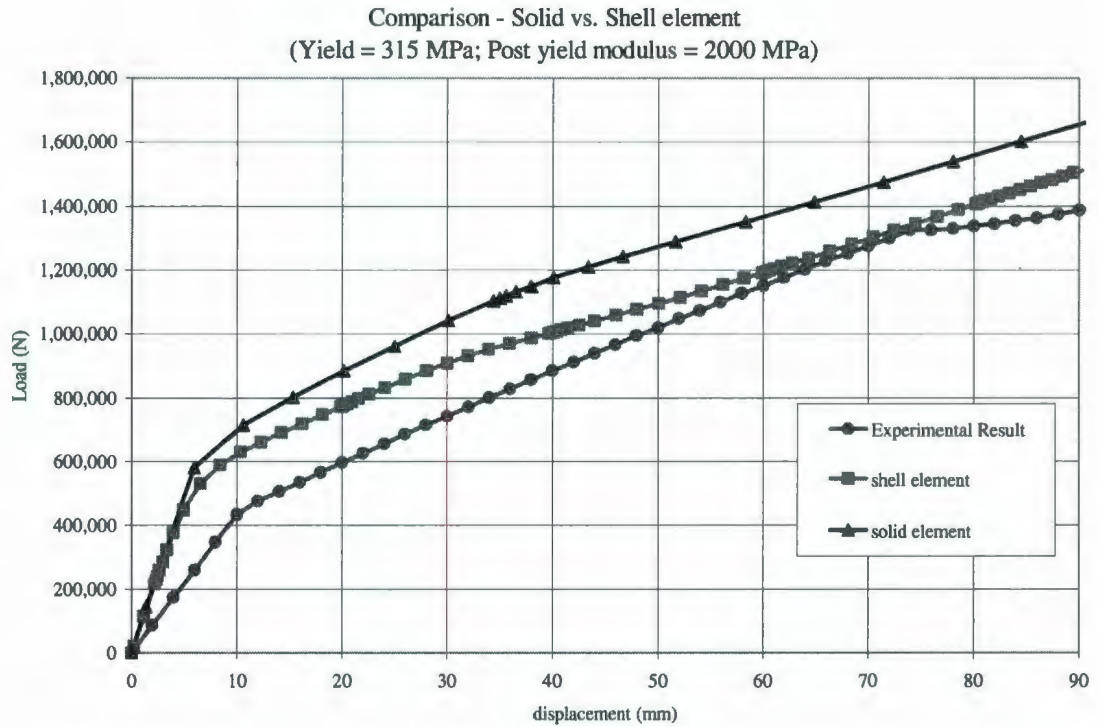


Figure 2.7.2: Comparison of capacity using shell and solid elements (yield stress = 315 MPa and post yield modulus = 2000 MPa)

The load required to produce a displacement of 90mm (the maximum displacement in laboratory test) is 10.6% higher for the solid element compared to shell element, for the 315 yield stress and 2000 MPa post yield modulus case (Figure 2.7.2).

The results of finite element analysis have shown that for a given set of material properties, the estimate of load carrying capacity using solid element is higher than that using shell element, so that shell elements give conservative results for design.

### 2.7.2 Deformed shape comparison

Figure 2.7.3 presents the deformation pattern comparison of the finite element analysis using shell and solid elements.

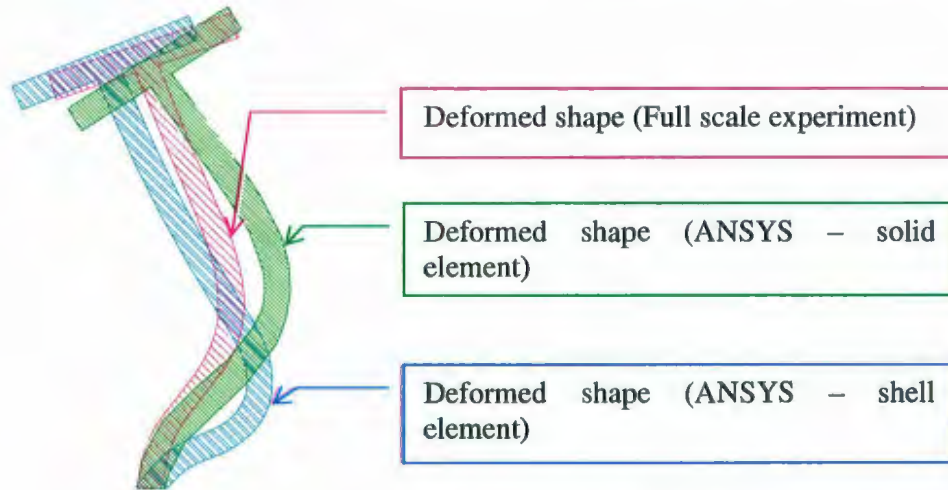


Figure 2.7.3: Comparison of deformed shape using shell and solid elements

The results of finite element analysis have shown that the deformation estimation using solid element is more realistic than that using shell element. Shell elements (without modeling of weld) showed excessive deformations particularly at the intersection of web and shell plate. The deformation results of shell element showed considerable improvement by modeling the weld.

## 2.8 Conclusions

The full scale laboratory test results were used to validate the finite element model. The lessons learned (in terms of element type, element sizes, iterative schemes etc) from the validation study were incorporated into the finite element models used for studying other topics of this research.

The results of analysis have shown that both shell and solid elements are suitable in estimating load carrying capacity of a frame. The deformations produced by the solid elements were similar to the experimental results. Shell elements (without modeling of weld) showed excessive deformations particularly at the intersection of web and shell plate. The deformation results of shell element showed considerable improvement by modeling the weld.

The choice of an element type is dependent on the type of problem being analyzed. For studying load carrying capacity, both shell and solid are suitable. The shell element however takes much lesser time for solution compared to solid element. For studying stability of stiffener web, which in turn depends on web deformation, the solid element is the better choice due to its greater accuracy in predicting deformation. Shell elements can also be used if the weld is modeled.

The time required to perform a non-linear analysis using solid elements is quite large compared to that using shell elements. Hence the number of elements should be kept to a minimum. This can be achieved by using larger element sizes at far regions and smaller elements near the point of application of load and the regions of large deformations.

The total load should be applied in steps and sub-steps should be used within each step to gradually increase the load. This makes sure that convergence is easily achieved. A large load increment step will require more iteration to converge and hence might not reduce the overall time required to achieve solution. An efficient method is to use default values so that the load increments are decided by ANSYS based on the physics of the problem.

ANSYS offers many iterative schemes for solving non-linear simultaneous equations. The most common and default method is the Newton-Raphson. Other schemes were only used once Newton-Raphson failed to converge.

ANSYS offers many convergence enhancement features like line search, automatic load stepping and bisection. These features reduces the time required for solution and hence were utilized whenever permitted by the iterative scheme used.

### **3 LOAD SHARING IN A GRILLAGE**

#### **3.1 Introduction**

Ship hull structure primarily consists of plate stiffened either longitudinally or transversely or a combination of both. In the case of longitudinal framing, the primary stiffeners run in the longitudinal direction. The stiffeners commonly used are flat bars, bulbs, angles and tees. The longitudinals are supported by heavy transverse frames running in the other direction.

The stiffened structure can be represented by a Single Frame, Small Grillage or a Large Grillage based on the structure considered as representative model for the whole grillage structure. Details of these structural representations are explained in Section 2.1.

Ship structure has been traditionally designed as single frames. A single frame can be considered as a representative model of the entire grillage structure when the loading is uniform. The symmetric boundary condition takes care of the support provided by the adjacent structure in a single frame. In case of ice loading - which is non-symmetric - the symmetric boundary condition may not accurately represent the true structural behavior. The main objective of the research is to study the difference in load carrying capacity when the single frame is in isolation and when it forms a part of a grillage, subjected to an unsymmetrical loading. The study further explores the behavior of various stiffener forms like flat bar and tee stiffener.

The study also verifies the accuracy of boundary conditions assumed in the cases of single frame, small grillage and large grillage. In a ship's structure, the web and flange of a stiffener are free to move both in vertical and horizontal direction. The shell plate is however restricted to move sideways due to the presence of adjacent structure. In a single frame, the support provided by adjacent side structure is simulated by symmetric boundary condition. In a small grillage, the side boundary conditions are incorporated by modeling the side structures rather than relying on the boundary condition. In a large grillage, both longitudinal and transverse boundary conditions are incorporated by modeling the longitudinal and transverse continuity in structure.

All the plating and stiffeners considered for the study satisfy the IACS requirements of polar class vessel.

### 3.2 Ice load

The ice pressure distribution on the vertical side of a ship is not uniform. The ice edges shear off and the pressure tends to concentrate to the center. As ice is crushed, rubble is formed. In the worst case scenario, solid ice presses through the ice rubble and makes direct contact with the structure. The ice exerts a concentrated high pressure on the structure, and the ice rubble exerts a relatively lower pressure on both sides. In this situation, the ice sheet is braced by the rubble, thus strengthening the ice sheet.

The ice pressure used in the study is based on the ice load proposed by Daley and Kendrick (2008). The ice loading is idealized as a distributed pressure load with a center peak, as shown in Figure 3.2.1.

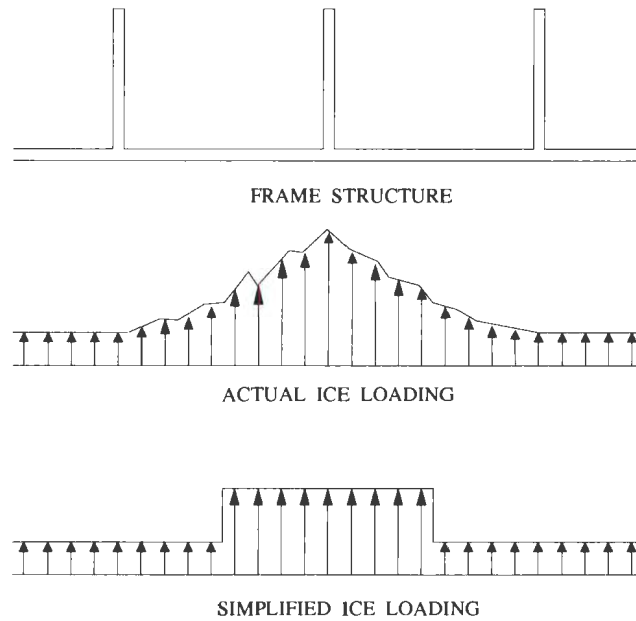


Figure 3.2.1: Frame, actual ice loading and simplified ice loading

The calculation of ice pressure distribution is included in Appendix A1. The ratio between the 'centre peak pressure' to the 'edge pressure' is calculated as 5.82 for a PC7 class vessel.

### **3.3 Single frame analysis**

#### **3.3.1 Structural model**

A single frame considers a stiffener with the attached shell plating as a representative model of the entire stiffened panel. The single frame idealizes the structure considered in design rules.

#### **3.3.2 Finite element model**

The Shell181 finite element was chosen due to its suitability to model thin to moderately thick shell structures.

For more details about the element, refer to Section 2.4.2.1.

#### **3.3.3 Material model**

Non-linear material behavior was considered for the analysis. The material was idealized as bilinear with linear strain hardening. The slope at elastic region was represented by Young's Modulus and the plastic region by Post Yield Modulus.

#### **3.3.4 Loading**

The pressure distribution during an ice structure interaction was considered for the analysis. The loading considered for the analysis is illustrated in Figure 3.3.1. For details of the pressure load, refer to Section 3.2.

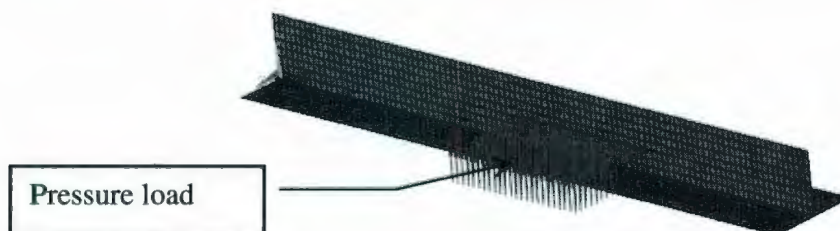


Figure 3.3.1: Loading considered for single frame analysis

### 3.3.5 Boundary conditions

Symmetric boundary conditions were applied at two transverse edges of the plate to simulate the supported provided by the neighboring structure. The two longitudinal ends were fixed to simulate the support provided by the continuing frame and transverse stringers. The boundary conditions considered for the analysis are presented in Figures 3.3.2 and 3.3.3.

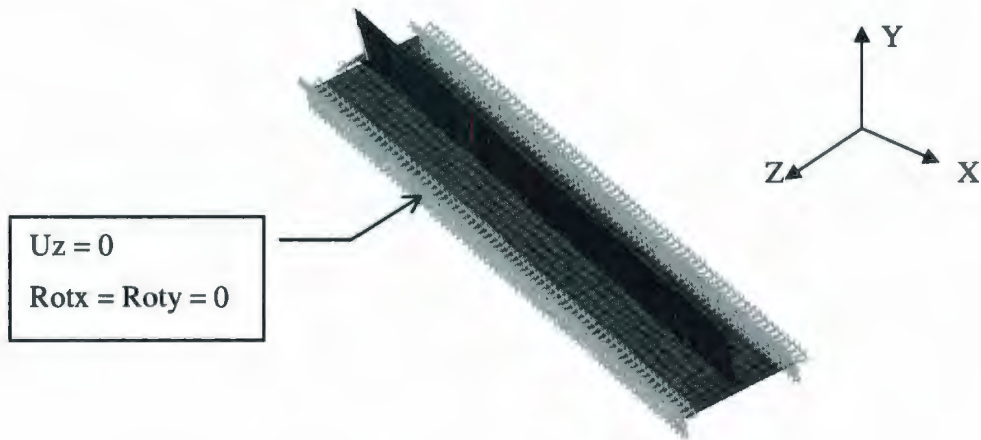


Figure 3.3.2: Symmetric boundary condition at transverse edges

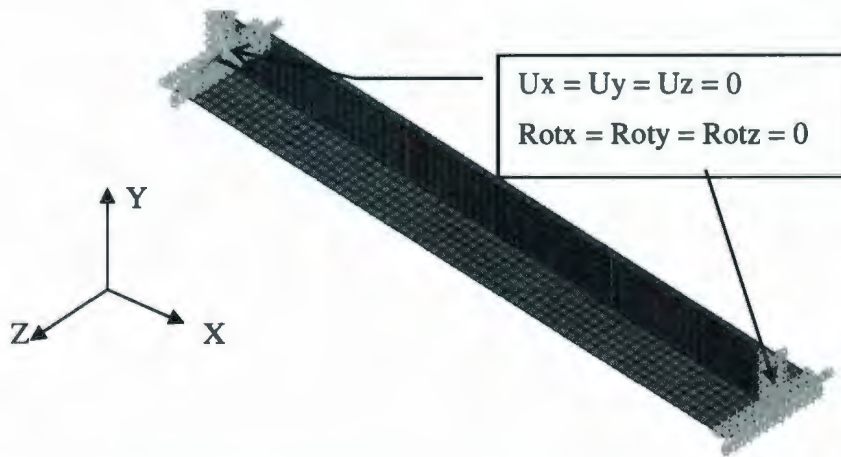


Figure 3.3.3: Fixed boundary condition at longitudinal ends

### 3.3.6 Solution process

A non-linear finite element analysis was carried out to find the response of the structure to the applied load. A detailed discussion about non-linear ANSYS solution process is presented in Section 2.3.

## 3.4 **Small grillage analysis**

### 3.4.1 Structural model

The small grillage consists of structure between two transverse stringers. The inclusion of adjacent side structures simulates the actual side boundary conditions for the middle stiffener. The two longitudinal ends were considered as fixed. However, the assumption of fixed boundary condition may not accurately represent the actual boundary condition provided by continuing frames beyond the transverse frames in a ship structure, which are both free to deform.

### 3.4.2 Finite element

The Shell181 element was used to model the structure. For more details about the element, refer to Section 2.4.2.1.

### 3.4.3 Loading

The pressure distribution during an ice structure interaction was considered for the analysis. The loading considered for the analysis is illustrated in Figure 3.4.1. For details of the pressure load, refer to Section 3.2.

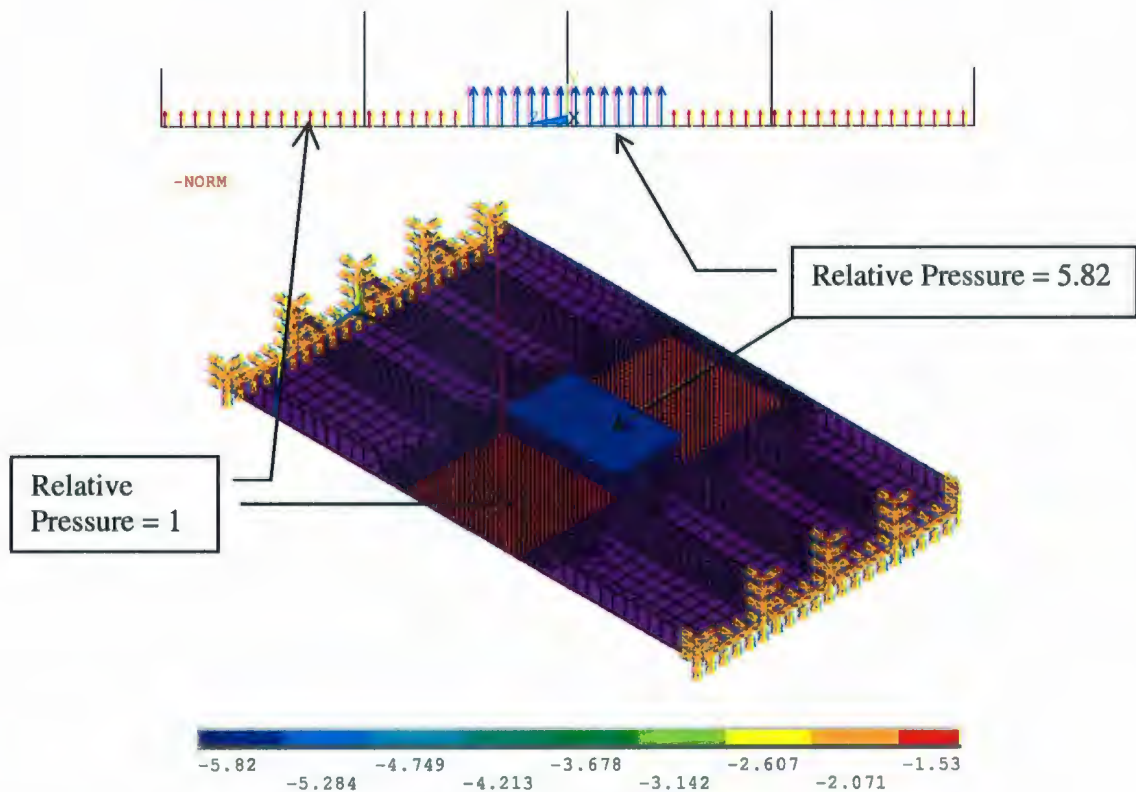


Figure 3.4.1: Loading considered for small grillage analysis

#### 3.4.4 Boundary conditions

The longitudinals are welded to the transverse stringers which are much heavier compared to the longitudinal stiffener. Since the stiffness of transverse stringer is significantly higher compared to that of the longitudinal, the displacements and rotations at the stringer locations are considered to be negligible and hence fixed boundary condition is assumed. The boundary conditions considered for the analysis are presented in Figure 3.4.2.

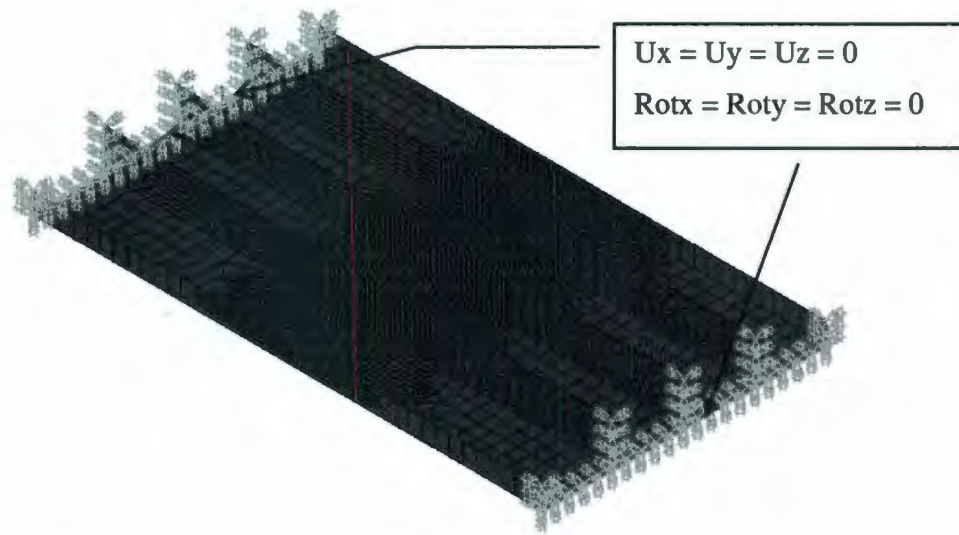


Figure 3.4.2: Boundary conditions considered for small grillage analysis

#### 3.4.5 Solution process

A non-linear finite element analysis was carried out to find the response of the structure to the applied load. A detailed discussion about non-linear ANSYS solution process is presented in Section 2.3.

### 3.5 Large grillage analysis

#### 3.5.1 Structural model

A large grillage consists of 3 neighboring frames, each with three frame spans in the longitudinal direction. At each span, a heavy transverse frame is provided which gives the necessary support at that location. The longitudinal frames ends and the two transverse frame ends of the large grillage are fixed. Since the points of fixities are far away from the point of application of load, it is considered that the boundary conditions have no significant effect on response of the frame. Thus in the large grillage both side and longitudinal boundary conditions are considered to be an accurate representation as in a real ship's structure.

### 3.5.2 Finite elements

The Shell181 element was used to model the structure. For more details about the element, refer to Section 2.4.2.1.

### 3.5.3 Loading

The pressure distribution during an ice structure interaction was considered for the analysis. The loading considered for the analysis is illustrated in Figure 3.5.1. For details of the pressure load, refer to Section 3.2.

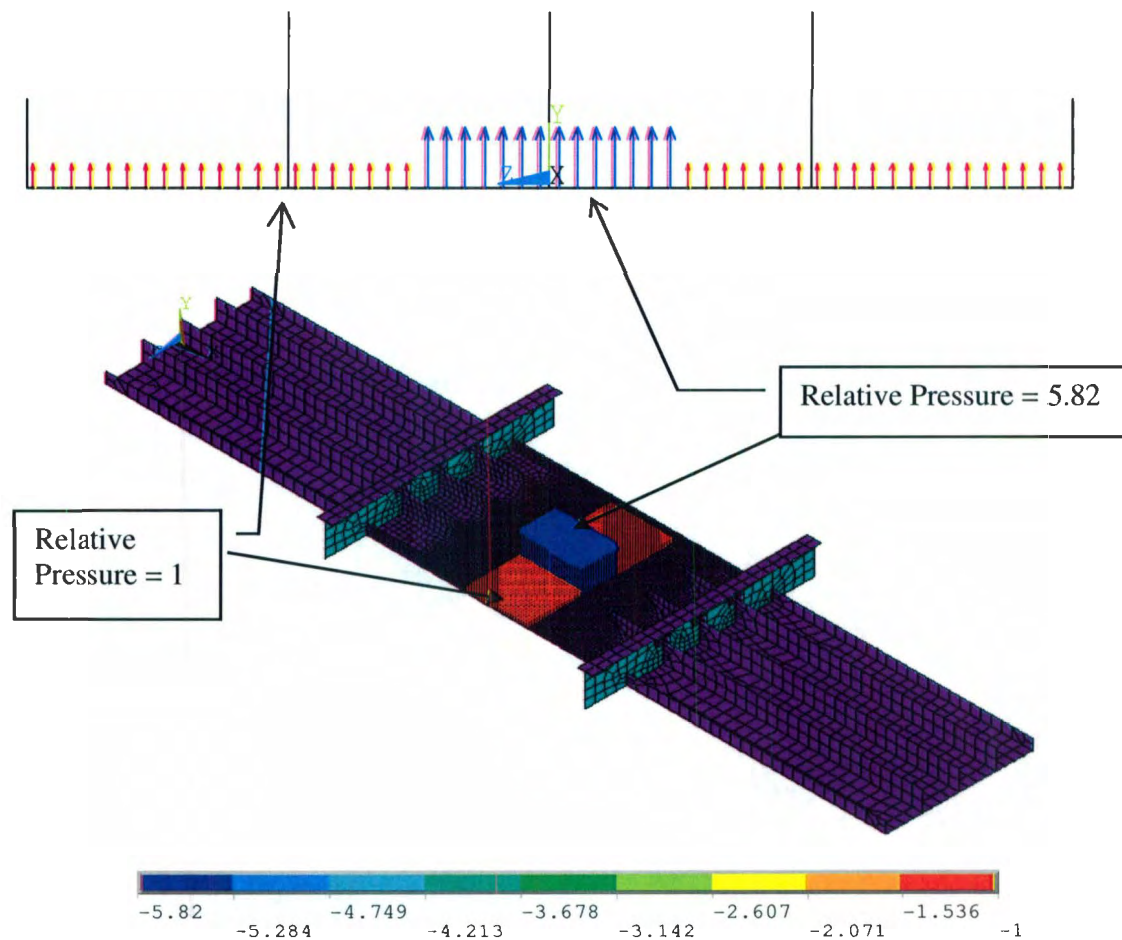


Figure 3.5.1: Loading considered for large grillage analysis

### 3.5.4 Boundary conditions

The boundary conditions considered for the analysis are presented in Figures 3.5.2. Fixed boundary conditions were set at both ends of transverse stringers and at the two longitudinal ends of the frames.

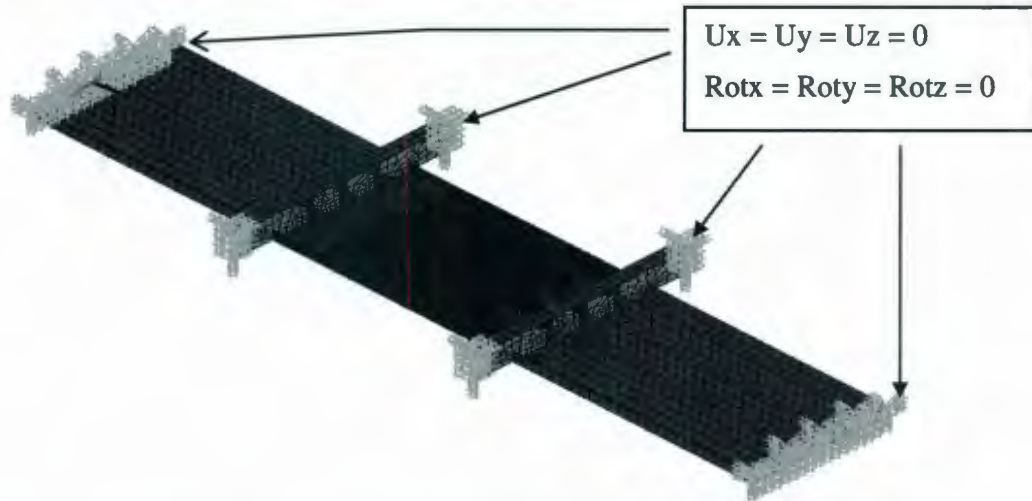


Figure 3.5.2: Boundary conditions considered for large grillage analysis

### 3.5.5 Solution

A non-linear finite element analysis was carried out to find the response of the structure to the applied load. A detailed discussion of the non-linear ANSYS solution process is presented in Section 2.3.

### 3.6 Capacity of a frame

The capacity of a structure can be defined as the load corresponding to a limit state. One of the limit states for a frame is the formation of three hinges. In an ideal case this is a situation where the deformation or strain increases infinitely without any appreciable increase in load. This hypothetical situation can be reached by an elastic perfectly plastic structure with no membrane effects. In real structures, this limit state does not occur due to strain hardening and membrane action of the plate. Therefore, various methods are used to determine the limit load value. Examples are the twice elastic slope method, tangent intersection method and 0.1% residual strain method (Mackenzie & Li, 2006 and Mourad, 1999).

#### 3.6.1 Twice elastic slope method

Figure 3.6.1 presents the definition of capacity using twice elastic slope method. A line is drawn with a slope equal to the initial slope ( $\theta$ ) of force displacement curve in the elastic region. A second line is drawn, with an angle  $\phi$  such that  $\tan \phi = 2 \tan \theta$ . The intersection of the force displacement curve with the second line is defined as the capacity.

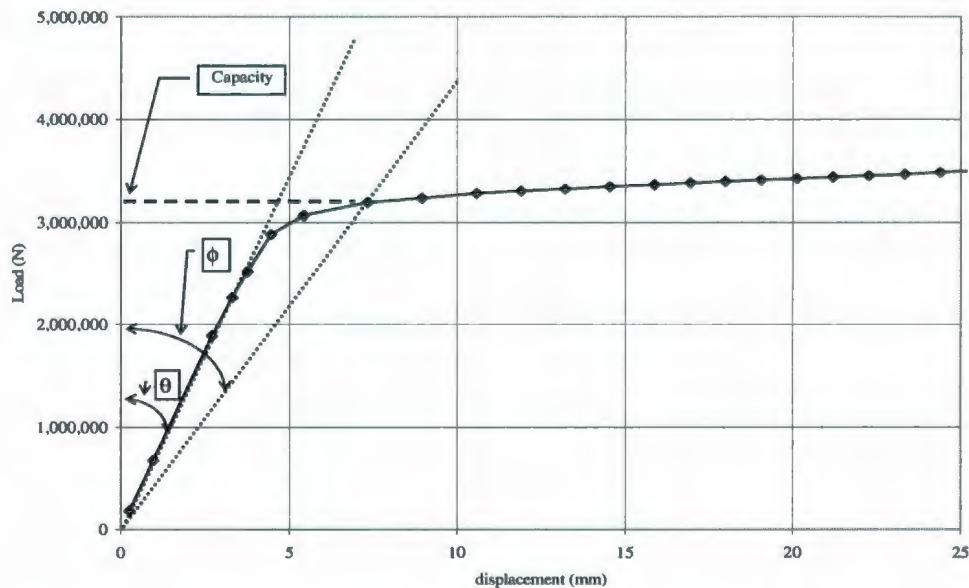


Figure 3.6.1: Definition of capacity using Twice Elastic Slope Method

### 3.6.2 Tangent intersection method

Figure 3.6.2 presents the definition of capacity using tangent intersection method. In this method the limit load is defined as the load at which the elastic and plastic tangents intersect. This method is also arbitrary as the slope in the plastic region is not constant and there can be infinite number of possible tangents in the plastic region.

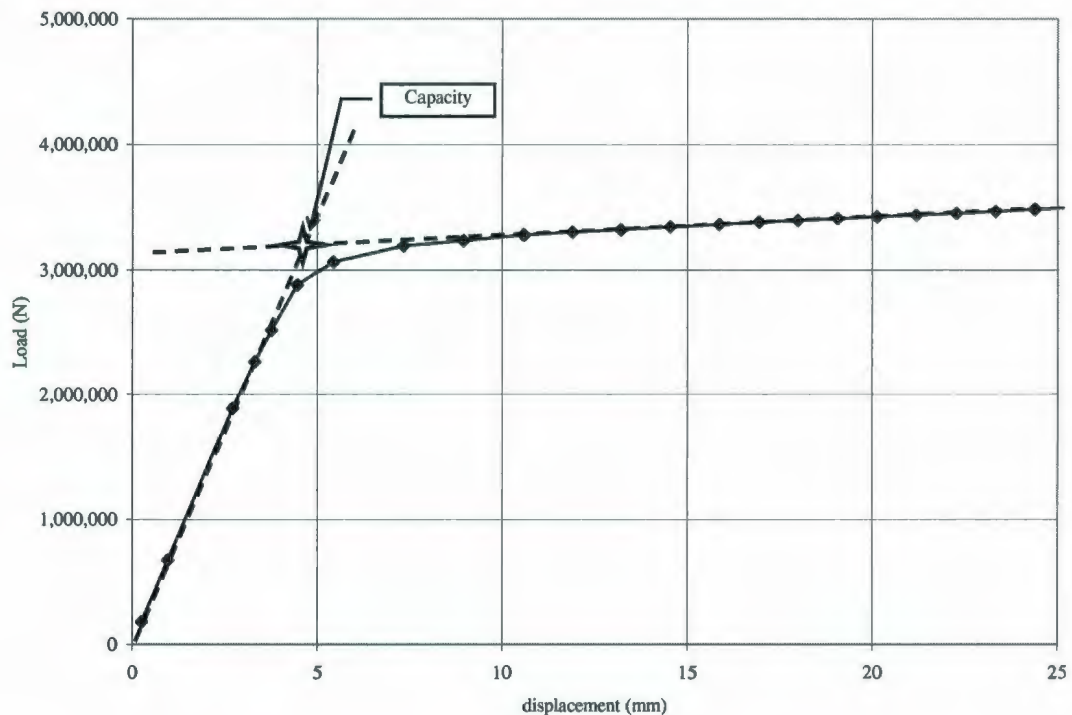


Figure 3.6.2: Definition of capacity using Tangent Intersection Method

### 3.6.3 0.1% residual strain method

Figure 3.6.3 presents the definition of capacity using 0.1% residual strain method. The capacity is equivalent to a load which causes a permanent strain of 0.1% of span.

A line is drawn with a slope equivalent to the elastic slope at a location which is offset from the origin by 0.1% of frame span. The intersection of this line with the force displacement curves is defined as the capacity.

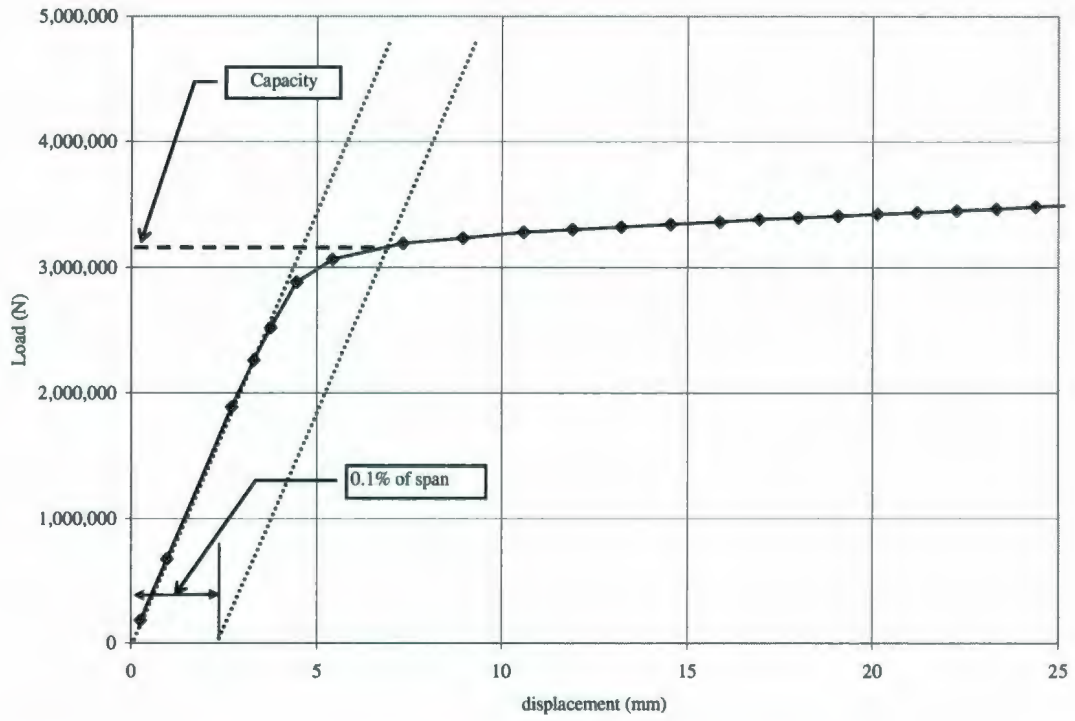


Figure 3.6.3: Definition of capacity using 0.1% Residual Strain Method

For the present study, 0.1% residual strain method has been used to estimate the capacity of single frame and large grillage.

### 3.7 T Stiffener analysis

Single frame, small grillage and large grillage analysis were carried out for five different T stiffener frames as shown in Table 3.7.1. The frames chosen for the study represents frames satisfying a range of ice classes.

Table 3.7.1: T stiffener parameters

Factor	Frame				
	T1	T2	T3	T4	T5
Web height [mm]	308	410	484	547	621
Web thickness [mm]	11.4	21.6	15.8	37.8	37.5
Flange width [mm]	102.3	108.1	142.3	138.8	187.3
Flange thickness [mm]	16.5	21.6	22.9	31.9	31.8
Plate thickness [mm]	16.2	21.6	22.6	30.8	37.5
Frame spacing [mm]	350	350	350	350	350
Frame span [mm]	2500	3250	2500	2500	2500
Yield strength [MPa]	355	355	355	355	355
Post yield modulus [MPa]	2000	2000	2000	2000	2000
Capacity - IACS [MN]	1.17	2.3	3.1	7.1	8.95

In order to examine the load sharing behavior in ship structures, the load-deflection characteristics of the center stiffener in a large grillage model is compared to that of a single frame model.

Capacity factor is defined as the ratio of capacity of the center stiffener in a large grillage to that of a single frame. A higher capacity factor represents a higher degree of load sharing.

### 3.7.1 Frame T1

The geometric and material properties of the T1 frame are listed in Table 3.7.2.

Table 3.7.2: T1 stiffener parameters

Web height	308 mm
Web thickness	11.4 mm
Flange width	102.3 mm
Flange thickness	16.5 mm
Plate thickness	16.2 mm
Frame spacing	350 mm
Frame span	2500 mm
Yield strength	355 MPa
Post yield modulus	2000 MPa
IACS Capacity	1.17 MN

The load-deflection behaviors of single frame, small grillage and large grillage for the Frame T1 are presented in Figure 3.7.1. Capacity estimation of Frame T1 is presented in Figure 3.7.2.

The single frame capacity is 1.3 MN and the large grillage capacity is 1.6 MN. The capacity of the large grillage is thus 23% more than that of the single frame.

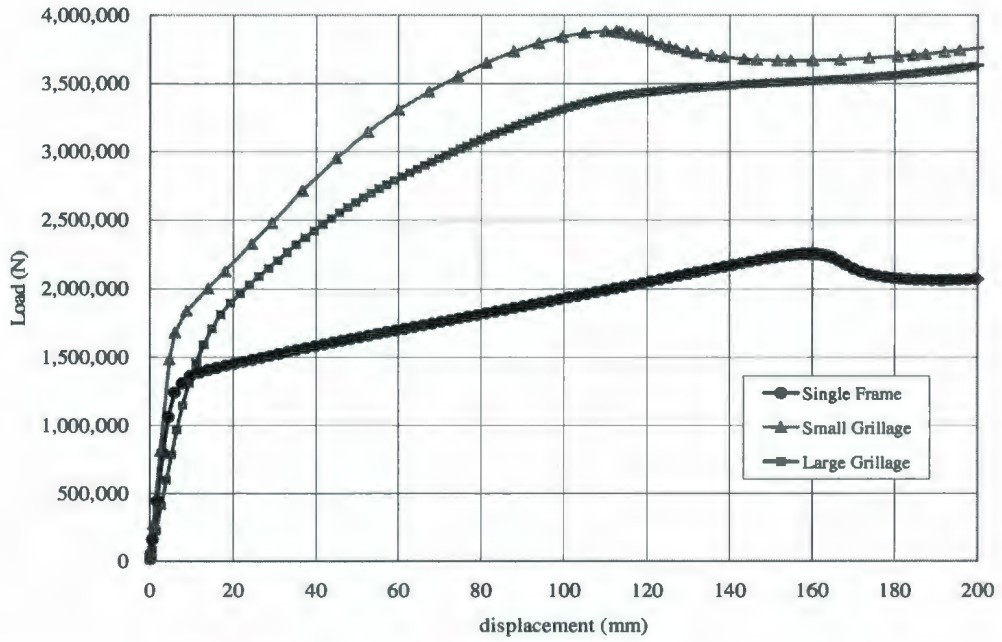


Figure 3.7.1: Results of ANSYS analysis – Frame T1

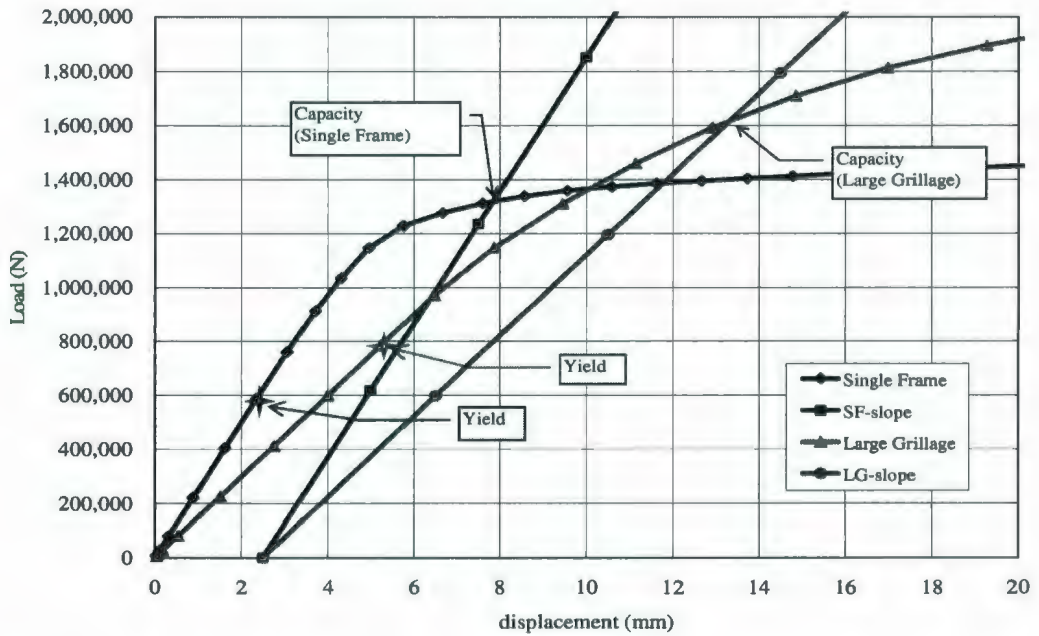


Figure 3.7.2: Capacity - Frame T1

### 3.7.2 Frame T2

The geometric and material properties of the T2 frame are listed in Table 3.7.3:

Table 3.7.3: T2 stiffener parameters

Web height	410 mm
Web thickness	21.6 mm
Flange width	108.1 mm
Flange thickness	21.6 mm
Plate thickness	21.6 mm
Frame spacing	350 mm
Frame span	3250 mm
Yield strength	355 MPa
Post yield modulus	2000 MPa
IACS Capacity	2.3 MN

The load-deflection behaviors of single frame, small grillage and large grillage for the Frame T2 are presented in Figure 3.7.3. Capacity estimation of Frame T2 is presented in Figure 3.7.4.

The single frame capacity is 2.5 MN and the large grillage capacity is 3.4 MN. The capacity of the large grillage is thus 36% more than that of the single frame.

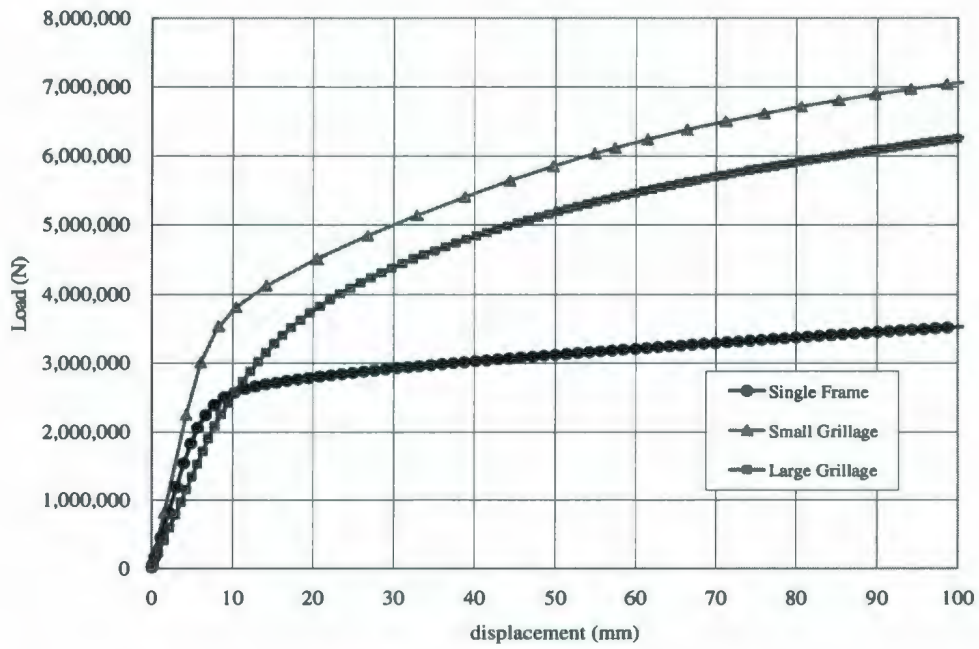


Figure 3.7.3: Results of ANSYS analysis – Frame T2

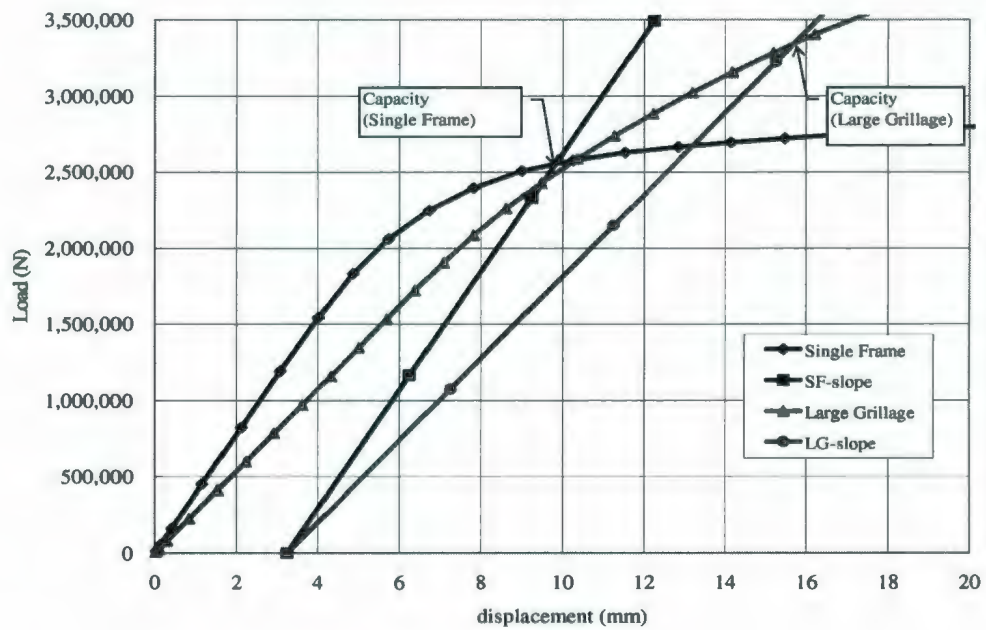


Figure 3.7.4: Capacity - Frame T2

### 3.7.3 Frame T3

The geometric and material properties of the T3 frame are listed in Table 3.7.4:

Table 3.7.4: T3 stiffener parameters

Web height	484 mm
Web thickness	15.8 mm
Flange width	142.3 mm
Flange thickness	22.9 mm
Plate thickness	22.6 mm
Frame spacing	350 mm
Frame span	2500 mm
Yield strength	355 MPa
Post yield modulus	2000 MPa
IACS Capacity	3.1 MN

The load-deflection behaviors of single frame, small grillage and large grillage for the Frame T3 are presented in Figure 3.7.5. Capacity estimation of Frame T3 is presented in Figure 3.7.6.

The single frame capacity is 3.2 MN and the large grillage capacity is 3.8 MN. The capacity of the large grillage is thus 18% more than that of the single frame.

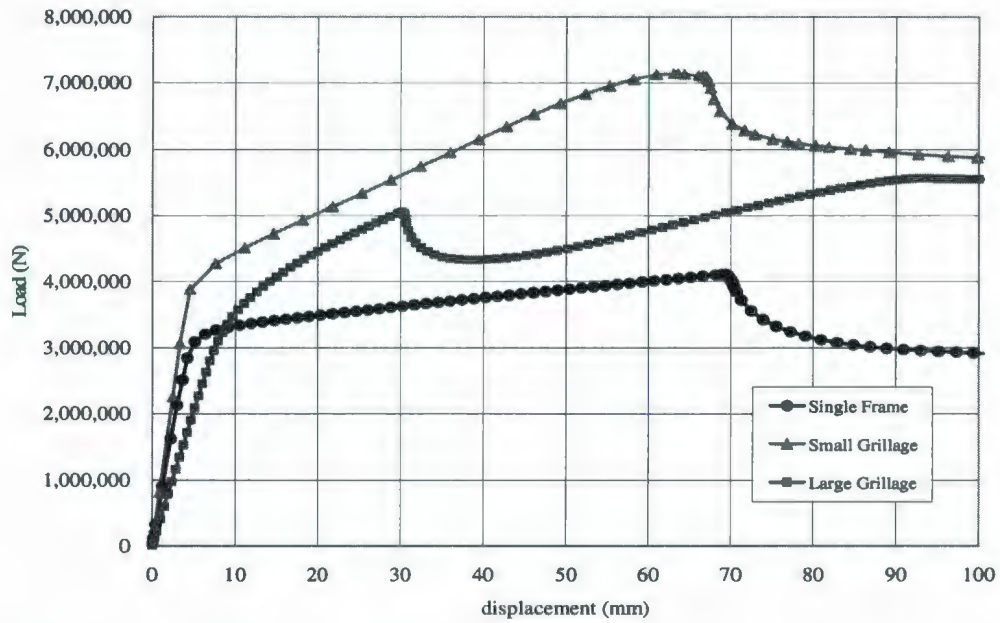


Figure 3.7.5: Results of ANSYS analysis – Frame T3

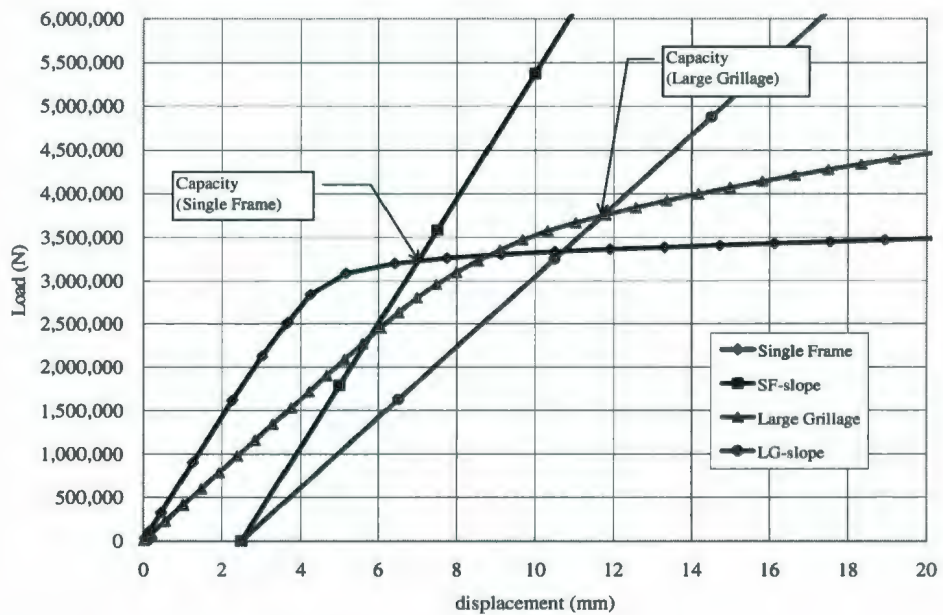


Figure 3.7.6: Capacity - Frame T3

### 3.7.4 Frame T4

The geometric and material properties of the T4 frame are listed in Table 3.7.5:

Table 3.7.5: T4 stiffener parameters

Web height	547 mm
Web thickness	37.8 mm
Flange width	138.8 mm
Flange thickness	31.9 mm
Plate thickness	30.8 mm
Frame spacing	350 mm
Frame span	2500 mm
Yield strength	355 MPa
Post yield modulus	2000 MPa
IACS Capacity	7.1 MN

The load-deflection behaviors of single frame, small grillage and large grillage for the Frame T4 are presented in Figure 3.7.7. Capacity estimation of Frame T4 is presented in Figure 3.7.8.

The single frame capacity is 7.8 MN and the large grillage capacity is 9.0 MN. The capacity of the large grillage is thus 15% more than that of the single frame.

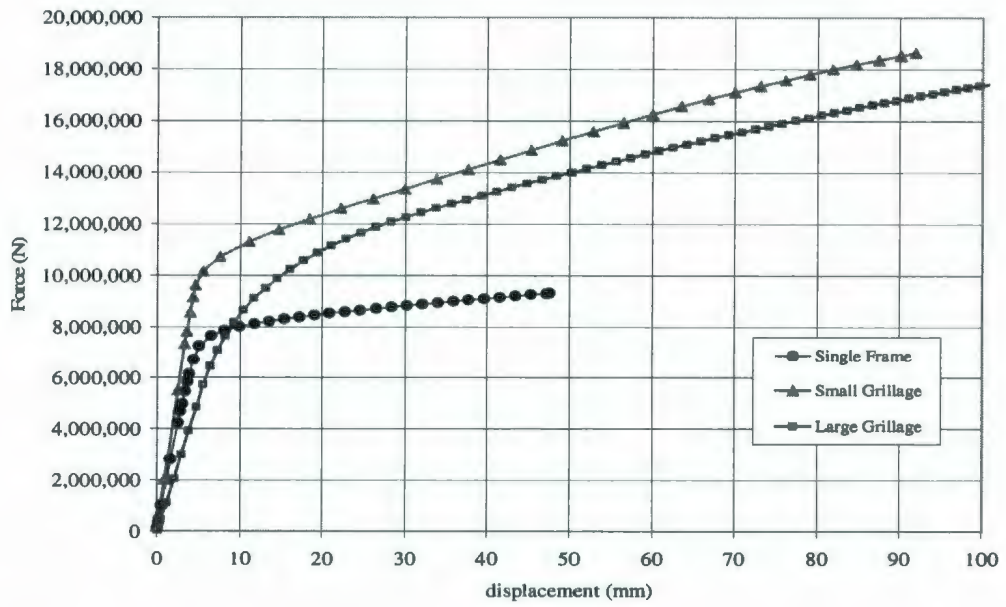


Figure 3.7.7: Results of ANSYS analysis – Frame T4

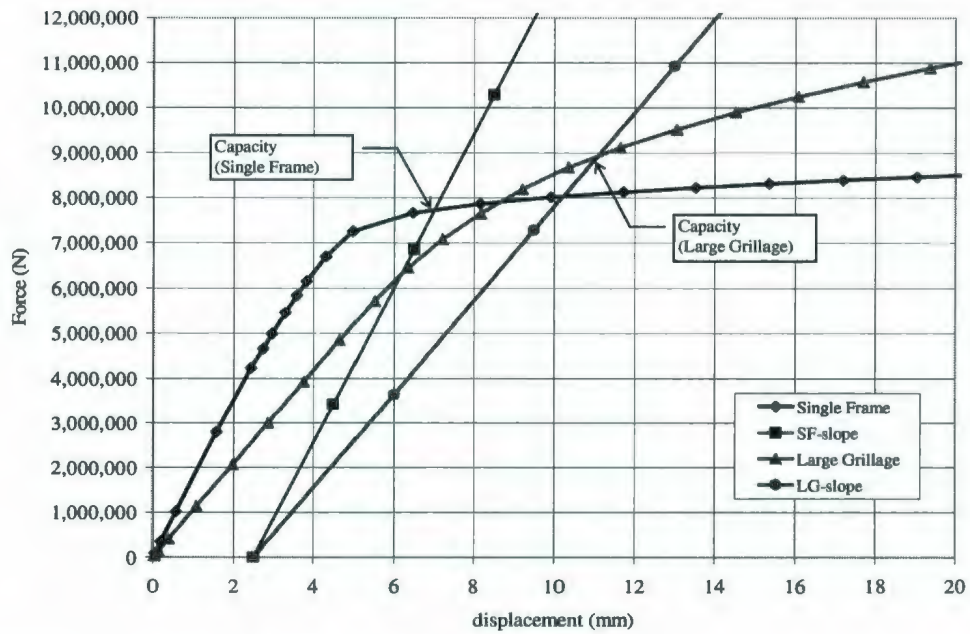


Figure 3.7.8: Capacity - Frame T4

### 3.7.5 Frame T5

The geometric and material properties of the T5 frame are listed in Table 3.7.6:

Table 3.7.6: T5 stiffener parameters

Web height	621 mm
Web thickness	37.5 mm
Flange width	187.3 mm
Flange thickness	31.8 mm
Plate thickness	37.5 mm
Frame spacing	350 mm
Frame span	2500 mm
Yield strength	355 MPa
Post yield modulus	2000 MPa
IACS Capacity	8.95 MN

The load-deflection behaviors of single frame, small grillage and large grillage for the Frame T5 are presented in Figure 3.7.9. Capacity estimation of Frame T5 is presented in Figure 3.7.10.

The single frame capacity is 9.5 MN and the large grillage capacity is 9.25 MN. The capacity of the large grillage is thus 3% less than that of the single frame.

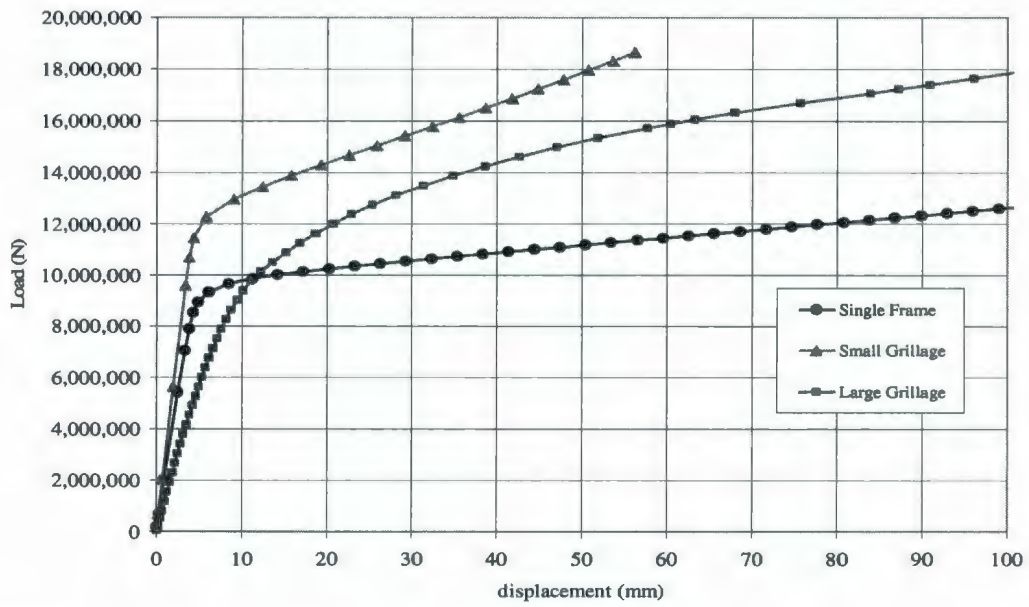


Figure 3.7.9: Results of ANSYS analysis – Frame T5

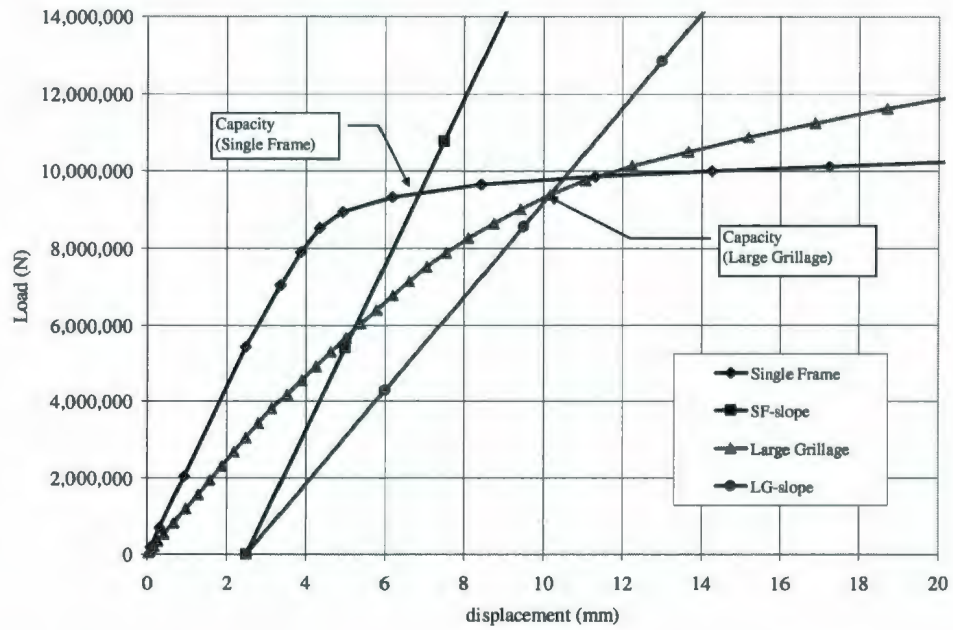


Figure 3.7.10: Capacity - Frame T5

### 3.7.6 Discussion of T stiffener results

Table 3.7.7 presents the summary of the results of finite element analysis carried out for different T stiffeners.

Table 3.7.7: Summary of T stiffener results

Factor	Frame				
	T1	T2	T3	T4	T5
Web height [mm]	308	410	484	547	621
Web thickness [mm]	11.4	21.6	15.8	37.8	37.5
Flange width [mm]	102.3	108.1	142.3	138.8	187.3
Flange thickness [mm]	16.5	21.6	22.9	31.9	31.8
Plate thickness [mm]	16.2	21.6	22.6	30.8	37.5
Frame spacing [mm]	350	350	350	350	350
Frame span [mm]	2500	3250	2500	2500	2500
Yield strength [MPa]	355	355	355	355	355
Post yield modulus [MPa]	2000	2000	2000	2000	2000
IACS Capacity [MN]	1.17	2.3	3.1	7.1	8.95
<b>ANSYS Results</b>					
Capacity - Single Frame [MN]	1.3	2.5	3.2	7.8	9.50
Capacity - Large Grillage [MN]	1.6	3.4	3.8	9.0	9.25
Capacity Factor	<b>1.23</b>	<b>1.36</b>	<b>1.18</b>	<b>1.15</b>	<b>0.97</b>

The results of the analysis have shown that large grillage is stronger than the single frame in almost all cases. The increase in capacity ranged from 0% to 36% for the frames

studied. It is also observed that as the thickness of the frame increases, the increase in capacity of the large grillage decreases and tends to become comparable to that of the single frame. In fact there was one case (frame T5) reported with capacity of the large grillage being marginally lower than that of a single frame.

The deformation pattern of the various frames has shown that thinner frames deform as a whole structure whereas thicker frames tend to deform only locally.

The single frame becomes stronger when it is a part of a grillage due to the load sharing between adjacent frames. The load sharing is more in case of thin frames compared to that of thick frames. The thin frames deflect more and distribute the load whereas the thick frame deforms only locally and takes the load without much sharing with adjacent members.

The behavior noted has important implications for ice class ship structures. Larger, higher ice class structures are less well able to distribute the loads. This implies that higher class vessels will not only need to withstand higher loads, but will need to do so more locally than lower class vessels. As most practical experience has been gained with lower class vessels, this issue should be of concern for the many new large and high ice class vessels that are currently on the drawing boards.

### 3.8 Flat bar stiffener analysis

Single frame and large grillage analysis were carried out for four different flat bar stiffener frames as shown in Table 3.8.1. The frames chosen for the study represents frames satisfying a range of ice classes.

Table 3.8.1: Flat bar stiffener parameters

Factor	Frame			
	FB1	FB2	FB3	FB4
Web height [mm]	190.8	315	445	547
Web thickness [mm]	13.0	21.7	30.5	37.8
Plate thickness [mm]	10.0	24.1	30.5	30.8
Frame spacing [mm]	350	350	350	350
Frame span [mm]	2500	2500	2500	2500
Yield strength [MPa]	355	355	355	355
Post yield modulus [MPa]	2000	2000	2000	2000

In order to examine the load sharing behavior in ship structures, the load-deflection characteristics of the center stiffener in a large grillage model is compared to that of a single frame model.

Capacity factor is defined as the ratio of capacity of the center stiffener in a large grillage to that of a single frame. A higher capacity factor represents a higher degree of load sharing.

### 3.8.1 Frame FB1

The geometric and material properties of the FB1 frame are listed in Table 3.8.2.

Table 3.8.2: FB1 stiffener parameters

Web height	190.8 mm
Web thickness	13 mm
Plate thickness	10 mm
Frame spacing	350 mm
Frame span	2500 mm
Yield strength	355 MPa
Post yield modulus	2000 MPa

The load-deflection behavior and capacity estimation of single frame and large grillage for the Frame FB1 are presented in Figure 3.8.1.

The single frame capacity is 0.325 MN and the large grillage capacity is 0.44 MN. The capacity of the large grillage is thus 35% more than that of the single frame.

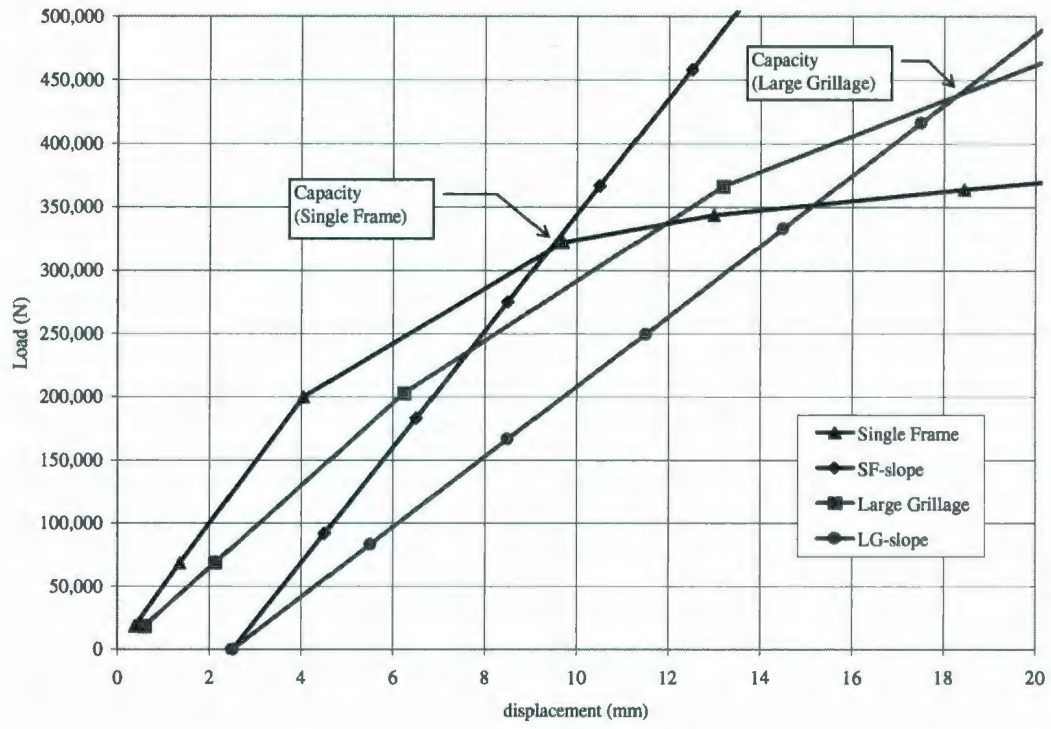


Figure 3.8.1: Results of ANSYS analysis – Frame FB1

### 3.8.2 Frame FB2

The geometric and material properties of the FB2 frame are listed in Table 3.8.3.

Table 3.8.3: FB2 stiffener parameters

Web height	315 mm
Web thickness	21.7 mm
Plate thickness	24.1 mm
Frame spacing	350 mm
Frame span	2500 mm
Yield strength	355 MPa
Post yield modulus	2000 MPa

The load-deflection behavior and capacity estimation of single frame and large grillage for the Frame FB2 are presented in Figure 3.8.2.

The single frame capacity is 1.5 MN and the large grillage capacity is 2.1 MN. The capacity of the large grillage is thus 40% more than that of the single frame.

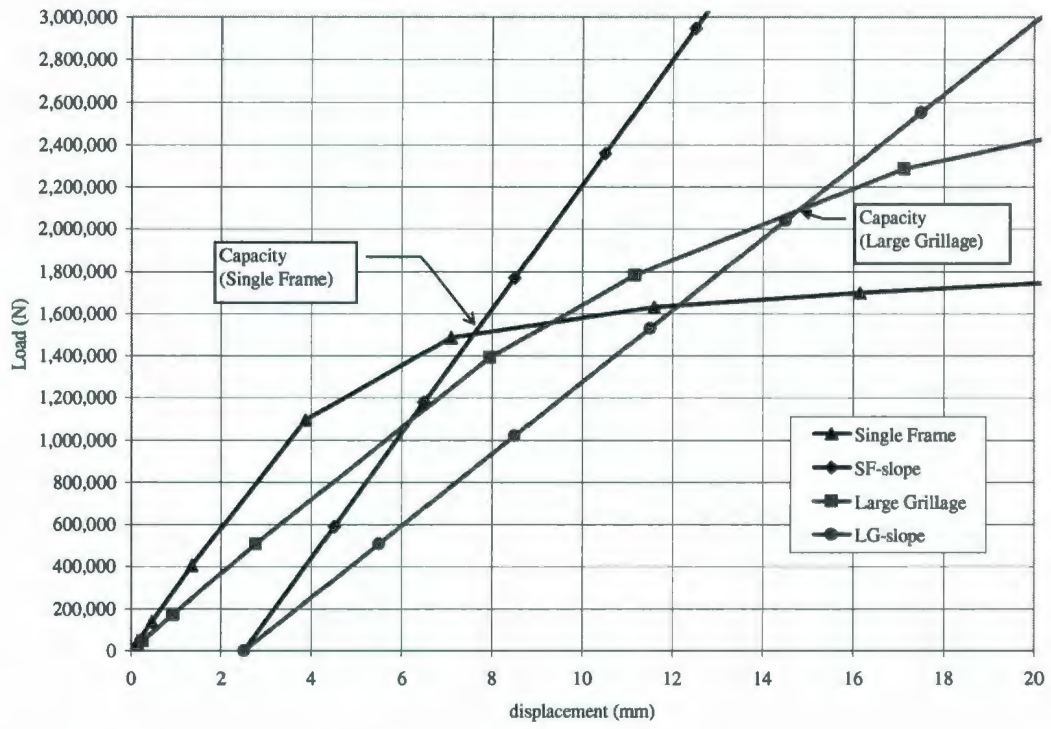


Figure 3.8.2: Results of ANSYS analysis – Frame FB2

### 3.8.3 Frame FB3

The geometric and material properties of the FB3 frame are listed in Table 3.8.4.

Table 3.8.4: FB3 stiffener parameters

Web height	445 mm
Web thickness	30.5 mm
Plate thickness	30.5 mm
Frame spacing	350 mm
Frame span	2500 mm
Yield strength	355 MPa
Post yield modulus	2000 MPa

The load-deflection behavior and capacity estimation of single frame and large grillage for the Frame FB3 are presented in Figure 3.8.3.

The single frame capacity is 3.8 MN and the large grillage capacity is 4.7 MN. The capacity of the large grillage is thus 23% more than that of the single frame.

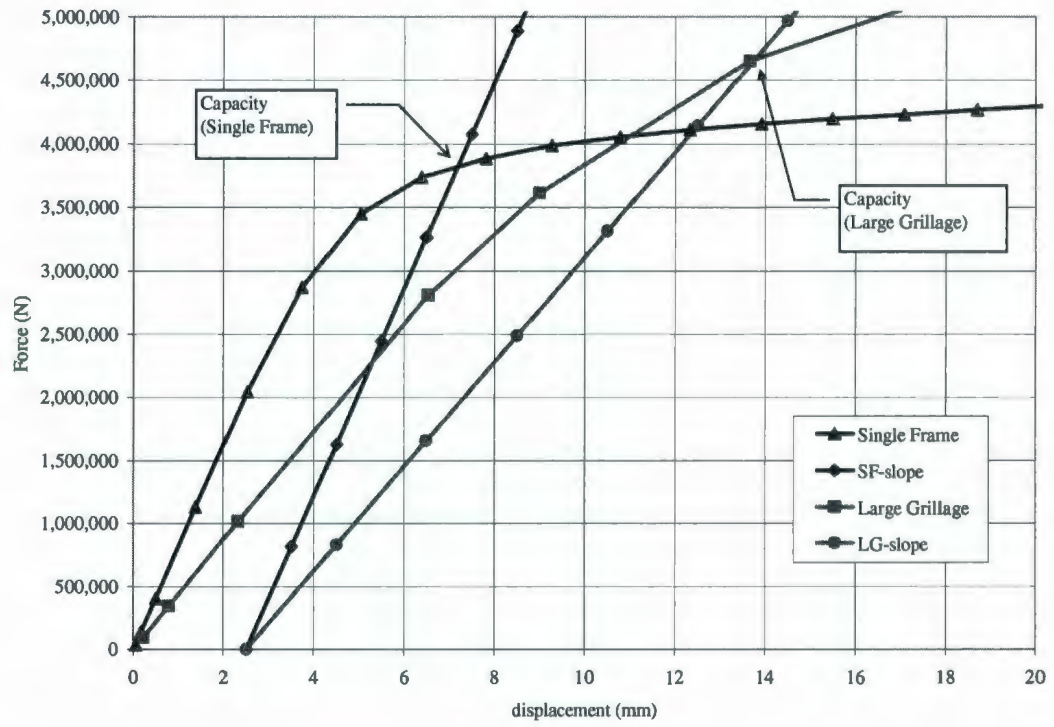


Figure 3.8.3: Results of ANSYS analysis – Frame FB3

### 3.8.4 Frame FB4

The geometric and material properties of the FB4 frame are listed in Table 3.8.5.

Table 3.8.5: FB4 stiffener parameters

Web height	547 mm
Web thickness	37.8 mm
Plate thickness	30.8 mm
Frame spacing	350 mm
Frame span	2500 mm
Yield strength	355 MPa
Post yield modulus	2000 MPa

The load-deflection behavior and capacity estimation of single frame and large grillage for the Frame FB4 are presented in Figure 3.8.4.

The single frame capacity is 6.0 MN and the large grillage capacity is 6.1 MN. The capacity of the large grillage is thus 1.6% more than that of the single frame.

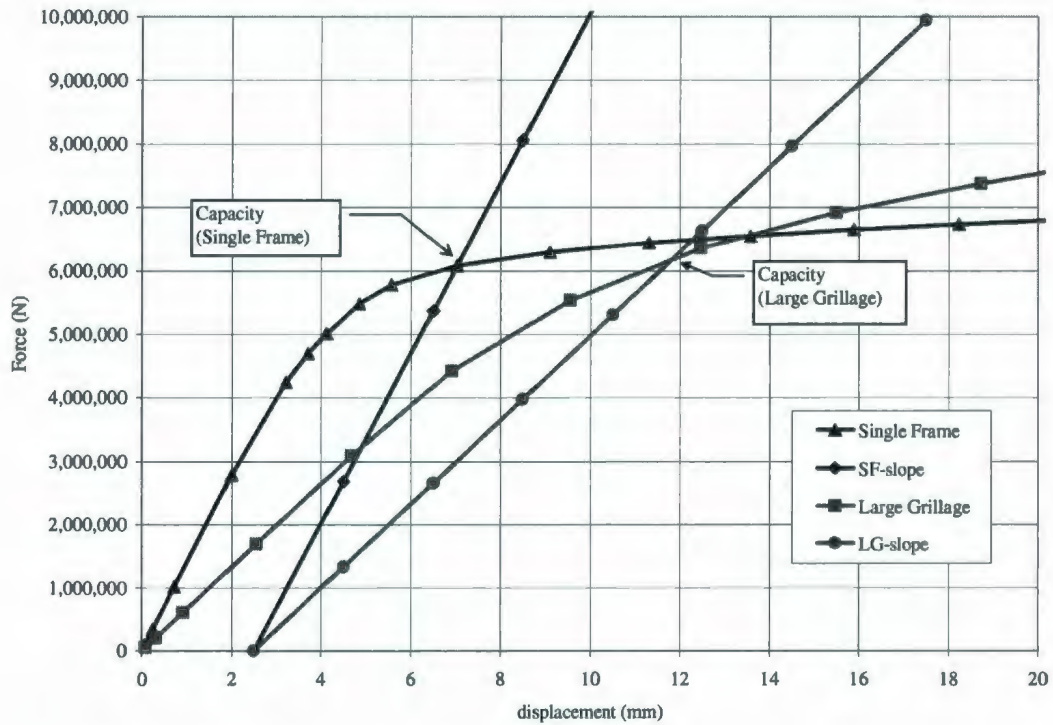


Figure 3.8.4: Results of ANSYS analysis – Frame FB4

### 3.8.5 Discussion of flat bar stiffener results

The results of the flat bar frame load sharing analysis are listed in Table 3.8.6. The results of the analysis of flat bar stiffener are similar to that of tee stiffener frame. The large grillage is stronger than the single frame in almost all cases. The increase in capacity ranged from 1% to 40% for the frames studied. It is also observed that as the thickness of the frame increases, the increase in capacity of the large grillage decreases and tends to become comparable to that of the single frame.

Table 3.8.6: Summary of flat bar stiffener results

Factor	Frame			
	FB1	FB2	FB3	FB4
Web height [mm]	190.8	315	445	547
Web thickness [mm]	13.0	21.7	30.5	37.8
Plate thickness [mm]	10.0	24.1	30.5	30.8
Frame spacing [mm]	350	350	350	350
Frame span [mm]	2500	2500	2500	2500
Yield strength [MPa]	355	355	355	355
Post yield modulus [MPa]	2000	2000	2000	2000
<b>ANSYS Results</b>				
Capacity - Single Frame [MN]	0.325	1.5	3.8	6.0
Capacity - Large Grillage [MN]	0.440	2.1	4.71	6.1
Capacity Factor	<b>1.35</b>	<b>1.40</b>	<b>1.23</b>	<b>1.016</b>

### 3.9 Conclusions

This chapter has examined a crucial aspect of ice class framing design. The response of stiffeners depends on the assumed boundary conditions. When considering localized patch loads, the issue of load sharing becomes important. The study compares the effect boundary conditions assumed in the cases of single frame, small grillage and large grillage, in order to assess the effect of load sharing in the plastic range.

The side boundary condition in the case of single frame is simulated by a symmetric boundary condition. The method is assumed to be an accurate representation of the support provided by the adjacent side structure, but in most cases underestimates the capacity of the frame.

In case of a small grillage, the side boundary condition is simulated by including the structure itself into the model, rather than relying on the symmetric boundary condition. However, the longitudinal boundary conditions are not realistic. In ship structure, the transverse frames are free to deform; hence the assumption of zero displacement/rotation at the longitudinal ends is not correct. The main effect of fixed longitudinal ends is the reduction of actual support span, which results in overestimation of capacity of the small grillage.

The side and longitudinal boundary conditions are accurately simulated in the case of a large grillage by modeling the longitudinal and transverse continuity of structure. Thus the large grillage represents the correct structural behavior as in the case of a real ships structure.

The results of analysis have shown that the large grillage is stronger than the single frame in most cases. The increase in strength ranged from approximately 0% to 40%. The increase in strength acts as a safety margin which takes care of the uncertainties in ice load estimation.

The single frame becomes stronger when it is a part of a grillage due to the load sharing between adjacent frames. The load sharing is more in case of thin frames compared to that of thick frames. The thin frames deflect more and distribute the load whereas the

thick frame deforms only locally and takes the load without much sharing with adjacent members.

Load sharing has important implications for ice class ship structures. If the effect were similar in all frames, then the practical significance would be small. However, the effect varies considerably. It is notable that larger, higher ice class structures are less well able to distribute the loads. This implies that higher class vessels will not only need to withstand higher loads, but will need to do so more locally than lower class vessels. Most practical experience has been gained with lower class vessels. Consequently this issue should be of concern for the many new large and high ice class vessels that are currently on the drawing boards.

## **4 PARAMETRIC STUDY OF CAPACITY**

### **4.1 Introduction**

Stiffened plates are the basic structural building blocks of many onshore and offshore structures. Ships hull structure consists of plate stiffened in both directions. The behavior of stiffened plate in the elastic region is well understood. In the recent years there has been a renewed interest in estimating plastic response of ship structures.

Ship design rules are changing from traditional working stress approach to new rules which allow plastic limit states, particularly in the case of ice class vessels. The rationale behind this move is the recognition that structure tends to have a large reserve capacity after it yields and before it finally collapses.

Figure 4.1.1 shows the response of a typical frame subjected to patch load, similar to an ice load. The initial response is linear until the material yields. The most highly stressed region yields first. The yield region grows as the loading is increased and results in an internal hinge when the complete cross section yields. More hinges will be formed as the applied load is further increased. The formation of three hinges is considered as one of the basic collapse mechanisms in the case of a fixed beam.

Beyond three-hinge formation, the beam can take more loads due to the additional support from membrane action (i.e., shape change) of plate and strain hardening. Even though the structure is deforming, the additional support of membrane and strain hardening enables the structure to bear increasing loads. Thus plastic limit state design can effectively and economically replace the traditional designs based on working stress, and still having sufficient reserve capacity.

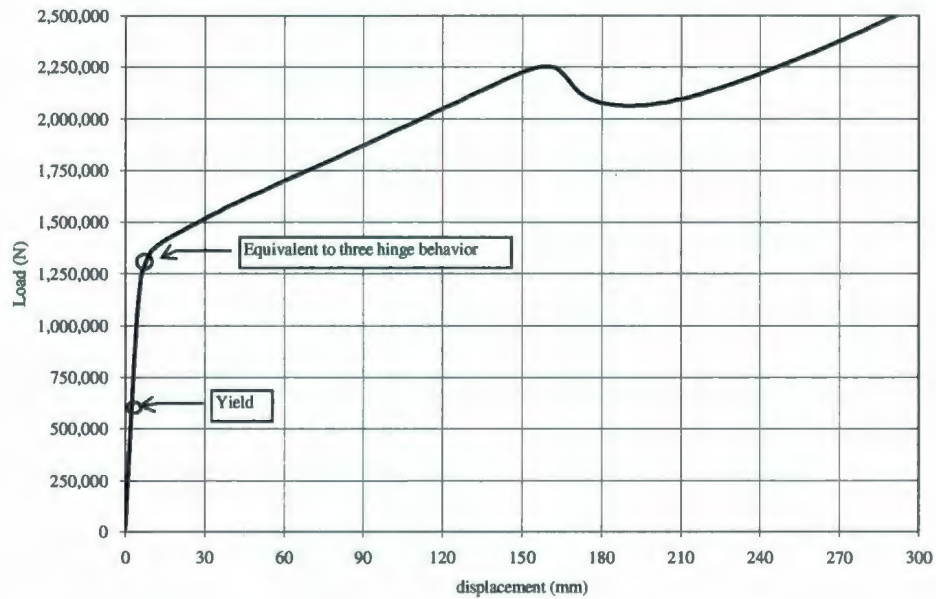


Figure 4.1.1: Load-deflection behavior of a typical frame

The capacity of a frame is currently estimated using the IACS rules. The pressure causing collapse in the case of a beam fixed at two ends and loaded at the center is given by IACS Polar Rules (Daley, 2002) as:

$$P_{3h} = \frac{(2 - kw) + kw \sqrt{1 - 48 \cdot Zpns \cdot (1 - kw)}}{12 \cdot Zpns \cdot kw^2 + 1} \cdot \frac{Zp \cdot \sigma_y \cdot 4}{\left[ S \cdot b \cdot L \cdot \left( 1 - \frac{b}{2 \cdot L} \right) \right]} \quad (4.1)$$

$$P_{shear} = \frac{2A_w \sigma_y}{\sqrt{3} S b} \quad (4.2)$$

The above pressure reflects the onset of significant plastic deformation as it ignores contributions from large deformations and membrane stresses.

The capacity of a frame is defined as the load the frame can withstand at the onset of three-hinge mechanism. The three-hinge mechanism can occur at relatively small deformations of the structure. In most cases the structure will be able to carry additional load at larger deformations, without collapsing. But the onset of three-hinge is considered as a design limit such that the frame has sufficient reserve capacity and hence inbuilt safety margin.

The capacity of a stiffened plate depends on many factors – geometric, material properties, loading type etc. The reliable methods to estimate capacity are either to conduct a full scale experiment or a nonlinear finite element analysis. Full scale experiments are very expensive and it is not practically possible to conduct a large number of experiments due the high cost and time required. Nonlinear finite element analyses are very complex and often face convergence issues. Hence there is a need for a simple regression equation which predicts capacity based on all the factors. The equation can serve as a quick guide for initial estimation of capacity.

The aims of the study were:

- to identify the major factors which affect the capacity of a stiffened plate
- to find a simple regression equation which can predict the capacity
- validate the regression equation for accuracy

#### **4.2 Factors considered for the study**

The factors which affect the capacity of stiffened plate can be broadly characterized as geometric factors, material properties, loading type, etc.

The major geometric factors considered for the study are

- Span
- Web height
- Web thickness
- Flange width
- Flange thickness
- Plate width (frame spacing)
- Plate thickness

The material properties considered are

- Yield strength
- Post yield modulus

The general case of T stiffener has been studied. The breadth of the flange towards left and right are considered as independent factors. When both left and right flanges are present, it will become a T stiffener. Removal of a flange towards one side will result in an L stiffener and removal of both flanges will result in flat bar stiffener. This allows the study of flat bar, L and T together, rather than having separate cases for each section type.

### 4.3 Design space

Frames can occur in various combinations of geometric and material properties. The design space explored covers the region between the practical low and high limits of each factor. The range of each factor considered for the study is presented in Table 4.3.1.

Table 4.3.1: Parameter ranges for capacity study

	<b>Factor</b>	<b>low</b>	<b>high</b>
1	web height [mm]	200	600
2	web height / thickness	15	40
3	flange width left [mm]	10	150
4	flange width right [mm]	10	150
5	flange thickness [mm]	12	40
6	plate width [mm]	300	600
7	plate thickness [mm]	10	40
8	plate length [mm]	2000	4000
9	Yield strength [MPa]	300	600
10	post yield modulus [MPa]	0	2000

The minimum flange width has been considered as 10 instead of zero. This avoids the situation of a flange with finite thickness but no width. The accuracy of the method has been independently verified and found to be within reasonable error margins.

#### **4.4 Design of Experiments**

An experiment is a series of tests or computer simulations on a system (e.g., structure) in which changes are made to the factors of the system (like geometric parameters or material properties) so as to identify and study the variation in the output response (e.g., capacity).

There are many ways of doing experiment by varying factors. One of the earliest methods was to change one factor at a time (OFAT) while keeping all other factors constant. The method was once considered to be the most efficient way of studying the many factors affecting a system, failed to address the effect of interaction of factors on the response.

An alternate and modern approach is to use statistically designed experiments. The method – known as Design of Experiments (DOE) - was introduced by Ronald Fisher in early 1920's. This method has found application in wide variety of fields including engineering, agriculture, finance, business, chemical and process industry. The method proposed by Fisher was expanded by other researchers like Box, Wilson etc and recently been implemented into computer software for easy statistical calculation.

DOE method starts by identifying all factors that are assumed to be important in the response of a system. The method will design the minimum number of experiments required to determine the major factors and interactions.

Statistical significance of each factor is tested using analysis of variance (ANOVA). Analysis of the experimental data is performed using statistical hypothesis testing, such that a p-value is found to assess significance. P-value of less than 0.05 is considered to be indicative of statistical significance.

DOE also generates a prediction model using regression analysis. The model is typically a low order polynomial function of the input variables. The prediction model is also tested for adequacy by performing certain statistical tests.

In general, DOE can be used to:

- Learn about the system
- Screen important variables
- Build a mathematical model
- Obtain prediction equations

The main advantage of DOE is the possibility of studying the effect of all factors with relatively small number of runs. In OFAT only one factor is changed at a time, so the effect of change in one variable can only be found out. In DOE method, more than one factor is varied at a time, resulting in filtering out the effect of many factors and interactions between them. Thus a relatively fewer number of runs are only required to study the main effect and their interactions. The method is hence best suited in situations where the system is affected by a large number of parameters.

There are many classes of DOE - of which two-level factorial, fractional factorial design (FFD) and response surface method (RSM) are the most common. There are also many variations of the above three basic classes of DOE.

RSM design is usually used when the behavior of the system is non-linear. The response surface will have significant curvatures and second order polynomial functions of input variables are required to define the non-linear behavior.

One of the popular RSM methods is Central Composite Design (CCD), which is built on the principles of fractional factorial design (FFD). Fractional factorial with resolution V makes sure that two-factor interaction terms are not aliased with other two-factor interaction terms, and can be considered as one of the best methods to study multi-factored experiments.

The total number of experiments required to study a multi factored problem considering all combinations of factors will become enormous. For example, if the above problem is to be studied in two levels (low and high) of each factor, it will result in 1024 ( $2^{10}$ ) ANSYS simulations. Considering the time required for solving each FE analysis and post

processing of results, it is clear that traditional methods are not efficient in studying these kinds of problems.

By using the DOE method, significant reduction in the number of experiments is achieved. The number of experiments required to study a ten factor problem by CCD with minimum run resolution V design is 77. The combinations of factors are generated using Design Expert™ software.

The details of experiment are given in Section 4.6

## **4.5 Finite element analysis**

### **4.5.1 Finite element**

The validation study of large grillage (Chapter 2) has shown that the capacity estimation using shell elements are in good agreement with the experimental results, even though the web tends to excessively twist at very large deformations. The three-hinge mechanism occurs at relatively small deformation, so it is assumed that shell elements are adequate for the present study of load carrying capacity. There is considerable saving in analysis time by using shell elements as compared to solid elements.

Shell 181 has been used to model the structure. The details of the element are presented in Section 2.4.2.1

### **4.5.2 Loading**

The study explores the capacity of a frame subjected to an ice loading. Ice loading manifests itself as areas of localized high pressure surrounded by regions of lower pressure. The local structure should be strong enough to withstand these local high pressures.

The nodes located on a small area (150mm x 150mm) at the center of the frame were applied with a high pressure so that the frame was loaded well beyond three-hinge mechanism. Loading considered for the analysis are presented in Figure 4.5.1

### **4.5.3 Boundary conditions**

The side shell structure of a longitudinally framed ice strengthened ship was considered for the study. Only a single frame was considered in order to reduce the analysis time.

The two longitudinal ends were fixed which idealizes the support provided by transverse stringers. The two transverse sides of the shell plate were given symmetric boundary condition to simulate the support provided by adjacent side structure.

Boundary condition considered for the analysis are presented in Figures 4.5.2 and 4.5.3

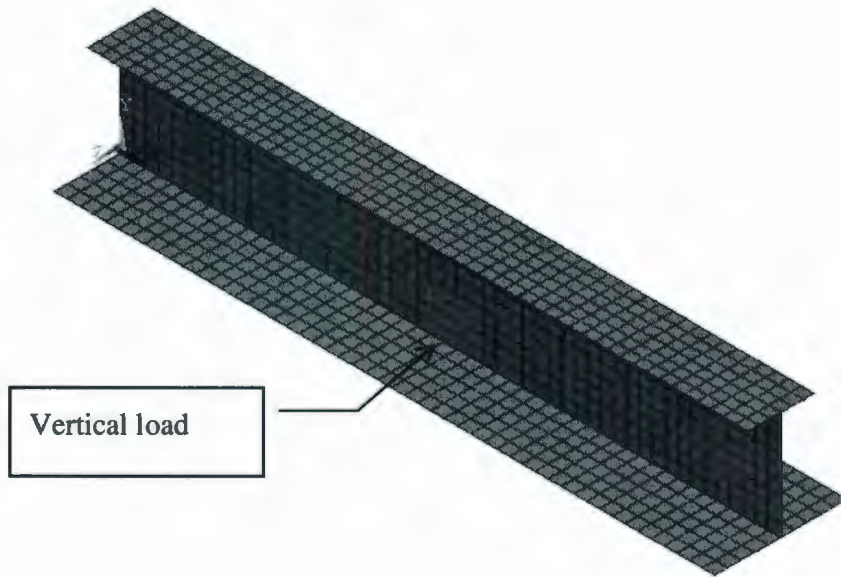


Figure 4.5.1: Loading considered for capacity study

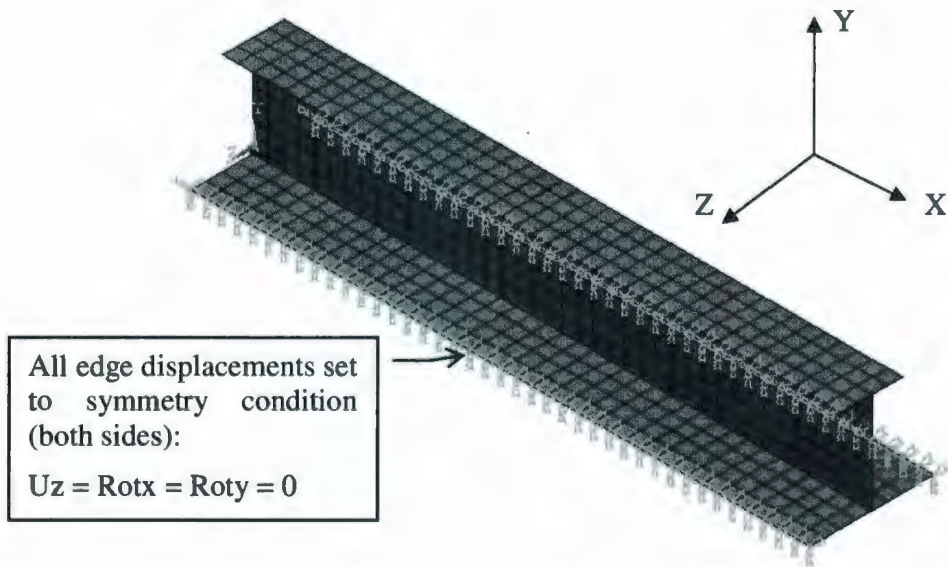


Figure 4.5.2: Symmetric boundary condition at transverse edges

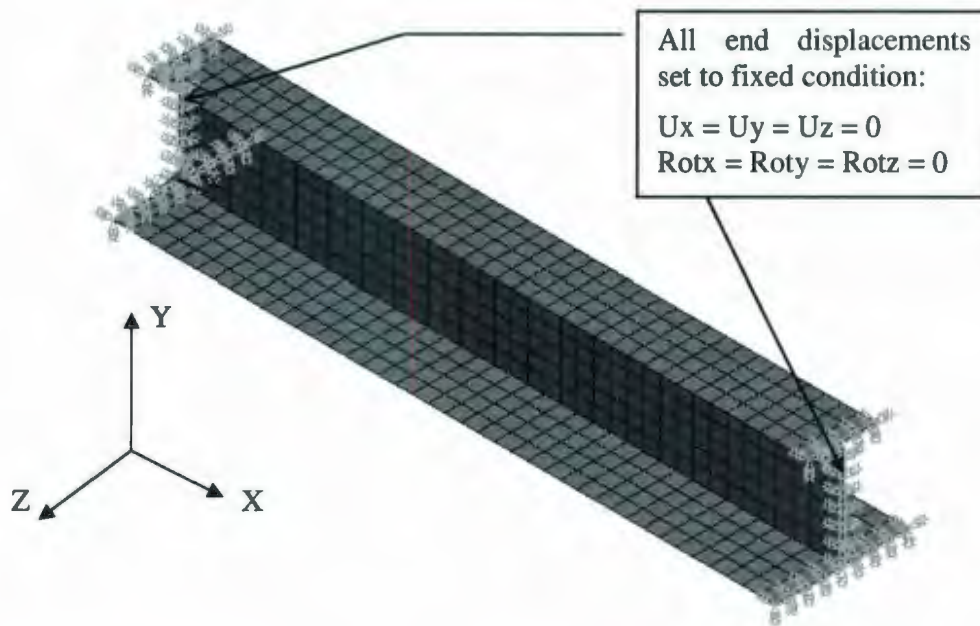


Figure 4.5.3: Fixed boundary condition at longitudinal ends

#### 4.5.4 Nonlinear analysis

A non-linear finite element analysis was carried out to find the response of the structure to the ice loading. Large deformation analysis usually encounters convergence issues; hence some refinements were done to achieve easier convergence.

The region near the application of load was defined with separate areas and very small elements were used. The region far away from the load application was modeled using larger elements. These modeling techniques resulted in faster solution without losing accuracy.

The material property was approximated as bi-linear with Young's modulus and post yield modulus as slopes in elastic and plastic region.

A large number of sub-steps were used such that load (pressure) was applied gradually.

#### 4.5.5 Result of finite element analysis

The major result of finite element analysis is the load vs. deflection of the frame. The capacity of the frame is estimated from the load-deflection behavior using the modified tangent intersection method.

The capacity of a structure can be defined as the load corresponding to a limit state. One of the limit states for a frame is the formation of three hinges. In an ideal case this is a situation where the deformation or strain increases infinitely without any appreciable increase in load. This hypothetical situation can be reached by an elastic perfectly plastic structure with no membrane effects. In real structures, this limit state does not occur due to strain hardening and membrane action of the plate.

#### 4.5.6 Modified tangent intersection method

The capacity of a frame can be defined by various methods. One of the most common methods used by the engineering industry is the tangent intersection method. Tangent intersection method describes the capacity as the load at which the elastic and plastic tangents intersect. This method is arbitrary as the slope in the plastic region is not a constant. There can be infinite number of possible tangents in the plastic region. A modification to the current method is proposed such that the ambiguity of slope at plastic region is avoided.

For defining the slope at the plastic region, two points along the response curve are required. The two points corresponds to the force which causes a permanent strain of 0.1% of span and 0.2% of span. A line connecting these two points is defined as the slope in the plastic region.

For finding the force causing permanent deformation of 0.1% and 0.2% of span, a line is drawn parallel to the initial elastic region at 0.1% L and 0.2% L (where L is the frame span). The intersection of these lines with the response curve gives the two required points.

Figure 4.5.4 presents the definition of capacity using modified tangent intersection method.

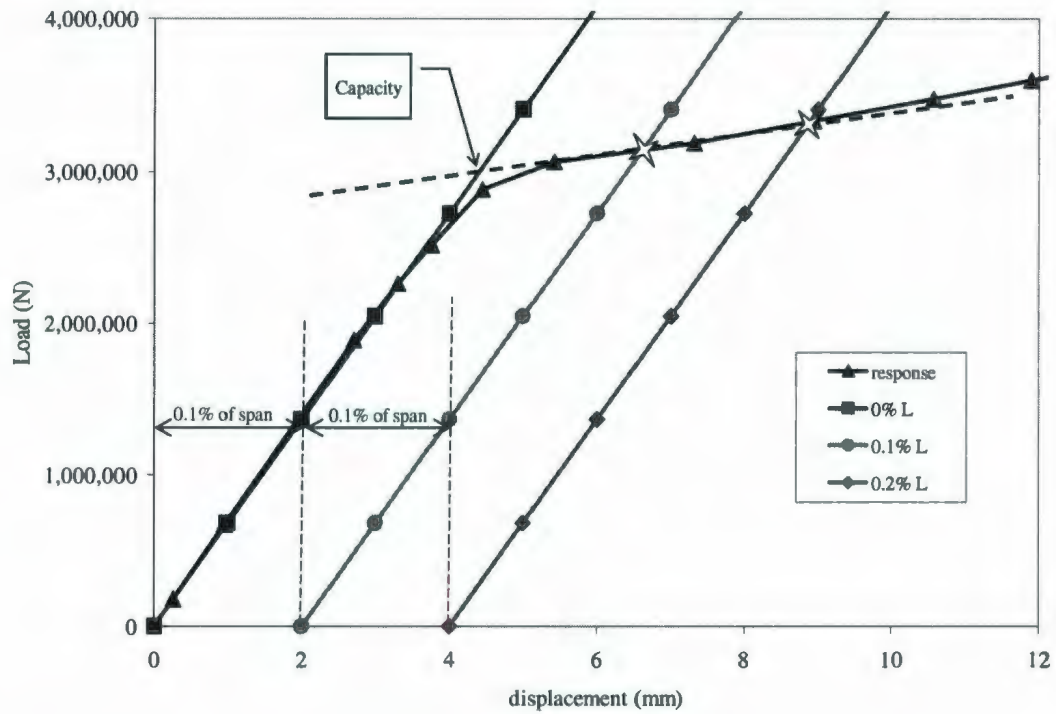


Figure 4.5.4: Definition of capacity using Modified Tangent Intersection Method

For situations where the capacity dropped due to web buckling, the highest value of capacity achieved before the drop was considered as the capacity of the frame.

#### 4.6 Analysis matrix

Table 4.6.1 presents the combinations generated by Design Expert software for a minimum run resolution V central composite design. The capacity of the frame for each run was found using ANSYS analysis. The output of ANSYS analyses is presented in Appendix-B1.

Table 4.6.1: Analysis matrix for capacity study

Run No.	web height	web ht/thk	flange width left	flange width right	flange thk	plate width	plate thk	plate length	yield	post yield modulus	Capacity (ANSYS)
1	200	27.5	80	80	26	450	25	3000	450	1000	842,500
2	600	15	10	10	12	300	40	4000	600	2000	7,100,000
3	200	15	10	150	40	600	40	4000	600	2000	1,720,000
4	400	27.5	80	80	26	450	25	2000	450	1000	2,060,000
5	600	40	150	10	40	600	10	2000	600	0	2,100,000
6	400	27.5	80	10	26	450	25	3000	450	1000	2,100,000
7	200	15	150	10	40	600	10	2000	300	2000	955,000
8	400	27.5	80	80	26	300	25	3000	450	1000	1,850,000
9	600	15	150	10	40	600	10	4000	300	0	2,600,000
10	200	40	150	150	12	600	10	2000	300	2000	361,000
11	200	40	150	150	40	600	40	4000	600	0	847,000
12	400	27.5	80	80	26	450	10	3000	450	1000	1,530,000
13	600	40	10	150	40	600	40	2000	300	2000	2,450,000
14	600	15	10	150	12	300	40	2000	600	0	7,300,000
15	600	40	150	10	40	300	40	2000	600	2000	3,800,000
16	200	15	10	10	40	300	40	2000	300	2000	750,000

Run No.	web height	web ht/thk	flange width left	flange width right	flange thk	plate width	plate thk	plate length	yield	post yield modulus	Capacity (ANSYS)
17	600	40	150	10	12	300	40	4000	600	0	3,200,000
18	200	40	10	150	12	600	40	4000	300	2000	255,000
19	400	27.5	150	80	26	450	25	3000	450	1000	2,300,000
20	600	40	10	10	12	600	40	2000	600	2000	3,700,000
21	200	15	10	10	12	600	10	4000	300	2000	195,000
22	600	15	150	150	40	300	10	2000	300	0	2,570,000
23	200	40	10	10	40	600	40	2000	300	0	440,000
24	400	27.5	80	80	26	450	25	3000	450	2000	2,250,000
25	200	40	150	10	12	600	10	4000	600	2000	390,000
26	200	15	150	10	40	300	10	4000	600	0	1,180,000
27	200	15	10	10	12	300	40	4000	300	0	240,000
28	400	27.5	80	150	26	450	25	3000	450	1000	2,250,000
29	400	27.5	80	80	26	450	25	3000	300	1000	1,620,000
30	400	27.5	80	80	26	450	40	3000	450	1000	2,980,000
31	600	15	150	10	12	600	10	2000	600	2000	5,200,000
32	600	40	150	150	12	300	40	2000	300	2000	2,000,000
33	600	15	10	150	40	300	10	4000	300	2000	2,900,000
34	200	40	10	150	12	300	10	2000	300	0	290,000
35	600	15	150	150	40	300	40	4000	300	2000	4,300,000
36	400	27.5	10	80	26	450	25	3000	450	1000	2,100,000
37	200	15	10	10	12	600	40	4000	600	0	490,000

Run No.	web height	web ht/thk	flange width left	flange width right	flange thk	plate width	plate thk	plate length	yield	post yield modulus	Capacity (ANSYS)
38	400	27.5	80	80	12	450	25	3000	450	1000	2,080,000
39	200	40	150	150	40	600	10	4000	300	0	383,000
40	200	40	10	150	12	300	10	4000	600	0	370,000
41	600	40	10	150	40	600	10	2000	600	0	2,100,000
42	400	27.5	80	80	26	450	25	4000	450	1000	2,350,000
43	600	15	10	150	40	300	40	2000	600	2000	7,400,000
44	200	15	150	150	12	300	10	4000	300	2000	560,000
45	600	40	150	10	12	300	10	4000	300	2000	1,300,000
46	200	15	10	150	40	300	10	2000	600	0	1,550,000
47	400	27.5	80	80	40	450	25	3000	450	1000	2,100,000
48	400	27.5	80	80	26	600	25	3000	450	1000	2,100,000
49	400	40	80	80	26	450	25	3000	450	1000	1,650,000
50	600	15	150	10	12	300	40	2000	300	0	3,900,000
51	200	15	150	150	12	600	40	2000	300	2000	1,030,000
52	600	15	10	150	40	600	40	4000	300	0	4,300,000
53	600	15	150	150	12	300	10	4000	300	0	2,550,000
54	400	27.5	80	80	26	450	25	3000	600	1000	2,750,000
55	400	27.5	80	80	26	450	25	3000	450	0	2,150,000
56	200	15	150	150	12	300	40	4000	600	0	1,400,000
57	200	40	10	150	40	300	40	4000	600	2000	770,000
58	600	27.5	80	80	26	450	25	3000	450	1000	3,000,000

Run No.	web height	web ht/thk	flange width left	flange width right	flange thk	plate width	plate thk	plate length	yield	post yield modulus	Capacity (ANSYS)
59	200	40	150	10	40	600	40	4000	300	2000	410,000
60	600	40	150	150	12	600	40	2000	300	0	2,100,000
61	200	40	10	10	12	300	40	2000	600	0	500,000
62	200	40	150	10	40	300	40	2000	300	0	450,000
63	200	15	150	150	12	600	10	2000	600	0	1,710,000
64	600	15	10	10	40	600	10	2000	600	0	4,700,000
65	200	40	10	10	40	300	10	4000	300	2000	182,000
66	400	15	80	80	26	450	25	3000	450	1000	3,450,000
67	600	40	150	150	12	600	40	4000	600	2000	4,350,000
68	200	15	150	10	40	600	40	2000	600	0	2,150,000
69	200	15	10	10	12	300	10	2000	600	2000	740,000
70	400	27.5	80	80	26	450	25	3000	450	1000	2,175,000
71	600	15	150	150	40	600	10	4000	600	0	5,100,000
72	200	40	150	150	40	300	10	2000	600	2000	720,000
73	600	40	10	10	12	300	10	2000	600	2000	1,800,000
74	600	15	10	150	12	600	10	2000	300	2000	2,800,000
75	600	40	10	10	12	600	10	4000	300	0	970,000
76	600	40	10	10	40	600	10	4000	600	2000	2,000,000
77	600	40	10	10	40	300	40	4000	300	0	1,915,000

#### 4.7 Capacity prediction model

The capacity of a frame for given set of geometric and material properties has been found using Design Expert™ software. The regression model has an adjusted R-squared of 0.99 and prediction R-squared of 0.98.

The capacity of a frame for given set of geometric and material properties is given by the following relation:

$$\begin{aligned} \text{Sqrt(Capacity)} &= -1065.17 + 5.12 * \text{Web Height} - 25.07 * \text{Web Height} / \text{Web Thickness} \\ &+ 0.93 * \text{Flange Width Left} + 2.15 * \text{Flange Width Right} \\ &+ 7.85 * \text{Flange Thickness} + 3.82 * \text{Frame Spacing} \\ &- 1.25 * \text{Plate Thickness} - 0.05 * \text{Span} + 0.88 * \text{Yield} \\ &- 0.05 * \text{Post Yield Modulus} - 0.03 * \text{Web Height} * \text{Web Height} / \text{Web Thickness} \\ &- 2.20\text{E-}003 * \text{Web Height} * \text{Flange Width Left} \\ &- 2.06\text{E-}003 * \text{Web Height} * \text{Flange Width Right} \\ &- 0.01 * \text{Web Height} * \text{Flange Thickness} \\ &+ 0.02 * \text{Web Height} * \text{Plate Thickness} \\ &+ 2.46\text{E-}004 * \text{Web Height} * \text{Span} + 1.88\text{E-}003 * \text{Web Height} * \text{Yield} \\ &- 0.02 * \text{Web Height} / \text{Web Thickness} * \text{Yield} \\ &- 4.64\text{E-}003 * \text{Flange Width Left} * \text{Flange Width Right} \\ &+ 1.83\text{E-}003 * \text{Flange Width Left} * \text{Yield} \\ &- 2.57\text{E-}004 * \text{Flange Width Right} * \text{Post Yield Modulus} \\ &- 1.42\text{E-}004 * \text{Frame Spacing} * \text{Span} - 1.33\text{E-}003 * \text{Plate Thickness} * \text{Span} \\ &+ 6.87\text{E-}003 * \text{Plate Thickness} * \text{Yield} \\ &+ 1.28\text{E-}003 * \text{Plate Thickness} * \text{Post Yield Modulus} \\ &+ 2.12\text{E-}005 * \text{Span} * \text{Post Yield Modulus} \\ &- 4.04\text{E-}003 * \text{Web Height}^2 + 0.54 * \text{Web Height} / \text{Web Thickness}^2 \\ &- 3.64\text{E-}003 * \text{Frame Spacing}^2 \end{aligned}$$

- Equation 4.3

The regression equation is quite long due to the statistical significance of the many factors and interactions of factors. The equation is best suited to be coded in some programming language like Matlab.

The actual vs. predicted values for the regression model is shown in Figure 4.7.1.

Design-Expert® Software  
Sqrt(Capacity)

Color points by value of  
Sqrt(Capacity):  
2720  
427

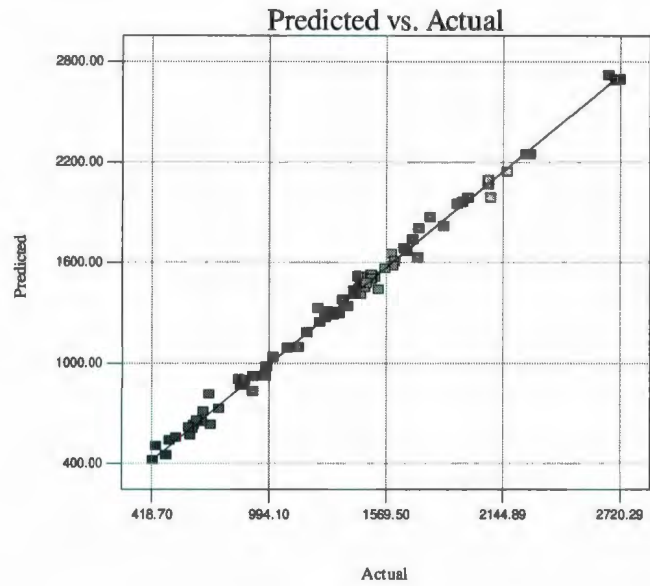


Figure 4.7.1: Predicted vs. Actual capacity

#### 4.8 Validation of capacity prediction model

The capacity prediction model has been independently checked against the results of finite element analysis for few randomly generated values of geometric and material properties. Results of the validation runs are given in Table 4.8.1. Appendix-B2 presents the output of ANSYS analyses.

Table 4.8.1: Validation runs of capacity

	Validation Run						
	V1	V2	V3	V4	V5	V6	V7
web height [mm]	492	598	390	542	337	554	318
web height/thickness	16	19	20	26	34	20	19
flange width left [mm]	122	101	17	58	79	38	140
flange width right [mm]	60	78	41	137	96	111	31
flange thickness [mm]	20	24	14	14	19	16	35
plate width [mm]	557	534	458	495	554	496	481
plate thickness [mm]	27	32	26	11	37	32	20
plate length [mm]	3082	3866	2230	3628	2209	3585	3398
yield strength [MPa]	495	511	499	342	313	313	450
post yield modulus [MPa]	109	600	268	605	717	443	302
Capacity [MN] (ANSYS)	4.00	5.00	2.80	1.60	1.30	2.90	2.00
Capacity [MN] (DOE) (Equation 4.3)	4.30	5.22	2.68	2.10	1.38	3.28	1.96
% Error	<b>7.49</b>	<b>4.34</b>	<b>-4.40</b>	<b>31.18</b>	<b>6.49</b>	<b>13.17</b>	<b>-1.77</b>
Capacity [MN] (IACS) (Equation 4.1 and 4.2)	6.71	8.13	3.17	2.69	1.20	3.78	2.78
% Error	<b>67.75</b>	<b>62.60</b>	<b>13.21</b>	<b>68.13</b>	<b>-7.69</b>	<b>30.34</b>	<b>39.00</b>

	Validation Run						
	V8	V9	V10	V11	V12	V13	V14
web height [mm]	247	341	582	600	600	200	600
web height/thickness	19	38	23	40	15	15	40
flange width left [mm]	122	91	127	150	150	10	10
flange width right [mm]	128	51	43	150	10	10	10
flange thickness [mm]	28	19	25	12	12	12	40
plate width [mm]	569	315	560	300	600	300	300
plate thickness [mm]	30	19	28	10	40	10	10
plate length [mm]	2607	3621	3406	2000	4000	2000	2000
yield strength [MPa]	489	416	455	600	300	300	300
post yield modulus [MPa]	1430	1229	1473	0	2000	0	0
Capacity [MN] (ANSYS)	2.00	0.95	3.50	1.83	4.45	0.41	0.95
Capacity [MN] (DOE) (Equation 4.3)	1.84	0.95	3.80	2.00	4.54	0.30	0.84
% Error	<b>-8.16</b>	<b>0.14</b>	<b>8.71</b>	<b>9.43</b>	<b>1.92</b>	<b>-24.86</b>	<b>-11.91</b>
Capacity [MN] (IACS) (Equation 4.1 and 4.2)	1.85	1.28	6.50	6.23	4.95	0.40	2.53
% Error	<b>-7.50</b>	<b>34.74</b>	<b>85.71</b>	<b>240.44</b>	<b>11.24</b>	<b>-1.23</b>	<b>166.32</b>

	Validation Run						
	V15	V16	V17	V18	V19	V20	V21
web height [mm]	600	200	600	200	600	600	200
web height/thickness	15	40	15	15	40	40	15
flange width left [mm]	150	150	10	10	150	10	150
flange width right [mm]	10	10	150	10	150	10	150
flange thickness [mm]	12	12	12	40	40	12	12
plate width [mm]	600	300	300	600	600	300	300
plate thickness [mm]	10	10	10	10	10	40	40
plate length [mm]	2000	2000	2000	2000	2000	2000	2000
yield strength[MPa]	300	300	300	300	300	300	300
post yield modulus [MPa]	0	0	0	0	0	0	0
Capacity [MN] (ANSYS)	2.38	0.29	2.40	0.61	0.96	1.90	1.04
Capacity [MN] (DOE) (Equation 4.3)	2.65	0.21	2.74	0.60	1.08	1.84	0.89
% Error	<b>11.29</b>	<b>-28.47</b>	<b>14.13</b>	<b>-0.84</b>	<b>13.26</b>	<b>-3.37</b>	<b>-13.96</b>
Capacity [MN] (IACS) (Equation 4.1 and 4.2)	6.32	0.35	5.68	0.54	3.10	2.79	0.92
% Error	<b>165.55</b>	<b>20.69</b>	<b>136.67</b>	<b>-10.74</b>	<b>224.61</b>	<b>46.84</b>	<b>-11.54</b>

The maximum error percentage associated with the new regression model is 31.18% (validation run 4) as compared to 240.44% (validation run 11) for the current IACS rule.

A graphical comparison of the results of the validation study is presented in Figure 4.8.1. The validation study has shown that the new regression model estimates capacity within reasonable error margins (less than 32%) for most of the cases. The current IACS rule has however produced much higher percentage errors.

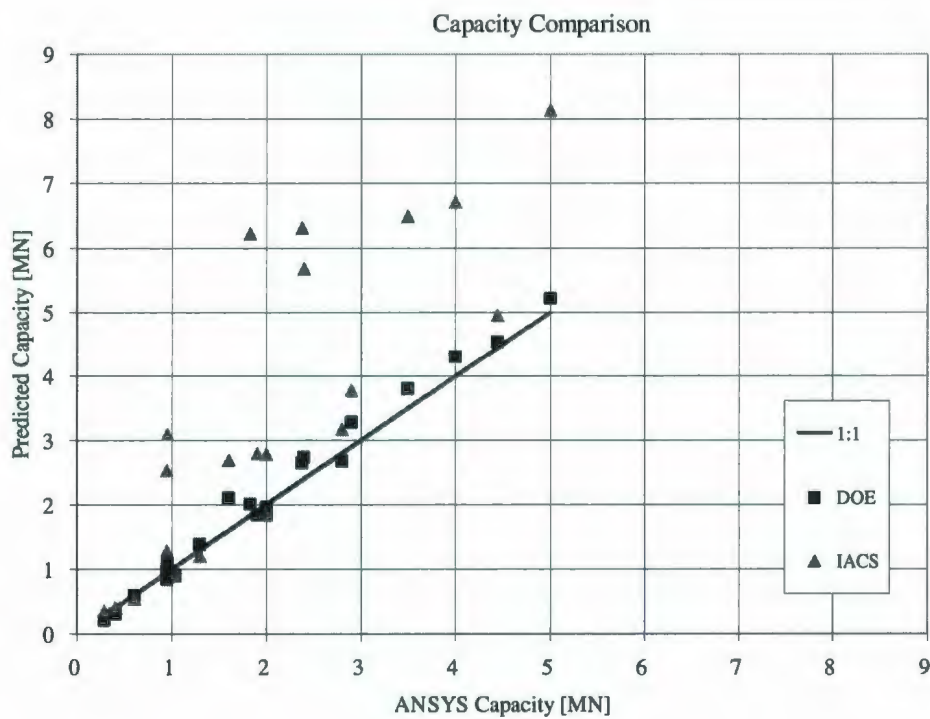


Figure 4.8.1: Predicted vs. Actual capacity

## 4.9 Major factors affecting capacity

Figures 4.9.1 to 4.9.9 presents the effect of various factors on the load carrying capacity of a frame. The units of the various factors shown in the figures are as follows:

web height	mm
flange width left	mm
flange width right	mm
flange thickness	mm
plate width	mm
plate thickness	mm
plate length	mm
yield strength	MPa
post yield modulus	MPa
Capacity	N

### 4.9.1 Capacity vs. web height

Design-Expert® Software  
Original Scale  
Capacity

● Design Points

X1 = A: Web Height

Actual Factors

B: Web Ht / Web Thk = 28

C: Flange Width Left = 80.00

D: Flange Width Right = 80.00

E: Flange Thickness = 26.00

F: Frame Spacing = 450.00

G: Plate Thickness = 25.00

H: Span = 3000.00

J: Yield = 450.00

K: Post Yield Modulus = 1000.00

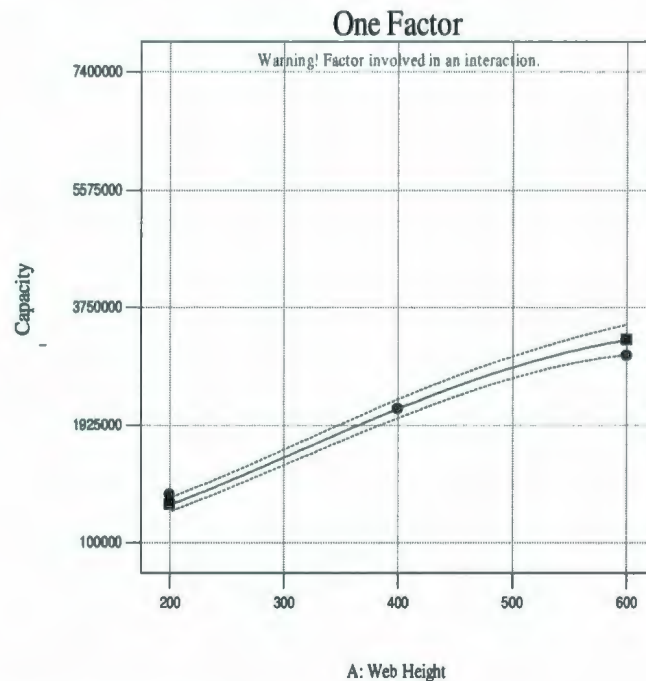


Figure 4.9.1: Capacity vs. web height

Figure 4.9.1 shows that the capacity of a frame increases with increase in web height.

## 4.9.2 Capacity vs. web height / web thickness

Design-Expert® Software  
Original Scale  
Capacity

● Design Points

X1 = B: Web Ht / Web Thk

Actual Factors

A: Web Height = 400  
C: Flange Width Left = 80.00  
D: Flange Width Right = 80.00  
E: Flange Thickness = 26.00  
F: Frame Spacing = 450.00  
G: Plate Thickness = 25.00  
H: Span = 3000.00  
J: Yield = 450.00  
K: Post Yield Modulus = 1000.00

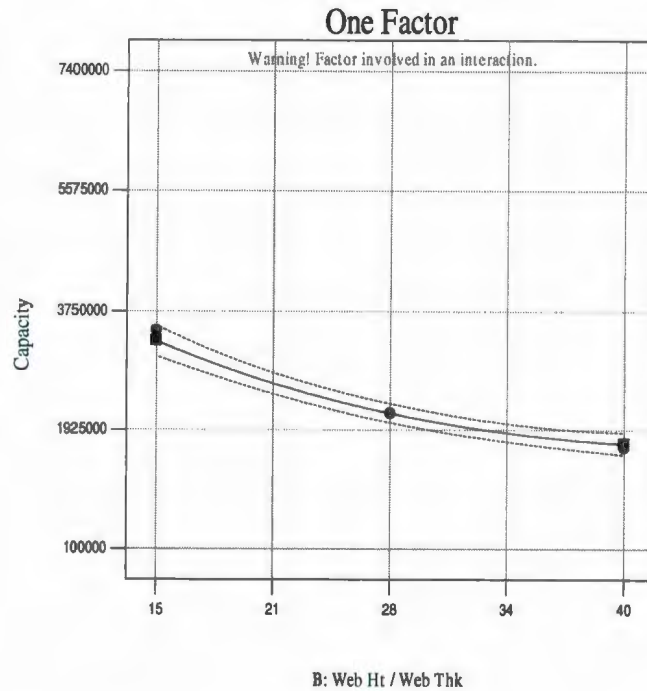


Figure 4.9.2: Capacity vs. web height / web thickness

Figure 4.9.2 shows that the capacity of a frame increases with decrease in web height to web thickness ratio (or increase in web thickness).

### 4.9.3 Capacity vs. shell thickness

Design-Expert® Software  
Original Scale  
Capacity

- Design Points

X1 = G: Plate Thickness

Actual Factors  
A: Web Height = 400  
B: Web Ht / Web Thk = 28  
C: Flange Width Left = 80.00  
D: Flange Width Right = 80.00  
E: Flange Thickness = 26.00  
F: Frame Spacing = 450.00  
H: Span = 3000.00  
J: Yield = 450.00  
K: Post Yield Modulus = 1000.00

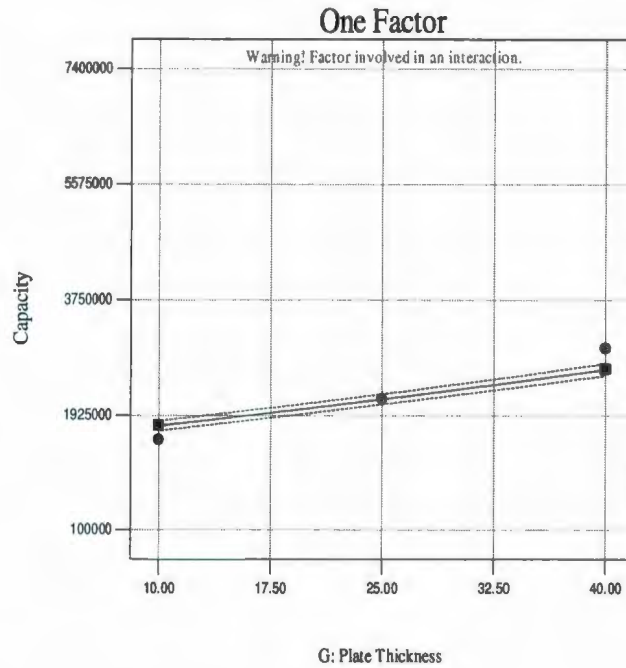


Figure 4.9.3: Capacity vs. shell thickness

Figure 4.9.3 shows that the load carrying capacity of a frame increases with increase in plate thickness.

#### 4.9.4 Capacity vs. yield strength

Design-Expert® Software  
Original Scale  
Capacity

● Design Points

X1 = J: Yield

Actual Factors

A: Web Height = 400  
B: Web Ht / Web Thk = 28  
C: Flange Width Left = 80.00  
D: Flange Width Right = 80.00  
E: Flange Thickness = 26.00  
F: Frame Spacing = 450.00  
G: Plate Thickness = 25.00  
H: Span = 3000.00  
K: Post Yield Modulus = 1000.00

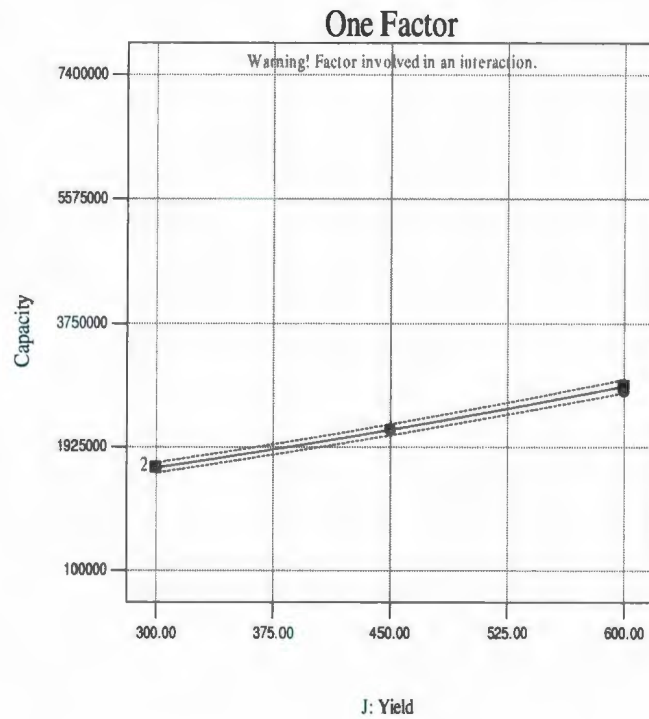


Figure 4.9.4: Capacity vs. yield strength

Figure 4.9.4 shows that the load carrying capacity of a frame increases with increase in yield strength.

#### 4.9.5 Interaction of web height and web height / thickness

Design-Expert® Software  
 Original Scale  
 Capacity

● Design Points  
 ■ B- 15.000  
 ▲ B+ 40.000

X1 = A: Web Height  
 X2 = B: Web Ht / Web Thk

Actual Factors  
 C: Flange Width Left = 80.00  
 D: Flange Width Right = 80.00  
 E: Flange Thickness = 26.00  
 F: Frame Spacing = 450.00  
 G: Plate Thickness = 25.00  
 H: Span = 3000.00  
 J: Yield = 450.00  
 K: Post Yield Modulus = 1000.00

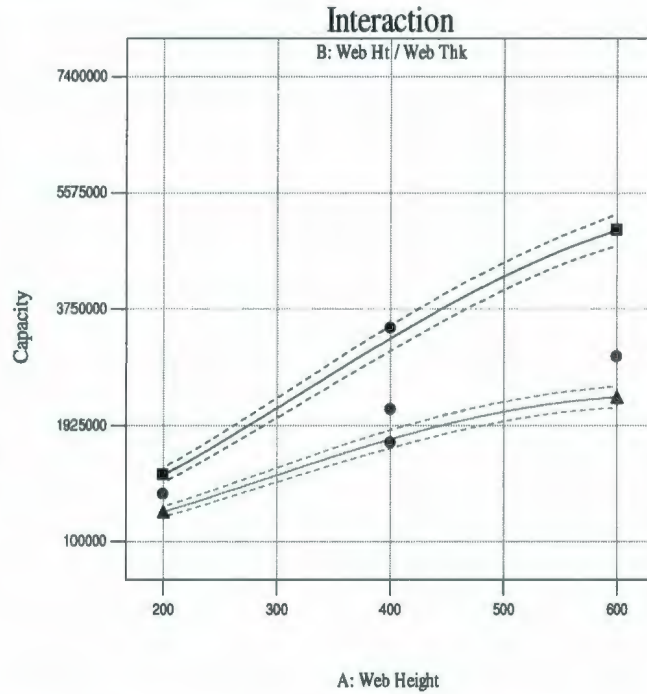


Figure 4.9.5: Interaction of web height and web height / thickness

Figure 4.9.5 shows that the rate of increase of capacity for increase in web height depends on the web thickness. For higher web thickness (or lower web height to thickness ratio), the rate of increase is more.

#### 4.9.6 Interaction of web height and plate thickness

Design-Expert® Software  
Original Scale  
Capacity

- Design Points
- G- 10.000
- ▲ G+ 40.000

X1 = A: Web Height  
X2 = G: Plate Thickness

Actual Factors

- B: Web Ht / Web Thk = 28
- C: Flange Width Left = 80.00
- D: Flange Width Right = 80.00
- E: Flange Thickness = 26.00
- F: Frame Spacing = 450.00
- H: Span = 3000.00
- J: Yield = 450.00
- K: Post Yield Modulus = 1000.00

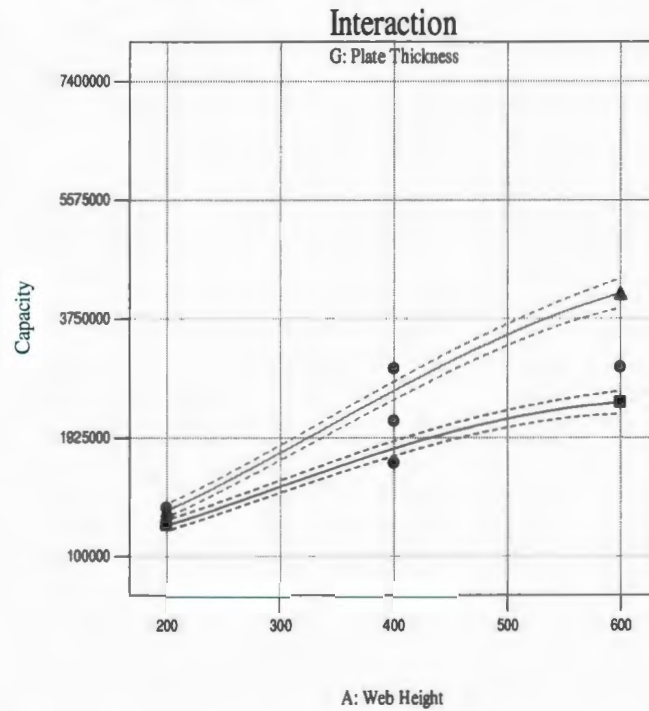


Figure 4.9.6: Interaction of web height and plate thickness

Figure 4.9.6 shows that the rate of increase of capacity for increase in web height depends on the plate thickness. For higher plate thickness, the rate of increase is more.

#### 4.9.7 Interaction of web height and yield strength

Design-Expert® Software  
Original Scale  
Capacity

- Design Points
- J- 300.000
- ▲ J+ 600.000

X1 = A: Web Height  
X2 = J: Yield

Actual Factors  
B: Web Ht / Web Thk = 28  
C: Flange Width Left = 80.00  
D: Flange Width Right = 80.00  
E: Flange Thickness = 26.00  
F: Frame Spacing = 450.00  
G: Plate Thickness = 25.00  
H: Span = 3000.00  
K: Post Yield Modulus = 1000.00

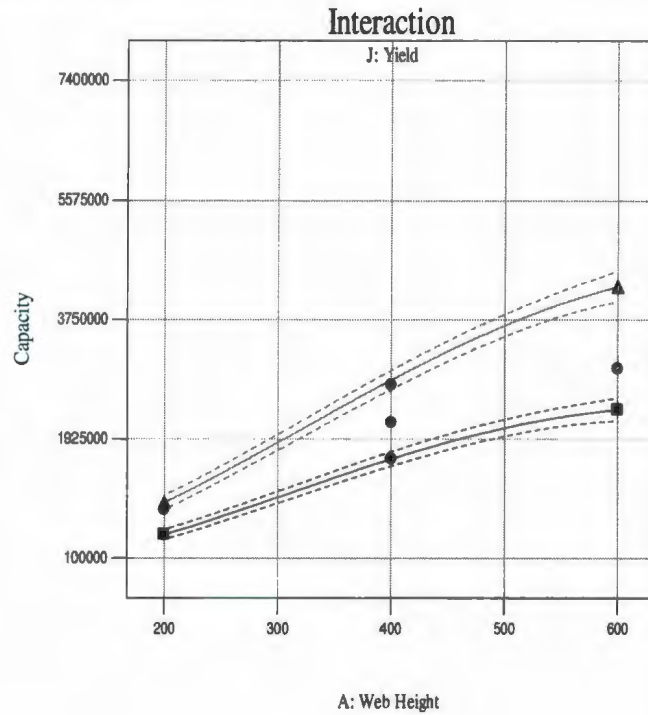


Figure 4.9.7: Interaction of web height and yield strength

Figure 4.9.7 shows that the rate of increase of capacity for increase in web height depends on the yield strength of the material. For higher yield strength, the rate of increase is more.

#### 4.9.8 Interaction of web height / thickness and yield strength

Design-Expert® Software  
 Original Scale  
 Capacity

● Design Points

■ J- 300.000  
 ▲ J+ 600.000

X1 = B: Web Ht / Web Thk  
 X2 = J: Yield

Actual Factors  
 A: Web Height = 400  
 C: Flange Width Left = 80.00  
 D: Flange Width Right = 80.00  
 E: Flange Thickness = 26.00  
 F: Frame Spacing = 450.00  
 G: Plate Thickness = 25.00  
 H: Span = 3000.00  
 K: Post Yield Modulus = 1000.00

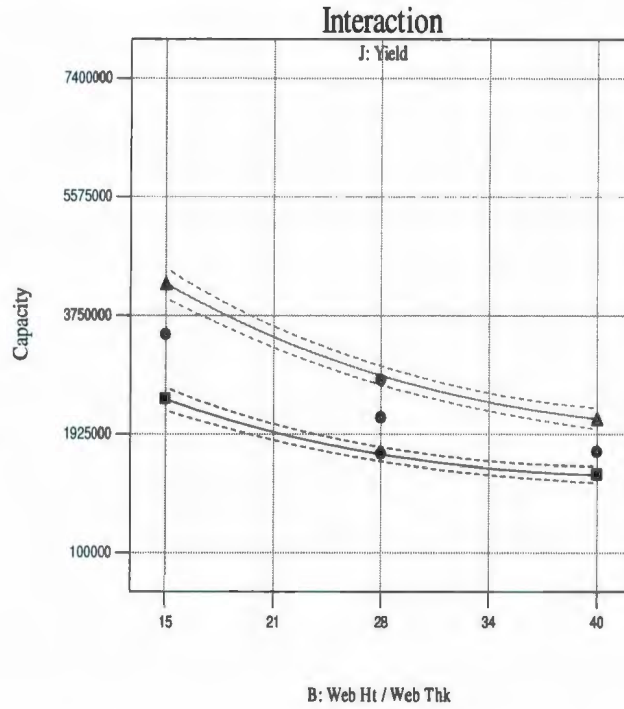


Figure 4.9.8: Interaction of web height / thickness and yield strength

Figure 4.9.8 shows that the rate of increase of capacity for increase in web thickness depends on the yield strength of material. For higher yield strength, the rate of increase is more.

#### 4.9.9 Interaction of plate thickness and yield strength

Design-Expert® Software  
 Original Scale  
 Capacity

● Design Points  
 ■ J- 300.000  
 ▲ J+ 600.000

X1 = G: Plate Thickness  
 X2 = J: Yield

Actual Factors  
 A: Web Height = 400  
 B: Web Ht / Web Thk = 28  
 C: Flange Width Left = 80.00  
 D: Flange Width Right = 80.00  
 E: Flange Thickness = 26.00  
 F: Frame Spacing = 450.00  
 H: Span = 3000.00  
 K: Post Yield Modulus = 1000.00

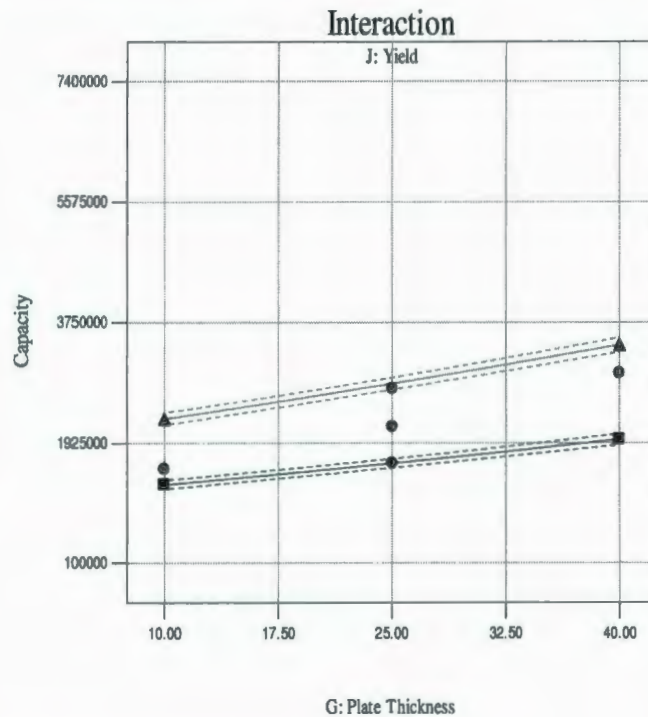


Figure 4.9.9: Interaction of plate thickness and yield strength

Figure 4.9.9 shows that the rate of increase of capacity for increase in plate thickness depends on the yield strength of material. For higher yield strength, the rate of increase is more.

#### 4.10 Conclusions

The DOE method has shown to be a useful tool in studying multi-factored systems with manageable number of numerical simulations. The method is particularly useful in situations where a full analytical solution is difficult to achieve due to the complexities involved. The confidence level in the regression equation produced by DOE can be increased by validating using independent FEA, which has been the approach used in the present study.

A regression equation has been generated using techniques of DOE for predicting capacity of frames with different stiffener forms. Even though the regression equation has the inherent deficiency of not representing any physical failure modes or the limited range of application, it offers a quick and reasonably accurate estimation of capacity. The capacity of various stiffener forms (like flat bar, angle and tee) are captured in the same equation such that the same equation can be used to estimate capacity of various types of frames.

The validation of the new regression equation has shown that it estimates capacity within lower error percentages (less than 32%) compared to IACS equation. The current IACS rule produced much higher percentage errors (maximum of 240% error for the cases studied). The major reason for this large error in IACS estimation is the fact that only certain failure modes are considered in IACS rule equations.

The major factors affecting capacity have also been found out using the parametric study.

The capacity of a frame generally increases with

- Increase in web height.
- Decrease in web height to web thickness ratio (or increase in web thickness).
- Increase in plate thickness.
- Increase in yield strength.

The rate of increase of capacity for increase in web height depends on the web thickness. For higher web thickness (or lower web height to thickness ratio) the rate of increase is more.

The rate of increase of capacity for increase in web height depends on the plate thickness. For higher plate thickness the rate of increase is more.

The rate of increase of capacity for increase in web height depends on the yield strength of material. For higher yield strength, the rate of increase is more.

The rate of increase of capacity for increase in web thickness depends on the yield strength of material. For higher yield strength, the rate of increase is more.

The rate of increase of capacity for increase in plate thickness depends on the yield strength of material. For higher yield strength, the rate of increase is more.

## 5 STABILITY OF FLAT BAR STIFFENER

### 5.1 Introduction

The total capacity of a frame is contributed by the shell plate and the stiffener. Some stiffener forms show tendency for local failure at very large deformations, thereby resulting in a reduction in total capacity. The three major local failure mechanisms in the case of a stiffener are local web buckling, tripping and shear buckling. These failures are critical and can result in structural collapse due to sudden loss of capacity.

Local web buckling (Figure 5.1.1) occurs as a result of direct compression of the web due to applied concentrated load. Lateral torsional buckling or tripping (Figure 5.1.2) occurs when the stiffener twists about the line of attachment to the shell plate. The stiffener susceptible to tripping will have high bending rigidity and low torsional rigidity. Shear buckling occurs typically in deep and thin webs.

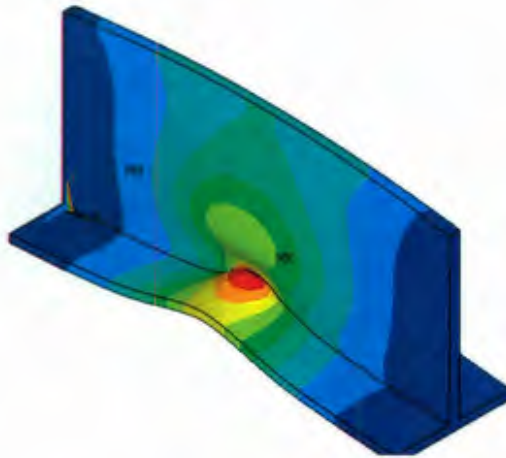


Figure 5.1.1: Local web buckling

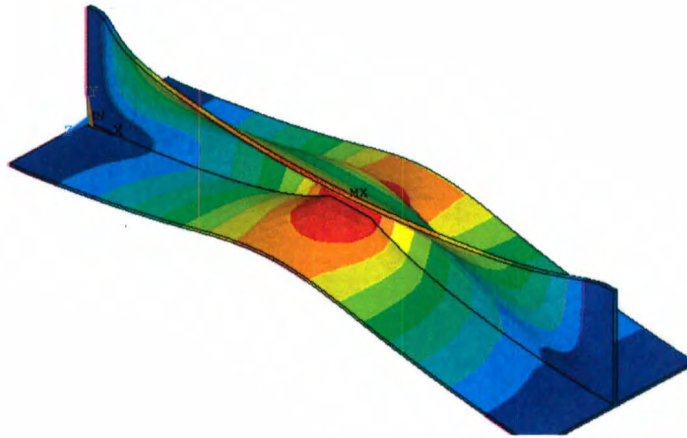
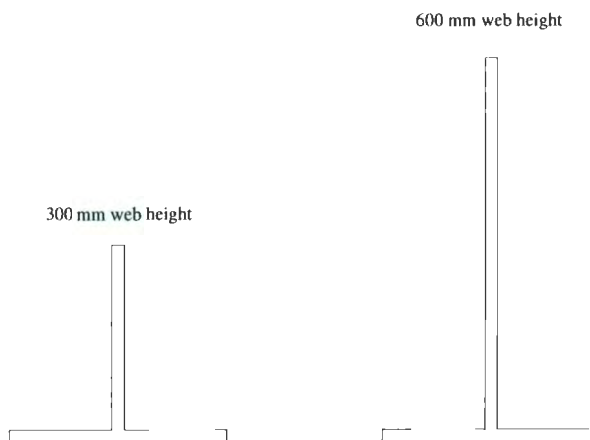


Figure 5.1.2: Lateral torsional buckling or tripping

Consider two frames as shown in Figure 5.1.3. The frames have different web heights (300 mm and 600 mm respectively) but all other geometric and material properties are the same.



Frame span = 2000 mm; Plate = 350 mm x 20 mm; Web thickness = variable  
 $E = 2,000,000$  MPa;  $E_t = 2,000$  MPa; Yield Strength = 300 MPa

Figure 5.1.3:: Two frames with different web heights

The responses of these frames to a concentrated patch load are presented in Figures 5.1.4 and 5.1.5. The frame with 300 mm web height shows stable load carrying characteristics even at large  $h_w/t_w$  ratios (i.e., small web thicknesses). The frame with 600 mm web height at large  $h_w/t_w$  ratios becomes unstable resulting in sudden drop in capacity.

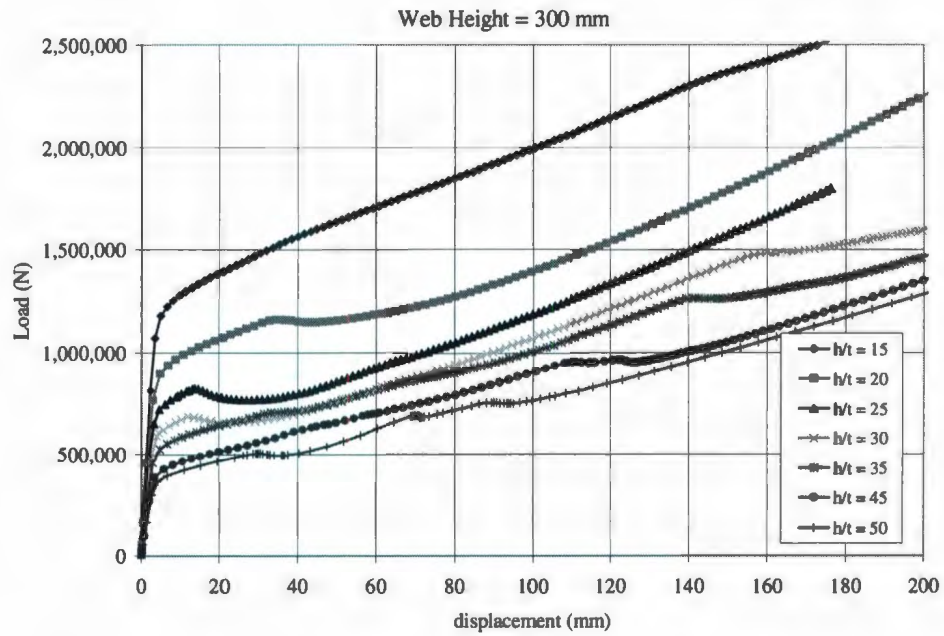


Figure 5.1.4: 300 mm web height frame (capacity vs.  $h_w/t_w$  ratio)

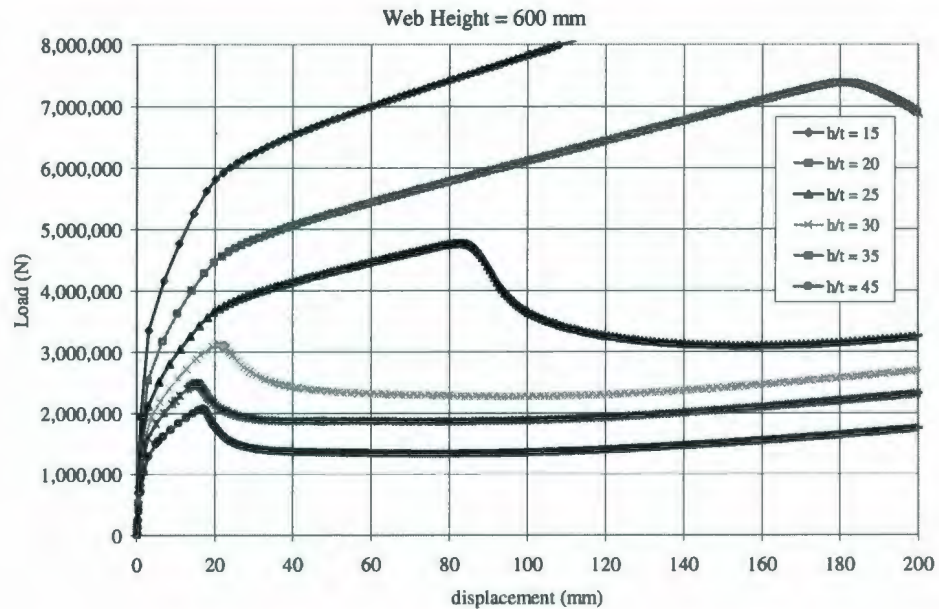


Figure 5.1.5: 600 mm web height frame (capacity vs.  $h_w/t_w$  ratio)

The result shows that, tall and thin stiffeners tend to locally fail resulting in sudden drop in capacity whereas short stiffeners tend to be stable even with small web thickness. This demonstrates that yield strength is not the only factor which affects stability of a stiffener as postulated by design rules. There could be more factors like span, frame spacing and thicknesses which might affect stability in addition to the yield strength.

The current IACS UR-I2 Polar rules (and various rules of classification societies) try to prevent web instabilities by specifying a maximum slenderness ratio ( $h_w/t_w$ ). These ratios are formulated so that the stiffener will not locally fail before yielding occurs. The current rule limiting  $h_w/t_w$  values depends only on the yield strength of the material. Current classification society rule limits of  $h_w/t_w$  for various stiffeners forms are presented in Table 5.1.1.

Non-linear analyses of the elasto-plastic response of flat bars to lateral loads have shown that the limits given by classification society rules are very conservative, particularly in

the case of a flat bar stiffener for the type of loading considered. Flat bar stiffeners can exhibit stable response even when considerably more slender than the allowed limits given in Table 5.1.1.

Table 5.1.1:  $h_w/t_w$  limits

	Flat Bar	Tee	Angle
IACS	$282/\sqrt{\sigma_y}$	$805/\sqrt{\sigma_y}$	$805/\sqrt{\sigma_y}$
ABS	$226/\sqrt{\sigma_y}$	$679/\sqrt{\sigma_y}$	

For practical ranges of yield strength for ship building steel, the  $h_w/t_w$  limit for flat bar stiffener based on IACS rule ranges from 12 to 18, corresponding to yield strength values of 500 MPa and 250 MPa respectively. The small  $h_w/t_w$  ratio limits the usage of tall flat bar sections without increasing the web thickness. The thickness of the stiffener is controlled by the thickness of the shell plate to which it is attached due to welding considerations. The combined effect of maximum allowable web thickness and maximum allowable  $h_w/t_w$  ratios limits the usage of a flat bar stiffener. Other stiffener forms like angle, bulb or T are to be used instead of a flat bar stiffener. Most of the sections suitable to stiffen a polar class vessel are much heavier than the cold formed sections produced by mills and hence will require expensive welding to create the required angle or T stiffeners. Welding will result in increase in fabrication time and cost.

The main factor hindering the wide spread use of flat bar stiffener is the  $h_w/t_w$  limit. Consequently, an investigation was carried out to check the possibility of increasing the rule  $h_w/t_w$  limits. In the absence of an analytical solution explaining the stability of a stiffener, combined use of finite element method (FEM) and design of experiment (DOE) was used in the study.

The aims of the study were:

- to identify the major factors that affects the stability of a flat bar stiffened plate

- study the various interactions between main factors
- to find simple regression equations to predict the maximum allowable web height and web height to thickness ( $h_w/t_w$ ) ratio
- validate the regression equations for accuracy

## **5.2 Factors considered for the study**

Stability of a flat bar stiffener is affected by a large number of factors – geometric, material property, loading type, boundary condition etc. The main geometric factors considered for the study are:

- Frame span
- Frame spacing
- Shell plate thickness
- Web height
- Web thickness

The main material properties considered for the study are:

- Yield strength
- Post yield modulus

The thickness of web is usually dictated by shell plate thickness due to welding considerations. The web thickness is specified as a percentage of the shell thickness. For the present study the ratio of web thickness to shell plate thickness is considered to be between 0.6 and 1.3. This corresponds to a web thickness of 6mm to 13mm for a shell plate thickness of 10 mm.

### 5.3 Design space

Stiffened plate can occur in various combinations of geometric and material properties. The total number of factors which influence stability of a flat bar stiffener is identified as six - four geometric factors and two material properties. The ranges of each factor considered for the study are presented in Table 5.3.1. The range of each factor was chosen such that it covers the practical range of stiffener properties found in ice capable vessels.

Table 5.3.1: Design space for stability study

	<b>Factor</b>	<b>low</b>	<b>high</b>
1	Frame span [mm]	2000	4000
2	Frame spacing [mm]	300	600
3	Plate thickness [mm]	10	40
4	Yield Strength [MPa]	250	500
5	Post yield modulus [MPa]	0	2000
6	Web thickness / plate thickness	0.6	1.3

The study of these six factors at two levels (at high and low values of each factor) will result in 64 ( $2^6$ ) possible combinations. Each combination requires an average of five trials to find the maximum allowable web height, making a total of 320 FEA analyses. Considering an average solution time of ten hours, the total time and effort required to carry out such an exercise will become enormous thereby making it practically impossible.

In order to overcome the requirement of large number of experiments (numeric simulations), principles of design of experiments (DOE) is utilized.

#### **5.4 Design of Experiment**

The Design of Experiments (DOE) method is a useful tool in studying multi-factored systems with manageable number of numerical simulations. The method is particularly useful in situations where a full analytical solution is difficult to achieve due to the complexities involved. A detailed discussion about DOE method is presented in Section 4.4.

The fractional factorial design (FFD) is an important class of DOE, which is used to screen the important factors affecting a system. FFD is categorized into different design resolutions according to the alias patterns it produces. Some of the commonly used design resolutions are III, IV and V.

Design resolution V has no main effect or two factor interaction aliased with any other main effect or two-factor interaction. Two-factor interactions are only aliased with three-factor interactions. The main effects and two factor interactions are resolved and hence resolution V is an efficient method for reducing number of runs.

The number of experiments required to study the six factored problem using a minimum run resolution V design is 22, compared to 64 experiments required for two-level factorial approach. The combinations of factors are generated using Design Expert™ software.

The details of experiment are given in Section 5.7

## **5.5 Finite element analysis**

### **5.5.1 Finite element**

The validation study of large grillage experiment (Chapter 2) has shown that shell elements tend to deform excessively, even though the capacity predictions were in good agreement. The shell element showed excessive deformation, particularly in the region of intersection of web and plate. The reason for the excessive deformation was found to be the absence of weld connecting web and shell in the model, which provides rotational restraint to the web. Including weld will result in complicating modeling and hence an easier solution is to use solid elements which have shown good agreement in predicting deflection as well as capacity. Solid model takes longer time to solve compared to shell element, hence in order to reduce analysis time larger elements were used except for regions of large deformations.

Solid92 has been used to model the structure. For the details of the element, refer to Section 2.4.2.1

### **5.5.2 Loading**

The study explores the stability of a flat bar stiffener subjected to an ice loading. Ice load manifests itself as areas of localized high pressure surrounded by regions of lower pressure. The local structure should be strong enough to withstand these high pressures.

The nodes located at the center of the frame within a small area (150mm x 150mm) are given a vertical prescribed displacement of 10% of the frame span. This simulates displacement of nodes due to a concentrated ice pressure from a ship-ice collision.

Loading considered for the analysis are presented in Figure 5.5.1.

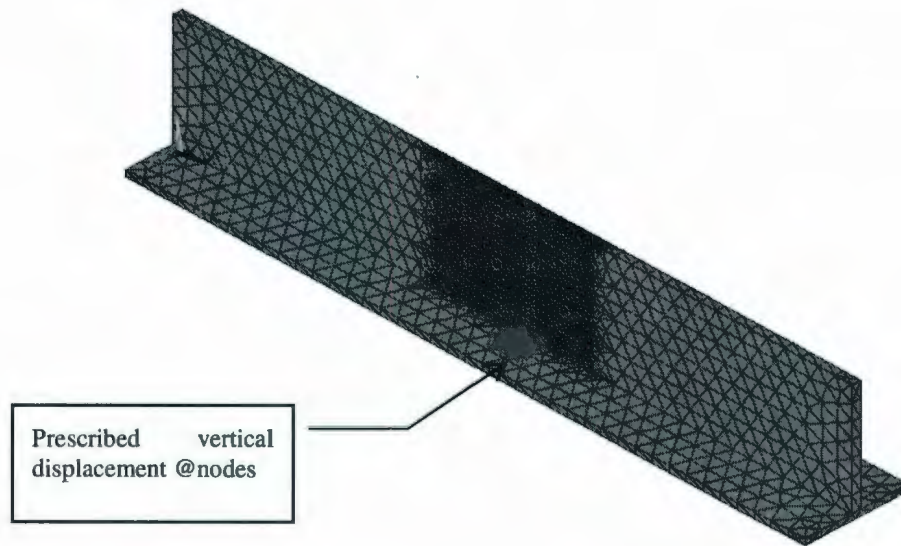


Figure 5.5.1: Loading considered for stability study

### 5.5.3 Boundary conditions

The side shell structure of a longitudinally framed ship is considered for the study. Results of load sharing in a grillage (Chapter 3) have shown that capacity predictions using single frame are in good agreement with that of a large grillage. A single frame is only considered for the study in order to reduce the analysis time.

The two longitudinal ends are fixed which idealizes the support provided by stringers. The two transverse sides of the shell plate are given symmetric boundary condition to simulate support provided by the adjacent structure.

Boundary conditions considered for the analysis are presented in Figure 5.5.2 and Figure 5.5.3.

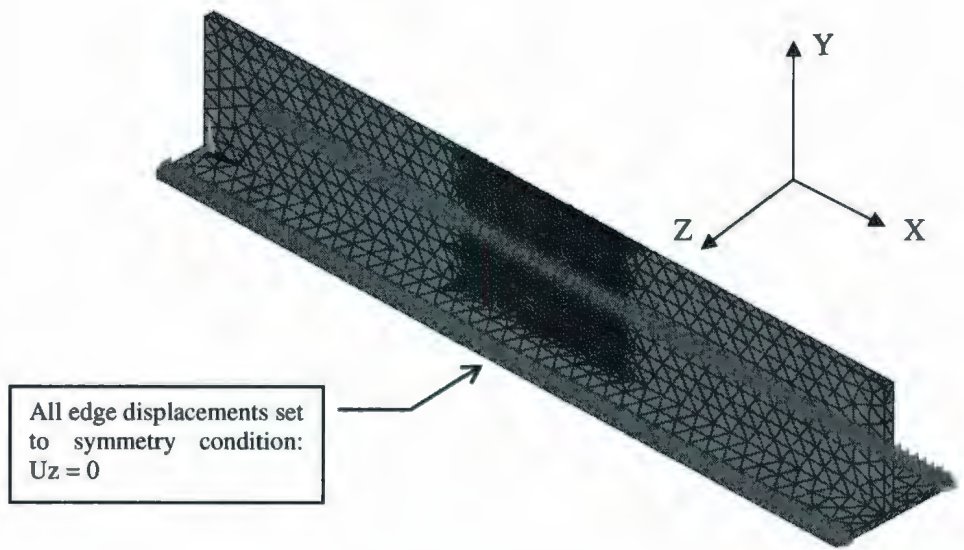


Figure 5.5.2: Symmetric boundary condition at transverse edges

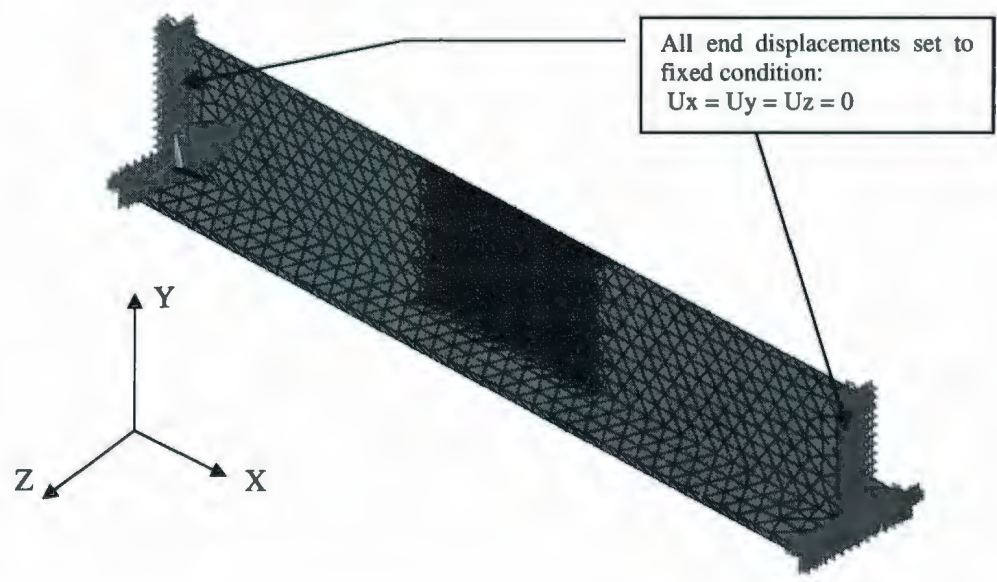


Figure 5.5.3: Fixed boundary condition at longitudinal ends

#### 5.5.4 Nonlinear analysis

A non-linear finite element analysis was carried out to find the response of the structure to an ice collision loading. Large deformation analysis usually encounters convergence issues; hence some refinements were required to achieve easier convergence.

In order to reduce analysis time, large elements were used wherever possible and small elements at locations where large deformations were expected. The web near the application of load was refined to accommodate large sideways deformation. In case of shear buckling failure, the whole web was refined using small elements because shear buckling occurred near the support location and covered large areas.

A large number of sub-steps were used such that load (prescribed displacement) was applied gradually.

The default iterative scheme of Newton-Raphson was used to solve simultaneous non-linear equations. Other iterative schemes were only used once Newton-Raphson failed to converge. Solution enhancement features like line search, bisection and automatic load stepping were used as permitted by the selected iterative scheme.

The reactions at supporting nodes were summed up to get the total applied force, for each load step. The deformation of the center node was extracted from post processor. A macro was used to sum up the nodal reactions and extract the deformations of the center node.

## 5.6 Defining stability

The flat bar stiffener can sometimes accommodate very large deformations without sudden drop in capacity, even after the three-hinge formation. The drop in capacity due to stiffener failure is compensated by the growing membrane action of the plate and post yield modulus, thus making the frame stable. The present study is based on defining a frame as stable in situations where the capacity drop is less than or equal to 10%. Even though the stiffener at large deformations may have experienced local buckling or various types of local folding and stretching, only when the drop in capacity is more than 10% is the frame considered to be unstable.

Figure 5.6.1 shows the response of a frame for increasing web heights. All other geometric and material properties are kept constant. An increase in web height results in an increase in the capacity of the frame, but the stability characteristics at large deformations may not be good. At some critical height the web becomes increasingly unstable resulting in sudden drop in capacity.

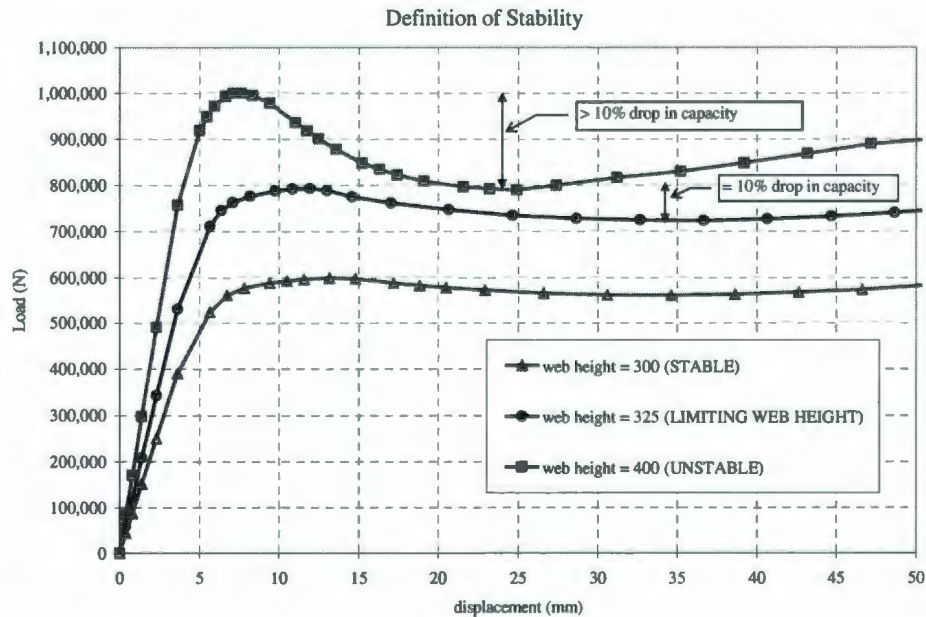


Figure 5.6.1: Definition of stability

Table 5.6.1: Stability vs. web height

Web height [mm]	Drop in capacity (%)	Remarks
300	4 %	Stable
325	10 %	Limiting web height
400	20 %	Unstable

Table 5.6.1 summarizes the effect of web height on stability of the frame. Based on the above results, the limiting web height for the frame is estimated as 325 mm. An increase in web height will result in frame becoming unstable, i.e., the drop in capacity of more than 10%.

The analysis starts with a conservative initial guess of web height. Subsequent web height increase is based on the stability nature of the force-displacement curve. A limiting value of web height was found, such that any further increase in web height will result in unstable frame i.e., more capacity drop.

## 5.7 Analysis matrix

Table 5.7.1 presents the combinations generated by Design Expert software for a minimum run resolution V fractional factorial design. The limiting web height for each run was found using ANSYS analysis. Appendix-C1 presents the output of ANSYS analyses.

Table 5.7.1: Analysis matrix for stability study

DOE Run No	Length (mm)	Frame Spacing (mm)	Plate Thk (mm)	Yield (MPa)	Post Yield Modulus (MPa)	Web / Plate Thk	Web Height (ANSYS)	Web height/thk (ANSYS)
1	4000	600	40	250	0	0.6	660	27.50
2	2000	300	10	250	0	1.3	300	23.08
3	2000	600	10	250	2000	1.3	410	31.54
4	4000	600	10	250	0	0.6	420	70.00
5	4000	600	40	250	0	1.3	1000	19.23
6	4000	600	40	250	2000	0.6	825	34.38
7	2000	300	40	250	2000	1.3	850	16.35
8	2000	300	40	500	2000	0.6	575	23.96
9	2000	300	10	500	0	0.6	300	50.00
10	2000	600	10	500	0	1.3	325	25.00
11	4000	600	40	500	0	0.6	600	25.00
12	4000	600	10	500	2000	1.3	500	38.46
13	4000	300	10	500	2000	0.6	250	41.67
14	2000	600	40	250	0	0.6	600	25.00
15	4000	300	10	500	0	1.3	400	30.77

DOE Run No	Length (mm)	Frame Spacing (mm)	Plate Thk (mm)	Yield (MPa)	Post Yield Modulus (MPa)	Web / Plate Thk	Web Height (ANSYS)	Web height/thk (ANSYS)
16	2000	600	40	500	2000	1.3	850	16.35
17	2000	600	10	500	2000	0.6	325	54.17
18	4000	300	40	500	2000	1.3	925	17.79
19	4000	300	40	250	0	0.6	500	20.83
20	4000	300	10	250	2000	1.3	500	38.46
21	2000	300	10	250	2000	0.6	325	54.17
22	2000	300	40	500	0	1.3	1000	19.23

## 5.8 Results of stability study

### 5.8.1 Major factors affecting web height

Figure 5.8.1 presents the half-normal probability plot of the web height study. The main factors affecting the maximum allowable web height are shell plate thickness (factor C) and web thickness (factor F).

The current design rule limits the maximum web height based on material yield strength alone. An interesting conclusion of the study is that the maximum allowable web height of a frame is independent of material yield strength. The main factors affecting the web height of a frame are the geometric parameters like shell plate thickness and web thickness.

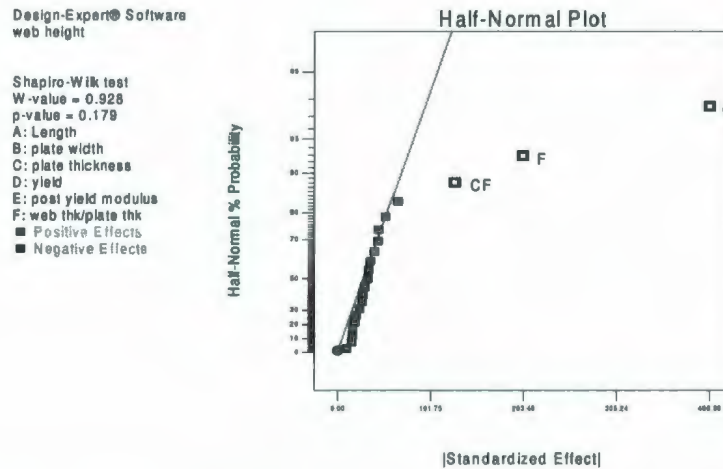


Figure 5.8.1: Half normal plot of web height study

### 5.8.2 Web height prediction

The maximum web height that can be achieved for a given set of geometric and material properties has been found by using Design Expert software. The regression model has an adjusted R-squared of 0.90 and prediction R-squared of 0.86.

The predicted vs. actual values for the web height regression model is shown in Figure 5.8.2.

Design-Expert® Software  
web height

Color points by value of  
web height:

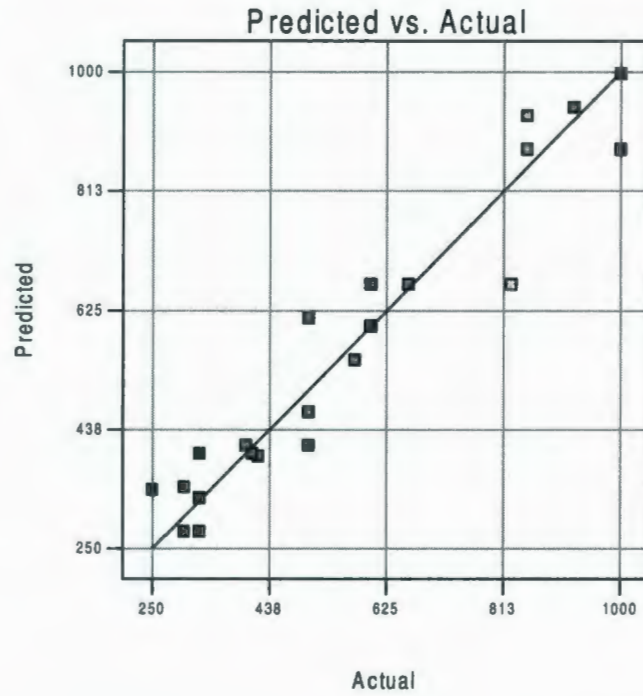


Figure 5.8.2: Predicted vs. Actual web heights

The maximum web height that can be achieved with a maximum allowable drop in capacity of 10% is given by:

$$\begin{aligned}
 \text{web height} = & 81.44 + 0.033 * \text{Length} + 0.17 * \text{plate width} \\
 & + 1.59 * \text{plate thickness} - 23.97 * \text{web thickness}/\text{plate thickness} \\
 & + 12.38 * \text{plate thickness} * \text{web thickness} / \text{plate thickness} \quad (5.1)
 \end{aligned}$$

Figure 5.8.3 shows that the maximum web height depends on the thickness of web and shell plate. The allowable web height increases with increasing shell plate thickness and web thickness.

Design-Expert® Software

web height

■ F- 0.600  
▲ F+ 1.300

X1 = C: plate thickness  
X2 = F: web thk/plate thk

Actual Factors

A: Length = 3000.00  
B: plate width = 450.00  
D: yield = 375.00  
E: post yield modulus = 1000.00

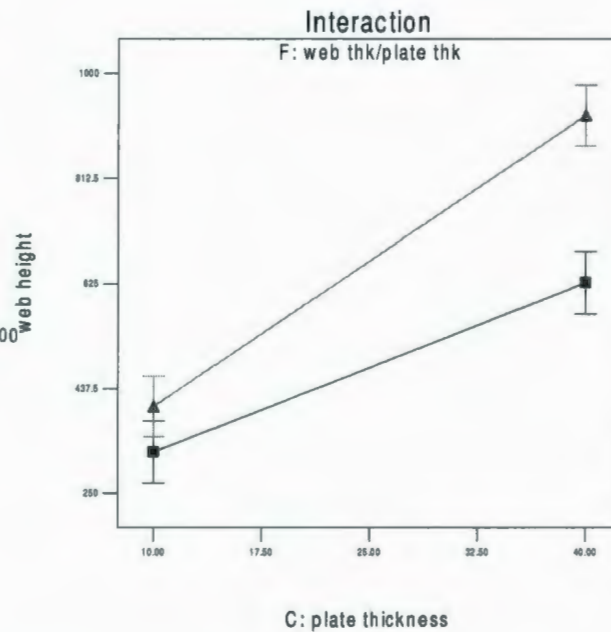


Figure 5.8.3: Allowable web height vs. plate thickness and web thickness

### 5.8.3 Major factors affecting web height / web thickness ratio

Figure 5.8.4 presents the half-normal probability plot of the  $h_w/t_w$  study. The main factors affecting the maximum allowable  $h_w/t_w$  are shell plate thickness (factor C) and web thickness (factor F).

The current design rule limits the maximum allowable web height to thickness ratio based on material yield strength alone. An interesting result from the analysis is that the web height to thickness ratio does not depend on yield strength. The main factors affecting the  $h_w/t_w$  ratio are the geometric parameters like web thickness and shell plate thickness.

Design-Expert® Software  
1/(h/t)

Shapiro-Wilk test  
W-value = 0.954  
p-value = 0.457  
A: Length  
B: plate width  
C: plate thickness  
D: yield  
E: post yield modulus  
F: web thk/plate thk  
■ Positive Effects  
■ Negative Effects

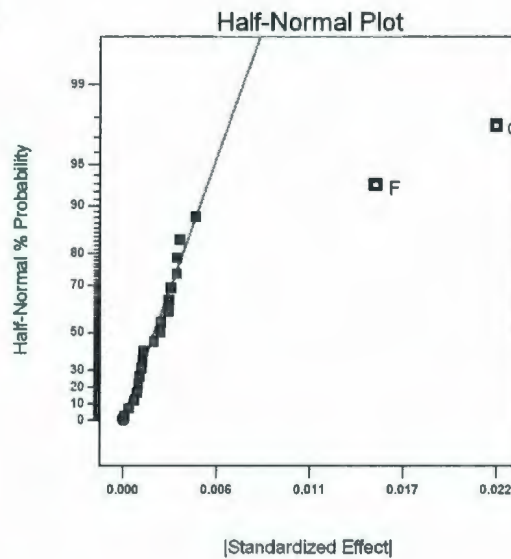


Figure 5.8.4: Half normal plot of  $h_w/t_w$  study

#### 5.8.4 Web height / thickness ratio prediction

Results of finite element analysis presented in Table 5.7.1 have shown that some frames can have much higher  $h_w/t_w$  ratios than that permitted by the design rules. The maximum value of  $h_w/t_w$  ratio among the combinations studied is 70 and the minimum is 16. The large range of  $h_w/t_w$  ratio shows that it cannot be increased for all the frames.

The maximum web height to thickness ratio for a given set of geometric and material properties has been found using Design Expert software. The regression model has an R-squared of 0.89 and prediction R-squared of 0.83.

The maximum web height to thickness ratio that can be achieved with a maximum allowable drop in capacity of 10% is given by:

$$\begin{aligned}
 1/(h_w/t_w) &= 0.009 - 2.15E-06 * \text{Length} - 1.12E-05 * \text{plate width} \\
 &+ 0.0007 * \text{plate thickness} \\
 &+ 0.021 * \text{web thickness /plate thickness}
 \end{aligned} \tag{5.2}$$

Figures 5.8.5 and 5.8.6 shows that  $h_w/t_w$  ratio depends on thickness of web and shell plate. The  $h_w/t_w$  ratio decreases with increasing shell plate thickness and web thickness.

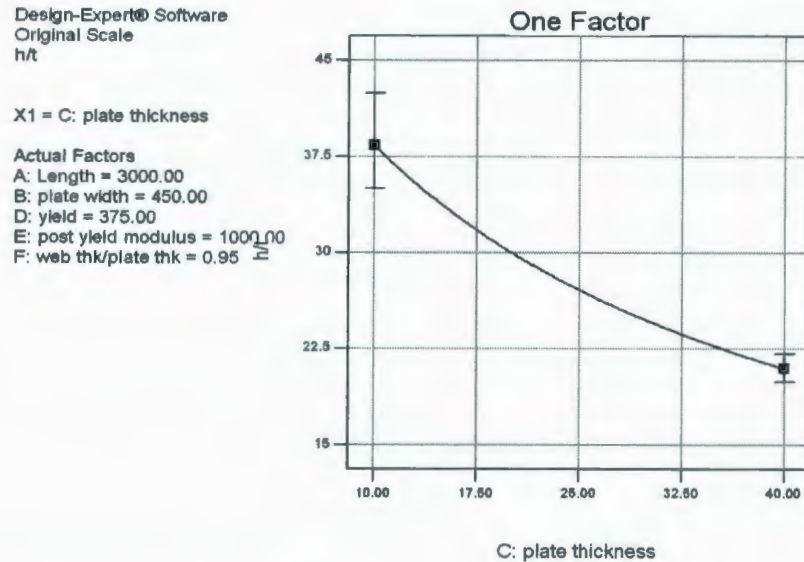


Figure 5.8.5:  $h_w/t_w$  ratio vs. plate thickness

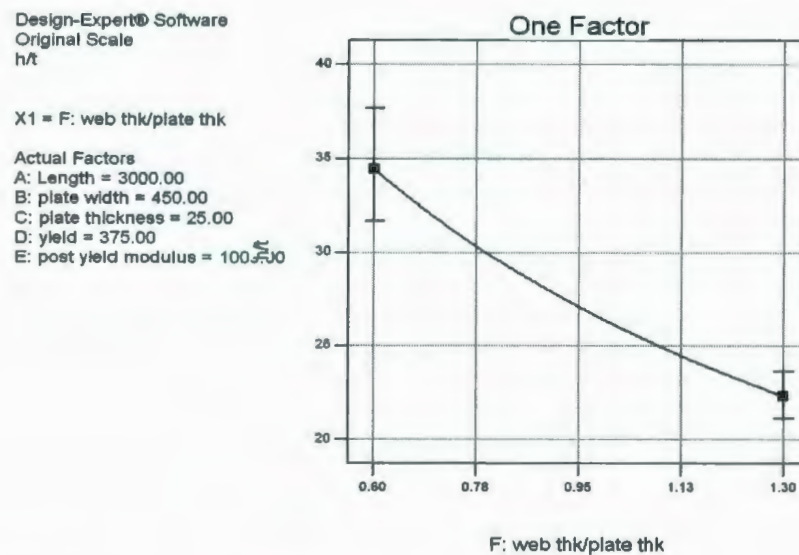


Figure 5.8.6:  $h_w/t_w$  ratio vs. web thickness

### 5.9 Validation of prediction models

The regression model for predicting web height and  $h_w/t_w$  ratio has been independently verified by separate finite element analyses. Results of validation runs are presented in Table 5.9.1. Appendix-C2 presents the output of ANSYS analyses.

Table 5.9.1: Validation runs of stability

Factor	Validation Runs							
	V1	V2	V3	V4	V5	V6	V7	V8
Span [mm]	3000	4000	3126	2500	2500	2500	2500	2500
Frame spacing [mm]	450	450	319	600	450	450	450	450
Plate Thickness [mm]	25	40	22	25	10	40	25	25
Yield Strength [MPa]	375	375	420	250	250	250	250	250
Post yield modulus [MPa]	1000	1000	1500	1000	1000	1000	1000	1000
Web thickness / plate thickness	0.95	0.95	1	0.95	0.95	0.95	0.6	1.3
<b>Results</b>								
Web height (FE Analysis) [mm]	550	820	530	620	410	760	520	650
Predicted Web Height (Equation 5.1) [mm]	571	804	524	581	354	755	454	654
% Error	<b>3.88</b>	<b>-1.84</b>	<b>-1.00</b>	<b>-6.23</b>	<b>-13.5</b>	<b>-0.61</b>	<b>-12.5</b>	<b>0.75</b>
$h_w/t_w$ (FE Analysis)	23.1	21.5	24.0	26.1	43.1	20.0	34.6	20.0
Predicted $h_w/t_w$ (Equation 5.2)	27.0	21.7	27.0	27.5	37.2	20.3	32.8	21.9
% Error	<b>16.9</b>	<b>0.85</b>	<b>12.2</b>	<b>5.48</b>	<b>-13.6</b>	<b>1.66</b>	<b>-5.26</b>	<b>9.72</b>
$h_w/t_w$ (FE Analysis)	23.1	21.5	24.0	26.1	43.1	20.0	34.6	20.0
$h_w/t_w$ (IACS)	14.5	14.5	13.7	17.8	17.8	17.8	17.8	17.8
% Error	<b>-37.1</b>	<b>-32.5</b>	<b>-42.8</b>	<b>-31.6</b>	<b>-58.6</b>	<b>-10.8</b>	<b>-48.5</b>	<b>-10.8</b>

Factor	Validation Runs							
	V09	V10	V11	V12	V13	V14	V15	V16
Span [mm]	2500	2500	2500	2500	2500	2500	2500	2500
Frame spacing [mm]	600	300	600	300	600	300	600	300
Plate Thickness [mm]	10	40	40	10	10	40	40	25
Yield Strength [MPa]	250	250	250	250	250	250	250	250
Post yield modulus [MPa]	1000	1000	1000	1000	1000	1000	1000	1000
Web thickness / plate thickness	0.6	0.6	0.6	1.3	1.3	1.3	1.3	0.95
<b>Results</b>								
Web height (FE Analysis) [mm]	380	625	690	410	450	875	850	560
Predicted Web Height (Equation 5.1) [mm]	345	563	616	362	415	893	946	528
% Error	<b>-8.97</b>	<b>-9.79</b>	<b>-10.6</b>	<b>-11.5</b>	<b>-7.59</b>	<b>2.16</b>	<b>11.4</b>	<b>-5.65</b>
$h_w/t_w$ (FE Analysis)	63.3	26.0	28.7	31.5	34.6	16.8	16.3	23.5
Predicted $h_w/t_w$ (Equation 5.2)	56.8	23.0	25.0	27.7	30.5	17.1	18.1	25.1
% Error	<b>-10.1</b>	<b>-11.3</b>	<b>-12.8</b>	<b>-12.1</b>	<b>-11.6</b>	<b>1.69</b>	<b>11.1</b>	<b>6.82</b>
$h_w/t_w$ (FE Analysis)	63.3	26.0	28.7	31.5	34.6	16.8	16.3	23.5
$h_w/t_w$ (IACS)	17.8	17.8	17.8	17.8	17.8	17.8	17.8	17.8
% Error	<b>-71.8</b>	<b>-31.5</b>	<b>-37.9</b>	<b>-43.4</b>	<b>-48.4</b>	<b>5.99</b>	<b>9.11</b>	<b>-24.3</b>

For the web height prediction, the maximum error percentage of the new regression model is 13.5% (validation run 5) as compared to 71.8% (validation run 9) for the current IACS rule.

For the  $h_w/t_w$  prediction, the maximum error percentage of the new regression model is 16.9% (validation run 1) as compared to 71.8% (validation run 9) for the current IACS rule.

A graphical comparison of the results of the validation study is presented in Figures 5.9.1 and 5.9.2. The results of the validation analyses have shown that the new regression model is reasonably accurate (less than 14% error) in predicting web height. The predicted  $h_w/t_w$  ratio is also much better than the current rule estimations.

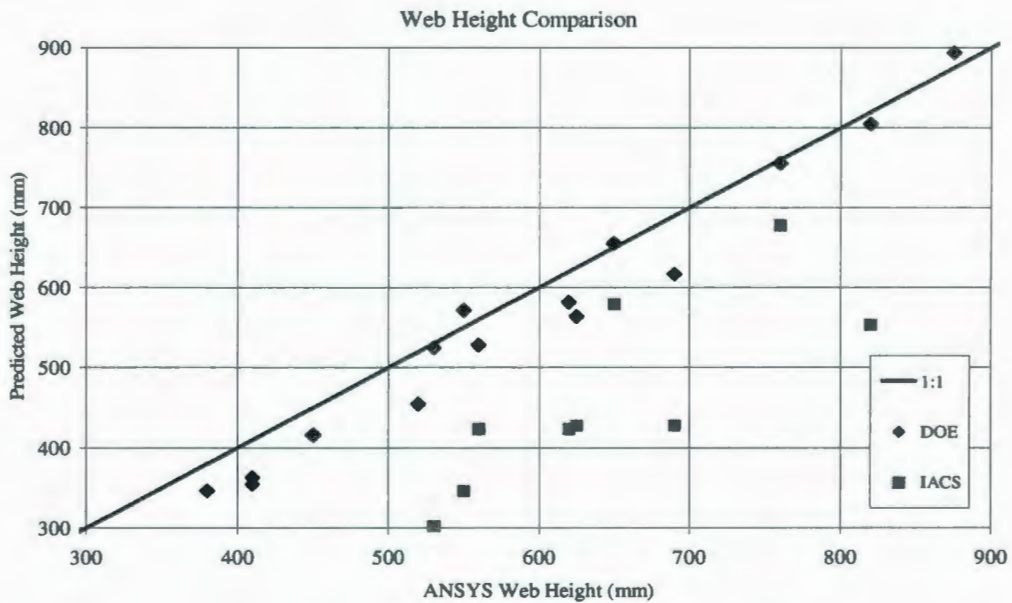


Figure 5.9.1: Web height – actual vs. predicted values

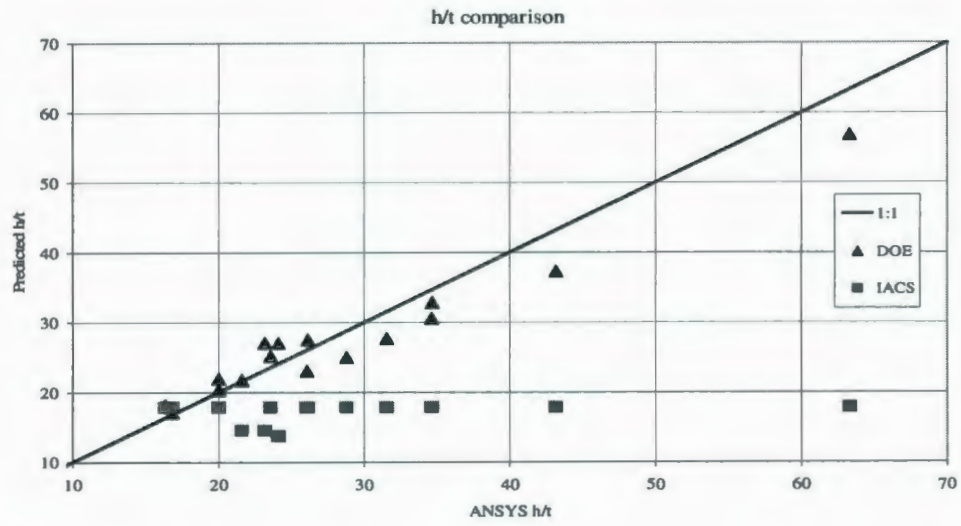
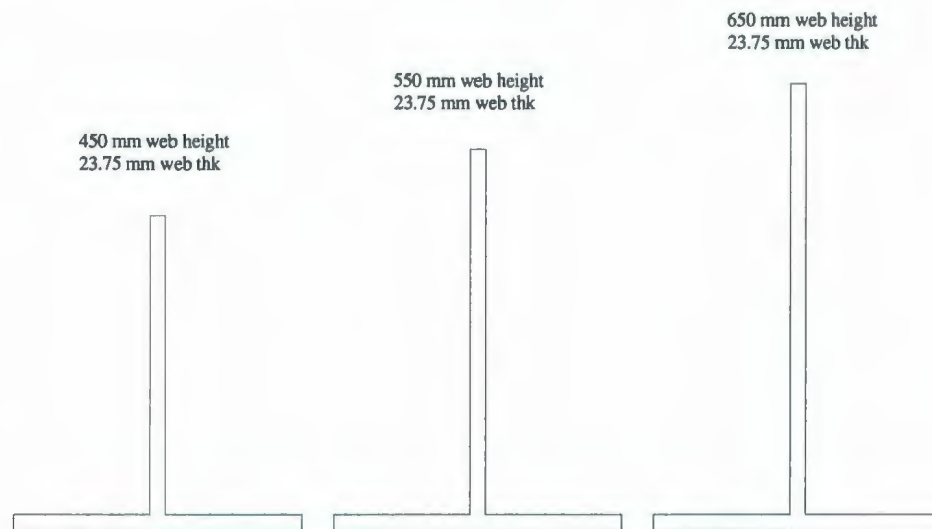


Figure 5.9.2:  $h_w/t_w$  ratio – actual vs. predicted values

## 5.10 Conclusions

The capacity of a frame depends on both material and geometric properties. Post yield web stability does not appear to depend on the same ratios that govern the elastic buckling mechanisms. Instead it depends on geometric properties like span, frame spacing, plate thickness, web height and thicknesses. This is likely because post yield instabilities are the result of plastic folding mechanisms, rather than a re-direction of elastic deformation that controls elastic buckling. The current IACS I2 stability rule limits are only a function of yield stress, but the study has shown that post yield stability is independent of yield stress.

Consider three frames as shown in Figure 5.10.1. The frames have different web heights (450, 550 and 650mm) and all other properties are kept constant.



Frame span = 3000 mm; Plate = 450 mm x 25 mm; Web thickness = 23.75 mm  
 $E = 2,000,000$  MPa;  $E_t = 1,000$  MPa

Figure 5.10.1: Three frames with different web heights

The responses of the frame are presented in Figures 5.10.2 to 5.10.4. It can be seen that web height of 450 mm is stable whereas web height of 650 mm is unstable. The stability pattern remains the same for the three different yield strength values. This demonstrates that yield strength is not a major factor affecting the stability of a frame.

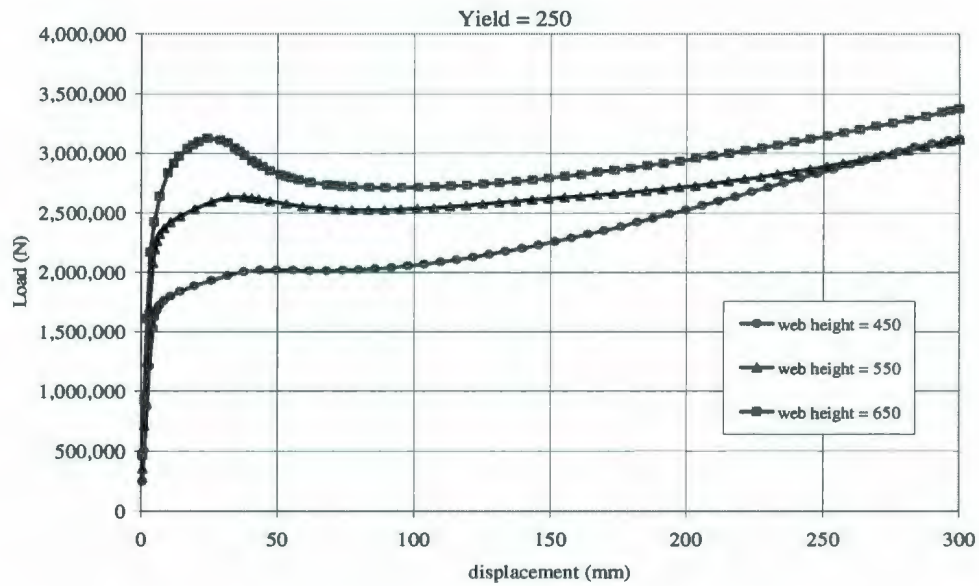


Figure 5.10.2: Capacity vs. Web Height (Yield strength = 250 MPa)

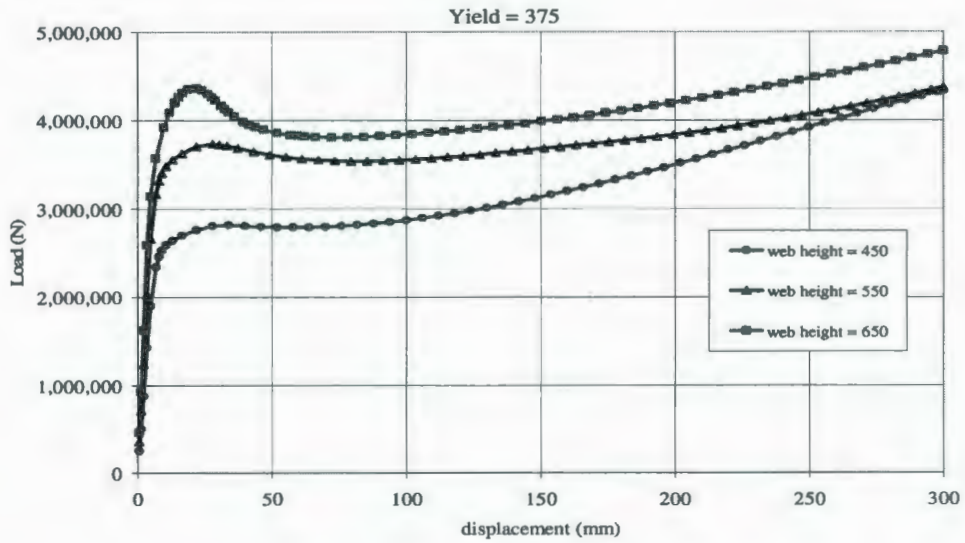


Figure 5.10.3: Capacity vs. Web Height (Yield strength = 375 MPa)

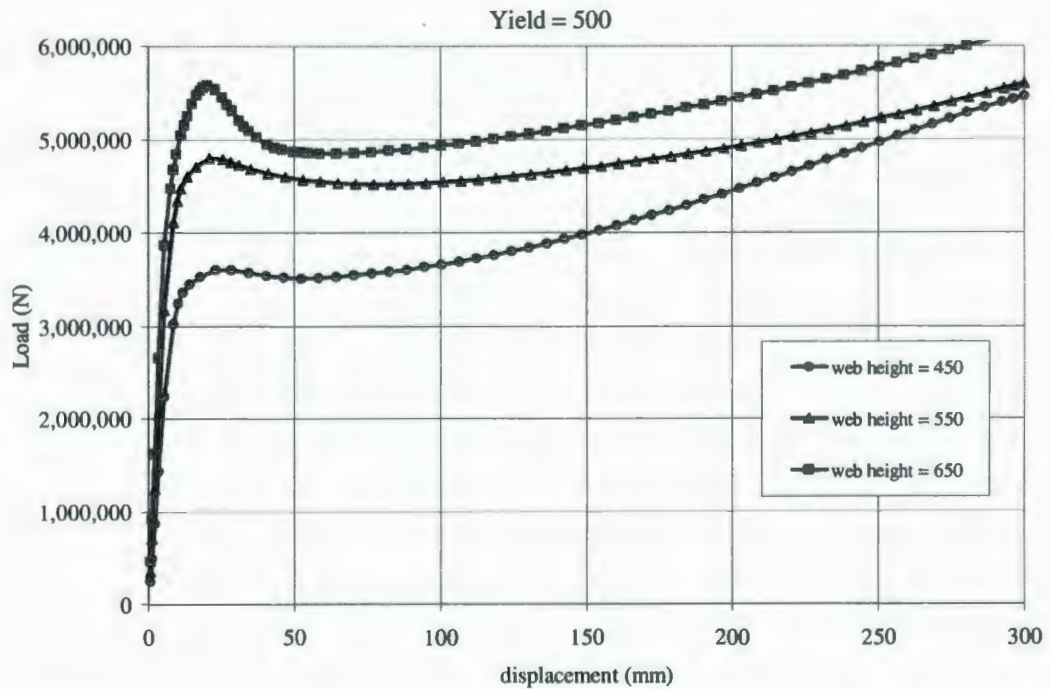


Figure 5.10.4: Capacity vs. Web Height (Yield strength = 500 MPa)



## **6 CONCLUSIONS AND RECOMMENDATIONS**

The research has addressed a few topics within the plastic behavior of stiffened plate subjected to ice loading. Plastic behavior was studied in terms of load sharing within the grillage, total capacity of the frame and stability of flat bar stiffener. Even though closure is not achieved for many of the problems, the research had achieved its intended goal of extending the currently available knowledge.

### **6.1 Conclusions**

The major conclusions of the study are as follows:

#### **6.1.1 FE validation study**

The FE validation study has shown that both shell and solid elements are suitable in estimating capacity of a frame. For a given set of material properties, capacity estimate using solid element is higher than that using shell element, so that shell elements give conservative results for design.

The deformation results using solid elements are similar to the experimental results. Shell elements (without modeling of weld) showed excessive deformations particularly at the intersection of web and shell plate. The deformation results of shell element showed considerable improvement by modeling the weld.

#### **6.1.2 Load sharing in a grillage**

The effect of boundary conditions (assumed in the cases of single frame, small grillage and large grillage) was studied, in order to assess the effect of load sharing in the plastic range.

The side boundary condition in single frame was simulated by symmetric boundary condition. The use of symmetric boundary condition, in most cases, underestimates the capacity of the frame.

In small grillage, the side boundary condition was simulated by including transverse continuity of the structure. The longitudinal ends were considered as fixed. In ships structure, the transverse frames (to which the single frames are connected) have finite

stiffness and can deform. The assumption of fixed longitudinal ends reduces the actual support span, which results in overestimation of the capacity of small grillage.

In a large grillage, the side and longitudinal boundary conditions were simulated by modeling the longitudinal and transverse continuity of the structure. Thus the large grillage represents the actual structural behavior as in a real ships structure.

The capacity of a large grillage is more than the single frame in most cases by approximately 0% to 40%. This increase in strength acts as a safety margin which takes care of the uncertainties in ice load estimation.

The single frame becomes stronger when it is a part of a grillage due to the load sharing between adjacent frames. The load sharing is more in case of thin frames compared to thick frames. The thin frame deforms and distributes the load, whereas, thick frame deforms only locally without much sharing with adjacent members.

Load sharing has important implications for ice class ship structures. If the effect were similar in all frames then the practical significance would be small. However, the effect varies considerably. It is notable that larger, higher ice class structures are less well able to distribute the loads. This implies that higher class vessels will not only need to withstand higher loads, but will need to do so more locally than lower class vessels. Most practical experience has been gained with lower class vessels. Consequently this issue should be of concern for the many new large and high ice class vessels that are currently on the drawing boards.

### 6.1.3 Parametric study of capacity

Capacity of a frame depends on geometric factors and material properties. A new regression equation has been developed using the DOE method to estimate capacity of a frame.

The new regression equation is quite long due to the statistical significance of the various factors and their interactions. The equation is best suited to be coded in some programming language like Matlab. The new regression equation has been validated

using independent FEA. The error associated with the new regression equation is relatively small compared to current IACS rule.

The major factors affecting capacity have been identified by the parametric study. The capacity of a frame generally increases with increase in web height, increase in web thickness, increase in plate thickness and increase in yield strength.

The rate of increase of capacity for increase in web height depends on the web thickness. For higher web thickness, the rate of increase is more.

The rate of increase of capacity for increase in web height depends on the plate thickness. For higher plate thickness, the rate of increase is more.

The rate of increase of capacity for increase in web height depends on the yield strength of material. For higher yield strength, the rate of increase is more.

The rate of increase of capacity for increase in web thickness depends on the yield strength of material. For higher yield strength, the rate of increase is more.

The rate of increase of capacity for increase in plate thickness depends on the yield strength of material. For higher yield strength, the rate of increase is more.

#### 6.1.4 Stability of flat bar stiffener

The capacity of a frame depends on geometric and material properties but stability depends only on geometric properties (like span, frame spacing, plate thickness, web height and thicknesses). The current IACS rule limits stability based on yield strength alone, but the study has shown that stability is independent of yield strength.

A new relationship has been proposed for calculating the limiting web height using DOE. The regression model depends only on geometric properties of the frame.

A new relation has also been proposed for estimating the limiting  $h_w/t_w$  ratio of the web. The new web slenderness prediction model shows good agreement with the finite element results. The current IACS rule gives very conservative estimates of web slenderness, thereby limiting the use of flat bar stiffener. If the allowable web slenderness of the flat

bar stiffener can be increased, flat bar stiffener can be used more widely instead of other expensive stiffener forms like angle, bulb or T.

## **6.2 Recommendations**

The regression equation for predicting capacity is quite long due to the large number of factors and the range of each factor considered. The study also combines various stiffener forms into a single equation. The regression equation can be simplified by separating the study for various stiffener forms and taking smaller ranges of each factor. This will result in a family of smaller equations rather than a very long equation.

The stability study of a flat bar stiffener is based on the behavior of structural response alone. A closer inspection of some of the acceptable web heights has shown local failure of the web. A re-examination of the results is required for establishing a conservative estimate of web height by thickness ratio. The study also can be extended to other stiffener forms like T, angle and bulb.

The latest version of ANSYS offers capabilities of parametric study without using additional software for designing statistical experiment. This might result in defining parameters within ANSYS itself and specifying its ranges, thus avoiding the need for preparing data files for each run.

## 7 REFERENCES

- ANSYS Inc. (2007). Release 11.0 Documentation for ANSYS. USA: ANSYS Inc.
- Bond, J., Srinivasan, J., Basu, R., & Kennedy, S.J. (1995). Finite element and Physical Modelling of Post Yield Stability of Icebreaker Structure. Transport Canada Report TP12528E.
- Bridges, R., Hasolt, S., Kim, M.S., & Riska, K. (2005). Current Hull and Machinery Ice Class Rules Requirements and Impact of IACS Polar Rules. Project: GRD2/2000/30112 – ARCOP
- Bruneau, M., Uang, C.M., & Whittaker, A. (1998). Ductile Design of Steel Structures. NY, USA: McGraw-Hill.
- Butler, T.R. (2002). An Analysis of Stiffened Plate Subject to Extreme Ice Loads. M.Eng Thesis, Memorial University of Newfoundland.
- Caldwell, J.B. (1965). Ultimate Longitudinal Strength. Transactions of RINA, 107, 411-430.
- Cui, W., & Mansour, A.E. (1999). Generalization of a Simplified Method for Predicting Ultimate Compressive Strength of the Panels. Int. Shipbuilding Progress 46:447, 291-303.
- Daley, C. G. (1991). Ice Edge Contact - A Brittle Failure Process Model. Acta Polytechnica Scandinavica, Mechanical Engineering Series No. 100, Helsinki 1991. Published by the Finnish Academy of Technology.
- Daley, C.G., Tuhkuri, J., & Riska, K. (1998). The Role of Discrete Failures in Local Ice Loads. Cold Regions Science and Technology, Vol 27, 197-211.
- Daley, C.G., Kendrick, A., & Appolonov, E. (2001). Plating and Framing Design in the Unified Requirements for Polar Class Ships. In: Proceedings of the 16th International Conference on Port and Ocean Engineering under Arctic Conditions, Vol 3, Ottawa, Canada, 779-91.

- Daley, C.G. (2002). Derivation of Plastic Framing Requirements for Polar Ships. *Marine Structures* 15, 543-559.
- Daley, C.G. (2004). A Study of the Process Spatial Link in Ice Pressure Area Relationships. Panel on Energy Research and Development / Canadian Hydraulics Centre, PERD/CHC Report 7-108.
- Daley, C.G., Pavic, M., Hussein, A., & Hermanski, G. (2004). Ship Frame Research Program – A Numerical Study of the Capacity of Single Frames Subject to Ice Load. Ocean Engineering Research Centre, Memorial University of Newfoundland, OERC Report 2004-02.
- Daley, C.G., & Hermanski, G. (2005). Ship Frame/Grillage Research Program - Investigation of Finite Element Analysis Boundary Conditions. Ocean Engineering Research Centre, Memorial University of Newfoundland, OERC Report 2005-02.
- Daley, C.G., Hermanski, G., Pavic, M., & Hussein, A. (2007). Ultimate Strength of Frames and Grillages Subject to Lateral Loads – An Experimental Study. 10th International Symposium on Practical Design of Ships and Other Floating Structures, Houston, Texas, USA.
- Daley, C.G., & Kendrick, A. (2008). Direct Design of Large Ice Class Ships with Emphasis on the Mid-Body Ice Belt. In: Proceedings of the 27th International Conference on Offshore Mechanics and Arctic Engineering, OMAE2008-57846.
- Dome Petroleum Ltd. (1982). Report on Full Scale Measurements of Ice Impact Loads and Response Of The CANMAR Kigoriak – August and October 1981. Technical Report, Dome Petroleum Ltd.
- Dow, R.S. (1991). Testing and Analysis of 1/3-Scale Welded Steel Frigate Model. Proceedings of the International Conference on Advances in Marine Structures, Dunfermline, Scotland, 749-773.

- Frederking, R. (2000). Local Ice Pressures from the Louis S. St. Laurent 1994 North Pole Transit. Canadian Hydraulics Centre, National Research Council Canada, Ottawa, Technical Report HYDTR-054.
- Fujikubo, M., Yao, T., Khedmati, M.R., Harada, M., & Yanagihara, D. (2005a). Estimation of Ultimate Strength of Continuous Stiffened Panel under Combined Transverse Thrust and Lateral Pressure Part 1: Continuous Plate. *Marine Structures*, 18:5-6, 383-410.
- Fujikubo, M., Harada, M., Yao, T., Khedmati, M.R., & Yanagihara, D. (2005b). Estimation of Ultimate Strength of Continuous Stiffened Panel under Combined Transverse Thrust and Lateral Pressure Part 2: Continuous Stiffened Panel. *Marine Structures*, 18:5-6, 411-427.
- Hong, L., & Amdahl, J. (2007). Plastic Design of Laterally Patch Loaded Plates for Ships. *Marine Structures* 20, 124–142.
- Hughes, O.F. (1983). Ship structural design: A Rationally Based Computer Aided Optimization Approach. Published by the Society of Naval Architects and Marine Engineers, New York, 1988.
- Hughes, O., & Ma, M. (1996), Elastic Tripping of Asymmetrical Stiffeners. *Computers and Structures* 60:3, 369-389.
- IACS. (2006). I2 Structural Requirements for Polar Class Ships. London: International Association of Classification Societies.
- Jirasek, M., & Bazant, Z. (2002). *Inelastic Analysis of Structures*. West Sussex, UK: John Wiley & Sons.
- John, S.J., Package, D., & Kennedy, S. (2002). Post Yield Behavior of the USCGC Jupiter (WLB 201) Hull Structure. US Coast Guard Engineering Logistics Centre, MD, USA. Report No: DTG23-94-D-EN3119.
- Kurdyumov, V.A., & Khesin, D.E. (1976). A Hydrodynamic Model of Solid/Ice Impact. *Applied Mechanics*, Kiev, Vol XII, No 10, pp 103-109.

- Mackenzie, D., & Li, H. (2006). A Plastic Load Criterion for Inelastic Design by Analysis. *Journal of Pressure Vessel Technology*, Volume 128, Issue 1, 39-45.
- Madenci, E., & Guven, I. (2007). *The Finite Element Method and Applications in Engineering Using ANSYS*. New York Inc, USA: Springer-Verlag.
- Mahendran, M. (1997). Local Plastic Mechanisms in Thin Steel Plates under In-Plane Compression, *Thin-Walled Structures* 27:3, 245-261.
- Mourad, H.M. (1999). Elastic-Plastic Behavior and Limit Load Analysis of Pipe Bends under Out-Of-Plane Moment Loading and Internal Pressure. Master of Science Thesis, The American University in Cairo.
- Nyseth, H., & Holtmark, G. (2006). Analytical Plastic Capacity Formulation for Plates Subject to Ice Loads and Similar Types of Patch Loadings. In: *Proceedings of 25th International Conference on Offshore Mechanics and Arctic Engineering (OMAE2006)*, Hamburg, Germany.
- Paik, J.K., & Pedersen, P.T. (1996). A Simplified Method for Predicting Ultimate Compressive Strength of Ship Panels. *International Shipbuilding Progress*, 43 (434), 139-157.
- Paik, J.K., Thayamballi, A.K., & Kim, D.H. (1999). An Analytical Method for the Ultimate Compressive Strength and Effective Plating of Stiffened Panels, *J. of Constructional Steel Research* 49, 43-68.
- Paik, J.K., Thayamballi, A.K., & Kim, B.J. (2001). Advanced Ultimate Strength Formulations for Ship Plating Under Combined Biaxial Compression/Tension, Edge Shear, and Lateral Pressure Loads. *Marine Technology*, Vol. 38, No. 1, January 2001, 9-25.
- Paik, J.K., & Thayamballi, A.K. (2003). *Ultimate Limit State Design of Steel-Plated Structure*. West Sussex, England: John Wiley & Sons.
- Paik, J.K., & Thayamballi, A.K. (2007). *Ship Shaped Offshore Installations*. NY, USA: Cambridge University Press.

- Paik, J.K., Kim, B.J., & Seo, J.K. (2008a). Methods for Ultimate Limit State Assessment of Ships and Ship-Shaped Offshore Structures: Part I un-stiffened plates. *Ocean Engineering*, 35: 2, 261-270.
- Paik, J.K., Kim, B.J., & Seo, J.K. (2008b). Methods for Ultimate Limit State Assessment of Ships and Ship-Shaped Offshore Structures: Part II Stiffened Panels. *Ocean Engineering*, 35: 2, 271-280.
- Paik, J.K., Kim, B.J., & Seo, J.K. (2008c). Methods for Ultimate Limit State Assessment of Ships and Ship-Shaped Offshore Structures: Part III Hull Girders. *Ocean Engineering*, 35: 2, 281-286.
- Riska, K., Rantala, H., & Joensuu A. (1990). Full Scale Observations of Ship-Ice Contact. Helsinki University of Technology, Laboratory of Naval Architecture and Marine Engineering, Report M-97.
- Save, M.A., Massonnet, C.E., & Saxce, G.D. (1997). Plastic Limit Analysis of Plates, Shells and Disks. Amsterdam: Elsevier.
- Sheikh, I.A., Grondin, G.Y., & Elwi, A.E. (2001). Stiffener Tripping in Stiffened Steel Plates. Structural Engineering Report No. 236, Department of Civil and Environmental Engineering, University of Alberta.
- Smith, C.S. (1975). Compressive Strength of Welded Steel Ships Grillages. *Trans. RINA*, Vol.117, 325-359.
- Smith, C.S. (1977). Influence of Local Compressive Failure on Ultimate Longitudinal Strength of a Ship's Hull. *Proceedings of International Symposium on Practical Design in Shipbuilding*, Tokyo, Japan, 73-79.
- Stat-Ease Inc. (2008). Design Expert version 7.1.3 manual. Minneapolis, USA: Stat-Ease Inc.
- Suneel, K.M., Alagusundaramoorthy, P., & Sundaravadivelu, R. (2006). Ultimate Strength of Ship Plating Under Axial Compression. *Ocean Engineering*, 33:8-9, 1249-1259.

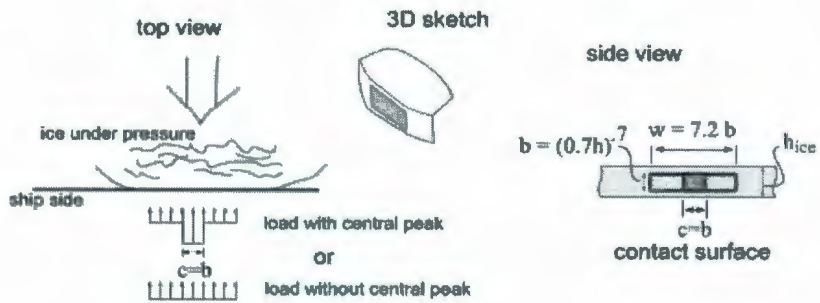
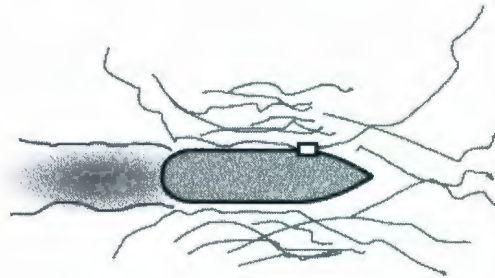
- Varsta, P., Droumev, I.V., & Hakala, M. (1978). On Plastic Design of Ice Strengthened Frame. Research Report No 27, Winter Navigation Research Board, Finnish Board of Navigation.
- Yao, T., & Nikolov, P.I. (1991). Progressive Collapse Analysis of a Ship's Hull Under Longitudinal Bending. *Journal of the Society of Naval Architects of Japan*, 170, 449-461.

## **APPENDIX**

APPENDIX A:  
LOAD SHARING IN A GRILLAGE

Appendix A1  
Ice Load Estimation

**Close Pack Pressure Load (Daley & Kendrick, 2008)**



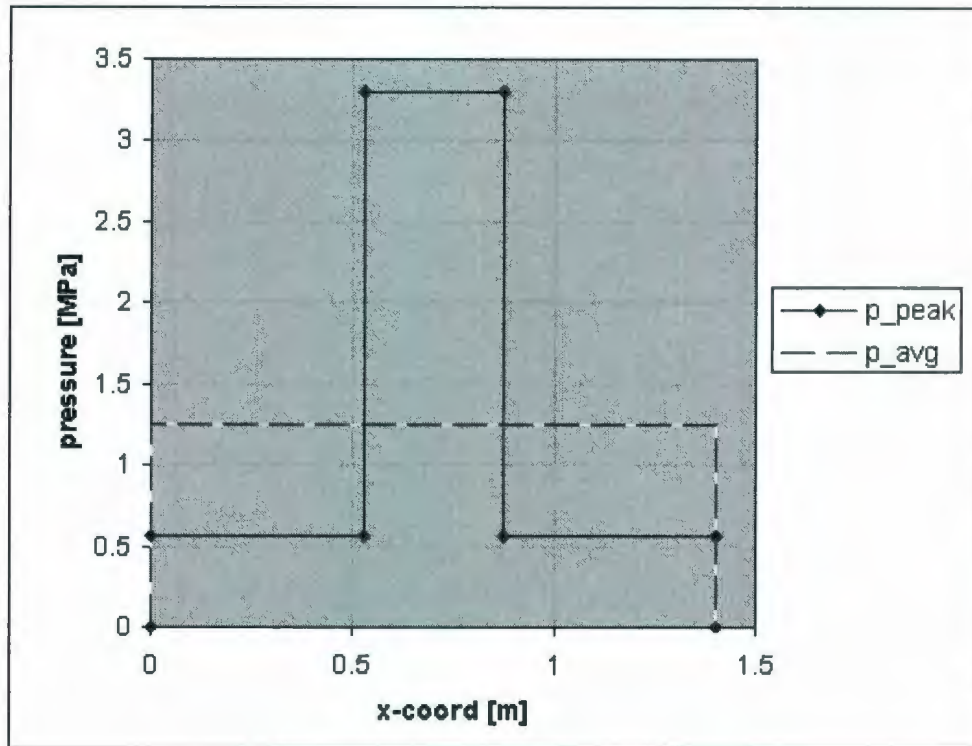
**Ship Main Parameters**

	<u>variable</u>	value	units
Ship Name	SN	LNG1	text
Ice Class	PC	7	#
Operational Ice thickness	h	0.70	m
Ice strength Index	k	1	-
factor of safety	fos	1.00	

**Results**

Height of patch	b	0.61	m
width of patch	w	1.40	m
Line Load	Q	0.76	MN/m
Nomal Force	Fn	1.1	MN
Aveage Pressure	Pav	1.25	Mpa
Area	A	0.8	m <sup>2</sup>
peak length	c	0.35	m
peak line load	Qc	2.00	MN/m
peak force	Fc	0.70	MN
peak pressure	Pc	3.30	Mpa
edge pressure	Pe	0.57	Mpa

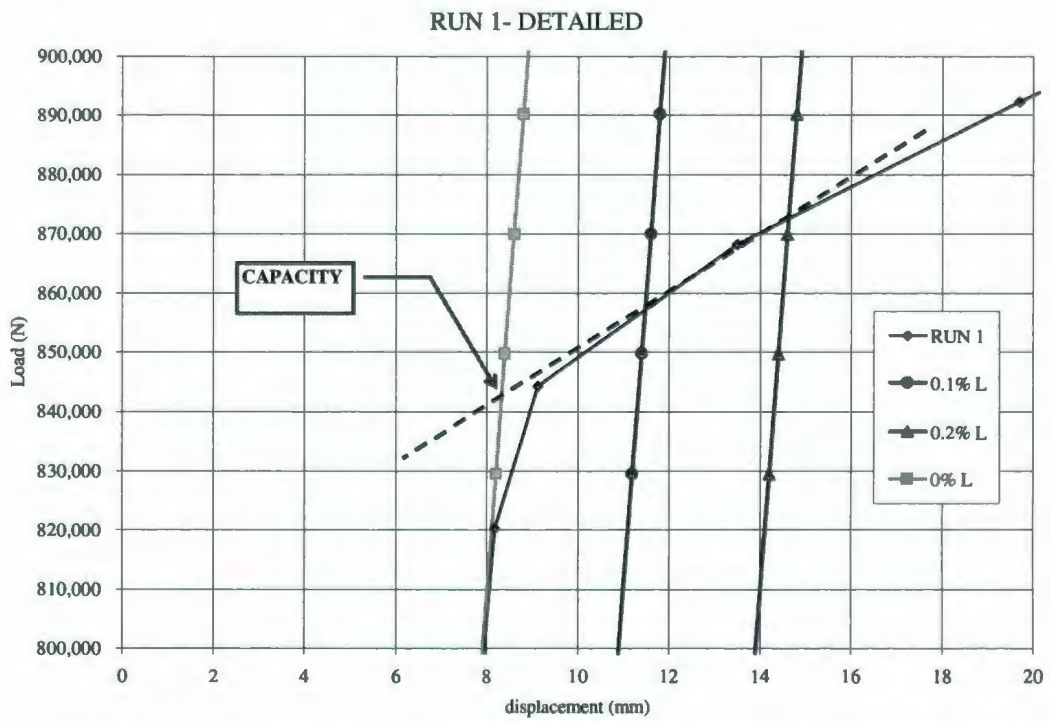
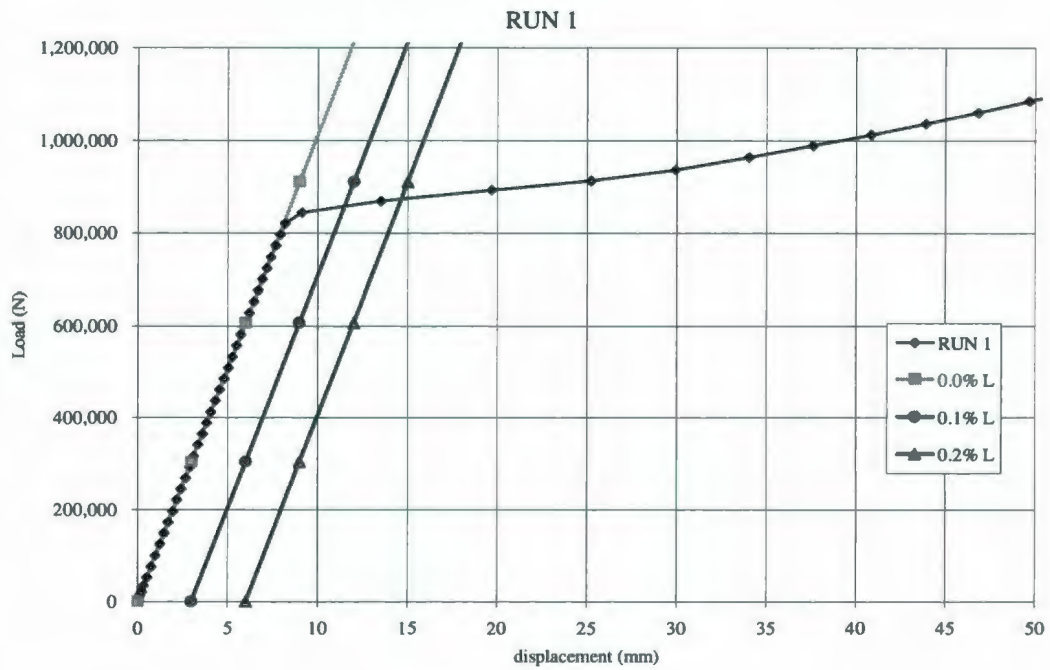
**Plot of load patch pressure**



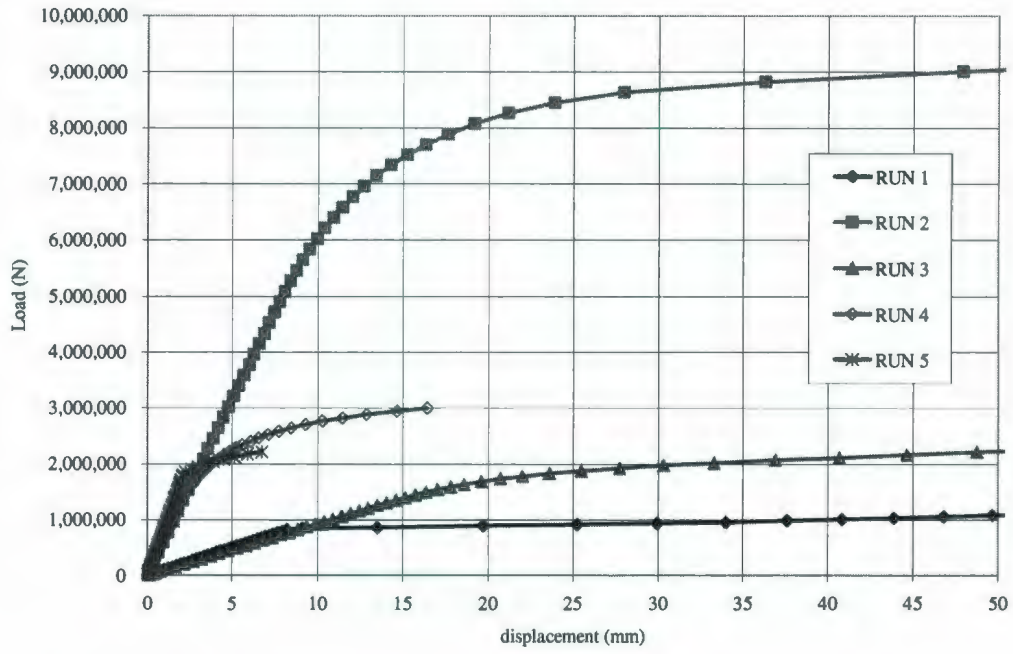
**Peak Pressure / Edge Pressure = 5.82**

APPENDIX B:  
PARAMETRIC STUDY OF CAPACITY

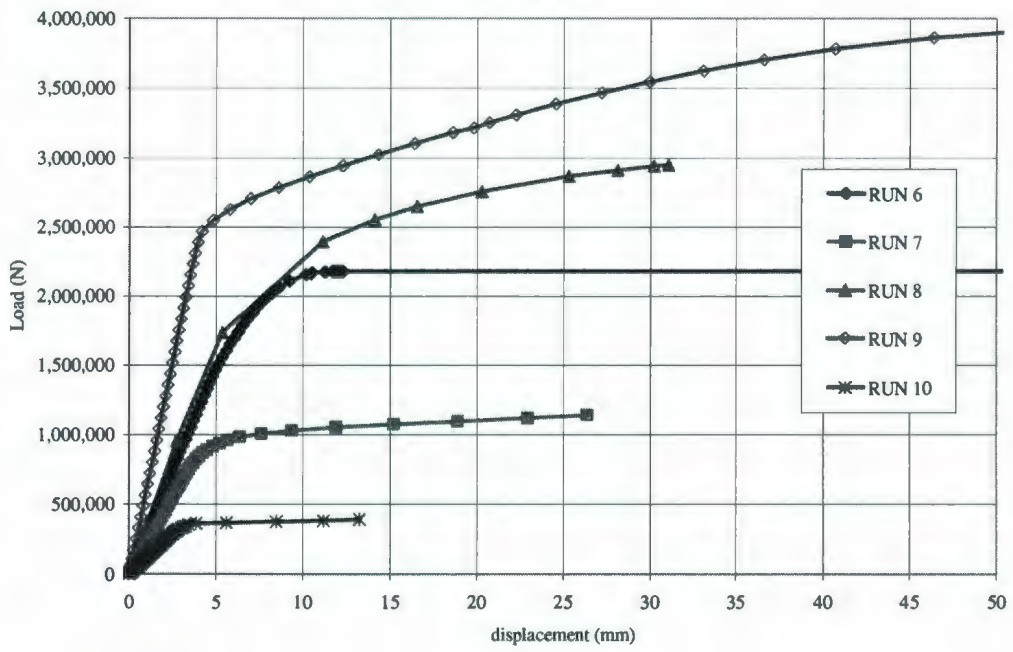
Appendix B1  
DOE Run Results



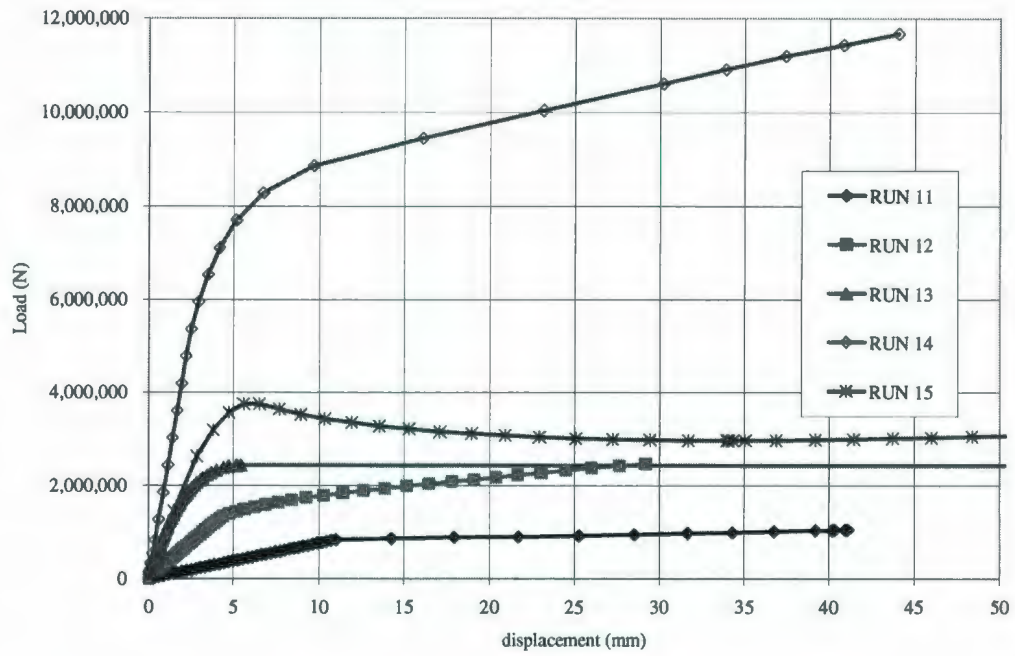
RUN 1-5



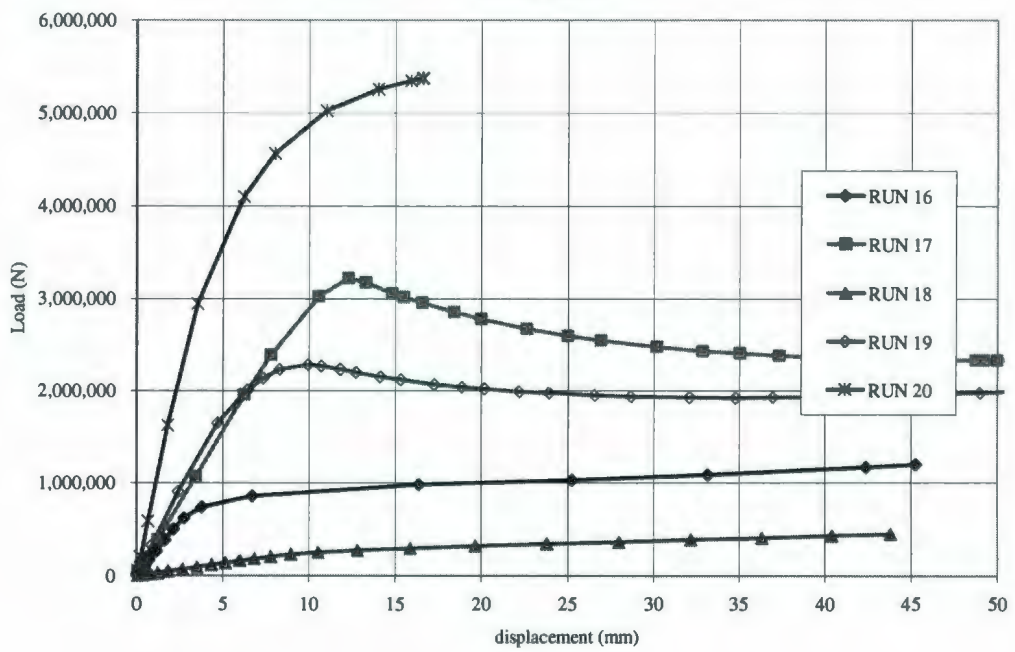
RUN 6-10



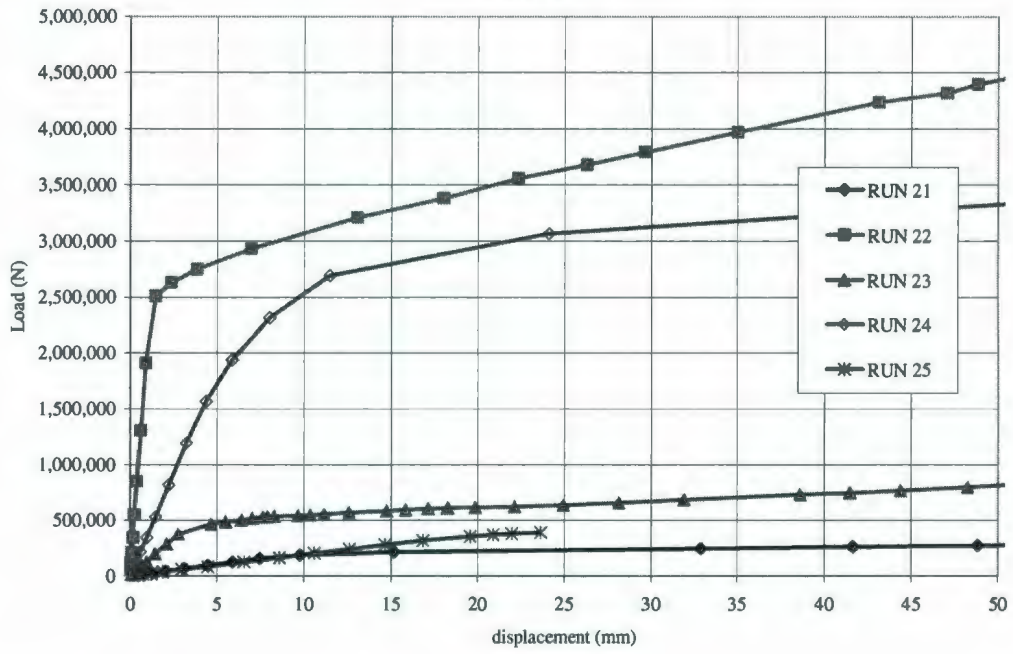
RUN 11-15



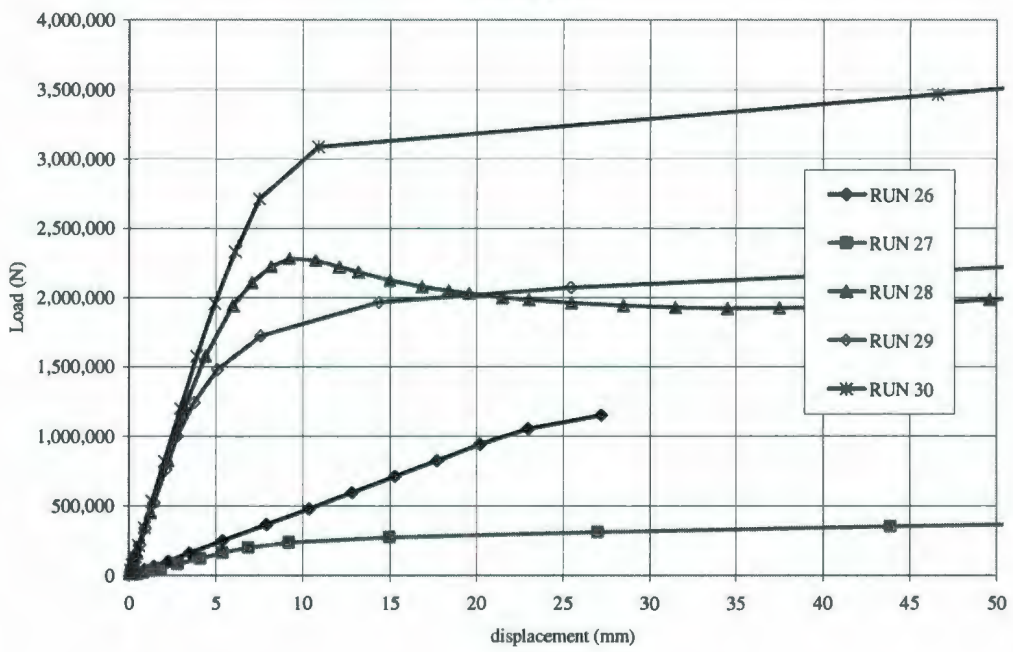
RUN 16-20



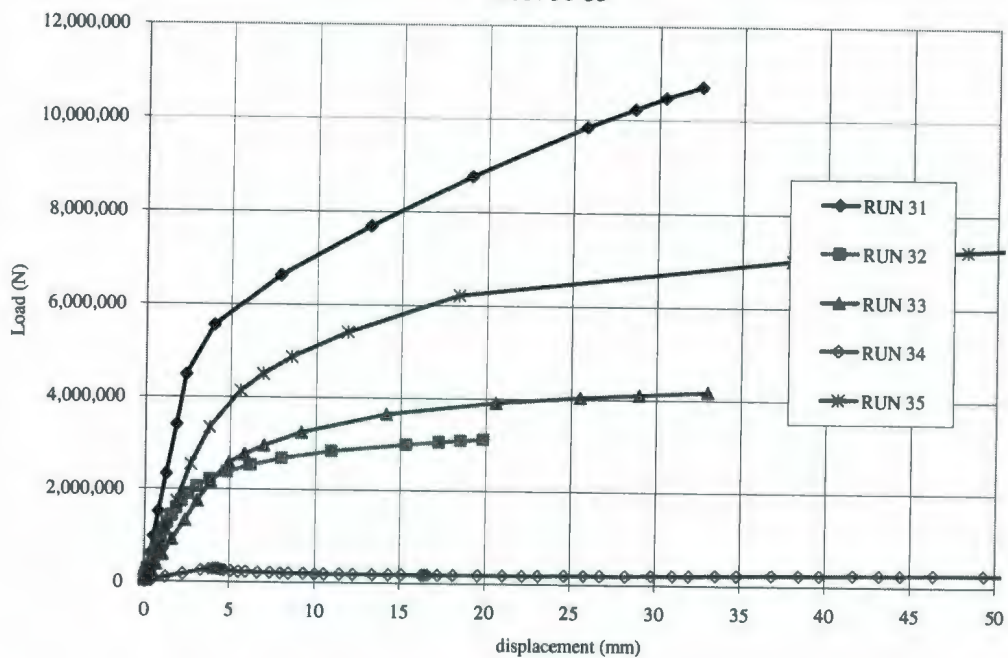
RUN 21-25



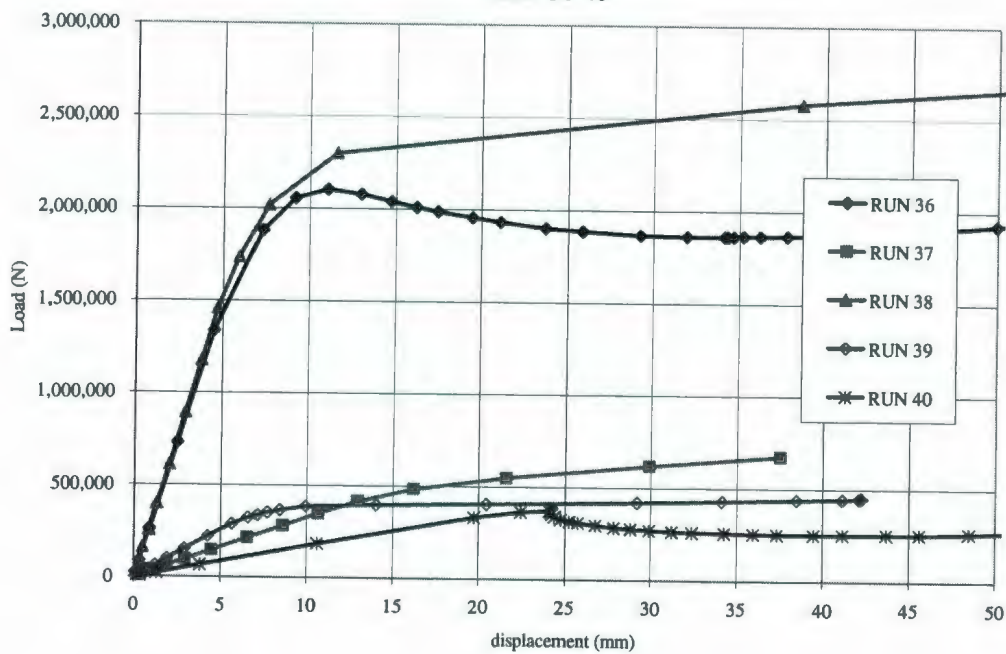
RUN 26-30



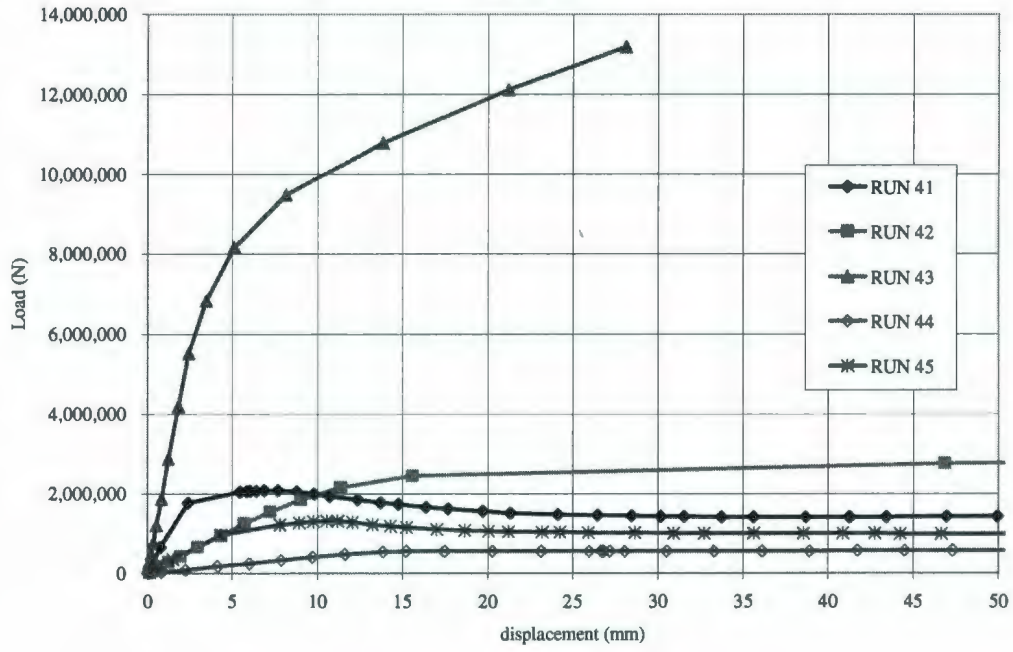
RUN 31-35



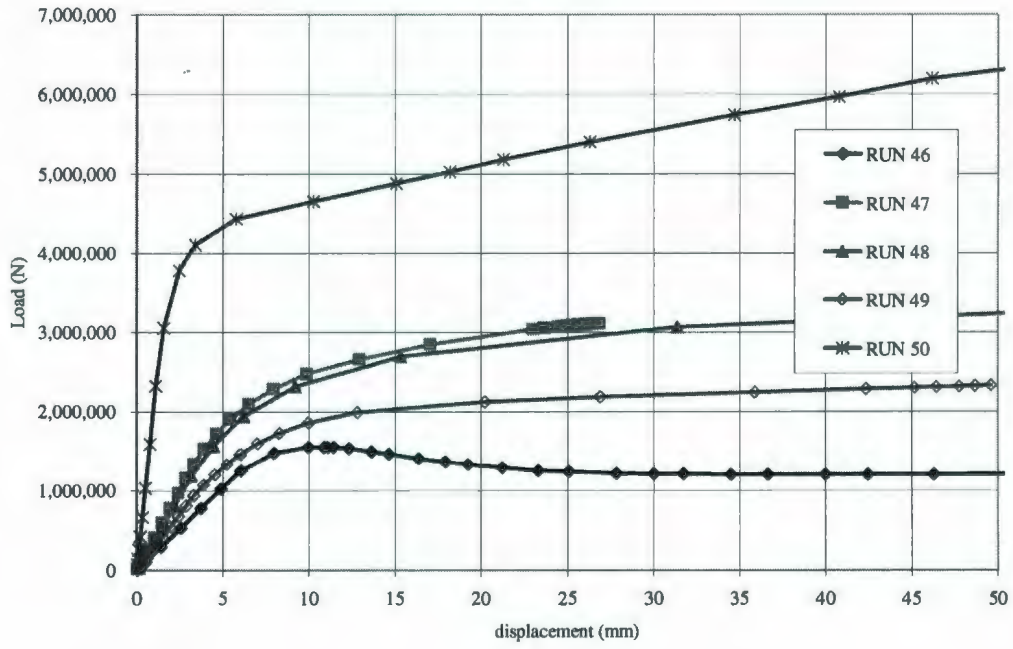
RUN 36-40



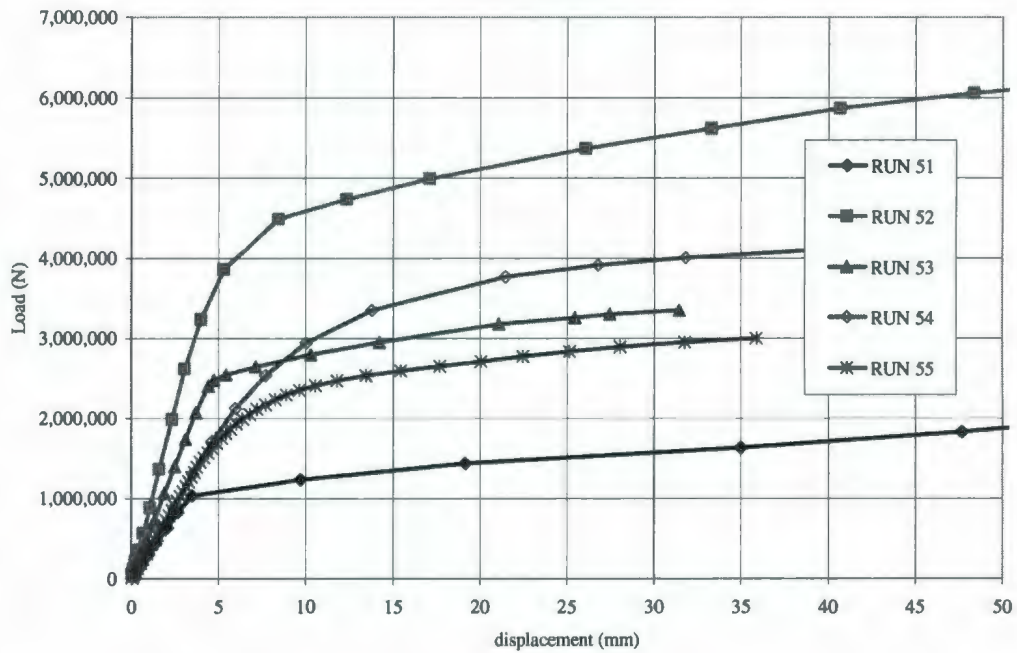
RUN 41-45



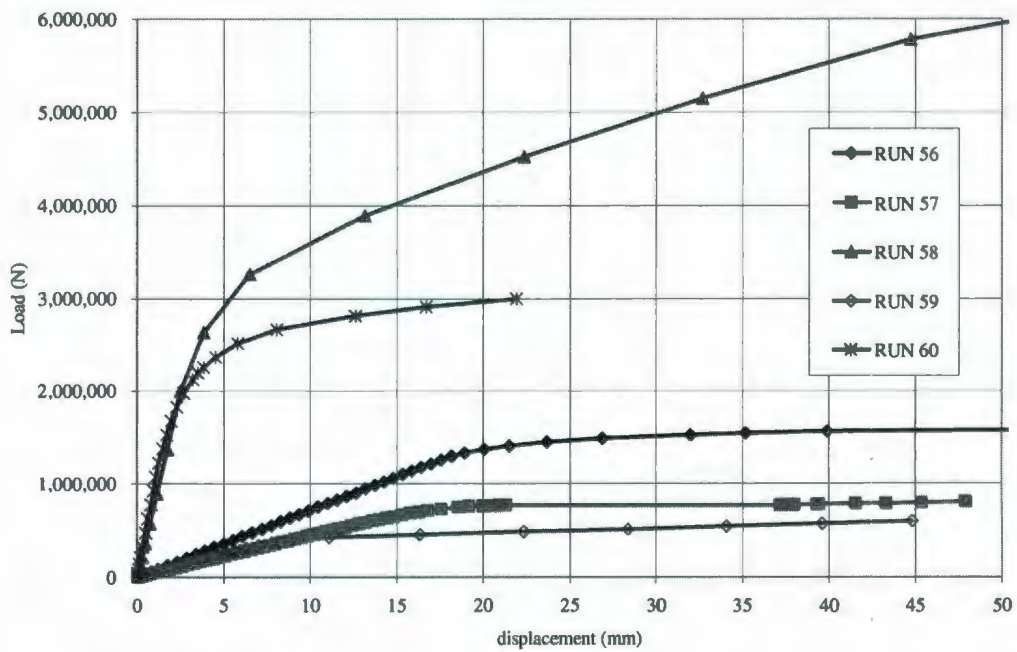
RUN 46-50



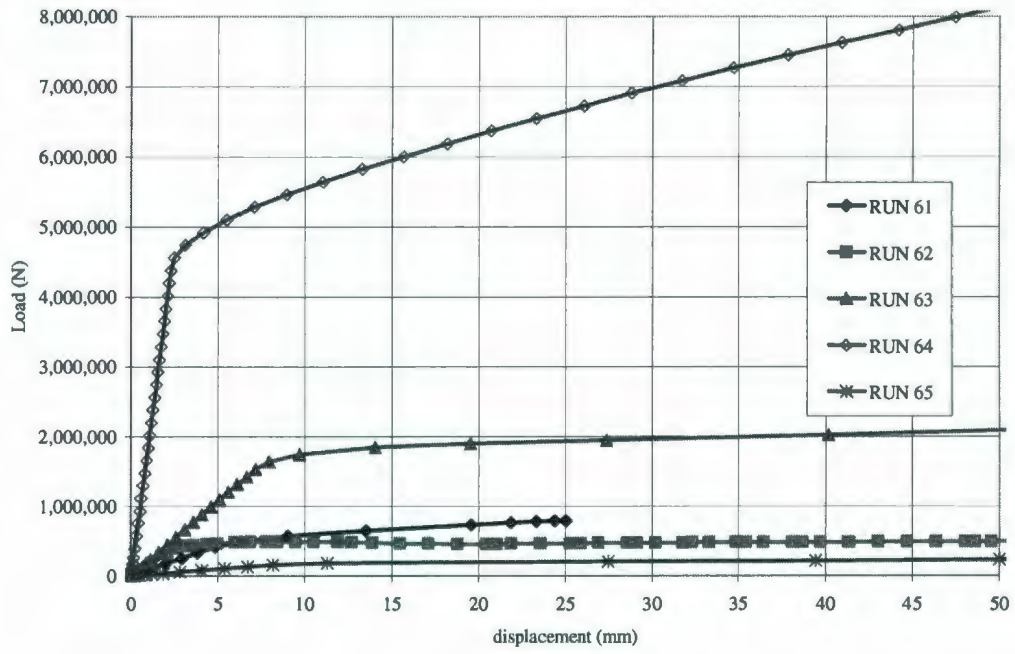
RUN 51-55



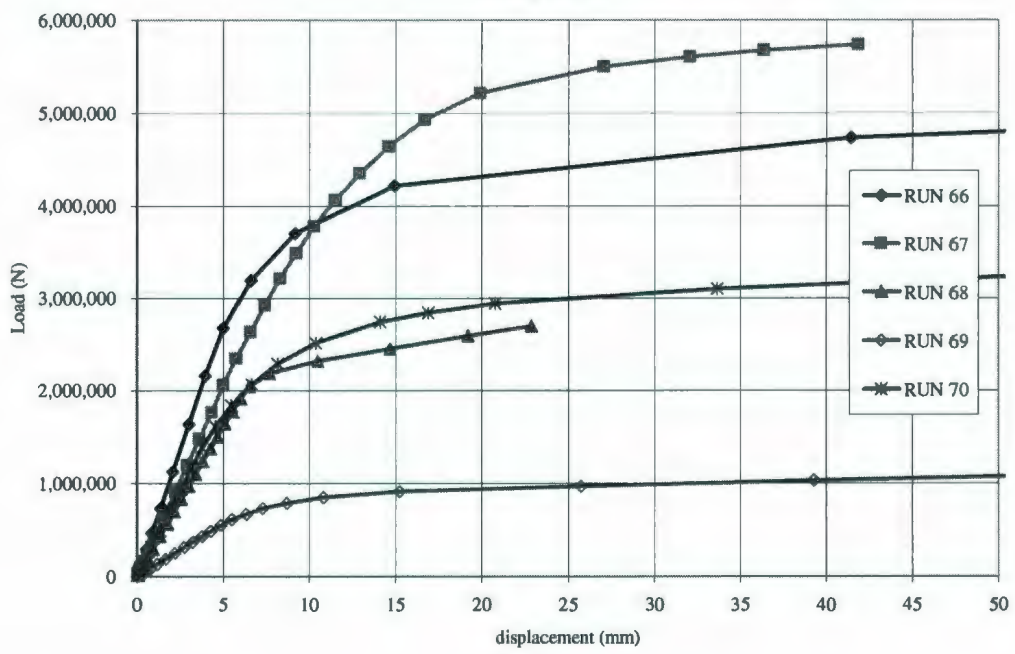
RUN 56-60



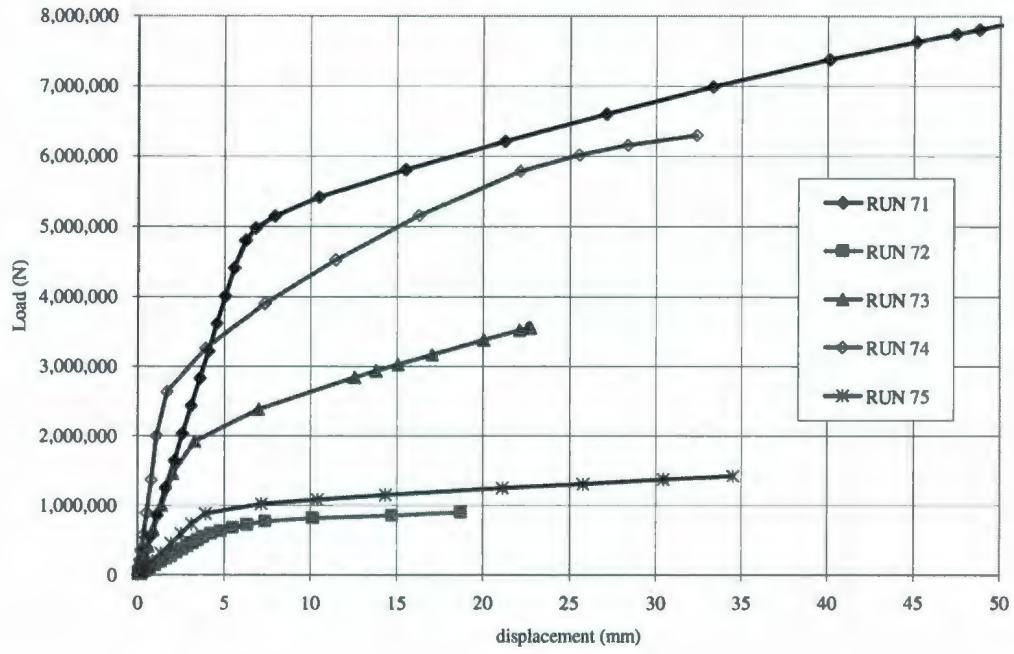
RUN 61-65



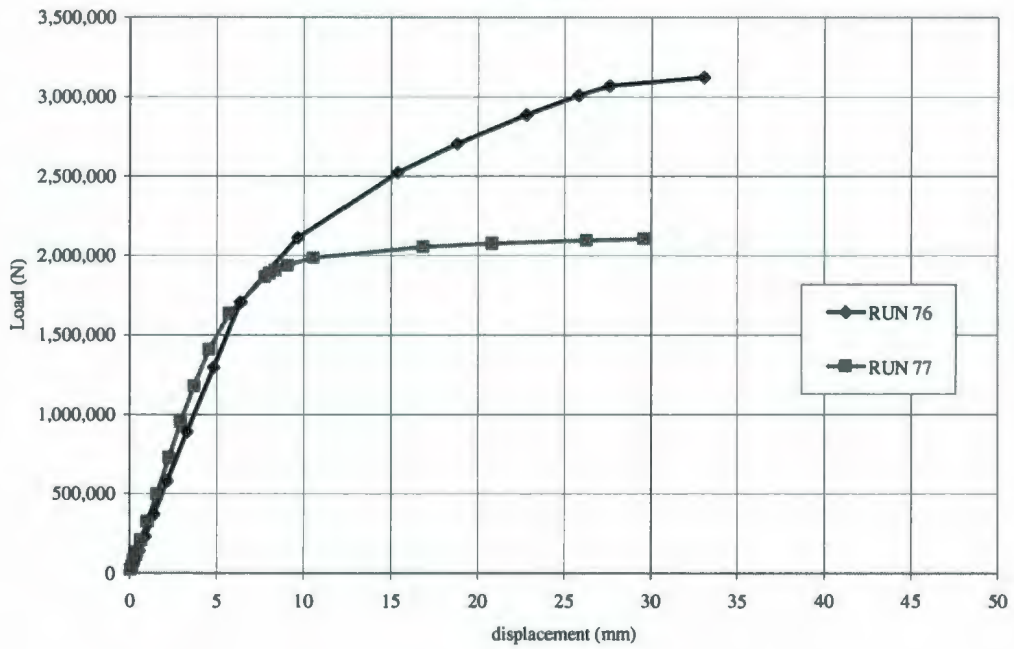
RUN 66-70



RUN 71-75

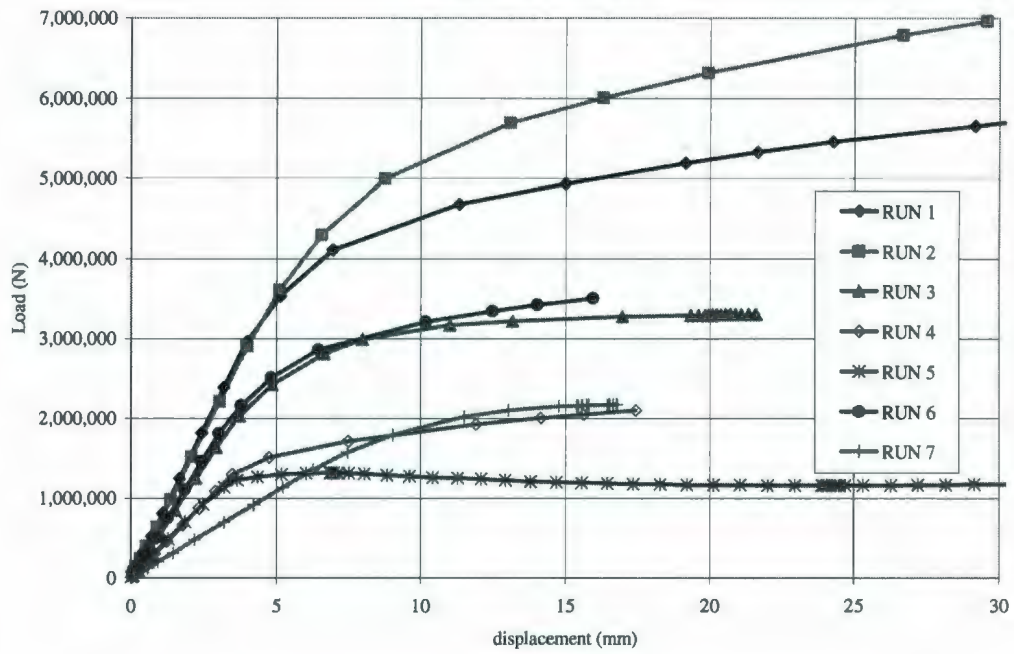


RUN 76-77

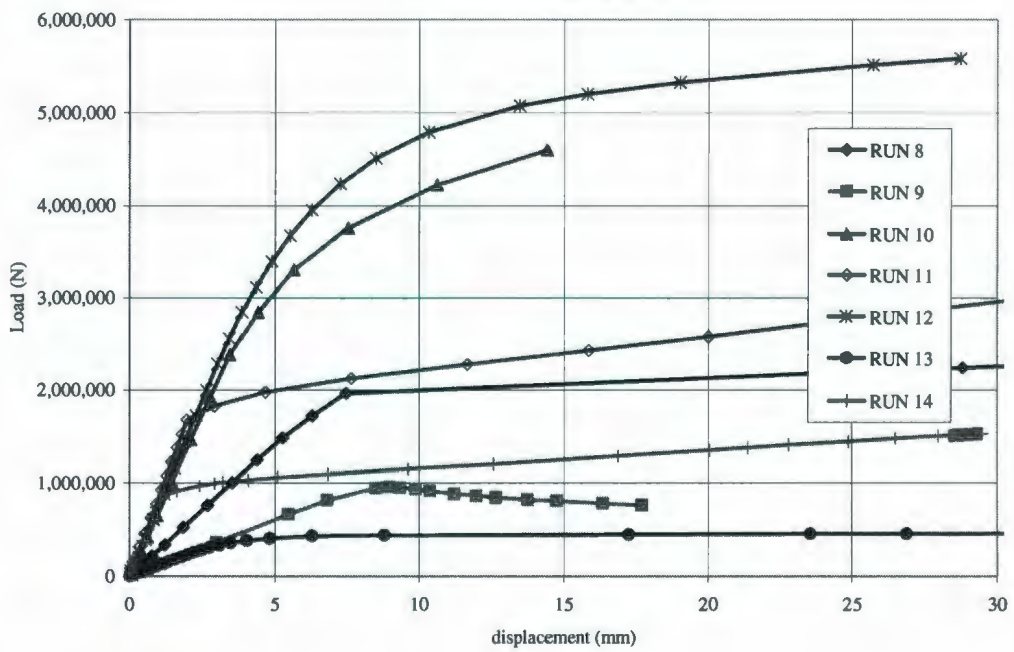


Appendix B2  
Validation Run Results

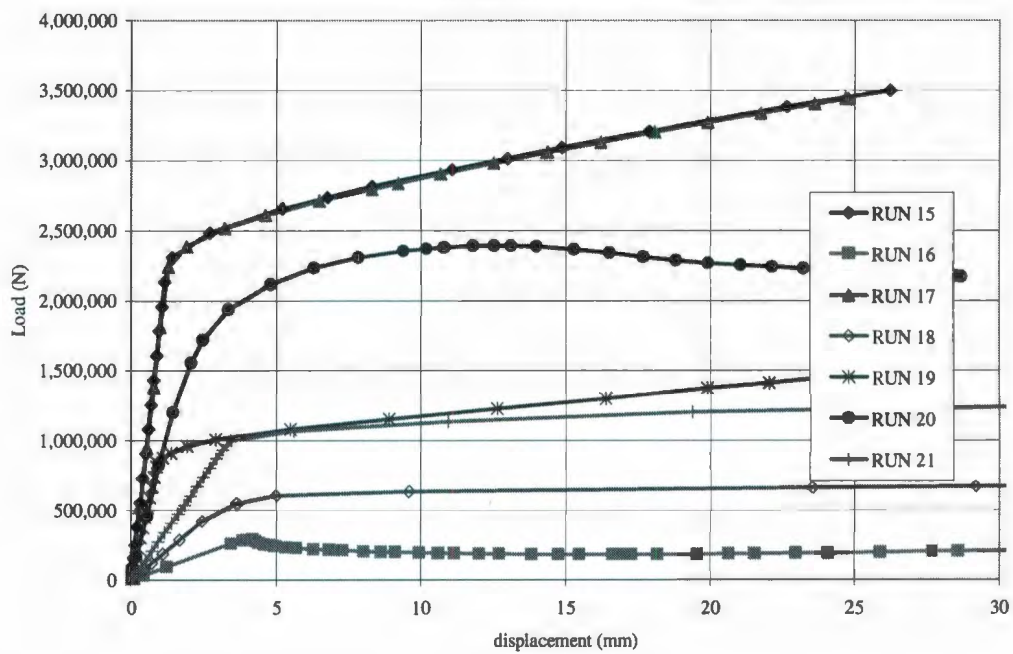
VERIFICATION RUN 1-7



VERIFICATION RUN 8-14



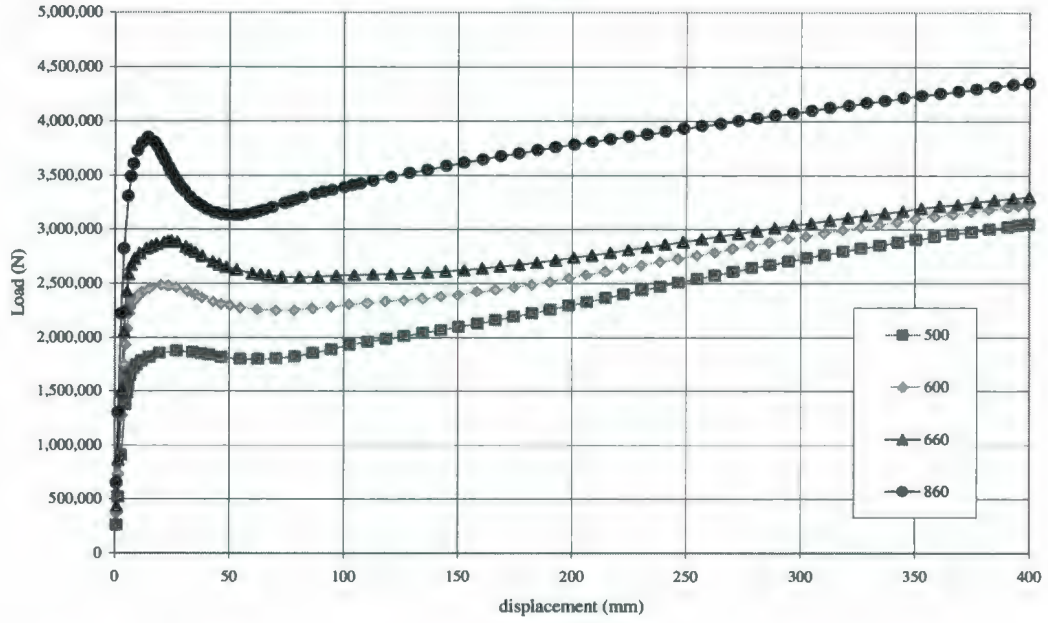
### VERIFICATION RUN 15-21



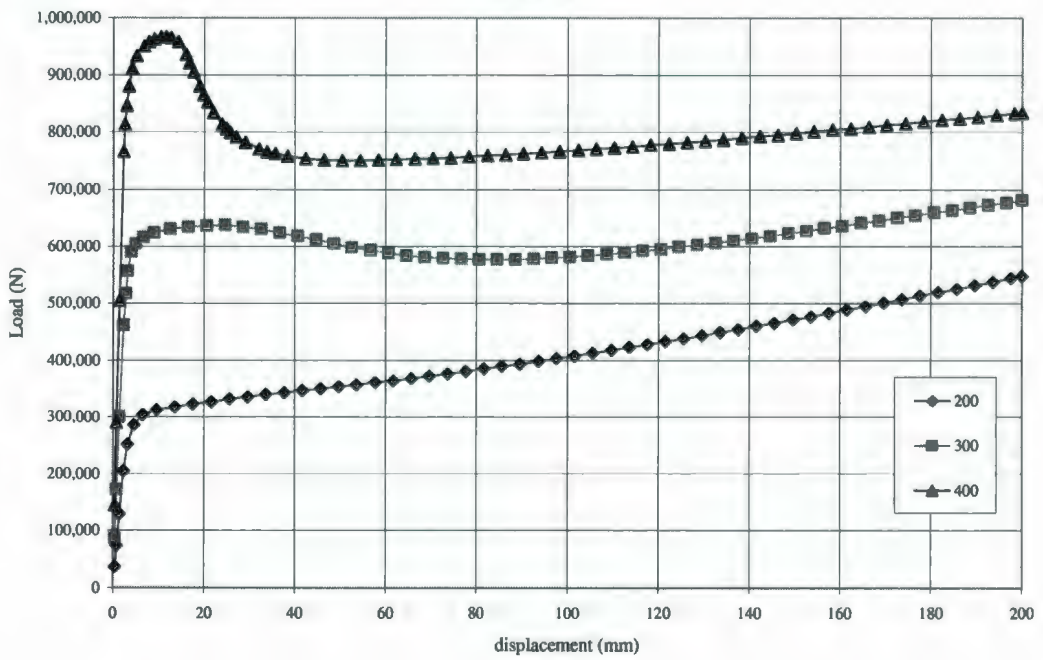
APPENDIX C:  
STABILITY OF FLAT BAR STIFFENER

Appendix C1  
DOE Run Results

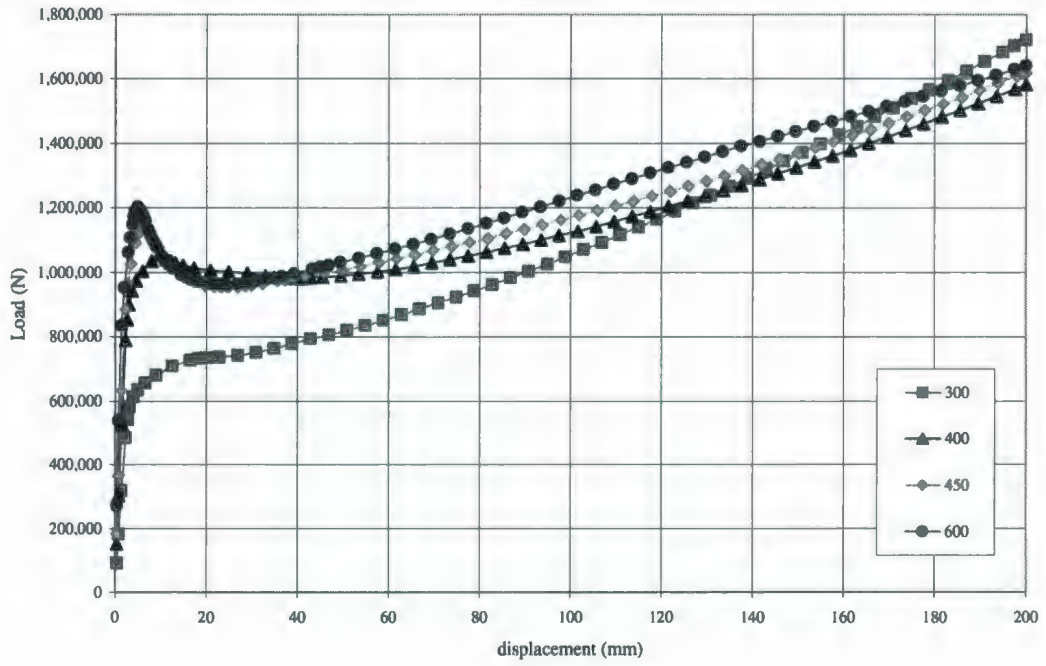
RUN 1



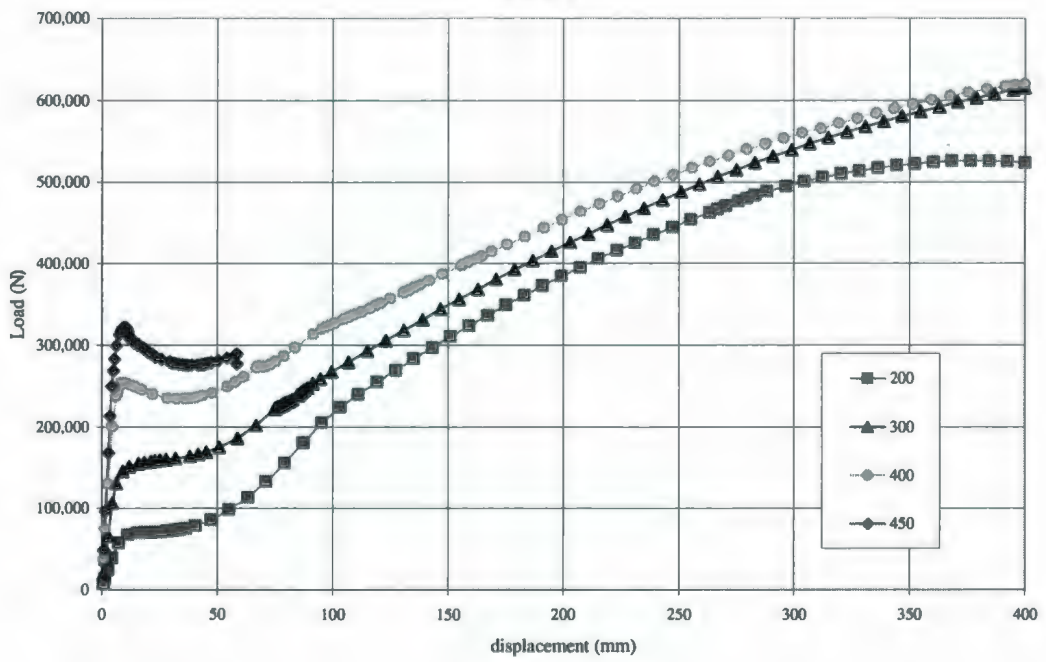
RUN 2



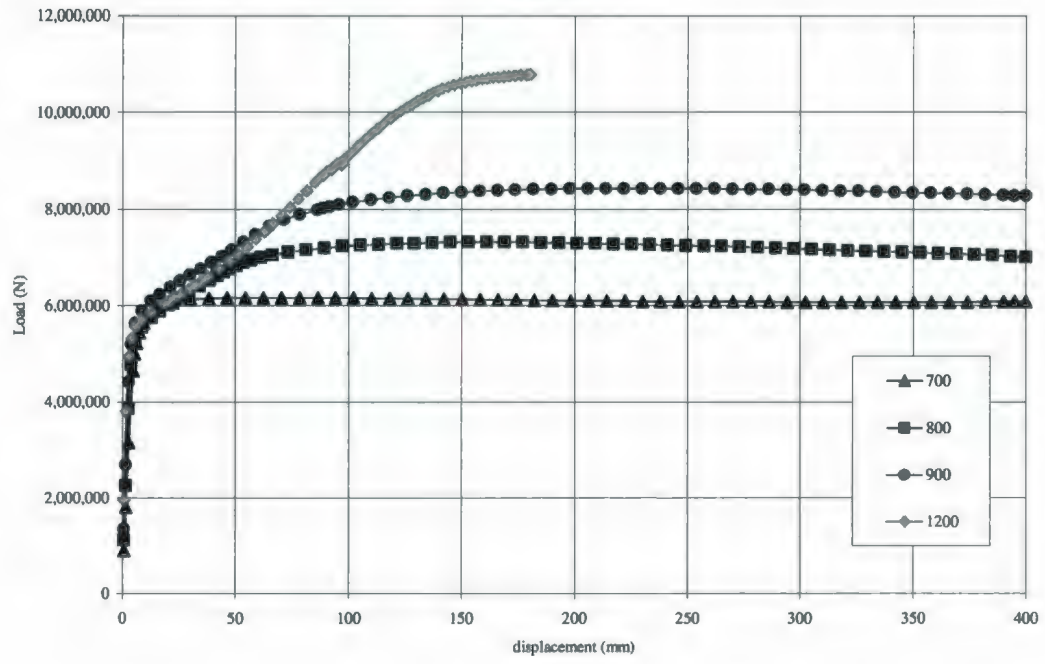
RUN 3



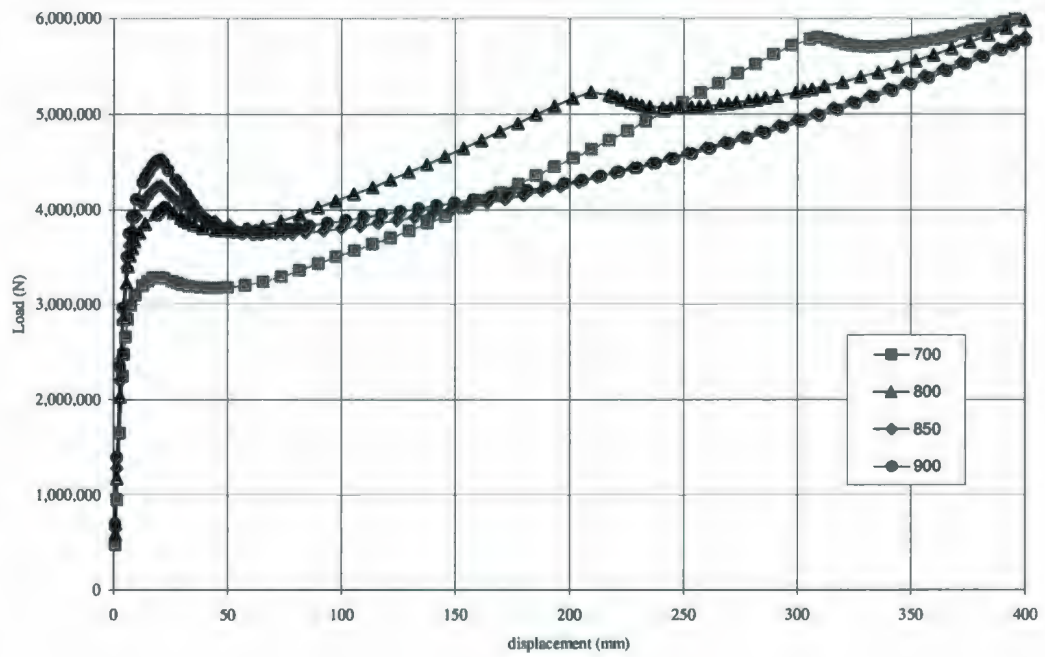
RUN 4



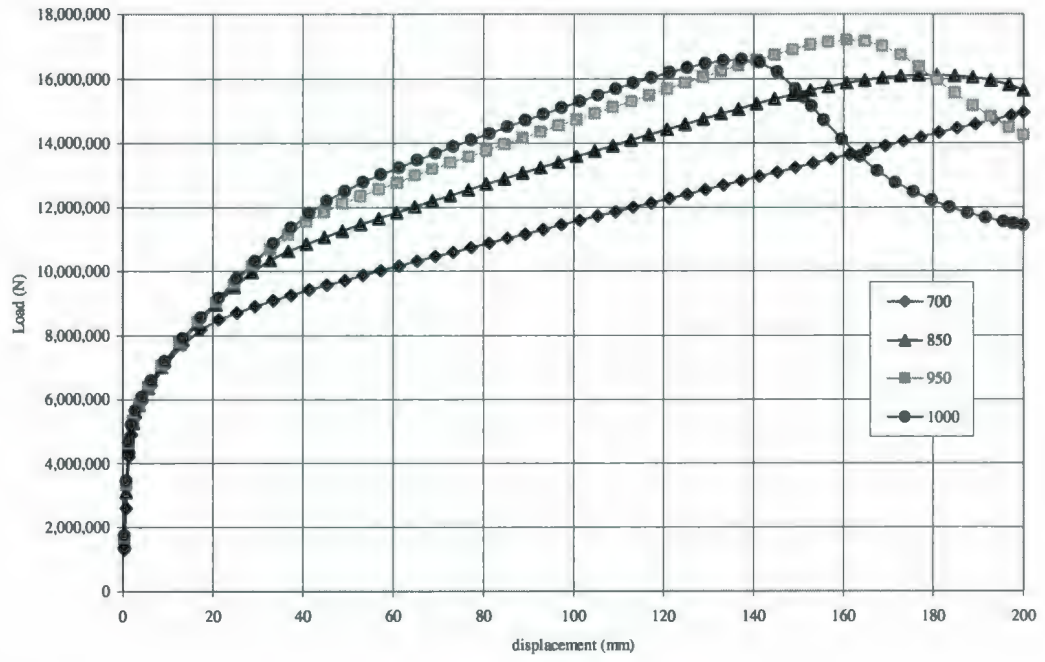
RUN 5



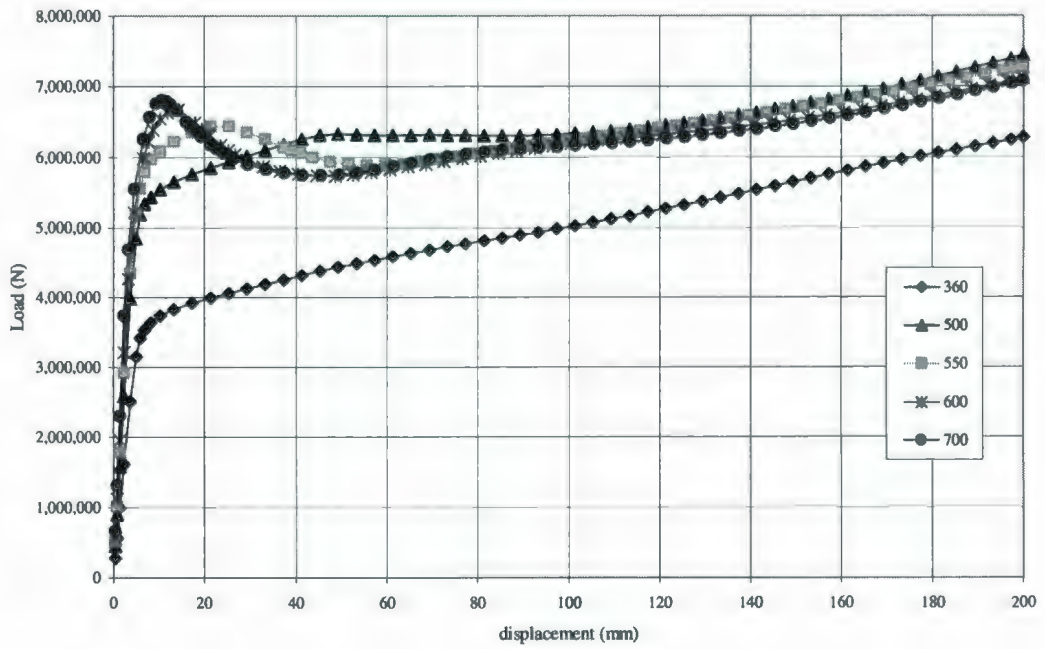
RUN 6



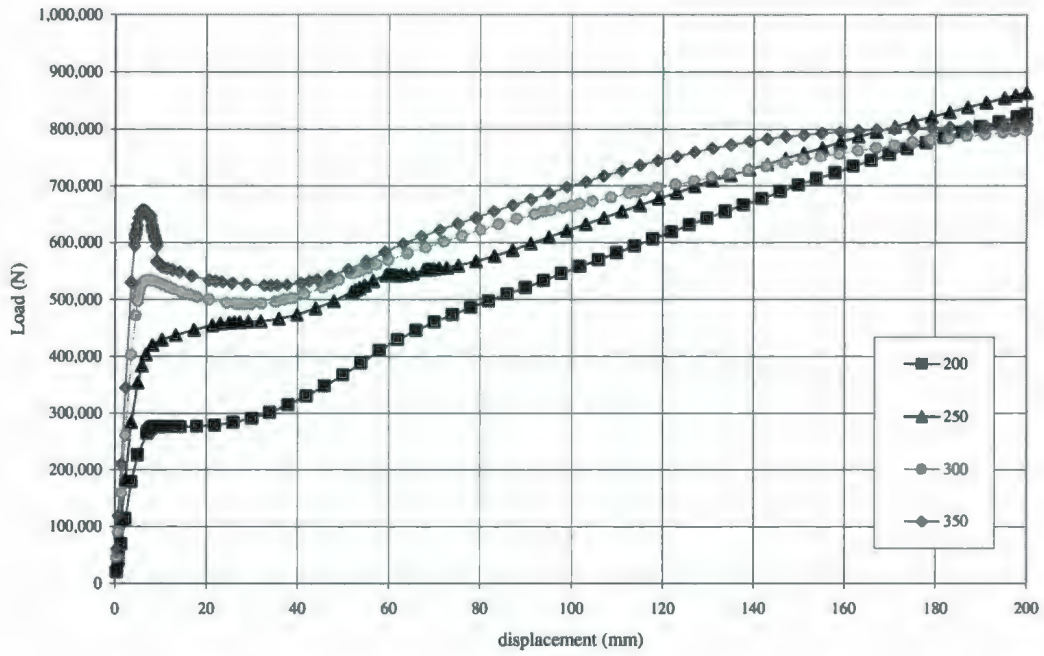
RUN 7



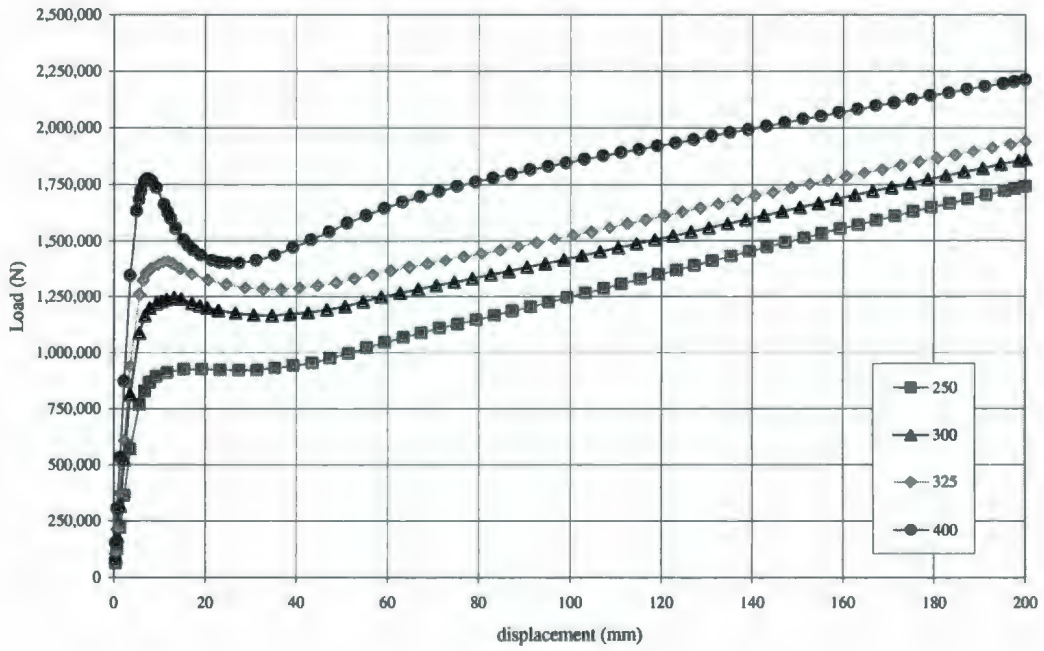
RUN 8



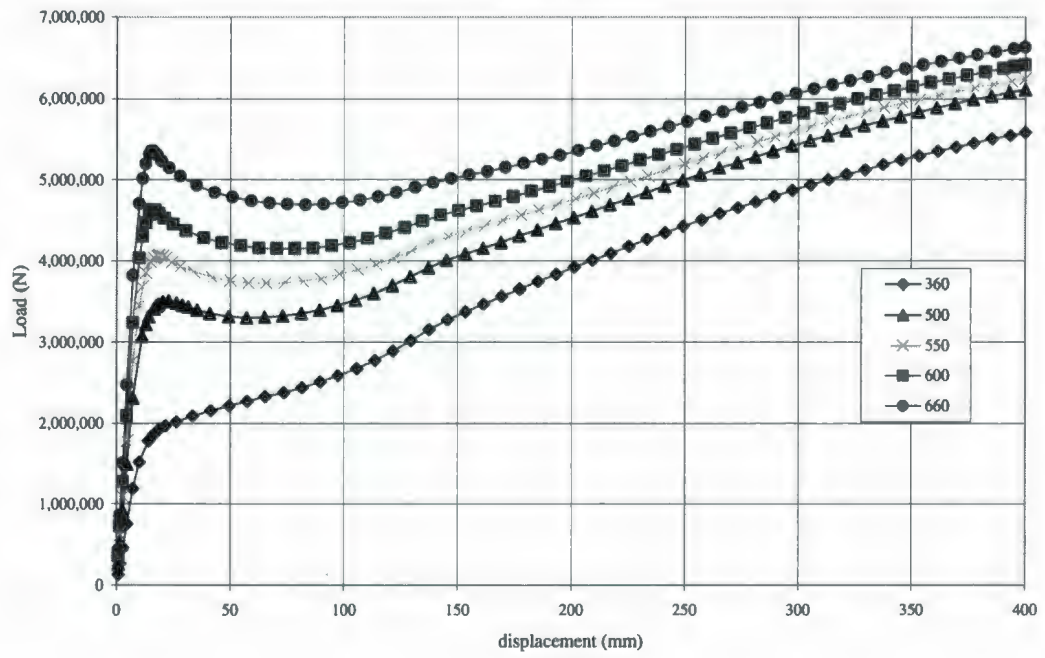
RUN 9



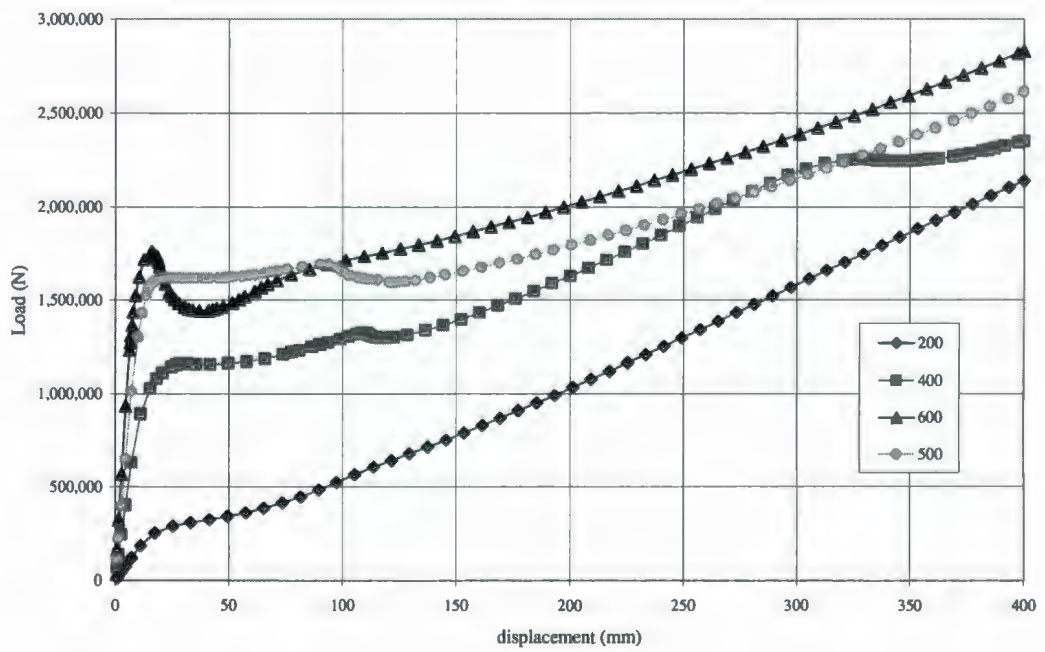
RUN 10



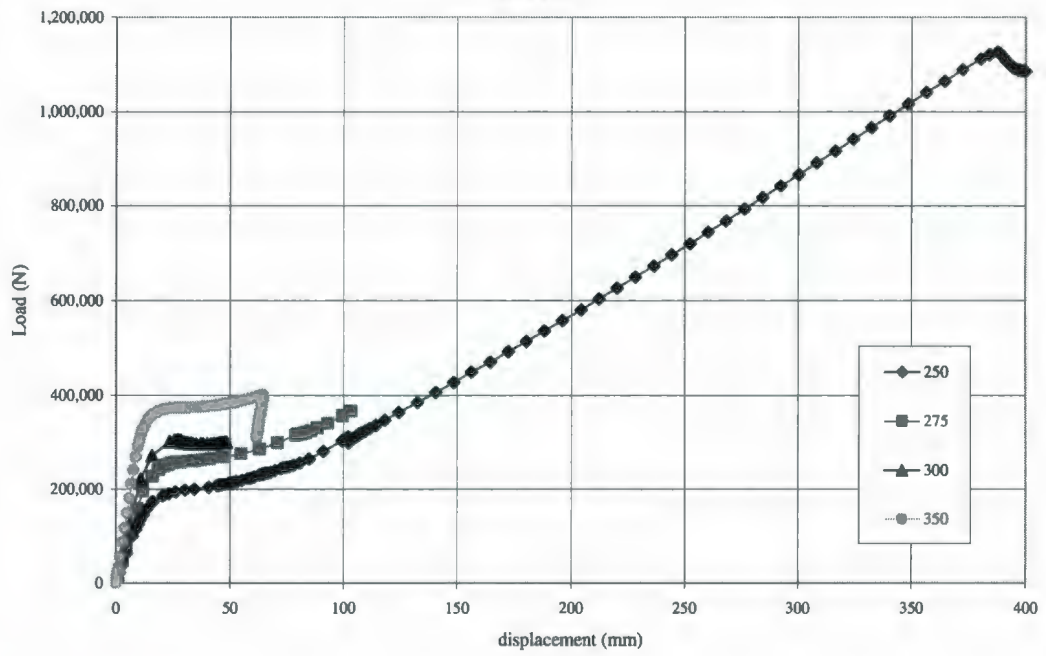
RUN 11



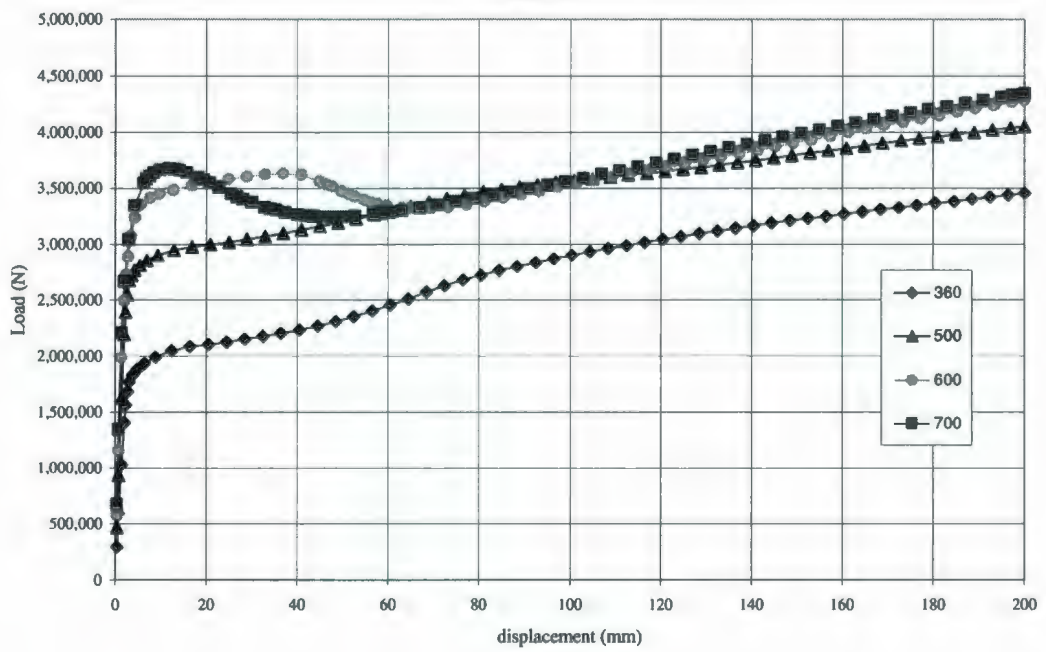
RUN 12



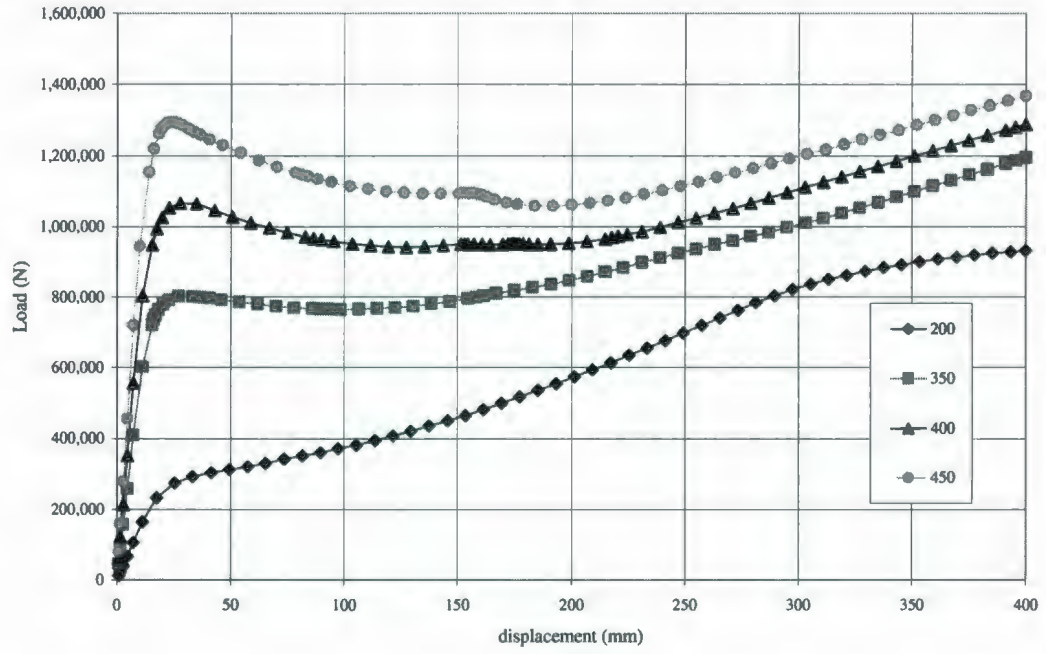
### RUN 13



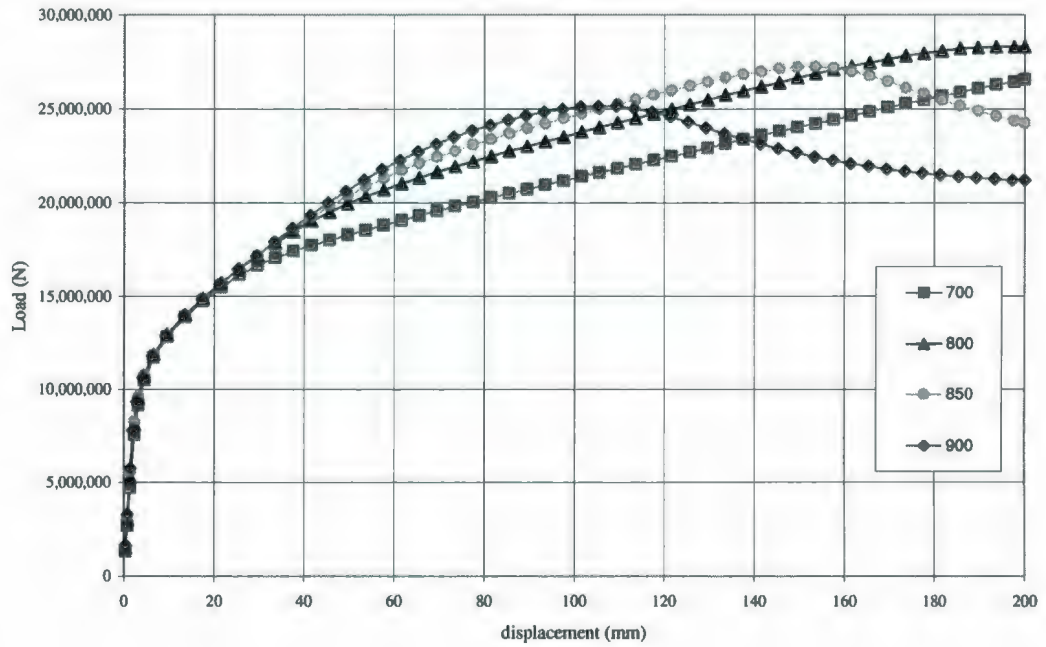
### RUN 14



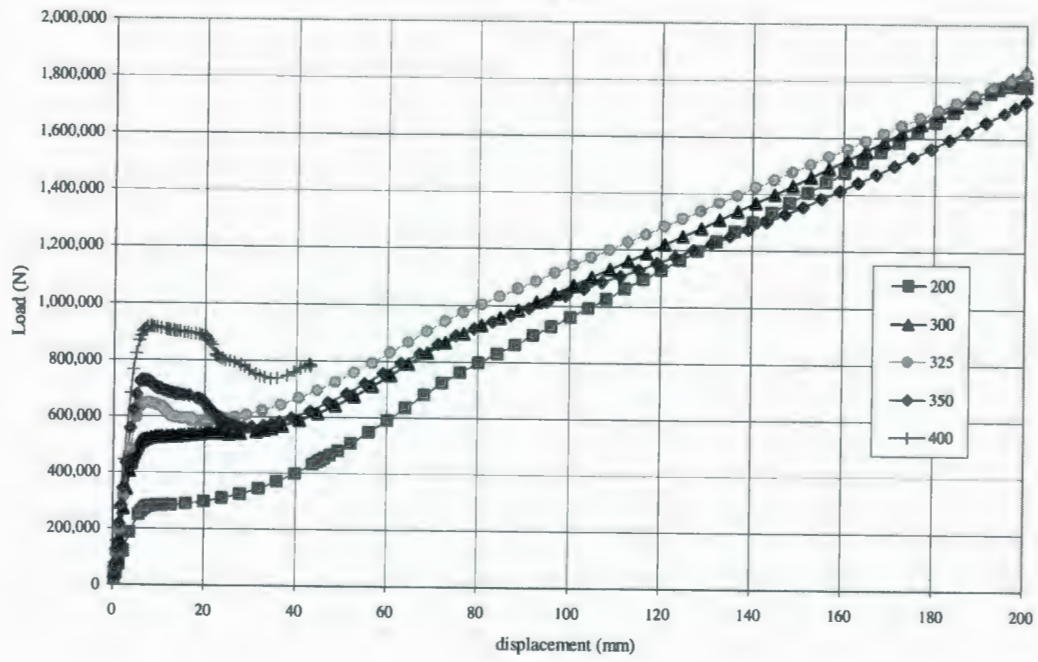
RUN 15



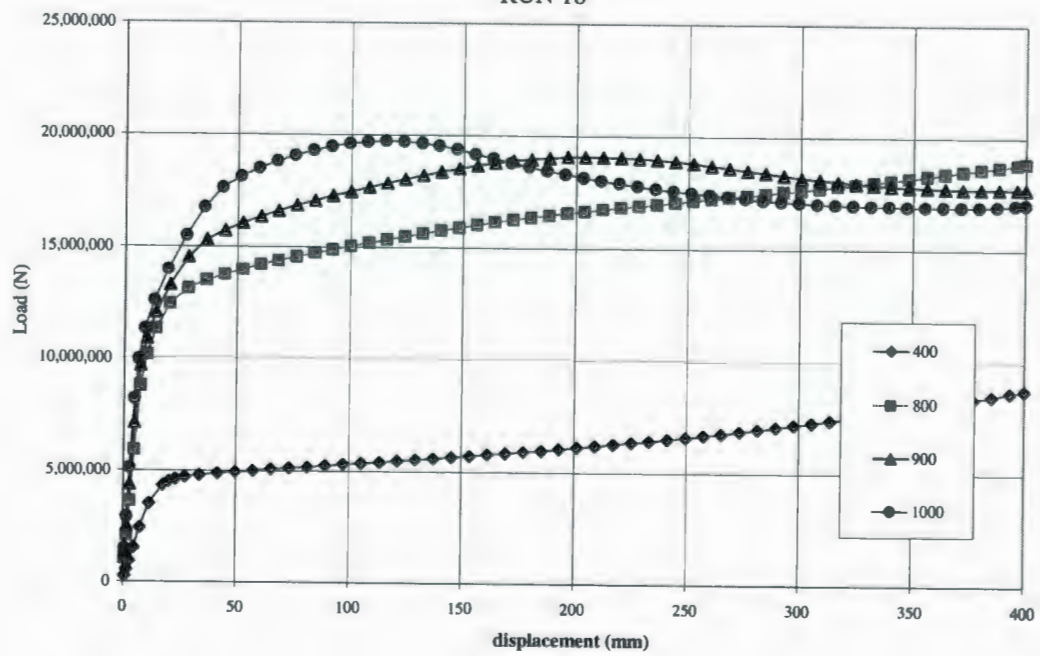
RUN 16



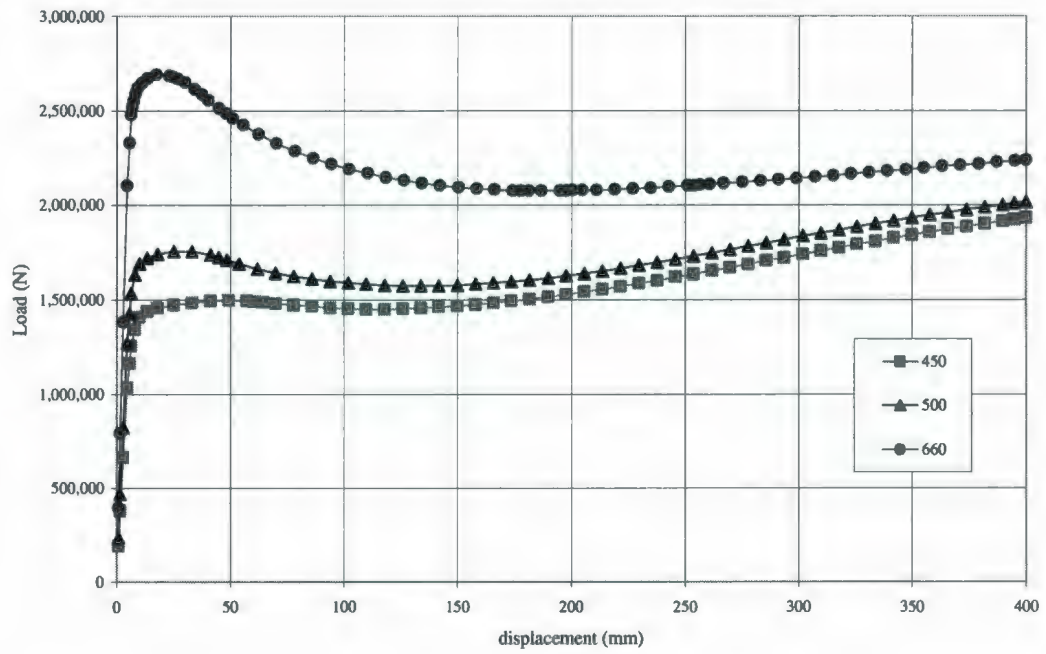
RUN 17



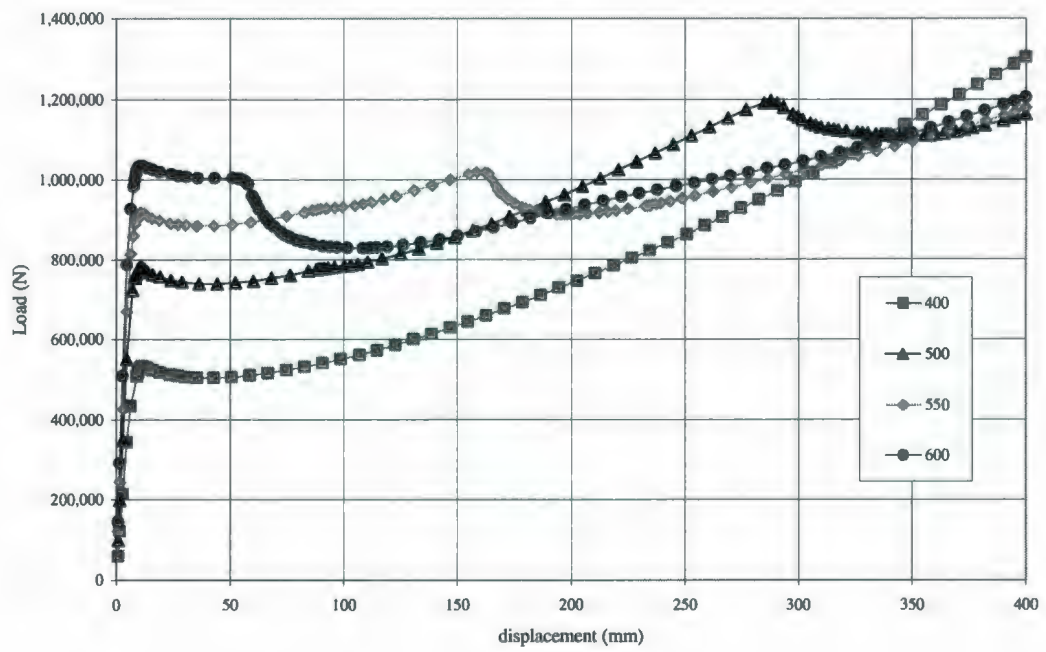
RUN 18



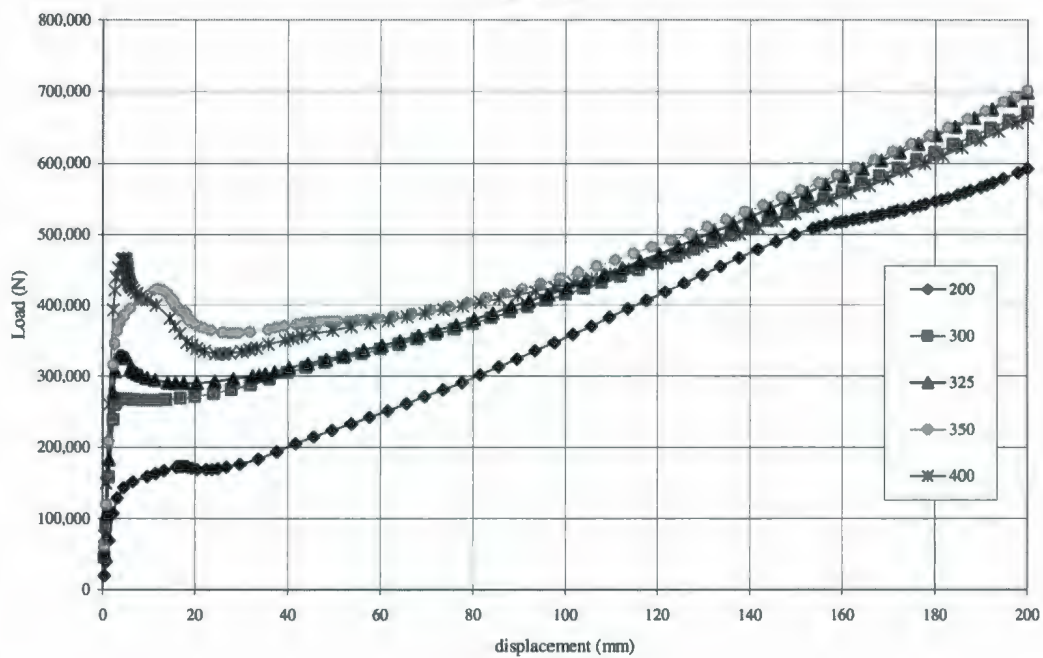
RUN 19



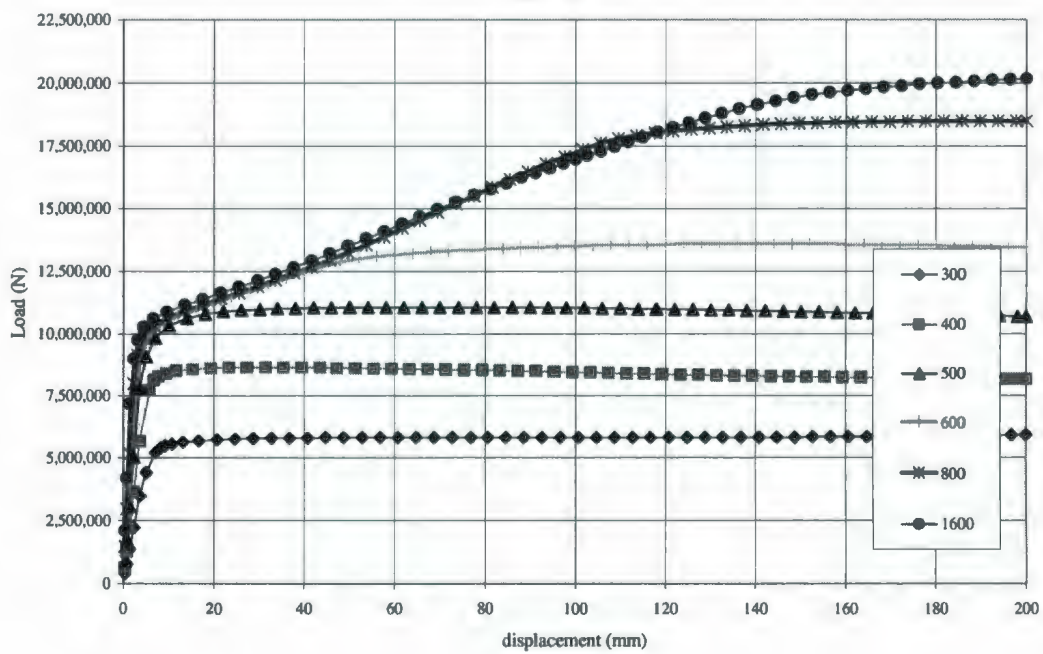
RUN 20



RUN 21

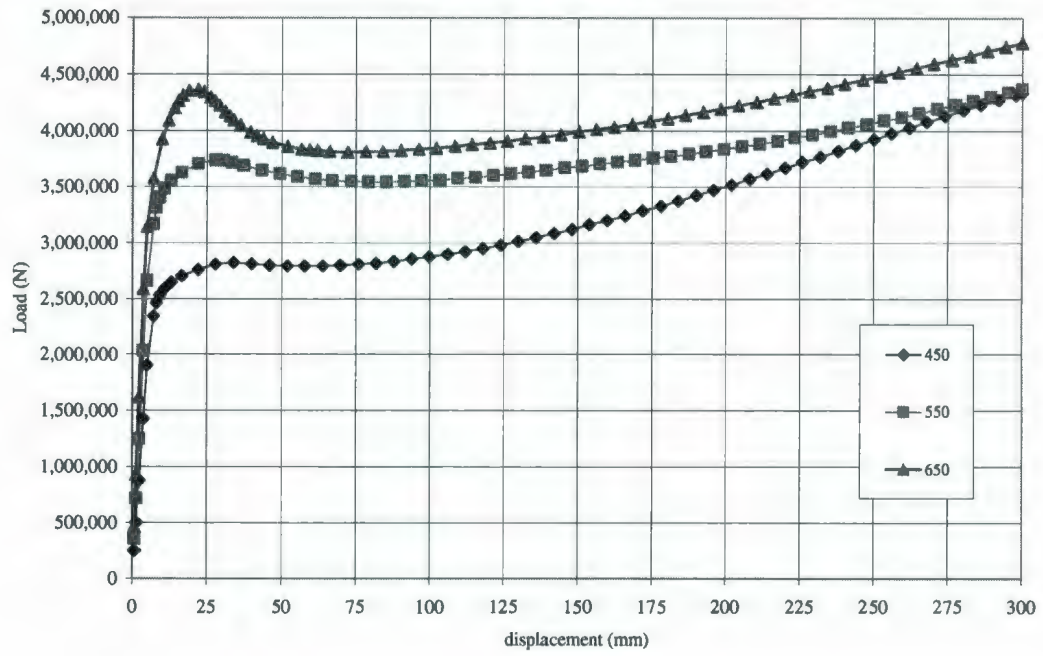


RUN 22

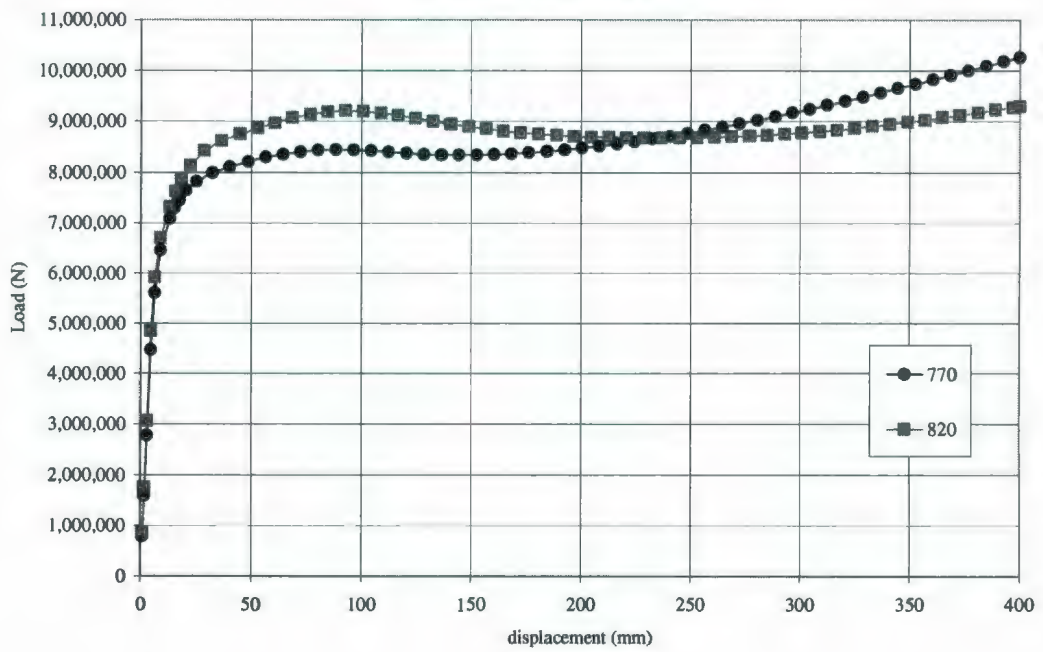


Appendix C2  
Validation Run Results

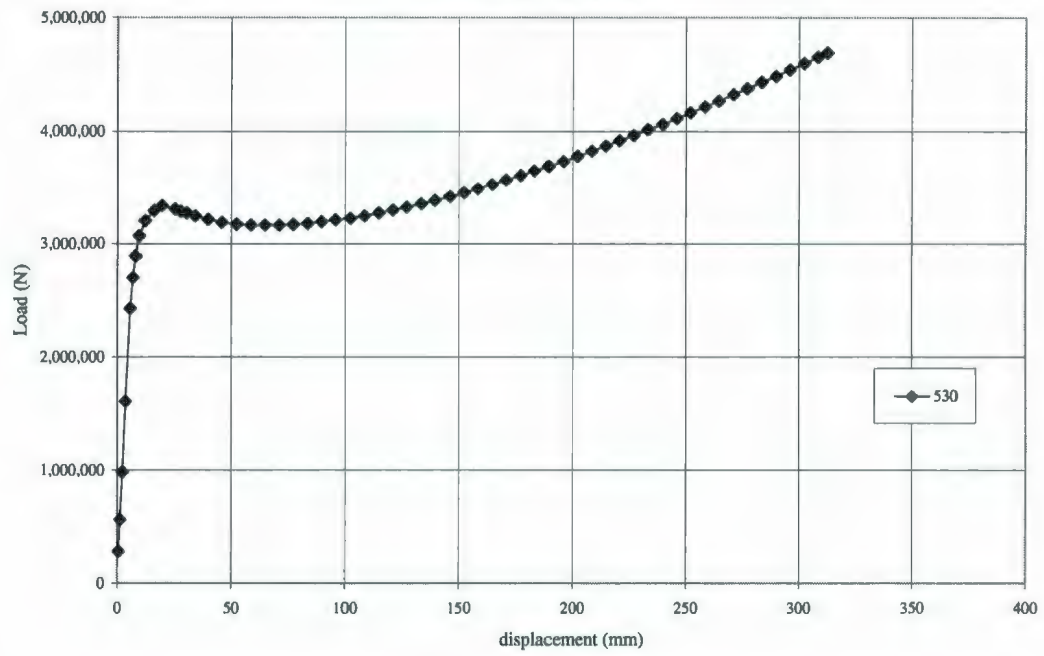
VALIDATION RUN V1



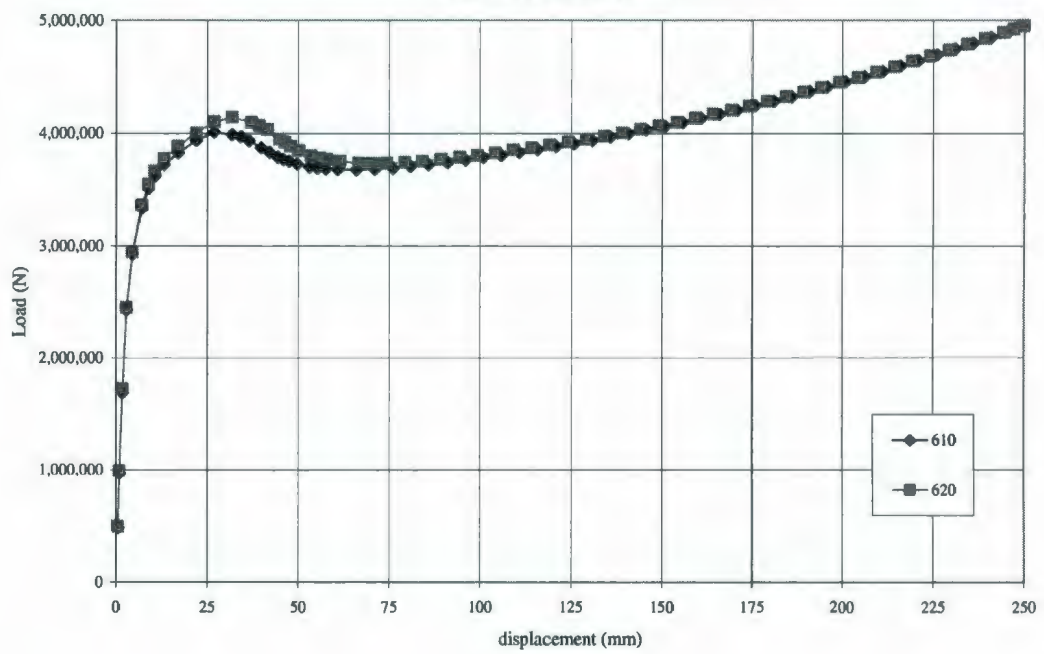
VALIDATION RUN V2



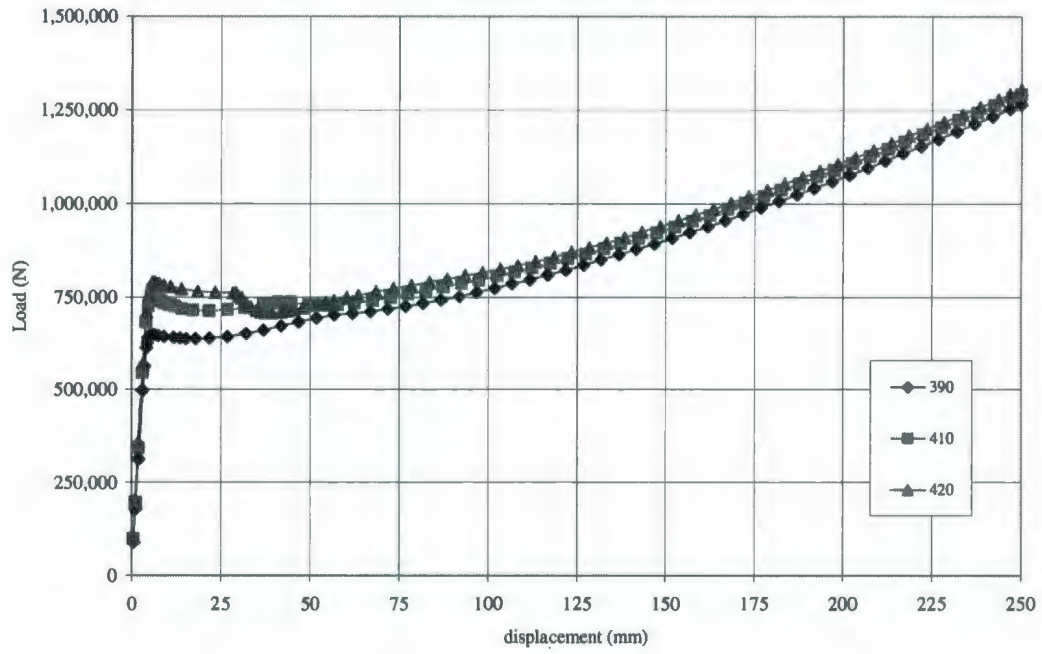
VALIDATION RUN V3



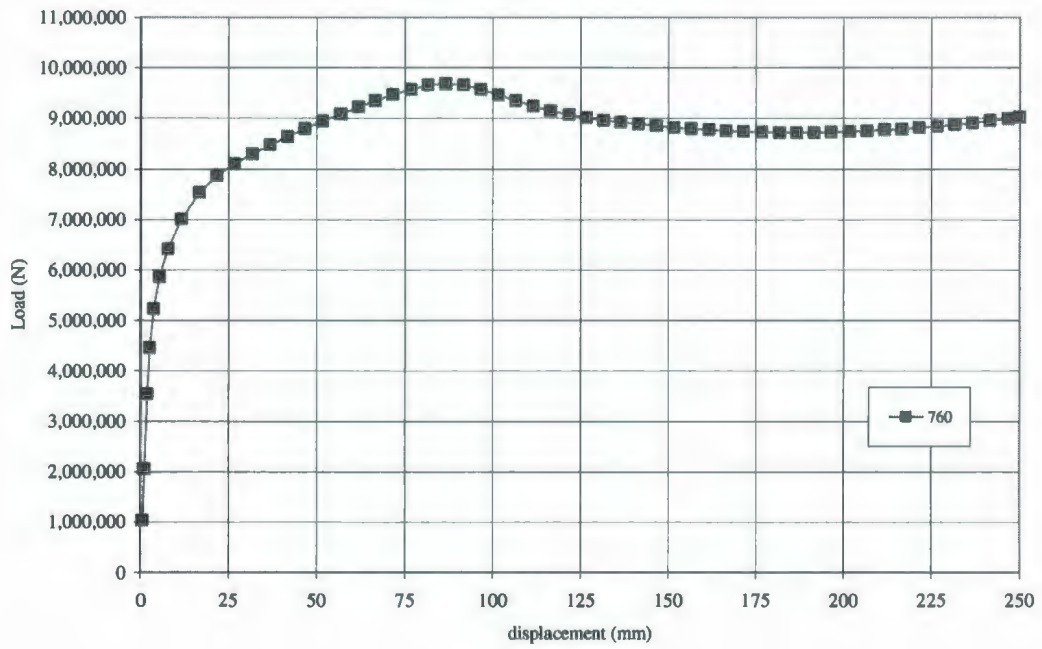
VALIDATION RUN V4



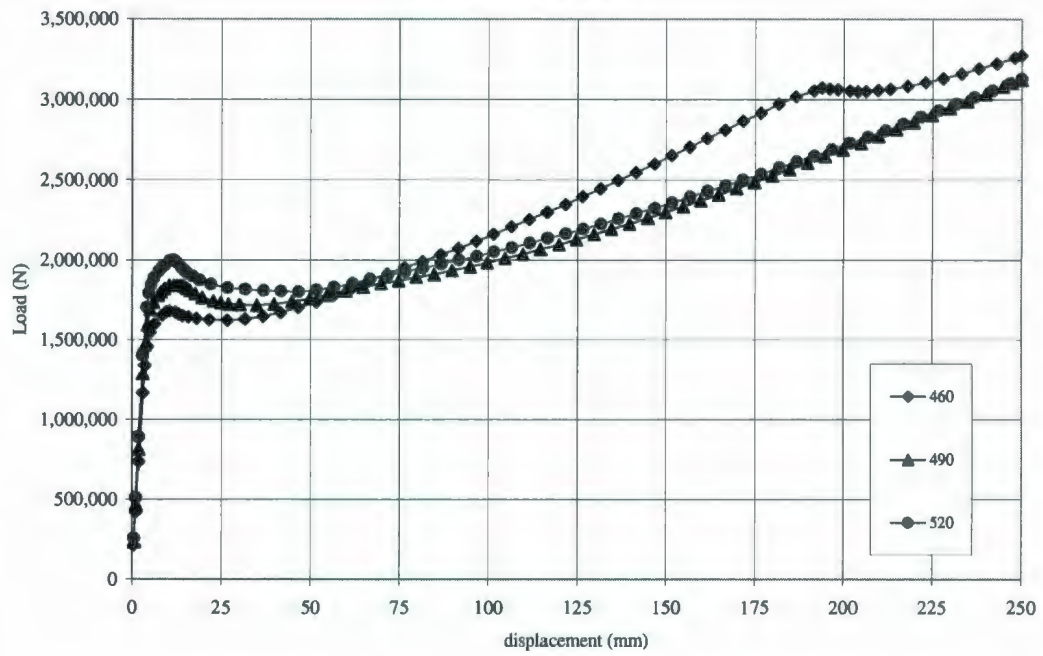
VALIDATION RUN V5



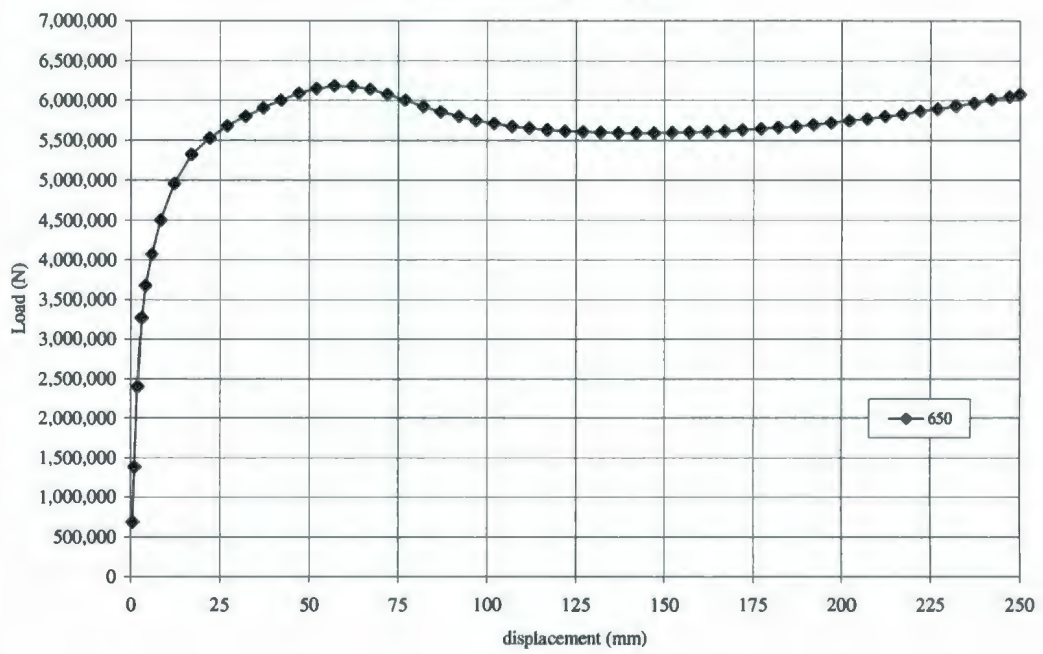
VALIDATION RUN V6



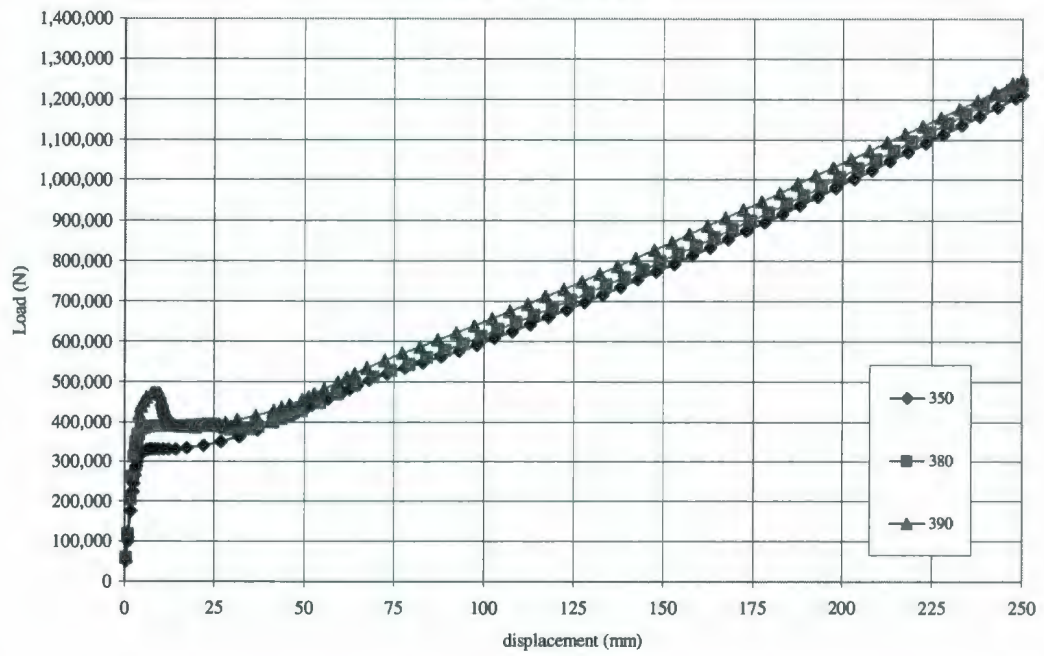
VALIDATION RUN V7



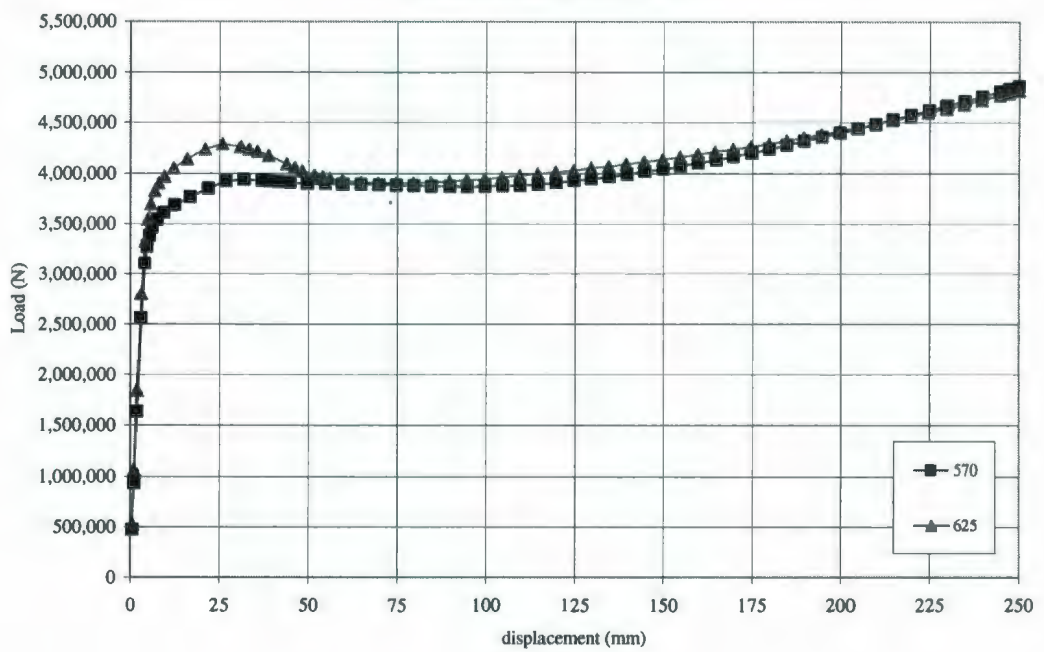
VALIDATION RUN V8



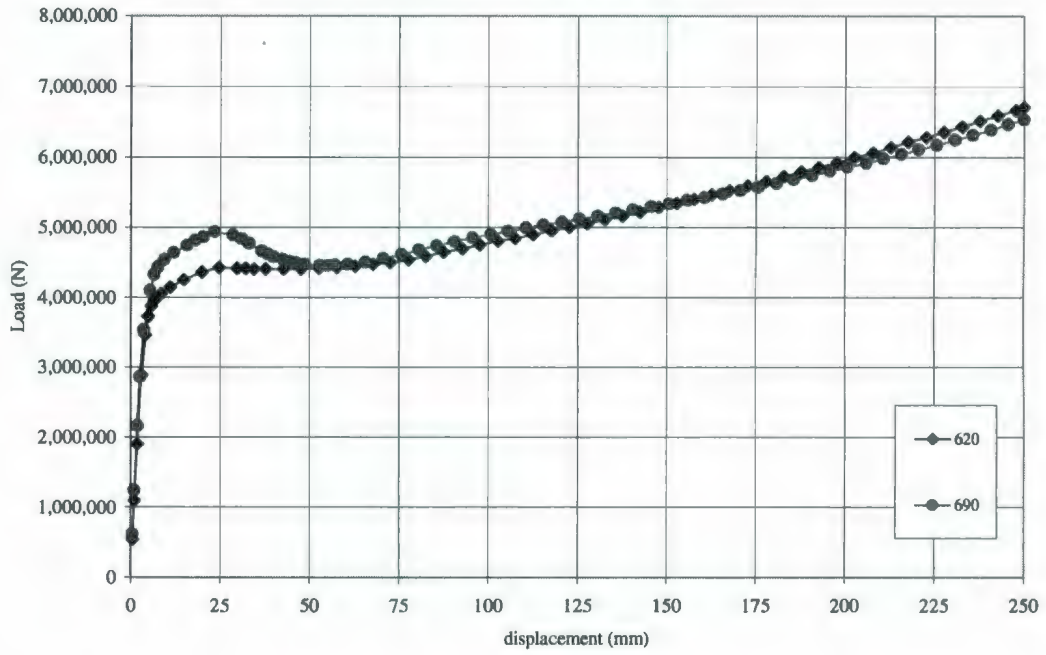
VALIDATION RUN V9



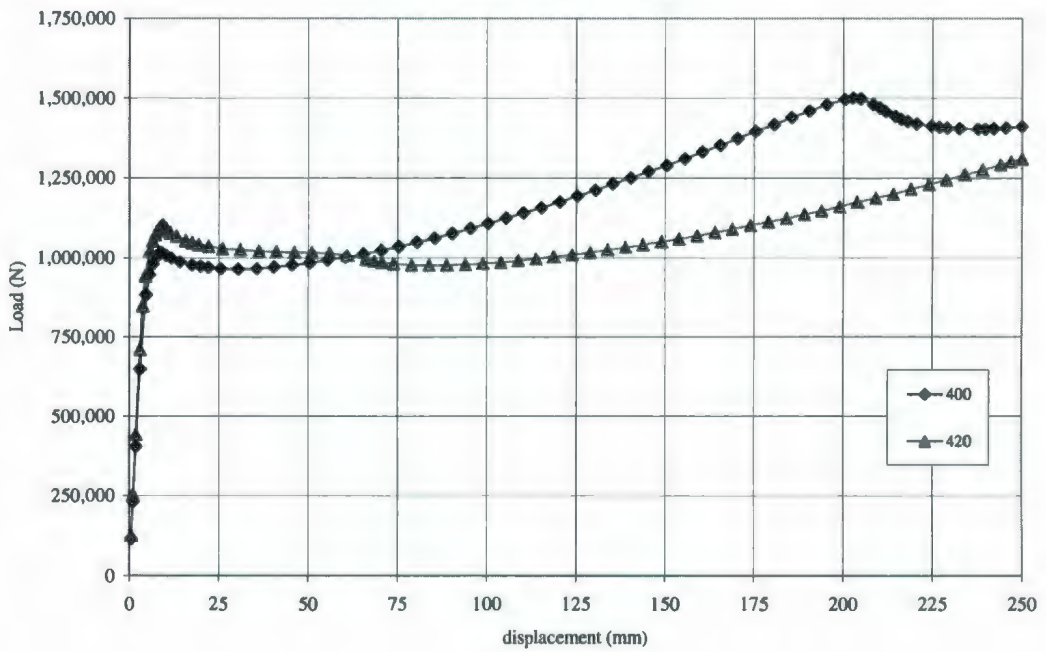
VALIDATION RUN V10



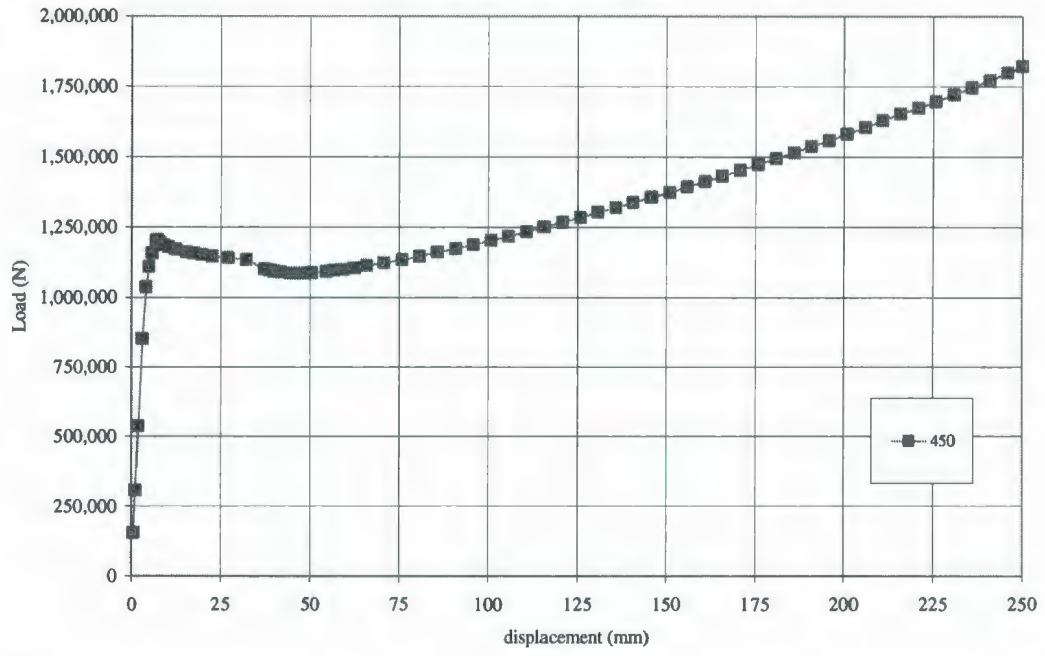
VALIDATION RUN V11



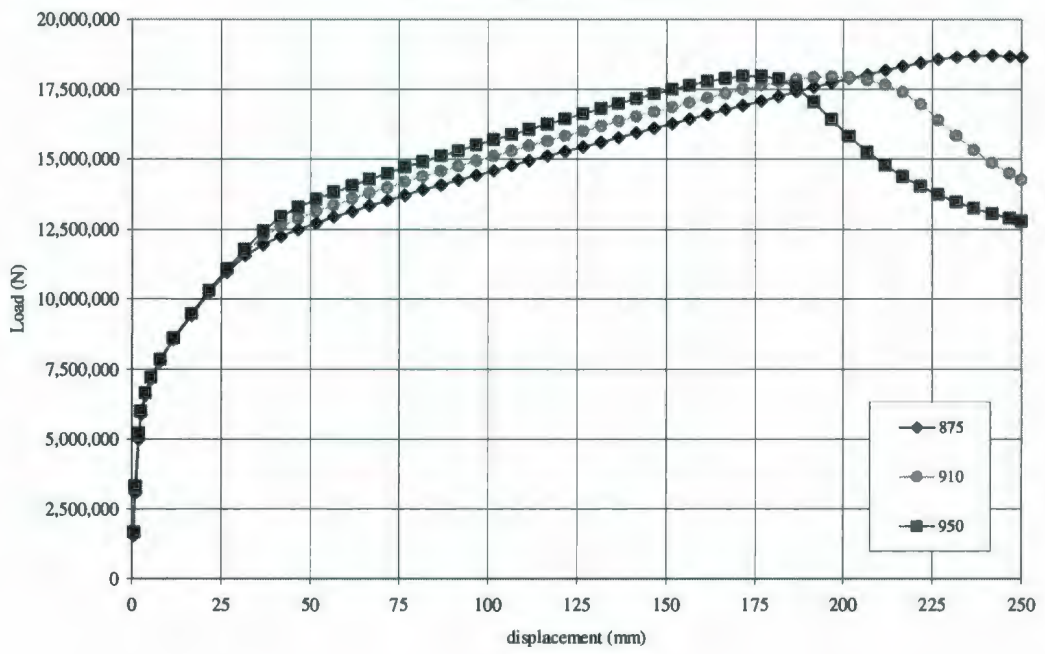
VALIDATION RUN V12



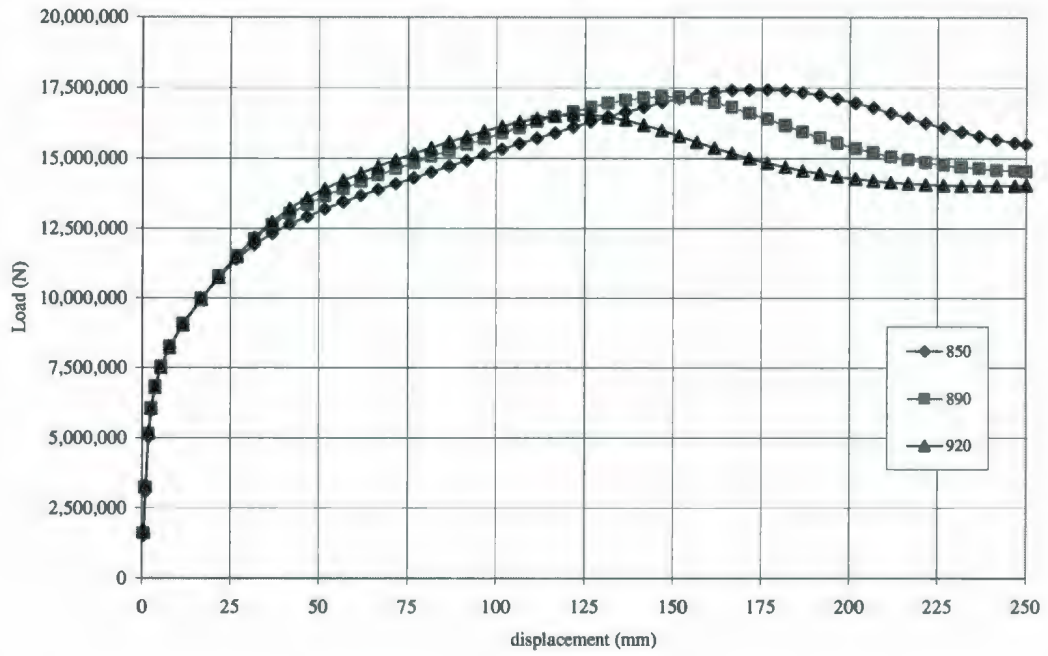
VALIDATION RUN V13



VALIDATION RUN V14



VALIDATION RUN V15



VALIDATION RUN V16

